



Genetic and chemical biology approaches for the
characterization of the yeast PDK1 orthologs in
Saccharomyces cerevisiae and *Candida albicans*

Dissertation zur Erlangung des Doktorgrades
des Naturwissenschaften

vorgelegt beim Fachbereich Biowissenschaften

der Johann Wolfgang Goethe-Universität in Frankfurt am Main

von Daniel Pastor-Flores
aus Zaragoza, Spanien
Frankfurt 2013

vom Fachbereich Biowissenschaften

Johann Wolfgang Goethe - Universität als Dissertation angenommen.

Dekan: Prof. Dr. Anna Starzinski-Powitz

Gutachter: Prof. Dr. A. Acker-Palmer

Datum der Disputation: 7. März 2014

This study was performed from March 2009 to October 2013 in the Research Group PhosphoSites located in the Biomedical Research Lab of the Medical Clinic I at the Goethe University Hospital in Frankfurt am Main under supervision of Dr. Ricardo Biondi.

The writing and the experiments presented here were performed by myself, unless otherwise stated.

Index

Figure Index	V
Table Index	VI
Abbreviations	VII
Zusammenfassung	1
Summary	6
Chapter I: Introduction	10
1. Introduction	11
1.1 Protein kinases	11
1.2 AGC protein kinases in eukaryotic organisms	11
1.2.1 The PDK1 master kinase in mammalian cells	13
1.2.2 PDK1 substrates	15
1.2.2.1 PKB/Akt	15
1.2.2.2 PKA	16
1.2.2.3 PKC	16
1.2.2.4 PKN	17
1.2.2.5 SGK	17
1.2.2.6 S6K	18
1.2.3 Mechanism of regulation by PDK1, the PIF-pocket	18
1.3 Opportunistic pathogens	19
1.3.1 Common opportunistic fungal infections	19
1.3.1.1 Candidiasis	20
1.3.1.1.1 The different morphogenic states of <i>C. albicans</i>	21
1.3.1.1.2 Signaling pathways and transcriptional regulators	23
1.3.1.1.2.1 The Ras1 Interrelated Networks	23
1.3.1.1.2.1.1 The MAPK signaling pathways	23
1.3.1.1.2.1.2 Cek1 pathway	23
1.3.1.1.2.1.3 Hog1 pathway	24
1.3.1.1.2.1.4 Cell Wall Integrity pathway	25
1.3.1.1.2.2 The cyclic AMP-dependent PKA pathway	25
1.3.2 Antifungal drugs and resistance	26
1.3.2.1 Efflux pumps in <i>S. cerevisiae</i> and <i>C. albicans</i>	29
1.4 <i>S. cerevisiae</i> , a model organism to study molecular networks and processes in <i>C. albicans</i>	30

1.5 The cell wall of yeast	30
1.5.1 The Cell Wall Integrity pathway in <i>S. cerevisiae</i>	30
1.5.1.1 The signal through the transmembrane sensors.....	31
1.5.1.2 The signal through Pkh.....	33
1.5.2 Pkh substrates in yeast.....	34
1.5.2.1 Sch9.....	34
1.5.2.2 PKA.....	35
1.5.2.3 Ypk1/2	37
1.5.2.4 Pkc1	38
1.6.1 Signal transduction function of sphingolipids	42
1.6.2 Organization in the plasma membrane	43
Chapter II: Materials and Methods	46
2. Materials and Methods	47
2.1 Bacterial strains.....	47
2.2 General molecular biology methods.....	47
2.3 Mammalian and insect cell lines.....	48
2.4 MTT Assay	49
2.5 Transfection and expression in HEK293 cells by PEI method.....	49
2.6 Bacmid production, transfection and protein expression in Sf9 cells.....	50
2.6.1 Virus production	51
2.6.2 Start a new culture of the Sf9 cells	52
2.6.3 Sf9 cell culture methods	52
2.6.4 Infection and harvest of Sf9 cells for protein production.....	52
2.6.5 Freezing and preserving a Sf9 cell culture	52
2.6.6 Purification of recombinant protein from Sf9 cells	53
2.6.7 Purification analysis of recombinant protein from Sf9 cells.....	54
2.7 Isoelectric focussing	55
2.8 Western Blot	56
2.9 In vitro measurement of protein kinase activity	56
2.10 His-CaPkh2 and His-PDK1 interaction with biotin-PIFtide and displacement of the Interaction using AlphaScreen technology	57
2.11 Interaction of GST-Pkh2 with lipids.....	58
2.12 Yeast cell strains and culture conditions.....	59
2.13 Construction of mutated yeast strains	61
2.13.1 Insertion of <i>tetO₇</i> promoter.....	61

2.13.2 Depletion of Pkh	62
2.14 RNA isolation.....	62
2.15 DNA microarray analysis	63
2.16 Preparation of yeast extracts and immunoblot analysis	64
2.17 Reactive Oxygen Species detection	64
2.18 Programmed cell death assays	64
2.19 Generation of Pkh2 <i>Candida albicans</i> synthetic gene	65
2.20 Two-hybrid screening.....	65
2.20.1 RNA isolation of the different morphogenetic states of <i>C. albicans</i>	66
2.20.2 LiAc yeast transformation for Two-hybrid assay.....	67
2.20.3 cDNA library <i>C. albicans</i> and pGBKt7-Pkh1 generation	67
2.20.4 Constructing and Screening the Two-Hybrid Library	68
2.20.5 Set-up for control Two-hybrid contrasformation	68
2.21 Novel protocols performed for testing compounds in vivo.....	69
2.21.1 Assay for testing compounds in yeast cells on agar	69
2.21.2 Test compounds in suspension growth in 96 well plates	69
2.21.3 Heat shock assay for Cell Wall Integrity pathway (CWI) kinases	72
2.22 Reproducibility of the results	74
Chapter III: Results.....	75
3. Results.....	76
3.1 Part I. Pkh <i>S. cerevisiae</i>. Genetic characterization	76
3.1.1 Characterization of depleted strains	76
3.1.2 Pkh-depleted cells are defective in the activation of the CWI pathway.....	78
3.1.3 Global transcriptional changes resulting from the depletion of Pkh.....	80
3.1.3.1 Cells depleted of Pkh accumulate mRNAs involved in stress responses	80
3.1.3.1.1 Short term depletion of Pkh alters glycogen	82
3.1.3.1.2 Unfolded Protein Response genes induced after 24 hours treatment	83
3.1.3.2 The absence of Pkh affects the transcriptional response to heat shock	84
3.1.3.3 Pkh is important for regulating the Hsf1 and Msn2/Msn4 transcription factors after heat stress	85
3.1.4 Cells depleted for Pkh accumulate ROS.....	86
3.1.5 Activation of the Slr2 MAP kinase pathway reduces the oxidative stress of cells depleted of Pkh	88
3.1.6 Depletion of Pkh induces PCD in a Mca1-independent manner	89
3.2 Part II Characterization of CaPkh2	91

3.2.1 Biochemical similarities and differences between CaPkh2 and PDK1.....	91
3.2.2 Design of <i>PKH2 C. albicans</i> synthetic gene for protein expression in mammalian and insect cells.....	92
3.2.3 Two-hybrid system.....	93
3.2.4 CaPkh2 as antifungal target.....	95
3.2.4.1 CaPkh2 crystal structure and the PIF-pocket as a target for the modulation of PDK1 activity	95
3.2.4.3 Biochemical differences at the PIF-pocket between PDK1 and CaPkh2	101
3.2.4.4 Small molecule PS77 is a CaPkh2 PIF-pocket allosteric inhibitor with selectivity over PDK1	103
3.2.4.5 Small molecule PS77 inhibited the growth of <i>S. cerevisiae</i> strains with ABC transporter deletions.....	105
3.2.5 Characterization of a putative CaPkh2 PH domain	105
3.2.5.1 In vitro activity and binding to lipids of Pkh constructs	106
Chapter IV: Discussion	112
Discussion	113
4.1 Perspectives	119
Bibliography	121
Bibliography	122
Appendix	132
Appendix	133
A.1 codon usage frequency vs. relative adaptiveness.....	139
A.2 Initial hits found targeting Aurora B in mammalian cells inhibited Ipl1 in <i>C. albicans</i> .	145
Acknowledgement	146

Figure Index

Figure 1.1 Catalytic domain of PKA	13
Figure 1.2 Schematic representation of PDK1 and its interaction mechanism with PKB/Akt	15
Figure 1.3 General regulation mechanism of AGC kinases	19
Figure 1.4 Schematic representation of the main MAPK pathways in <i>Candida</i>	24
Figure 1.5 PKC family in mammalian cells in comparison to Pkc1 in <i>S. cerevisiae</i>	39
Figure 1.6 Sphingolipid biosynthetic pathway	42
Figure 1.7 Signaling pathways regulated by LCBs	43
Figure 2.1 Schematic representation of virus production in insect cells	50
Figure 2.2 Analysis of CaPkh2 purification constructs	55
Figure 2.3 Conditions for AlphaScreen	58
Figure 2.4 Interaction between proteins activates a set of reporter genes in AH109 strain	66
Figure 2.5 Toxicity of PSX137 in <i>C. albicans</i> strains in solid growth	71
Figure 2.6 Toxicity of PSX137 in <i>C. albicans</i> strains in suspension growth	71
Figure 2.7. Compounds targeting the PIF-pocket inhibit growth of yeast cells	74
Figure 3.1 <i>S. cerevisiae</i> cells having reduced expression of <i>PKH2</i> are not viable	78
Figure 3.2 Depletion of Pkh decreases the ability of yeasts to activate the CWI pathway	80
Figure 3.3 Clustering of the genes differentially expressed when Pkh is depleted	82
Figure 3.4 Depletion of Pkh affects the glycogen metabolism	83
Figure 3.5 Cells with low Pkh expression are affected under reducer agent	84
Figure 3.6 The transcriptional response to heat shock requires Pkh	85
Figure 3.7 Transcription factors that are affected by the lack of Pkh under heat shock	86
Figure 3.8 Low expression of Pkh exacerbates the cell lethality of oxidizing agents	87
Figure 3.9 Depletion of Pkh activity induces oxidative stress in <i>S. cerevisiae</i>	88
Figure 3.10 <i>BCK1-20</i> expression reverts the accumulation of ROS in the absence of Pkh	89
Figure 3.11 Depletion of Pkh causes DNA fragmentation	90
Figure 3.12 Activity assay of CaPkh2 and PDK1 activated by PIFtide	96
Figure 3.13 Structural characterization of CaPkh2	97
Figure 3.14 Effect of ATP-competitive inhibitors KP-372 and Compound 7	98
Figure 3.15 Comparison of the ATP-binding sites of CaPkh2 and human PDK1	100
Figure 3.16 Comparison of the PIF-pocket of CaPkh2 and human PDK1	103
Figure 3.17 Novel compound PS77 is a selective allosteric inhibitor of CaPkh2	104
Figure 3.18 PS77 is toxic to YPP66 and YPP64T	105
Figure 3.19 Specific activity of PDK1 and CaPkh2 constructs in basal conditions	107
Figure 3.20 Lipid strips interact with PDK1 and CaPkh2 constructs	108
Figure 3.21 Aligment of the N-terminal Pleckstrin Homology Domain of TAPP2	109

Figure 3.22 Pkh constructs activity with structural lipids and regulatory lipids	111
Figure A.1 Codon usage of alternative yeast <i>C. albicans</i> by frequency.....	141
Figure A.2 Codon usage of alternative yeast <i>C. albicans</i> by relative adaptiveness.....	142
Figure A.3 Codon table of 50 first aminoacids coded by wild type <i>CaPKH2</i> gene.....	143
Figure A.4 Effect of PS77 on yeast strains and a mammalian cell line.....	144
Figure A.5 PSX137 inhibit growth in <i>S. cerevisiae</i> targeting Ipl1.....	145

Table Index

Table 1.1 AGC kinase families in eukaryote organisms.....	12
Table 1.2 Antifungal drugs with their targets and resistance mechanisms	28
Table 1.3 Main Glycerolphospholipids in <i>S. cerevisiae</i>	41
Table 2.1 Bacterial strains	47
Table 2.2 Oligonucleotides used	48
Table 2.3 Cell lines used	49
Table 2.4 Yeast strains used	60
Table 2.5 Small scale control.....	68
Table 3.1 Candida Pkh2 constructs	92
Table 3.2 Proteins interacting with CaPkh2 by Two-hybrid system	94
Table 3.3 Effect of Compounds on PDK1 and CaPkh2 ordered by families	102
Table A.1 Genes up-regulated by depletion of Pkh.....	133
Table A.2 Genes down-regulated by depletion of Pkh	137

Abbreviations

123-DHR	Dihydrorhodamine 123
1H	Hydrogen
Å	Angstrom
aa	Amino Acid
ABC transporter	ATP-binding cassette transporter
Abs	Absorbance
ADP	Adenosine 5'-diphosphate
Amp	Ampicillin
AMP	Adenosine monophosphate
ATP	Adenosine 5'-triphosphate
BAC	Bacterial Artificial Chromosome
Bcy1	Bypass of cyclic-AMP requirement
bp	Base pair
BSA	Bovine serum albumin
<i>C. albicans</i>	<i>Candida albicans</i>
Ca ²⁺	Calcium
cAMP	Cyclic AMP (adenosine 3',5'-cyclic monophosphate)
CAP	GTPase-activating protein
CD	Catalytic domain
Cek1	<i>C. albicans</i> ERK-like Kinase1 (Fus3 in <i>S. cerevisiae</i>)
C-terminal /c-terminus	Carboxy-terminal
CWI	Cell wall integrity
Da	Dalton
DAG	Diacylglycerol
DMEM	Dulbecco's Modified Eagles Medium
DMSO	Dimethyl sulfoxide
DNA	Deoxyribonucleic acid
dNTPs	Equal mixture of dATP, dCTP, dGTP and TTP
ds	Double stranded
DTT	Dithiothreitol
<i>E. coli</i>	<i>Escherichia coli</i>
EDTA	Ethylene diamine tetraacetic acid
EGTA	Ethyleneglycol bis (2-aminoethylether)-N'N'tetraacetic acid
ER	Endoplasmatic reticulum
FBS	Fetal bovine serum
FL	Full length
G418	Geneticin (neomycin analogue)

GEF	Guanosine exchange factors
GSH	Glutathione sepharose
GSK3	Glycogen synthase kinase-3
GST	Glutathione-S-transferase
GTP	Guanosine-5'-triphosphate
h	Hour
H-bond	Hydrogen bond
HEK293	Human embryonic kidney-293
HEPES	N-(2-Hydroxyethyl)piperazine-N'-(2-ethanesulfonic acid)
His-tag	Hexahistidine-tag
HM	Hydrophobic motif
HOG	High Osmolarity Glycerol
Hr1	Rho effector or protein kinase C-related kinase Homology region 1 homologues
HRP	Horseradish Peroxidase
IEF	Isoelectric focussing
KDa	Kilo Dalton
KO	Knock-Out
Kpb	Kilo pair bases
LA	Lipid activator
LB	Luria-Bertani medium
LCB	Long chain base
LD-PCR	Long distance PCR
loxP	Locus of recombination in P1
M	Molar
MAPK	Mitogen activated protein kinase
MCC	Membrane compartment of Can1
MCP	Membrane compartment of Pma1
MCT	Membrane compartment of TOR2
MDR	Multidrug resistance
MFS	Major facilitator superfamily
min	Minute
Mkc1	MAP Kinase from <i>C. albicans</i> (Slk2 in <i>S. cerevisiae</i>)
mol	Mol
mRNA	Messenger ribonucleic acid
MRP	Multidrug resistance-associated protein
mTORC	mTOR complex
mV	Millivolt
MW	Molecular weight
neo	Neomycin
Ni-NTA	Nickel-nitriloacetate matrix
No	Number
nt	Nucleotide

N-terminal/N-terminus	Amino-terminal
OD	Optic density
ORF	Open Reading Frame
PA	Phosphatidic acid
PAGE	Polyacrylamide gel electrophoresis
PB1	Phox Bem 1
PBS	Phosphate-buffered saline
PCR	Polymerase chain reaction
PDB	Protein database bank
PDK1	3-phosphoinositide dependent protein kinase-1 (PDK1)
PDR	Pleiotropic drug resistance
PE	Phosphatidylethanolamine
PEG	Polyethylene glycol
PH	Pleckstrin homology
pHM	Phosphorylated Hydrophobic Motif
PHS	Phytosphingosine
Pi	Inorganic phosphate
PI(3,5)P2	Phosphatidylinositol-3,5-bisphosphate
PI(4,5)P2	Phosphatidylinositol-4,5-bisphosphate
PIF-pocket	Docking site for PIFtide and HM
PIFtide	Synthetic PIF including the HM sequence of PRK2
Pins	Phosphatidylinositol
PIP3	Phosphatidylinositol (3,4,5)-triphosphate
PKA	cAMP dependent protein kinase
PKB	Protein kinase B, also called Akt
PKC	Protein kinase C
Pkh1-3	Pkb-activating Kinase Homolog
PKN	PKC-related kinase
PM	Plasma membrane
PMSF	Phenylmethylsulfonylfluorid
PRK	PKC-related kinase
PS compounds	Small chemical compounds synthesized at the Research Group Phosphosites
PSer	Phosphatidyl-serine
PSR	Pseudo substrate region
PTM	Phosphorylated Z/Turn motif
PX	Phox (Phagocyte Oxydase) homology
RNA	Ribonucleic acid
ROS	Reactive oxygen species
RP-HPLC	Reversed-phase high-performance liquid chromatography
rpm	Revolutions per minute
RSK	p90 ribosomal S6 kinase

RT	Room temperature
RT-PCR	Real time - Polymerase chain reaction
<i>S. cerevisiae</i>	<i>Saccharomyces cerevisiae</i>
S6K	p70 ribosomal S6 kinase
SDS	Sodium dodecyl sulfate
sec	Seconds
Sf9	Cell Spodoptera frugiperda-9 cell
SGK	Serum and glucocorticoid induced kinase
ss	Single stranded
STRE	Stress Responsive Element
T308tide	Synthetic peptide derived from the activation loop of PKB
TBE	Tris, Boric acid, EDTA
TBS-T	(TNT) Tris-Buffered Saline-Tween
TE	Tris-EDTA buffer
TM	Z/Turn motif
TOR	Target of rapamycin
Tpk1-3	Takashi's Protein Kinase (PKA)
Tris	Tris (hydroxymethyl) aminomethane
TUNEL	terminal deoxynucleotidyl transferase-mediated dUTP nick end labeling
U	Unit
UCN-01	7-hydroxystaurosporine
UV	Ultraviolet
V	Volt
v/v	Volume to volume
vol	Volume
w/o	Without
w/v	Weight to volume
WT	Wild type
YPD	Yeast Peptone Dextrose
μ	Micro

Amino Acid Code

Amino acid	Three letter code	One letter symbol
Alanine	Ala	A
Arginine	Arg	R
Asparagine	Asn	N
Aspartic acid	Asp	D
Cysteine	Cys	C
Glutamic acid	Glu	E
Glutamine	Gln	Q
Glycine	Gly	G
Histidine	His	H
Isoleucine	Ile	I
Leucine	Leu	L
Lysine	Lys	K
Methionine	Met	M
Phenylalanine	Phe	F
Proline	Pro	P
Serine	Ser	S
Threonine	Thr	T
Tryptophan	Trp	W
Tyrosine	Tyr	Y
Valine	Val	V
any amino acid	Xaa	X

Zusammenfassung

Pilze, einschließlich des am meisten verbreiteten Humanpathogens *Candida* spp., sind als kommensale Untermieter ein häufiger Bestandteil der menschlichen Flora. Pilzinfektionen sind meistens lokale Infektionen, die das Leben des Patienten nicht beeinträchtigen. Pilzkrankungen können jedoch lebensgefährlich sein, wenn sie zu systemischen Infektionen werden. Die Häufigkeit des Auftretens von systemischen Pilzinfektionen ist in den letzten drei Jahrzehnten parallel zur Anzahl an immungeschwächten Menschen gestiegen, wozu es in Folge von Krankheiten (z.B. HIV/AIDS) oder das Immunsystem schwächenden therapeutischen Maßnahmen (z.B. Chemotherapie zur Krebsbehandlung oder nach Organtransplantationen verwendete Immunsuppressiva) gekommen ist. Dies führte zu höherer Nachfrage von neuen Antimykotika zur Bekämpfung neuer durch diese opportunistischen Pilzerreger hervorgerufenen Infektionen. Die meisten der heute verfügbaren Präparate weisen jedoch unzulängliche pharmazeutische Eigenschaften wie ein enges Wirkungsspektrum, Anfälligkeit zum Ausschleusen durch Effluxpumpen oder eine mangelnde Spezifität auf, weshalb sie sich nicht zur klinischen Anwendung beim Menschen eignen. Die Behandlung von Pilzinfektionen und Parasitosen war seit jeher schwierig, denn bei diesen infektiösen Organismen handelt es sich um eukaryotische Zellen, die die meisten Stoffwechselwege und Enzyme mit den menschlichen Zellen teilen. Um Nebenwirkungen zu vermeiden und eine gezielte Therapie zu entwickeln, konzentrierte sich die Forschung üblicherweise auf die wenigen Enzyme und Wege, die im infektiösen Organismus, aber nicht im Menschen vorhanden sind. Bis heute sind die Therapieoptionen zur Behandlung von Pilzkrankungen begrenzt, und es werden vorwiegend Sterol-Biosynthese-Inhibitoren der Klasse der Azole zur Hemmung der Ergosterol-Synthese eingesetzt, einem essentiellen Bestandteil der Zellmembran von Pilzen. Da menschliche Zellen keine Zellwand haben, konzentrierte man sich bei der Entwicklung von wirkungsvollen und sicheren Antimykotika auch auf die für die Synthese der Zellwand erforderlichen Enzyme. Alternativ ist es theoretisch möglich, auf in Pilzen und im Menschen vorhandene Enzyme abzielen, wenn: 1) eine ausreichende Selektivität erreicht werden kann und 2) die Hemmung des Pilzenzyms für den Pilz tödlich ist, aber beim Menschen keine nennenswerten Nebenwirkungen hervorruft. In diesem

Sinne wäre es ideal, die Entwicklung von selektiven Enzyminhibitoren zu evaluieren, die bereits als Wirkstoffziele bekannt sind, wie z.B. Proteinkinasen.

Proteinkinasen spielen im Menschen und im Pilz eine wichtige Rolle bei der Regulierung des Phosphorylierungsstatus von Proteinen in Abhängigkeit von intra- oder extrazellulären Signalen. Der Phosphorylierungsstatus eines Proteins ist das Ergebnis eines koordinierten Zusammenspiels zwischen Kinasen und Phosphatasen. Bei Säugetieren ist die Phosphoinositid-abhängige Proteinkinase-1 (PDK1) in der AGC-Gruppe von Proteinkinasen (benannt nach einigen repräsentativen Mitgliedern dieser Gruppe, der cAMP-abhängigen Proteinkinase (PKA), cGMP-abhängigen Proteinkinase (PKG) und Proteinkinase C (PKC)) eines der zentralen ubiquitären Mitglieder. PDK1 reguliert die Aktivität von bis zu 23 verschiedenen Proteinkinasen der AGC-Gruppe, indem sie den sogenannten „activation loop“ phosphoryliert. In Hefen sind Pkh1 und Pkh2 die orthologen Gene der PDK1 beim Säugetier und phosphorylieren den „activation loop“ von Ypk1/2 (ähnlich SGK und PKB), Pkc1 (ähnlich den Mitgliedern der PKC-Familie), Sch9 (ähnlich der S6-Kinase) und Tpk1, eine der katalytischen Untereinheiten der PKA. Somit hat Pkh durch verschiedene Substrate vermittelte pleiotrope Effekte, insbesondere ist Pkh eine vorgeschaltete Kinase im Zellwand-Integritätsweg, der zur Erhaltung der Zellform erforderlich ist und auf Zellwandbeschädigung reagiert. Aufgrund der Mitwirkung von Pkh1 und 2 im Zellwand-Integritätsweg gelten diese Proteine als potentielle Ziele für die Entwicklung von Antimykotika.

Die große Mehrheit der heute verfügbaren Proteinkinase-Inhibitoren sind mit ATP konkurrierende Verbindungen. Da die ATP-Bindungsstelle in allen Proteinkinasefamilien, einschließlich der von phylogenetisch weit entfernten Organismen, ähnlich ist, fehlt es diesen mit ATP konkurrierenden Präparaten an Selektivität, und sie würden demzufolge wahrscheinlich Nebenwirkungen haben. Alternativ bieten allosterische Proteinkinase-Inhibitoren einen weitaus höheren Grad an Selektivität und können einen Weg für die selektive Inhibition von Proteinkinasen in Pilzen darstellen. Im Laufe der Jahre hat unsere Forschungsgruppe den Regulierungsmechanismus verschiedener Vertreter der großen Gruppe der AGC-Kinasen charakterisiert. Insbesondere hat das Team eine Tasche, die sogenannte PIF-Tasche beschrieben, der eine wichtige Rolle bei der Regulierung vieler Mitglieder dieser Gruppe zukommt. Unserem Team ist es sodann gelungen, kleine Moleküle zu

entwickeln, die durch die Interaktion mit der regulatorischen PIF-Tasche bei Säugetieren die Proteinkinase PDK1 allosterisch aktivieren können. Außerdem haben wir kleine Moleküle entwickelt, die durch die Interaktion mit der PIF-Tasche von atypischen PKCs deren Aktivität allosterisch hemmen können. Da die PIF-Taschen innerhalb der AGC-Familie scheinbar mehr Unterschiede aufweisen als die ATP-Bindestelle, kann die Technologie zur selektiven Inhibition von Pilz- oder Parasitenproteinkinasen in Betracht gezogen werden, ohne dass die menschlichen Gegenstücke beeinträchtigt werden.

Das Hauptziel meiner Arbeit lag in der Anwendung eines chemisch-genomischen Ansatzes zur Untersuchung der Rolle der Proteinkinase Pkh in Hefen und der Evaluierung von Pkh als mögliches Ziel für selektive Antimykotika. Meine Abhandlung besteht aus zwei Hauptteilen: 1- Untersuchung der Folgen der genetischen Depletion von Pkh in der Hefe *Saccharomyces cerevisiae*. Insbesondere beschreibe ich in diesem Teil der Arbeit, dass die Depletion von Pkh die Anreicherung von reaktiven Sauerstoffspezies, DNA-Fragmentierung und programmierten Zelltod fördert. 2- Biochemische, strukturelle und chemisch-biologische Charakterisierung der Pkh von *Candida albicans*. Zunächst habe ich CaPkh2 exprimiert, gereinigt, biochemisch charakterisiert und kristallisiert. Dann habe ich den möglichen physiologischen Regulationsmechanismus von CaPkh2 durch Lipide untersucht. Abschließend habe ich neue selektive kleine Verbindungen beschrieben, die an die PIF-Tasche binden und über menschliches PDK1 selektiv CaPkh2 im Vergleich zu menschliche hemmen.

Vorangehende Arbeiten haben gezeigt, dass Knock-outs von *PKH1* und *PKH2* in *S. cerevisiae*-Genen zu nicht lebensfähigen Zellen führt. Der Großteil der Erkenntnisse über Pkh-Proteinfunktionen wurde mittels Verwendung eines temperaturempfindlichen Allels gewonnen. Im ersten Teil des Projektes stelle ich eine andere Strategie zur Untersuchung dieser Proteine vor, die auf der Verwendung eines Doxycyclin-reprimierbaren Promotors basiert, der keine Inkubation bei hohen Temperaturen erforderlich macht, welche ansonsten Reaktionen auf den Zellwandstress hervorrufen würden, wobei Pkh involviert wäre. Die neue Strategie besteht in der Unterbrechung der *PKH1* und *PKH3* Gene in Verbindung mit der Depletion von Pkh2. Diese Strategie hat die Bedeutung von Pkh im Zellwand-Integritätsweg nachgewiesen. Ich zeige anhand der Microarray-Technologie, dass

Pkh bei der Transkriptionsantwort auf Wärmeschocks eine Rolle spielt, was hauptsächlich auf die Transkriptionsfaktoren Hsf1 und Msn2/Msn4 zurückzuführen ist. Ich bestimme zudem durch Genexpression, Durchflusszytometrie und Konfokalmikroskopie, dass die Depletion von Pkh oxidativen Stress auslöst und DNA-Doppelstrangbrüche induziert, die allgemein mit programmierten Zelltod in Zusammenhang stehen. Diese Phänotypen sind, zumindest teilweise, die Folge eines Defekts bei der Aktivierung des Zellwand-Integritätswegs, da sie teilweise rückgängig gemacht wurden als der Signalweg durch die Expression des *BCK1-20* Allels aktiviert wurde, was für ein im Wesentlichen aktives Bck1 kodiert, die MAP-Kinase-Kinase-Kinase des Zellwand-Integritätswegs. Zusätzlich habe ich festgestellt, dass der oxidative Stress und die DNA-Doppelstrangbrüche, die durch die Pkh-Depletion verursacht worden waren, nicht von der Metacaspase Mca1 abhängen. Zusammengefasst haben unsere Daten aufgezeigt, dass die Depletion von Pkh in Hefezellen zu Zelltod, dem angestrebten Ziel von Antimykotika, führte. Daher heben meine Ergebnisse das Interesse an der Untersuchung des Pkh-Homologs in Krankheitserregern wie *C. albicans* hervor, um dessen PIF-Tasche als potentielles Wirkstoffziel bei der Arzneimittelentwicklung zu verwenden.

Im zweiten Teil des Projektes beschreibe ich die Eigenschaften der Pkh von *C. albicans* mithilfe von biochemisch-kristallographischen und chemisch-biologischen Methoden. Meine Analyse der Daten vom *C. albicans*-Genom haben ergeben, dass dieses zwei ORFs für *PKH* besitzt: orf19.5224, der ein Protein kodiert, das eher Pkh1 und Pkh2 (CaPkh2) ähnelt, und orf19.1196, der ein Protein kodiert, das eher Pkh3 (CaPkh3) ähnelt. Ich habe eine cDNA-Bibliothek von *C. albicans* in deren drei morphologisch definierten Formen (sprossende Hefe, Pseudohyphe und Hyphe) erstellt und mittels der Zwei-Hybrid-Technik mit CaPkh2 interagierende Proteine identifiziert. Überraschenderweise gehörten die gefundenen Treffer nicht zur Kinasefamilie, wie dies von PDK1 erwartet wurde. Um eine mögliche Regulierung von Pkh durch Lipide zu untersuchen, habe ich verschiedene CaPkh2-Konstrukte gereinigt und entdeckt, dass CaPkh2-Proteine über mindestens zwei hochaffine lipidbindende Domänen verfügen, die mit den Strukturlipiden Phosphatidylserin und Phosphatidsäure und mit dem Signallipid Phosphatidylinositoldiphosphat interagieren, die die CaPkh2-Aktivität hemmen. Andererseits zeige ich, dass Dihydrosphingosin CaPkh2 in vitro aktiviert und die durch das Phosphatidylserin produzierte Inhibition aufhebt, was darauf hindeutet, dass die spezifische Aktivität

von CaPkh2, im Gegensatz zu PDK1, aktiv durch die Interaktion mit den Strukturlipiden der Plasmamembran reguliert werden kann. Die Proteinexpression in Sf9 Insektenzellen und eine hochwertige Reinigung mittels FPLC dienten uns zur Aufklärung der Kristallstruktur von CaPkh2 und zur Identifizierung der Unterschiede in der PIF-Tasche zwischen Pkh und dessen menschlichem Ortholog PDK1. Zum ersten Mal wurde ein Kinaseprotein der Candida-Familie kristallisiert, was auch zur zusätzlichen Validierung der PIF-Tasche von mykotischem Pkh als antimykotisches Target beiträgt. Ich beschreibe in biochemischer und struktureller Hinsicht bemerkenswerterweise eine neue allosterische kleine Verbindung, PS77, die spezifisch an die PIF-Tasche bindet und vorzugsweise CaPkh2 gegenüber menschlichem PDK1 inhibiert.

Zusammen ebnet diese Ergebnisse den Weg für die Entwicklung von Arzneimitteln zur Behandlung von Pilzinfektionen basierend auf der Verwendung von selektiven allosterischen Proteinkinase-Inhibitoren, die den Erreger töten und im Gegensatz zu mit ATP konkurrierenden Inhibitoren für den menschlichen Wirt jedoch keine nennenswerten Nebenwirkungen aufweisen.

Summary

Fungal organisms, including the most common human pathogens *Candida* spp., are commensal organisms that are widely present as part of the human flora. Fungal infections are, most frequently, local infections that do not compromise the life of patients. However, mycotic diseases can be life-threatening if they become systemic infections. Systemic fungal infections have risen over the last three decades in parallel to the increased immune-compromised population as a consequence of diseases (e.g. HIV/AIDS) or therapeutic interventions that affect the immune system (e.g. chemotherapy for cancer treatment and immunosuppressors used for patients with organ transplants). This has resulted in the demand of new antifungal drugs that can eradicate the new infections caused by these opportunistic fungal pathogens. However, most of the current compounds have poor pharmaceutical properties such as narrow spectrum of activity, susceptibility to be extruded by efflux pumps or lack of specificity, which make them not suitable for human clinical applications. The treatment of fungal and parasitic infections has been traditionally difficult because the infective organisms are eukaryotic cells that share most of the pathways and enzymes with human cells. To avoid side effects and to develop a targeted therapy, the research has traditionally been centered on the very few enzymes and pathways existing in the infectious organism but absent in humans. Until now, antifungal therapeutic options are limited and are almost dominated by azole class of sterol biosynthesis inhibitors affecting the synthesis of ergosterol, a major constituent of the fungal cell membrane. Because human cells do not have a cell wall, the development of effective and safe antifungal agents has also been directed to enzymes required for the synthesis of the cell wall. Alternatively, it is theoretically possible to target enzymes that are present in fungal organisms and in humans, when: 1) sufficient selectivity can be achieved, and 2) inhibition of the fungal enzyme is lethal to the fungus but does not produce major side effects to humans. In this line, it would be ideal to evaluate the development of selective inhibitors of enzymes which are already known to be drug targets, like protein kinases.

Protein kinases play an important role in humans and fungal organisms by regulating the state of phosphorylation of proteins in response to intra or extracellular signals. The phosphorylation state of a protein is the result of coordinated action of kinases

and phosphatases. In mammals, the Phosphoinositide-dependent kinase 1 (PDK1) is one of the key members of the ubiquitously present in the AGC group of protein kinases, named after some representative members from this group, cAMP-dependent protein kinases (PKA), cGMP-dependent protein kinases (PKG), and protein kinase C (PKC). PDK1 regulates the activity of up to 23 different protein kinases from the AGC group by phosphorylating their activation loop. In yeast, Pkh1 and Pkh2 are the orthologs of the mammalian PDK1 and phosphorylate the activation loop of Ypk1/2 (similar to SGK and PKB), Pkc1 (similar to the PKC family members), Sch9 (similar to the S6 kinase) and Tpk1, one of the catalytic subunits of PKA. Thus, Pkh has pleiotropic effects mediated by different substrates, most notably Pkh is an upstream kinase in the Cell Wall Integrity pathway that is required to maintain cell shape and provides a response to the cell wall damage. Due to the involvement of Pkh1 and 2 in the Cell Wall Integrity pathway these proteins are considered potential targets for the development of antifungals.

The vast majority of current protein kinase inhibitors are compounds that compete with ATP. Since the ATP-binding site is similar in all families of protein kinases including those from phylogenetically distant organisms, those ATP-competitor compounds lack selectivity and, consequently, would be likely to produce side effects. As an alternative, allosteric protein kinase inhibitors provide much higher degree of selectivity and may provide a path for fungal-selective inhibition of protein kinases. Over the years, our research group has characterized the mechanism of regulation of several representatives from the large group AGC kinases. In particular, team characterized a pocket, termed PIF-pocket, that plays an important role in the regulation of many members of this group. Our team then succeeded in the development of small molecules, which, by interacting with the PIF-pocket regulatory site, can allosterically activate the mammalian protein kinase PDK1. In addition, we have developed small molecules that, interacting with the PIF-pocket of atypical PKCs, can allosterically inhibit their activity. Since the PIF-pocket appears more diverse than the ATP-binding site within the AGC family, the technology can be envisaged to be employed for selectively targeting fungal or parasitic protein kinases without affecting the human counterparts.

The main objective of my thesis was to employ a chemical-genomic approach to investigate the role of the protein kinase Pkh in yeasts and to evaluate Pkh as a

possible target for selective antifungal agents. In particular, the thesis consists of two parts: 1- Investigation of the effects of genetic depletion of Pkh in the yeast *Saccharomyces cerevisiae*. As a highlight of this part of the thesis I describe that the depletion of Pkh promotes the accumulation of reactive oxygen species, DNA fragmentation and programmed cell death. 2- Biochemical, structural and chemical biology characterization of the Pkh from *Candida albicans*. I first expressed, purified, biochemically characterized and crystalized CaPkh2. I then investigated the possible physiological mechanism of regulation of CaPkh2 by lipids. Finally, I described novel selective small compounds that, binding to the PIF-pocket, selectively inhibit CaPkh2 over human PDK1.

Previous work had shown that the deletion of the *PKH1* and *PKH2* in *S. cerevisiae* genes results in non-viable cells, and the majority of knowledge on Pkh protein functions have been obtained using a temperature-sensitive allele. In the first part of this project, I present a different strategy for the study of these proteins based on the use of a doxycycline-repressible promoter that does not require incubation at high temperatures that trigger the response to the cell wall stress, in which Pkh protein has been involved. The new strategy consists in the disruption of the *PKH1* and *PKH3* genes, in combination with the depletion of Pkh2. This strategy has established the importance of Pkh in the cell wall integrity pathway. I reveal by microarray technology that Pkh plays a role in the transcriptional response to heat shock that is mainly driven by the transcription factors Hsf1 and Msn2/Msn4. I also determine by gene expression, Flow cytometry and confocal microscope that depletion of Pkh induces oxidative stress and DNA double-strand breaks, which are commonly associated with programmed cell death. These phenotypes are, at least in part, consequence of a defect in the activation of the Cell Wall Integrity pathway because they were partially suppressed when the pathway was activated by expressing the *BCK1-20* allele, which encodes for a constitutively active Bck1, the MAP kinase kinase kinase of the Cell Wall Integrity pathway. In addition, I determined that the oxidative stress and DNA double-strand breaks caused by Pkh depletion are independent of the metacaspase Mca1. Together, our data indicated that the depletion of Pkh in yeast cells resulted in cell death, the ultimate goal of antifungal agents. Therefore, my results highlighted the interest in the investigation of the

homolog of Pkh in pathogen organisms such as *C. albicans* to employ its PIF-pocket as a potential target site for drug development.

In the second part of the project, I describe the properties of Pkh of *C. albicans* using biochemical crystallographic and chemical biology tools. My analysis of the data from the *C. albicans* genome revealed that it possesses two *PKH* related ORFs: orf19.5224, encoding a protein more similar to Pkh1 and Pkh2 (CaPkh2) and orf19.1196, which encodes a protein more similar to Pkh3 (CaPkh3). I generated cDNA library of *C. albicans* in its three morphological defined forms (Budding yeast, pseudohyphae and hyphae) and by Two-Hybrid technology I identified interacting proteins with CaPkh2. Surprisingly, the hits found did not belong to the kinase family as it was expected from PDK1. To investigate a possible regulation of Pkh by lipids, I purified different constructs of CaPkh2 and I identified that CaPkh2 proteins have at least two high affinity lipid binding domains that interact with the structural lipids phosphatidylserine and phosphatidic acid and with signaling lipid phosphatidyl inositol bisphosphate, which inhibit CaPkh2 activity. On the other hand, I show that the dihydrosphingosine is an activator of CaPkh2 in vitro and releases the inhibition produced by phosphatidylserine, suggesting that the specific activity of CaPkh2, in contrast with PDK1, may be actively regulated by the interaction with the plasma membrane structural lipids. Protein expression in Sf-9 insect cells and high quality purification using FPLC served us to determine the crystal structure of CaPkh2 and to identify differences in the PIF-pocket, between Pkh and its human ortholog PDK1. It is the first time that a kinase protein from *Candida* family was crystallized which also contributes to the further validation of the PIF-pocket of fungal Pkh as an antifungal target. Remarkably, I describe biochemically and structurally a novel allosteric small compound, PS77, which specifically binds to the PIF-pocket and preferentially, inhibits CaPkh2 over human PDK1.

Together, these results clear the path for drug development of antifungal agents based on the use of selective allosteric protein kinase inhibitors that will kill the pathogen and do not have major side effects in the human host in contrast to ATP-competitive inhibitors.

Chapter I: Introduction

1. Introduction

1.1 Protein kinases

Protein phosphorylation has evolved along unicellular organisms and maintained in pluricellular organisms to regulate cellular and organism-wide functions, by reversibly modifying proteins to allow intracellular signaling. It is estimated that around 30% of all proteins in a single cell are phosphorylated. The importance of protein kinases in eukaryotic organisms is reflected by the abundance of genes coding for protein kinases: e.g., they represent 1.7% of the human genome, 4% of the plant *Arabidopsis thaliana*, 2% in the budding yeast *Saccharomyces cerevisiae*, and 1.6% of the protozoan parasite *Plasmodium falciparum*. With such number of protein kinases and the extraordinarily large number of cellular proteins that require to be phosphorylated, the signal transduction evolved in sophisticated mechanisms for the regulation of multiple cellular functions and responses.

1.2 AGC protein kinases in eukaryotic organisms

The AGC protein kinase group was named after 3 representative structurally related protein kinases, the cAMP dependent protein kinase (PKA), the cGMP dependent protein kinase (PKG) and the protein kinase C (PKC). AGC kinases corresponds to one of the most evolutionary conserved groups, represented widely within eukaryotes, in all vertebrates, invertebrates, fungi, plants, unicellular algae and protozoa. Prokaryotic protein kinases, on the other hand, include a large number of eukaryotic-like protein kinases that are distantly related and do not contain members of eukaryotic protein kinase groups. According to their evolutionary relationships in their catalytic domains, human protein AGC kinases comprise 12% of the kinome (Manning et al, 2002). Similarly, they represent 15% and 20% of the kinomes of yeast-like and filamentous fungi, respectively, 4% of plants, 6-8% of trypanosome, leishmania and amoeba and 6% of giardia kinomes. In humans, there are 63 genes coding for AGC kinases, distributed in 14 families (Table 1.1). The group also includes 6 pseudogenes; those are predicted to express protein kinases that lack essential features for activity. In more distant eukaryotic organisms, the number of families within the AGC group varies, with PKA/PKG, PDK1, RSK, MAST and NDRs family members widely present throughout eukaryotic kingdoms. The yeast AGC

kinase group is formed by 17 members sharing a high degree of similarity with mammalian AGC kinases (Table 1.1). The human AGC kinase group is well studied and is involved in many fundamental cellular signaling functions like glucose and lipid metabolism, cell growth, apoptosis, transcription, membrane structure modulation, protein synthesis, cell proliferation, etc. Therefore, multiple signaling pathways are regulated and an alteration in the protein phosphorylation balance leads, in some cases, to serious pathologies like cancer, diabetes, stroke and Alzheimer's disease (Arencibia, Pastor-Flores et al. 2013).

Table 1.1 AGC kinase families in eukaryote organisms

Domain Kingdom	Eukaryota				
	Animalia	Fungi	Plantae	Protist	Chromista
Representative organism	<i>H. sapiens</i>	<i>S. cerevisiae</i>	<i>A. thaliana</i>	<i>P. falciparum</i> <i>D. discoideum</i>	<i>P. infestans</i>
AGC kinases				<i>T. gondii</i>	
PDK1	●	●	●	●	●
AKT/PKB	●	●			●
SGK	●	●		●	●
RSK	●	●	●	●	●
PKA	●	●	●	●	
PKG	●		●	●	●
PKC	●	●		●	
PKN /PRK	●				
NDR	●	●	●	●	●
MAST	●	●	●	●	●
YANK	●	●		●	●
DMPK	●	●		●	
GRK	●				●
SGK494	●				
Aurora ^a	●	●		●	●
Phototropin ^b		●	●	●	

AGC kinase families in Fungi represented by the kinomes of *Saccharomyces cerevisiae*, in Plantae by that of *Arabidopsis thaliana*, in Protists that of *Plasmodium falsiparum*, in *Dictyostelium discoideum*, *Toxoplasma gondii* and Chromista represented by that of *Phytophthora infestans*, in comparison to the human kinome (Animalia), complemented by the AGC-related Aurora kinase (a) and Phototropin (b). AGC kinases are not found in the remaining kingdom, Prokaryotes. MAST, YANK and Phototropin were identified by the Conserved Domains and Protein Classification resource from the National Center for Biotechnology Information (NCBI) (Arencibia, Pastor-Flores et al. 2013).

The general structure of the AGC kinases consists of a typical kinase catalytic domain, shared in all the protein kinase families, which is composed of a small lobe and a large lobe with the ATP-binding lying in between the two lobes (Figure 1.1). The small lobe is formed by anti-parallel β -strands, a α B-helix and a α C-helix. The large lobe is formed exclusively by α -helices and participates in the substrate binding

and catalysis. Many AGC kinases have at least two regulatory Ser/Thr phosphorylation sites (three for some of them) that confer distinctive and unique features for this kinase family. These sites are the activation loop, the hydrophobic motif (HM) and, in some cases, a third one called Zipper/Turn motif (TM) phosphorylation site. A fully activated kinase needs to be phosphorylated in both HM and activation loop (and TM in some cases) (Hauge, Antal et al. 2007).

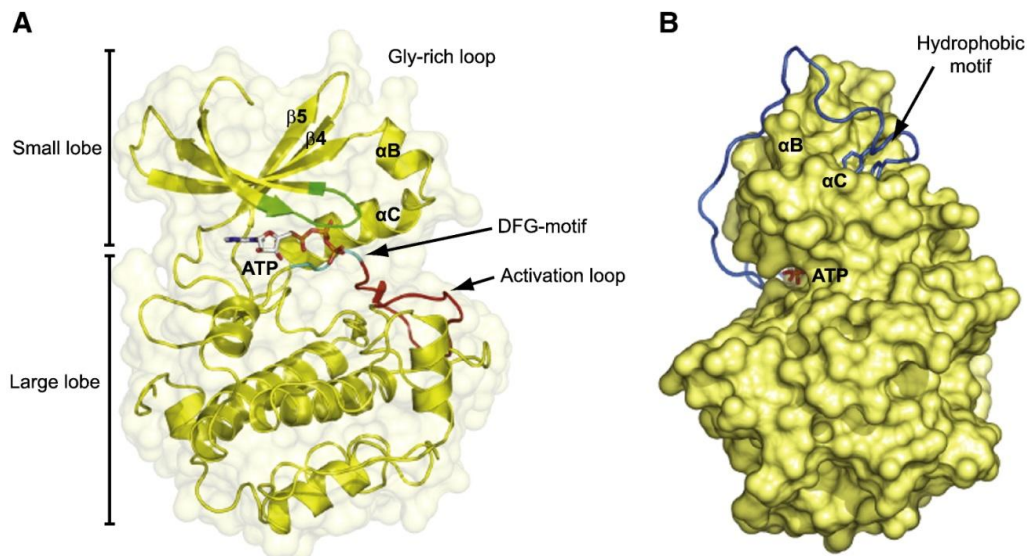


Figure 1.1 Catalytic domain of PKA A) Ribbon representation of the catalytic domain of PKA. The structure shows the small lobe, large lobe, ATP binding site, activation loop, DFG motif. B) Solid surface representation of the catalytic domain of PKA (yellow) and the C-terminal extension with the partial Phe-Xaa-Xaa-Phe hydrophobic motive (HM) at the end (blue). The C-terminal extension folds back onto the catalytic domain and ends in the partial HM. A homologous C-terminal extension is present in most AGC kinases but absent in PDK1.

To date, apart from the crystal structure of the catalytic and regulatory subunits of PKA, Tpk1 and Bcy1, from *S. cerevisiae* (Mashhoon, Carmel et al. 2001; Rinaldi, Wu et al. 2010), all the solved crystal structures of AGC kinases belong to the Animalia Kingdom and especially to the Mammalian Class. Thus, a structural approach is still missing to understand better the differences in the molecular mechanism of regulation of AGC kinases in the rest of eukaryotes.

1.2.1 The PDK1 master kinase in mammalian cells

The Phosphoinositide-dependent kinase 1 (PDK1) is the AGC master kinase that activates, by phosphorylating the activation loop, at least 23 other AGC kinases including PKB/Akt, PKC kinase family, SGK, S6K and also non AGC kinases such PLK1 (Tan, Li et al. 2013). Regarding the rest of AGC kinases, PDK1 is composed by

a catalytic and a pleckstrin homology (PH) domains. The catalytic domain comprises approximately the first 350-400 aa's and is formed by an N-region small lobe and a C-region large lobe. The PH domain of around 95 aminoacids is present at the end C-terminal segment (Fig 1.2A). The PH domain of PDK1 binds to phosphatidylinositol 3,4,5-triphosphate (PIP₃), a phospholipid found in the membrane that acts as an anchor to co-localize PDK1 close to its substrate PKB/Akt which contains a PH domain (Fig. 1.2B). In this manner, PDK1 phosphorylates the activation loop of PKB/Akt in the presence of PIP₃. A different mechanism is required for the rest of PDK1 substrates, where a docking interaction between the protein substrate and PDK1 is necessary. PDK1 mediates the phosphorylation in the activation loop inducing changes in the structure of the catalytic domain site that in turn, allows the substrate phosphorylation. The activation loop is one of the most dynamic regions of the kinase core and is common to all PDK1 substrates, with the consensus sequence **Thr**-Phe-Cys-Gly-Thr-Xaa-Glu-Tyr, where Thr residue in bold represents the phosphorylated residue and Xaa any amino acid. The activation loop of all AGC kinases emerges from the DFG-motif in between the α -C helix in the small and large lobe and a Gly-rich loop that forms the upper part of the ATP-binding site (Figure 1.1A). The next phosphorylation site is the HM. The HM is a conserved motif located in the C-terminal extension of the catalytic domain with a consensus sequence Phe-Xaa-Xaa-Phe-**Ser/Thr**-Tyr/Phe, where Xaa is any aminoacid and **Ser/Thr** is the phosphorylation site. There are a few exceptions where the HM is not conserved in AGC kinases: PKA does not have a phosphorylation site and instead only possesses the Phe-Xaa-Xaa-Phe motif in the end of the C-terminal (Fig. 1.1B). Another exception is found in the Atypical PKC isoforms and PRK that have an acidic residue (phosphomimetic) instead of the Ser/Thr phosphorylation site. To end, PDK1 does not possess HM; interestingly, it was found by the yeast Two-hybrid system that PDK1 interacts with a fragment of 77 aminoacids containing the HM of PRK2 with the phosphomimetic Asp residue that replaces the canonical Ser/Thr residue (Balendran, Casamayor et al. 1999). A smaller polipeptide fragment comprising the PRK2-HM, termed PDK1-Interacting Fragment-peptide (PIFtide), binds to a hydrophobic pocket in PDK1 that was termed PIF-binding pocket (Biondi, Cheung et al. 2000). Further studies with crystal structures demonstrated a phosphate binding site where PDK1 substrates accommodate the phosphorylated residue of the HM (Biondi, Komander et al. 2002; Frodin, Antal et al. 2002).

The solved crystal structures of PDK1 comprise the conserved catalytic domain. Many efforts were done in the crystallization of the full length protein but to date have always failed. The same problem has been found in the rest of AGC kinases with the exception of the short forms of some proteins such as PKA, PKC β or some NDRs whose N-terminal and C-terminal region are shorter than the rest (Wu, Voegtli et al. 2010). The crystal structure of the catalytic domain has been used for many years in drug development for the rational design of selective drugs.

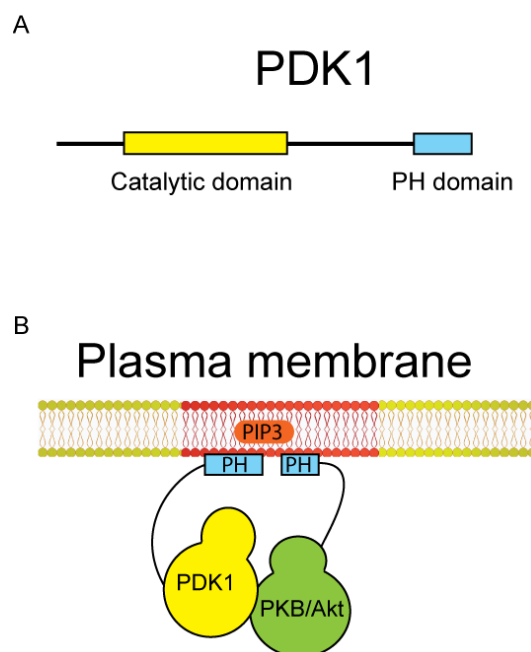


Figure 1.2 Schematic representation of PDK1 and its interaction mechanism with PKB/Akt. A) PDK1 is composed by a catalytic domain (CD) region and a pleckstrin homology domain (PH) at the C-terminal domain. B) Model in which the PH domain of both PDK1 and PKB/Akt is used to colocalize the kinases at the plasma membrane in the presence of PIP₃.

1.2.2 PDK1 substrates

1.2.2.1 PKB/Akt

The mammalian PKB/Akt kinase has three isoforms, PKB α /Akt1, PKB β /Akt2 and PKB γ /Akt3. The structure of the three of them share a N-terminal region with a PH domain, a common Ser/Thr catalytic domain which contains an activation loop that is phosphorylated by PDK1 and a C-terminal domain with a regulatory HM phosphorylated by mTORC2. The regulation mechanism of PKB/Akt by PDK1 differs to the rest by requiring the PH domain for the recruitment and colocalization of the protein to the PH (Figure 1.2B) (explained in Item 1.2.1). PKB/Akt has evolved to become phosphorylated by PDK1 in the presence of the second messenger PIP₃. In the crystal structure of the full length solved with an allosteric inhibitor, it is possible to

observe the PH domain blocking the side of the kinase core that contains the activation loop stabilizing the PIF-pocket in an inactive conformation. This explains why the PH domain must bind PIP₃ enabling the access of PDK1 to its phosphorylation site at the activation loop (Wu, Voegtli et al. 2010).

PKB/Akt is involved in numerous cellular processes downstream of PI3-kinase, and its deregulation leads to cancer, diabetes, cardiovascular and neurological diseases. (Arencibia, Pastor-Flores et al. 2013).

1.2.2.2 PKA

PKA is a holoenzyme formed by two regulatory subunits and two catalytic subunits. The catalytic subunit contains a typical catalytic domain and a truncated hydrophobic motif Phe-Xaa-Xaa-Phe at the end of the C-terminus that lacks a Ser/Thr phosphate binding site (Figure 1.1). Upon cAMP binding, the holoenzyme dissociates into a dimer of the regulatory subunit bound to cAMP and two free monomeric catalytic subunits. However, based in experimental evidences it is not yet clear if PKA is a direct substrate of PDK1 (Balendran, Hare et al. 2000) (Kornev, Haste et al. 2006).

The catalytic subunit of PKA was the first crystal solved structure on an AGC protein kinase (Knighton, Xuong et al. 1991; Knighton, Zheng et al. 1991). In the crystal structure, the HM binds the PIF-pocket, hydrophobic pocket situated on the small lobe of the catalytic core, between helix α -B, α -C and the β -4 and β -5 sheets (Figure 1.1B). PKA plays a major physiological role in glucose homeostasis and triglyceride storage. It is also involved in other fundamental processes like aging, tumorigenesis, cell migration, epithelial-mesenchymal transition and inflammation (Arencibia, Pastor-Flores et al. 2013).

1.2.2.3 PKC

The PKC family is divided into three different subfamilies based on the regulation by second messengers: The classical (α , β , γ), the novel (δ , ϵ , η , θ) and the atypical (ζ , λ) (see Item 1.5.2.4, Figure 1.4). Basically, the PKC family is formed by a long N-terminal domain followed by a catalytic domain and a short C-terminal extension. The catalytic domain and the C-terminal extension are common to all PKC kinases, while they differ in the long N-terminal domain. The classical PKCs include in the N-terminal domain, two C1 domains, a C2 domain and a Pseudosubstrate (PSR). They

can bind to diacylglycerol (DAG), lipids and Ca^{2+} . The novel PKC family has the same motifs, but it does not bind to Ca^{2+} . On the other side, the atypical family does not have a C2 domain but it has a PB1 and a single C1. However, the C1 domain is not able to bind neither DAG, nor Ca^{2+} .

PDK1 phosphorylates the activation loop of PKCs when the protein is newly synthesized. The phosphorylation in the turn motif is necessary in order to fully activate the kinase. Besides, the phosphorylation of the HM depends in specific PKC forms on mTORC2 (Ikenoue, Inoki et al. 2008). Although the phosphorylation in the activation loop, turn motif and HM are strictly necessary for the activation of the kinase, the regulation of PKC activity depends on the binding of the N-terminal domain to second messengers. The PKC proteins have different biological roles in mammalian cells. It was shown that aPKCs such PKC ζ has a high expression in different cancer cell types. Novel PKCs like PKC θ is involved in T cell activation and, therefore, is a potential target for allergic and autoimmune diseases (Arencibia, Pastor-Flores et al. 2013).

1.2.2.4 PKN

PKC-related serine/threonine-protein kinase (PKN) family is formed by 3 isoforms (PKN1-3) that share high similarity in the catalytic domain but differs in the N-terminal. PKN are composed in the N-terminal region by a PSR domain that as in PKC family is a PSR/autoinhibitory region, three Hr1 domains that bind to GTP a C2-like domain and a link. The C-terminal is composed by a HM motif and Zipp/Turn motif that regulates the intrinsic activity of PRK2 and its interaction with PDK1 (Dettori, Sonzogni et al. 2009). The kinase is activated by Rho proteins that bind to the Hr1 domain. Recent studies have shown that PRK2 is not inhibited intramolecularly in vitro but is forming oligomers, responsible for the inhibition (Bauer, Sonzogni et al. 2012).

1.2.2.5 SGK

There are three isoforms of the Serum Glucocorticoid regulated protein Kinases in mammalian cells: SGK1, SGK2 and SGK3. SGK is a homodimer disulfide-linked with the catalytic domain typical from AGC kinases (Zhao, Lehr et al. 2007). SGK family displays 54% sequence similarity with PKB/Akt. In contrast with PKB/Akt, SGK family does not contain a PH domain and therefore, phosphatidylinositols (Pins) are not

essential for the kinase activation. However, SGK3 has a PhoX domain (PX) that can bind to PIns. For the protein activation is essential the phosphorylation in the activation loop and HM by PDK1 and TORC2, respectively (Biondi, Kieloch et al. 2001; Hong, Larrea et al. 2008). SGK family regulates the epithelial sodium channel where it is localized to the cytoplasmic surface of the cell membrane. It also up regulates transcription factors and is involved in cell growth, migration survival, apoptosis and tumor growth (Arencibia, Pastor-Flores et al. 2013).

1.2.2.6 S6K

The Ribosomal protein S6 kinase family has two isoforms, S6K1 and S6K2 which the same domain regions. At the C-terminus, S6K family contains an autoinhibitory domain whose phosphorylation appears to release the domain and facilitate the phosphorylation of the activation loop by PDK1, necessary for the full activation of the kinase. S6K acts downstream of TOR and the phosphorylation by TOR is also required for a fully active kinase. S6K is involved in several biological processes such as cell growth, proliferation and differentiation by regulating ribosome biogenesis, protein synthesis, cell cycle progression and metabolism (Arencibia, Pastor-Flores et al. 2013).

1.2.3 Mechanism of regulation by PDK1, the PIF-pocket

PDK1 substrates, e.g., PKCs, RSKs, S6Ks, SGKs, and PKN/PRKs, are thought to require the docking interaction between their HM and the PIF-pocket of PDK1 (Figure 1.3). In substrates such as classical PKCs are unstable in the absence of a phosphorylated activation loop, suggesting that these substrates dock to the PIF-binding pocket of PDK1 as soon as they are synthesized and are constitutively phosphorylated. The mechanism by which PDK1 phosphorylates its substrates is different from the standard mechanism in which the phosphorylation of substrates is determined by the activation of the upstream kinase, as in MAPK signaling. Although all the substrates need to be phosphorylated on the activation loop by PDK1 to be active, none of these required Pins. As mentioned before, one of the characteristic features of PDK1 is that, in contrast with other AGC kinases, PDK1 does not possess HM in the c-terminal extension. The non existence of HM in PDK1 exposed the PIF-binding pocket for the activation mechanism of PDK1 substrates (Arencibia, Pastor-Flores et al. 2013).

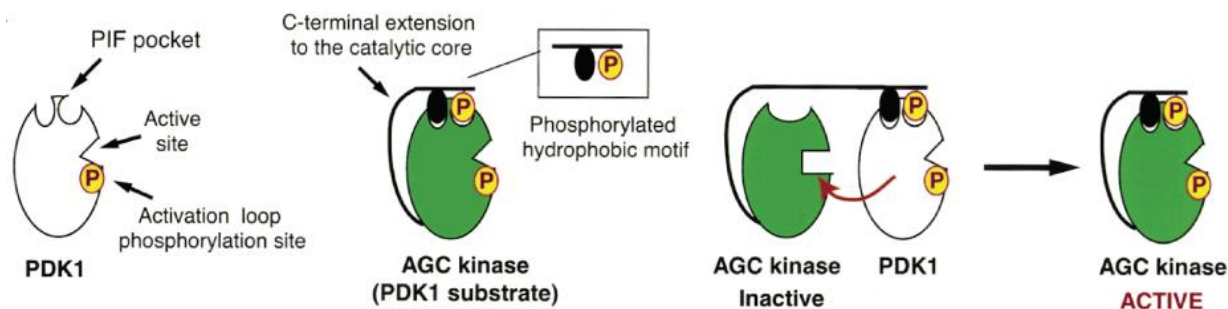


Figure 1.3 General regulation mechanism of AGC kinases. Regulation mechanism of interaction between PDK1 and its substrates. The binding of the substrate to the PIF-pocket regulatory site activates PDK1. Upon phosphorylation, the substrate acquires an active conformation. Adapted from (Biondi & Nebreda, 2003).

1.3 Opportunistic pathogens

Over the recent years new pharmacological treatments of diseases such as diabetes, HIV or some cancer tumors with a short life expectancy have increased the life expectancy, becoming chronic diseases where the patient can have an almost normal lifestyle. In many cases, a prolonged daily treatment with oral drugs compromise the immune system, changing the composition of non-specific defense system (intestinal flora, peristalsis, intestinal enzymes, etc...), which leads to the exposition of the host to opportunistic infections. These infections can be nosocomial or produced by a commensal organism that are normal resident in the flora and become pathogenic when the host defenses are altered. In many cases, it occurs in the same hospital where the patient is treated. The common opportunistic pathogens are bacterial (causing pneumonia, bartonellosis, syphilis...), parasitic (Malaria, Cryptosporidiosis...), virus (Hepatitis B and C, herpes Simplex, papillomavirus...) or fungal infections (Candidiasis, Aspergillosis, Cryptococcosis..).

1.3.1 Common opportunistic fungal infections

Fungal or mycotic infections affect a large population of patients with primary diseases and some of them are hard to diagnose, which contributes to their attributable mortality. Furthermore, in most immunocompetent patients, systemic mycoses typically have a chronic course, instead of being life-threatening (Roosen, Frans et al. 2000). From an estimated 1.5 million fungal known species, about 200 have been associated with human microflora (Cannon, Lamping et al. 2009). Those which are pathogenic have been classified in three categories: superficial cutaneous, subcutaneous and systemic mycoses. However, the classification has become

confusing since some agents that act as cutaneous opportunistic organism in immunocompromised patients can affect the subcutaneous tissue and could also promote systemic diseases by dissemination. Therefore, the border between the groups can be modified (Arenas, Moreno-Coutino et al. 2012).

1.3.1.1 Candidiasis

Candida yeasts cells are detectable in 96% of the neonate in the first month of life. From the third to the fifth year, the constitutional development process is complete, and each individual has a microflora compatible with his/her immunsystem. In healthy adults, fungi are detectable in about 70% of all gastrointestinal sections. Many of these are members of *Candida* genus (Kumamoto and Vines 2005).

Candidiasis is the most common fungal pathogen infection in immunocompromised patients. Oral fungal infections occur mainly during (39%) and after (33%) cancer treatment (Lalla, Latortue et al. 2010). Radiotherapy and Chemotherapy increase the risk of prevalence in the oral colonization up to 72%. In HIV, up to 90% of untreated advanced cases develop oral candidiasis. The esophageal candidiasis affects from 10% to 20% of HIV cases becoming the most common cause of esophageal disease among these patients. Vaginal candidiasis affects from 27% to 60% of women in child bearing age, and these rates are similar for HIV-infected and non-infected patients. Although 200 species of *Candida* are classified, only few of them such as *C. albicans*, *C. parapsilosis*, *C. glabrata*, *C. tropicalis*, *C. krusei* and *C. dubliniensis* are medically relevant. The prevalence of colonization by *Candida* species varies depending upon the strain. *C. albicans* is the most common *Candida* species. In a recent study followed for 7 years by ARTEMIS antifungal surveillance program, over 200.000 isolates from blood samples were obtained. It was shown that 64% of the isolates correspond to *C. albicans* strain followed for *C. glabrata* with 11,6%, *C. tropicalis*, 7,7%, *C. parapsilosis* 6,3%, *C. krusei*, 2,5% (Pfaller, Diekema et al. 2010). In the United States, 11.5 % of around 80.000 blood infections reported per year are caused by *Candida*, 30% of them leading to death (Chauhan, Latge et al. 2006). In addition, *C. albicans* is the yeast most frequently isolated from clinical material.

Candidiasis can appear as superficial or cutaneous mycosis affecting the outer layer of the skin, in most cases, coming from endogenous *Candida* blastospores. The cells selectively can also colonize oral, gastrointestinal and vaginal epithelium (Raz-

Pasteur, Ullmann et al. 2011). *Candida* can as well appear as subcutaneous mycoses where the skin and the subcutaneous tissue are affected. The inoculation usually is caused by traumatic implantation and this infection has a subacute or chronic evolution. In the worst of the cases, the infection becomes systemic which is caused either by outer infection or colonization.

1.3.1.1.1 The different morphogenic states of *C. albicans*

C. albicans, as *Saccharomyces cerevisiae*, is an Ascomycota fungi that belongs to the family of Saccharomycetaceae. *Candida* cells have the ability to grow in distinct morphological forms, from “true budding yeast” to “pseudohyphae” and “hyphae” forms. Those states are closely linked to the virulence of the cell and can vary depending on the environmental changes to which cells are exposed. Besides, other morphological forms such as the “opaque” form mating-component cells and the “chlamyospore” forms also naturally occurs under suboptimal growth conditions (Whiteway and Bachewich 2007).

The budding yeast form is also termed as “white form” and shares the cell shape similarity with *S. cerevisiae*. *C. albicans* grows as budding yeast in rich media as Yeast Peptone Dextrose (YPD) at a temperature below 30°C or pH 4.0. The division occurs by budding and forming a constriction at the neck of the mother cell which usually occurs next to the bud scar from a previous division or at the opposite side of the cell from the previous bud formed (Herrero, Lopez et al. 1999).

The pseudohyphae form is induced in environmental situations such as high phosphate concentrations, Nitrogen-limited growth on solid medium (SLAD) or a rise in temperature to 35°C with pH 6.0. In pseudohyphae cells, the division occurs similarly as in the blastopore with a constriction at the neck of the mother cell but also at every subsequent septal junction.

The hyphae form is the common infective form because cells in this morphogenetic state are better colonizers of the skin. They can also mate (Soll 2004). It is not then difficult to imagine that an environment close to the mammalian blood conditions, such as serum and a temperature of 37°C promotes the formation and division of hyphal cells. Indeed, in clinical diagnoses, the basis of the analysis used to distinguish *C. albicans* from other *Candida* species is the germ tube formation in response to serum. On the other side, synthetic poor mediums such as Lee’s

medium, 199 medium or N-acetylglucosamine pH 7.0 and 37°C, and cell density below 10^6 cells ml^{-1} also induce morphological changes into hyphae form (Sudbery, Gow et al. 2004). The hyphae developed from unbudded yeast do not have a constriction at the neck of the mother cell and have parallel sides along their entire length. This morphologic form is also found in mycelia ascomycetes that possesses an apical body and septa with simple pores (Sudbery, Gow et al. 2004). One hypothesis raised for the infectiveness of *C. albicans* when developing the hyphae form, is that it can penetrate easily into the tissue by tip extension generating significant pressure. Except few cases where the symptoms are caused by the host immune response (mould allergies and cutaneous dermatophyte infections), serious systemic mycoses involving deep tissues requires fungal dissemination and invasion throughout the body (Gow, Brown et al. 2002). This mechanic explanation for the linked virulence of the hyphae form goes along with morphogenic-related changes in the protein composition of the cell wall that allow the cell shape changes, as well as with the expression of a group of proteins covalently linked into the cell wall that promotes the adhesion to the host cells (Grubb, Murdoch et al. 2008; Wachtler, Wilson et al. 2011).

The cell wall proteome can be modulated depending on different external or internal factors. In addition to morphology, *C. albicans* can establish molecular networks within cells that function as quorum sensing. For example, *C. albicans* inoculated in a poor medium with a cell density below 10^6 ml^{-1} promotes the shift to hyphae form (Odds 1985). However, if the density is greater than 10^6 ml^{-1} , little germination will occur and cells will maintain the yeast morphology. Another example of quorum sensing is when *C. albicans* is in close contact with other microorganisms such as *Escherichia coli* and *Pseudomonas aeruginosa* in the infection process; bacterial-fungal and fungal-fungal interactions are established to contribute to pathogenicity in a density manner throughout the regulation of essential virulence factors.

The infection-associated conditions that promote shift to hyphae form include stress conditions such as iron starvation, hypoxia, oxidative and nitrosative stress as part of the defense of the innate immune system. In addition, a low pH environment as found in vagina, phagocytes or phagolysosomes, promotes the hyphae form (Piekarska, Mol et al. 2006). Therefore, significant efforts were applied to elucidate the molecular

networks and mechanism that promote the shift from budding yeast to the infective hyphae form.

1.3.1.1.2 Signaling pathways and transcriptional regulators

The molecular networks and the cross-talk between the pathways behind the morphological switch of *C. albicans* have become in the last decade a front sight for the scientific community. Four different research areas have been focused in the understanding of the molecular networks. Those are the Ras1 Interrelated Networks, the carbon dioxide sensing, the Quorum sensing and the pH regulation. This classification could be explained by the first-signal-sensors that carry out a morphological transformation. However, a global view communicates the molecular networks between them. The Ras1 Interrelated Networks are of special interest for the elaboration of this project.

1.3.1.1.2.1 The Ras1 Interrelated Networks

The two main pathways studied in detail that belong to the Ras1 interrelated networks are the mitogen-activated protein kinase pathway (MAPK) and the cAMP-dependent protein kinase A pathway (PKA).

1.3.1.1.2.1.1 The MAPK signaling pathways

The MAPK proteins comprise a group of protein Ser/Thr kinases, conserved in many eukaryotes. A variety of extracellular stimuli result in the signal transduction to the MAPK kinase kinase kinase (MAPKKK) that activates a MAPKK and subsequently act upon a MAPK kinase, end in the activation of a transcription factor. The Cek1, Hog1 and Mkc1 MAPK pathways are the best characterized of the five known pathways in *C. albicans* (Figure 1.4).

1.3.1.1.2.1.2 Cek1 pathway

Cek1 pathway (Kss1 in *S. cerevisiae*) was the first studied in *C. albicans* (Csank, Schroppe et al. 1998). The activation of Cst20/Ste20 (MAPKKKK) by the GTPase Ras1 activates the Cst20 and this the Ste11-Hst7(Ste7)-Cek1 module of MAPK (Monge, Roman et al. 2006) that finish with the activation of Cph1 transcription factor involved in the cell wall construction, morphogenesis and invasive growth (Figure 1.4). The double mutants of all the components of the cascade fail to produce hyphae upon induction on solid media, except in the presence of serum, suggesting

that this pathway is essential for filamentation. Cek1 is also negatively regulated by the kinase Hog1 and the phosphatase Cpp1. Both *cpp1* and *hog1* single mutants result in a hyper-filamentous morphology cell (Alonso-Monge, Navarro-Garcia et al. 1999).

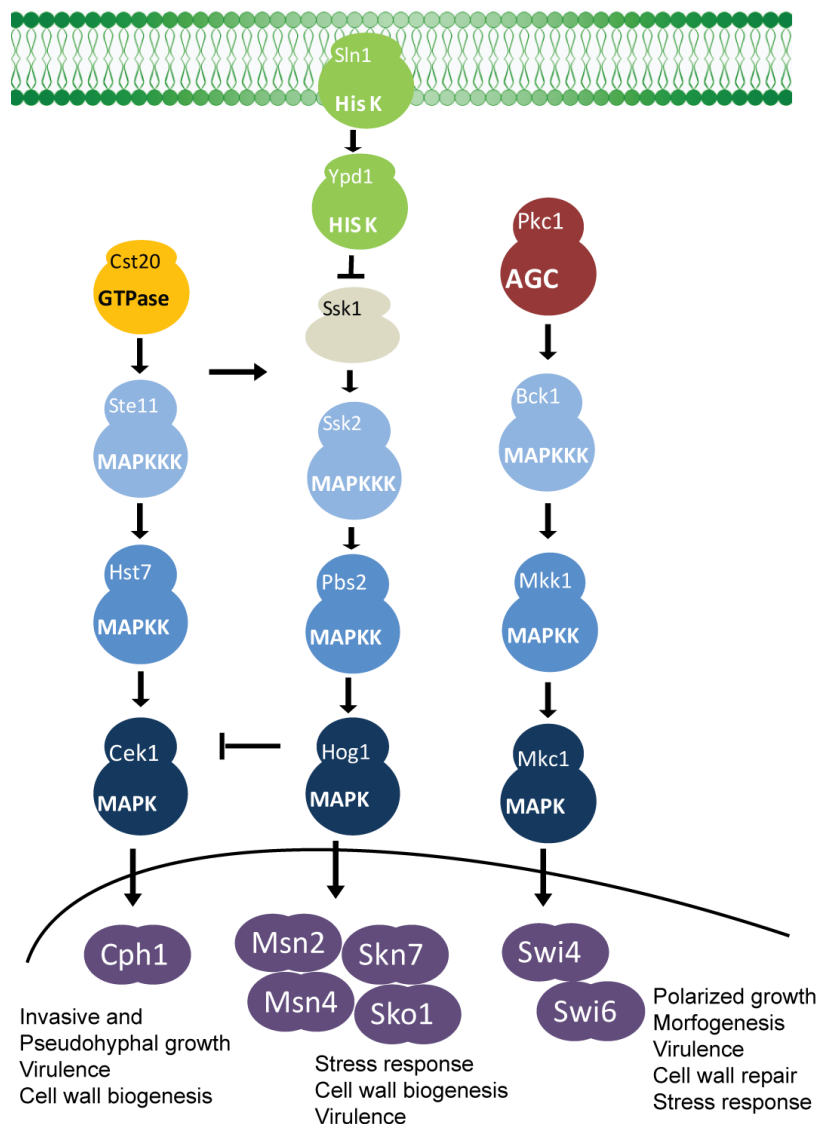


Figure 1.4 Schematic representation of the main mitogen-activated protein kinase signaling pathways in *Candida*.

1.3.1.1.2.1.3 Hog1 pathway

The Hog1 pathway is implicated in several stress resistance mechanisms such as osmotic stress, oxidative stress, heat-shock and many antifungal drugs. Hog1 pathway is composed by Sln1, Ypd1, Ssk2, Ssk1 (MAPKKK), Pbs2 (MAPKK) and Hog1 (MAPK) (Figure 1.4) (Nagahashi, Mio et al. 1998). The pathway is activated by the transmembrane histidine kinase Sln1 that that forms part of two-component regulatory system (see also Item in *S. cerevisiae* 1.5.1) with Ypd1. Under basal conditions or hyposmolarity, Sln1 and then Ypd1 are phosphorylated. Ypd1 transfers

the phosphorylation to the cytoplasmic regulator Ssk1 which inhibits the activation of the MAPK Hog1 pathway. Under hyperosmotic stress conditions, the Hog1 pathway is activated by inhibiting the two-component regulator Sln1-Ypd1 at the beginning of the pathway. Once in the nucleus, Hog1 can activate the transcription factors Msn2, Msn4, Skn7 or Sko1 (Figure 1.4). Single *sln1* or *ssk1*, but not *ssk2* or *pbs2* mutant cells present growth deficiencies under stress conditions (Arana, Nombela et al. 2005). However, this effect in the mutants can be explained taking into account a cross talk between the Cek1 and the Hog1 pathway (Cheetham, Smith et al. 2007).

1.3.1.1.2.1.4 Cell Wall Integrity pathway

The last MAPK pathway, the cell wall integrity (CWI) pathway, is not well characterized in *Candida*. It is composed of Pkc1, Bck1 (MAPKKK), Mkk2 (MAPKK) and Mkc1 (MAPK), the homolog of Slr2 in *S. cerevisiae* (Navarro-Garcia, Sanchez et al. 1995). Pkc1 activates by phosphorylation Bck1 that phosphorylates Mkk2 and, in turn, activates Mkc1 (Figure 1.3). Recently, it was shown that Mkc1 activates Swi4 and Swi6, two transcription factors components of the SBF transcription complex, involved in G1/S cell-cycle progression (LaFayette, Collins et al. 2010). Single null mutants of any of the three MAPK kinases results in hypersensitive to cell-wall stressors, such as caspofungin, an echinocandin that inhibits the enzyme (1→3)-β-D-glucan synthase used as antifungal agent because it disrupts the integrity of the cell wall (Blankenship, Fanning et al. 2010). The *mkc1* homozygous deletion mutants produce abnormal biofilms, reduce filamentation and are less pathogenic in mice than the parental strain (Diez-Orejas, Molero et al. 1997; Kumamoto 2005). The signaling cascade that regulates Pkc1 is not fully depicted; nevertheless, it is one of the best known in *S. cerevisiae* (Levin 2005) (See Item 1.5.1).

1.3.1.1.2.2 The cyclic AMP-dependent PKA pathway

Cyclic adenosine monophosphate (cAMP) is a widely spread molecule present in eukaryotic and prokaryotic organisms. It regulates many extra and intra cellular processes and has different roles depending on the species or tissue specific distribution. The enzyme that promotes the conversion from ATP to cAMP is the adenylate cyclase, a highly conserved protein in nature. In contrast with the majority mammalian cells, *C. albicans* only possesses one adenylate cyclase called Cyr1, and it is predicted to be a soluble protein due to the absence of the membrane domains

typically associated in mammalian adenylate cyclases. The *cyr1/cyr1* mutants grow slowly and only exhibit hyphal development in embedded conditions (Cao, Lane et al. 2006). In turn, Cyr1 is regulated by external signals such as serum or farnesol, via the GTPase Ras1 and peptidoglycans, or CO₂ that directly interacts with the cyclase (Feng, Summers et al. 1999; Klengel, Liang et al. 2005; Davis-Hanna, Piispanen et al. 2008). Those signals are transduced by different pathways that converge in Cyr1. The conversion from ATP to cAMP activates then the PKA pathway. The homolog of PKA kinase in *C. albicans* is called Tpk (two isoforms in *C. albicans* and three in *S. cerevisiae*) that, as in mammals, count with a regulatory subunit, named Bcy1 (See Item 1.5.2.2). Tpk and Bcy1 form an inactive holoenzyme; when cAMP binds to the Bcy1 regulatory subunit, it suffers a conformational change that releases and activates the Tpk catalytic subunits. Tpk1 and Tpk2 have distinct functions in *C. albicans*. While Tpk1 is required for hyphal formation on solid media, Tpk2 is necessary for hyphal development in suspension growth, agar invasion and biofilm formation (Bockmuhl, Krishnamurthy et al. 2001; Giacometti, Kronberg et al. 2009; Giacometti, Kronberg et al. 2011). Deletion of *tpk1/tpk1* but not of *tpk2/tpk2* results in a deficiency in glycogen biogenesis (Giacometti, Kronberg et al. 2009; Pastor-Flores, Schulze et al. 2013). The abundance of each subunit is at the same time tightly regulated by the others (Giacometti, Kronberg et al. 2012). In addition, Tpk2 phosphorylates Efg1 (Sok2 in *S. cerevisiae*), the major transcription factor involved in morphogenesis. It is likely that other kinases contribute to the activation of Efg1 because although in a *tpk2/tpk2* background, an overexpression of Efg1 can restore the filamentous morphological form, a *efg1/efg1* background cannot restore the morphological switch by an overexpression of Tpk2 (Tebarth, Doedt et al. 2003; Park, Myers et al. 2005). In addition, Efg1 works in concert with other transcriptional regulators such as Czf1, Efh1 or Flo8 directly involved in filamentation (Lengeler, Davidson et al. 2000; Ryan, Shapiro et al. 2012).

1.3.2 Antifungal drugs and resistance

The systemic fungal infections usually appearing in immunocompromised patients are hard to diagnose. The symptoms associated to the fungal infection in the early stages are nonspecific, and the most common methods used for their detection make difficult a fast diagnostic. Conventional fungal detection is based on culture techniques and direct microscopy that allows identification on cellular morphology

and staining properties. Therefore, the identification requires expertise microbiologist and identification based on morphology can often be equivocal. Other strategies based on growth, morphology and biochemical tests are available as commercial kits for identification of clinical isolates. Nevertheless, the culturing steps may take 36 to 48 h, and the results show in most of the cases poor discrimination between species.

Other non-culture techniques for fungus identification are based in the DNA, RNA or immunological detection. Those are less spread but have more sensitivity and specificity (Yeo and Wong 2002).

There are few antifungal agents available up to date, limiting the therapeutic options. One of the reasons of lacking antifungal drugs is the similarity between molecular pathways in eukaryotic organisms. Such similarity makes difficult the specificity of the antifungal agent. There are five antifungal classes classified regarding their target.

Table 1.2 Antifungal drugs with their targets and resistance mechanisms

Antifungal drugs, their targets and possible specific resistance mechanisms		
Antifungal class and members	Primary target (mode of action)	Resistance mechanisms
Fluorinated pyrimidine analogs 5-FC	RNA and DNA synthesis (misincorporation of 5-fluorouracil)	Mutation in Fur1 (uracil phosphoribosyl transferase)
Polyenes Nystatin AMB	Cell membrane ergosterol (increased membrane permeability creating pores and oxidative damage)	Induction of low membrane ergosterol content detected in some fungi
Allylamines Terbinafine Naftifine	Ergosterol biosynthesis (inhibition of squalene epoxidase; accumulation of toxic sterol intermediates)	Mutations in Erg1, efflux via ABC transporters, stress tolerance induction, induction of detoxification
Imidazoles MCZ, etc.	Ergosterol biosynthesis (inhibition of Erg11, the rate-limiting step in ergosterol biosynthesis; conversion of Erg11p substrate into toxic methylated sterols)	Mutations in Erg11, induced overexpression of Erg11, efflux via ABC and MFS transporters, tolerance to methylated sterols via mutation in <i>ERG3</i> , loss of heterozygosity for mutant <i>ERG11</i> and <i>TAC1</i> , aneuploidy (<i>C. albicans</i> chromosome 5), stress tolerance induction, import of host cholesterol (<i>C. glabrata</i>)
Triazoles FLC ITC VCZ POS Ravuconazole Isavuconazole Pramiconazole Albaconazole		
Echinocandins Caspofungin Micafungin Anidulafungin	Cell wall biosynthesis [inhibition of $\beta(1,3)$ -glucan synthase]	Mutation in $\beta(1,3)$ -glucan synthase, loss of heterozygosity for $\beta(1,3)$ -glucan synthase (<i>C. albicans</i>)

Adapted from (Cannon, Lamping et al. 2009).

Fungal cells can gain resistance to drugs, and the mechanisms of resistance vary between the different antifungal classes. The most common resistances to fungal drugs are to the fluorinated pyrimidine analogs, imidazoles and triazoles. In contrast, there are few isolates resistant to polyenes, allylamines and echinocandins. The resistance mechanisms are explained in Table 1.2, but the most common is the efflux by ATP-binding cassette (ABC) pump which uses the hydrolysis of ATP to carry ligands across the membrane in eukaryotic and prokaryotic organisms. The ABC transporters have been classified in three subfamilies in yeast cells: the multidrug resistance (MDR), the pleiotropic drug resistance (PDR) and the multidrug

resistance-associated protein (MRP). The ABC transporters often associated with antifungal drug resistance are members of the PDR transporter family. The second class of efflux pump is the major facilitator superfamily (MFS) transporters which use the proton-motive force across the plasma membrane (PM) as source of energy. Both families, ABC and MFS, exist in fungal lineages (e.g. *S. cerevisiae* and *C. albicans* family) (Gbelska, Krijger et al. 2006).

1.3.2.1 Efflux pumps in *S. cerevisiae* and *C. albicans*

Most of the acquired antifungal resistance comes from genetic mutations in transcription factors, drug targets or enzymes in metabolic pathways. However, antifungal compounds can also cause an alteration in the stress response. In contrast to the genetic mutations that have a long term resistance, the stress response is reversible and can be thought as short term phenotypic response.

In *S. cerevisiae* drug resistance most often involves the transcription factors ScPdr1 and ScPdr3. The combination of both or the single induction stimulates the expression of the majority ABC pumps in *S. cerevisiae*. ABC transporters, in turn, extrude the drug across the plasma membrane. The homolog in *C. albicans* of ScPdr1 and ScPdr3 is the transcription factor CaTac1. It controls at least the expression of the ABC transporters CaCdr1 and CaCdr2. Although the analysis of *C. albicans* genome identified 27 ORFs coding for ABC transporters, only CaCdr1 and CaCdr2 have been identified as functional transporters of known antifungal drugs (Sanglard, Ischer et al. 1997; Niimi, Niimi et al. 2004). From the 6 annotated MFS transporter proteins in the Candida Genome Database, only CaMdr1 and CaFlu1 have antifungal drugs as substrates (Calabrese, Bille et al. 2000).

Antifungal compounds that target the cell wall or plasma membrane can produce hypo-osmotic stress that derives in the activation of the CWI pathway. In addition, the protein phosphatase calcineurin is activated in response to many stresses and is essential in *C. albicans* for survival during the activation of the membrane stress. This PP2B phosphatase activates transcriptional regulators such as CaCrz1. It also plays a role in the tolerance of some antifungal drugs, such as Azoles, but in a CaCrz1-independent manner. In fact, if calcineurin activity is inhibited, the cytostatic azoles become cytotoxic which leads to the death of the cell (Sanglard, Ischer et al. 2003).

1.4 *S. cerevisiae*, a model organism to study molecular networks and processes in *C. albicans*

One of the major problems in the genetic work with *C. albicans* is the lack of haploid form. So far, it has not been possible to isolate by mating or sporulation *C. albicans* strains that lack either α or the a MTL allele (Jones, Federspiel et al. 2004). Therefore, since the key signaling pathways in *S. cerevisiae* are highly conserved in *C. albicans* and other more distantly related fungi, *S. cerevisiae* has provided a single model system to study in a haploid organism the molecular mechanisms and pathways in *C. albicans*. With the aim of finding whether or not *S. cerevisiae* is an appropriate model organism for the study of biological processes a recent study compares 704 organisms from various phyla with *S. cerevisiae*. It was found that from the 5880 annotated proteins in the genome of *S. cerevisiae*, 3864 (65.7%) are ortholog proteins, 754 (12.8%) are homolog proteins and 1262 (21.4 %) are absent in *C. albicans*. Within 704 organisms studied, *C. albicans* ranks in the 5th position in terms of sharing biological processes with *S. cerevisiae*. This data reassert the expected result, taking into account the genetic similarities shared between all the ascomycetes (Karathia, Vilaprinyo et al. 2011).

1.5 The cell wall of yeast

Yeast and other fungi can adapt rapidly to adverse conditions. Habitats such as fruits or flowers can drastically alter the growth conditions, varying the osmolarity, pH, oxygen, radiation and more specially the availability of water. The morphology and shape that provides the cell wall to the yeast are used to adapt to these adverse conditions. To regulate the intracellular water content necessary for biochemical reactions, yeasts have a thick and rigid cell wall that limit swelling and controls the osmotic gradient inside the cell (Hohmann 2002). The cell wall also is required to maintain the cell shape, necessary for cell division, mating, nutrient accession, endocytosis, cytokinesis, cell polarity, and to induce cell morphogenesis. An internal cytoskeleton formed by actin acts in combination with the cell wall regulation in yeast (Moseley and Goode 2006).

1.5.1 The Cell Wall Integrity pathway in *S. cerevisiae*

The CWI pathway in *S. cerevisiae* has been extensively characterized in the last decade. In contrast, it should be noted that the real importance of the CWI pathway

has not been elucidated yet in *C. albicans* (see Item 1.3.1.1.2.1.4). Basically, the CWI is formed by an AGC kinase and a MAP kinase cascade that respond to different stimuli coming from the cell surface, such as low osmolarity, heat and high pH, which activates several transcription factors that in turn participate in the cell wall remodeling. For activation of the CWI pathway, different transmembrane protein receptors and cytosolic proteins localized on the inner layer of the PM transduce the signals to common Rho1 small GTPase, which activates the protein kinase Pkc1, the core component of the CWI pathway.

1.5.1.1 The signal through the transmembrane sensors

The five known cell surface sensors belonging to the CWI pathway are composed by Wsc1-3, Mid2 and Mtl1. All of them detect and transmit the signal of the cell wall status to the redundant guanosine exchange factors (GEF) Rom1/2. Rom1 and Rom2 stimulate Rho1, the GTPase homolog of the mammalian RhoA. Loss of both *ROM1* and *ROM2* results in lethality. Rho1 is also an essential protein that controls the CWI signaling, activating Pkc1. It is as well important for the β 1,3-glucan-synthase activity and the actin cytoskeleton organization. Rom1 and Rom2 are highly conserved GTPases, although Rom2 has been found to play a more important role in the CWI regulation since deletion of *rom1* has no phenotype and *rom2* causes lysis to the cell (Krause, Cundell et al. 2012). Moreover, Rom2 has an important function in the feedback regulation of the CWI pathway (Guo, Shen et al. 2009). Another GEF that regulates the activity of Rho1 is Tus1. It is more distant to Rom1/2 and the function of this GEF has been found to be opposite to these of Rom1/2, since a *tus1* mutants result in the activation of the CWI pathway (Krause, Cundell et al. 2012). In addition, an inhibition regulatory role has been found for 4 of the 11 GTPase-activating proteins (GAPs) identified in *S. cerevisiae*. Therefore, Rho1, a small G protein with GTPase activity, is regulated by the specific guanosine nucleotide bound to it: it is active in the GTP-bound state and inactive when bound to GDP.

The main target of Rho1, that controls the regulation of CWI pathway, is Pkc1, the AGC kinase homolog to the PKC family members. The *pkc1* mutant is not viable even in normal growth conditions (by contrast with the downstream MAP kinases of the CWI, whose mutant genotypes cause lysis only at high temperatures) suggesting that Pkc1 not only plays an important role in the CWI remodeling but also in the regulation of additional targets separate from the MAP kinase cascade that may be

essential for the survival of the cell. However, the major role of Pkc1 is the regulation of CWI pathway since it is possible the rescue of the cell lysis the phenotype with the osmostabilizer sorbitol. The target of Pck1 in the CWI pathway is the MAPKKK Bck1. It is the MAP Kinase responsible to transmit the signal to Mpk1/2. The mutant *bck1* phenotype is viable at normal growth conditions of 28-30°C but requires an osmotic stabilizer at high temperatures. The *pkc1* suppression can be by-passed by Bck1 catalytic domain, but not by the full length molecule. In addition, a constitutively active allele of *BCK1* gen (*BCK1-20*) was found by Levin and Lee. *BCK1-20*, a mutant allele which has a mutation in the position 3520, G to C that results in replacement of Ala-1174 for Pro in a region immediately upstream of the catalytic domain (Lee and Levin 1992). This constitutively active allele is used to date as a control of the CWI implication in proteomic and genetic studies. Bck1 phosphorylates two redundant MAP kinase kinases, Mkk1 and Mkk2 since deletion of either *mkk1* or *mkk2* did not cause any phenotypic defect, but deletion of both did cause temperature sensitive cell lysis defect (Irie, Takase et al. 1993). The last MAP kinase in the CWI pathway is Slt2. Slt2 is a cytoplasmatic and nuclear kinase. It is responsible for phosphorylation of several transcription factors implicated in the cell wall remodeling such as Rlm1, the only known transcriptional regulator dependent of CWI pathway, and the SBF transcriptional activator composed of Swi4-Swi6 subunits, important regulator for the late G1 cell cycle transition and cell wall stress. The lysis phenotype at high temperature of *slt2* mutant cells can be suppressed by the overexpression of Swi4, the DNA binding component of the SBF complex, but not by overexpression the regulatory subunit Swi6. Moreover, as opposed to *swi6*, *swi4* mutant cells display temperature sensitive growth that can be suppressed by 1M sorbitol (Madden, Sheu et al. 1997). Slt2 also regulates both, the poli (A) length of the mRNA and the mRNA export factors under heat shock stress by the phosphorylation of Nab2, a nuclear polyadenylated RNA-binding protein (Carmody, Tran et al. 2010). Slt2 phosphorylation state is finely regulated by Sdp1, a dual-specificity MAP kinase phosphatase that is expressed under oxidative stress or following heat shock-induced conditions (Fox, Shafiq et al. 2007).

Typically the activation of Slt2 can be estimated using an antibody (anti phospho-Slt2) that detects the double Thr/Tyr phosphorylation in the activation loop. Another

method, less direct but efficient and simple, consists of measuring the expression of Rlm1 by a reporter gene such as *lacZ* under the control of the Rlm1 promoter.

1.5.1.2 The signal through Pkh

Pkh1 and Pkh2 are the orthologs of the mammalian master kinase PDK1, sharing 68% of homology in the catalytic domain. In contrast to PDK1 (see Item 1.2.1), Pkh1/2 do not have a characterized PH domain and it was postulated that their regulation is independent of PIP₃ (Casamayor, Torrance et al. 1999). *PKH1* and *PKH2* are functionally redundant genes with an essential function because deletion of both genes, but not of either single gene, results in lethality. PDK1 and Pkh proteins are evolutionary conserved because the expression of either human or plant PDK1 in the otherwise lethal *pkh1 pkh2* haploid cells rescues this lethality (Casamayor, Torrance et al. 1999; Deak, Casamayor et al. 1999). Pkh3 is a third and more distantly related protein. It was identified as a multicopy suppressor of the growth defect of *pkh1D398G pkh2 (pkh1^{ts} pkh2)* mutant cells at the restrictive temperature. The single *pkh3* deletion does not have an obvious phenotype (Inagaki, Schmelzle et al. 1999) and does not modify the overall transcriptomic profile (our unpublished results). Lack of *PKH3*, however, exacerbates the growth defect of the *pkh1^{ts} pkh2* mutant at the restrictive temperature (Voordeckers, Kimpe et al. 2011). Nevertheless, in contrast to what occurs with the *pkh1 pkh2* double-mutant cells, the *pkh1 pkh3* and *pkh2 pkh3* double-mutant cells grow normally.

As PDK1, yeast Pkh proteins exert pleiotropic effects by phosphorylating the activation loop of diverse yeast AGC protein kinases substrates and also by the direct phosphorylation of other regulatory proteins. Phosphorylation in the activation loop is indispensable for the activity of the protein kinases Ypk1/2, Pkc1 and Sch9 and Tpk1, one of the catalytic subunits of PKA (Voordeckers, Kimpe et al. 2011). Thus, phosphorylation of Pkc1 by Pkh is crucial to CWI by the activation of the Slr2 MAPK cascade. As part of a seemingly independent signaling pathway, the involvement of Pkh in the endocytic pathway relies on the direct phosphorylation of the Slm1 and Slm2 proteins, regulators of the cytoskeleton (Daquinag, Fadri et al. 2007) by Pil1 and Lsp1, which are constitutive proteins of eisosomes (Zhang, Lester et al. 2004; Walther, Aguilar et al. 2007) and Ypk, which leads to the activation of Ypk downstream signaling that regulates endocytosis (Grosshans, Andreeva et al. 2006).

Also through Ypk proteins, Pkh is involved in the maintenance of the asymmetric distribution of the aminophospholipids phosphatidylserine (PSer) and phosphatidylethanolamine (PE) between the two leaflets of the PM (Roelants, Baltz *et al.* 2010) and takes part in important aspects of the heat shock response. Finally, Pkh regulates chronological aging, cell size determination and nutrient-induced growth resumption by phosphorylation and activation of Sch9 (Liu, Zhang *et al.* 2005; Voordeckers, Kimpe *et al.* 2011) and controls, as well, the rate of mRNA decay at the deadenylation step and the assembly of processing body (P-body) induced by different stresses (Luo, Costanzo *et al.* 2011).

It has been reported that the long chain base phytosphingosine (PHS) directly activates Pkh (Friant, Lombardi *et al.* 2001; deHart, Schnell *et al.* 2002), thereby regulating translation initiation during heat stress. However, the identities of the sphingolipid-activating Pkh proteins *in vivo* are still controversial. It has recently been reported that complex sphingolipids, and not PHS, are the activators of Ypk1 phosphorylation by Pkh (Roelants, Baltz *et al.* 2010). A similar approach based on the use of a phospho-specific antibody was used to discard a role of PHS in the phosphorylation of Sch9 (Voordeckers, Kimpe *et al.* 2011).

1.5.2 Pkh substrates in yeast

1.5.2.1 Sch9

Based on the sequence comparison, the AGC kinase Sch9 was initially proposed as a PKB/Akt homolog. However, Sch9 in contrast to PKB/Akt, does not have PH domain. Recent work suggests that Sch9 might be more related to the mammalian S6K1 since the activity of both S6k1 and Sch9 is regulated by TORC1 (Sarbasov, Guertin *et al.* 2005). In addition, both have as a substrate the ribosomal protein S6 or its homolog in yeast Rps6 (Urban, Soulard *et al.* 2007). Other characteristic is that Sch9, as S6K, has a long C-terminal with a not yet cleared function but with a possible regulatory role.

Sch9 is phosphorylated by Pkh1/2 in the activation loop *in vivo* and *in vitro* and Pkh phosphorylation is required for Sch9 activity since a mutation in Sch9 activation loop cannot overcome the small colony phenotype and the slow growth in a *sch9* mutant cells (Roelants, Torrance *et al.* 2004; Voordeckers, Kimpe *et al.* 2011). Besides, TORC1 phosphorylates six residues in the carboxyl terminal of Sch9, including its

HM, and mutations in these phosphorylated residues eliminate Sch9 activity (Urban, Soulard et al. 2007). In addition to the HM regulatory motif, Sch9 possesses in its N-terminus a C2 domain, a typical Ca^{2+} -dependent lipid binding, although to date its function remains unclear.

Sch9 is involved in different cellular processes such as the regulation of transcription from RNA polymerases I-III, the regulation of cell size, the response to osmotic, heat and oxidative stresses, and is involved in cell aging (Fabrizio, Pozza et al. 2001; Jorgensen, Nishikawa et al. 2002; Jorgensen, Rupes et al. 2004; Huber, Bodenmiller et al. 2009). In addition, Sch9, like PKA, exerts similar physiological roles in response to nutrient availability. Indeed, Sch9 was isolated as a multicopy suppressor of the growth defect resulting from disruption of PKA signaling. A genome-wide expression analysis indicated that both Sch9 and PKA act in parallel in partially redundant pathways as well as being key elements of separate signaling cascades. Therefore Sch9 and PKA probably share common substrates although none have been described for Sch9 (Roosen, Engelen et al. 2005). However, transcriptional factors have been linked with the Sch9 activity. The heat shock transcriptional factor, Hsf1, contains both C-terminal and N-terminal transcriptional activation domains. A truncation of the C-terminal domain in a *hsf1* (1-583) mutant turns into a temperature-sensitive mutant with growth defect at 37°C. This phenotype is deficient in the expression of heat-inducible Hsp90 chaperone complex and can be restored by the deletion of *SCH9* gene that results in an increment of Hsp90 activity, compensating the low abundance of the chaperone (Morano and Thiele 1999). However, the relation between Hsp90 and Sch9 signaling pathway is still unclear.

1.5.2.2 PKA

PKA is a heterotetramer formed by two catalytic subunits that contain three catalytic isoforms, Tpk1, Tpk2 and Tpk3, and a regulatory subunit Bcy1. The sequences of the three Tpk's share high similarity in their C-terminal and CD regions, while the N-terminal region differs in length and similarity. In addition, the three Tpk's contain an activation loop site which is phosphorylated by Pkhs in vivo and in vitro. In a *pkh1^{ts} pkh2 pkh3* strain, the phosphorylation in the activation loop of both Tpk2 and Tpk3 is completely abolished at the restrictive temperature of 37°C (Levin and Zoller 1990; Haesendonckx, Tudisca et al. 2012) and mutations in the Tpk1 Phe-Xaa-Xaa-Phe motif drastically reduces Pkh1-Tpk1 interaction (Voordeckers, Kimpe et al. 2011). A

Non-phosphorylated activation loop conformation of Tpk1 decreases its association with Bcy1 and phosphorylation of the activation loop of Tpk1 is capable to interact with Bcy1 dimer to form the holoenzyme molecule (Haesendonckx, Tudisca et al. 2012). The PKA activity is essential for the survival of the cell since the deletion of the 3 catalytic subunits is lethal (Toda, Cameron et al. 1987). PKA is the effector kinase of the Ras-cAMP signaling pathway (see Item 1.3.1.1.2.2). cAMP, produced in response to fermentable sugars, binds to the Bcy1 regulatory subunit and, in turn, releases the Tpk catalytic subunits that becomes active. The cAMP is quickly degraded by the phosphodiesterases and acts as a negative feedback system to regulate the pathway (Ma, Wera et al. 1999). Besides, the phosphorylation in the activation loop by Pkh, the two signaling pathways that control the PKA activity work with glucose sensors: The Ras proteins that detect the intracellular glucose (Rolland, De Winde et al. 2000) and G-protein-coupled receptor Gpr1 and G-protein Gpa2 that sense the extracellular sugar (Colombo, Ma et al. 1998) bind independently to adenylate cyclase (Cyr1) and stimulate its production of cAMP; cAMP activates the catalytic subunits by binding to Bcy1 subunits and promoting dissociation of the complex that in turn activate the PKA pathway. Phosphodiesterases antagonize glucose signaling via enzymatic inactivation of cAMP (conversion to AMP). Another condition to activate PKA pathway in yeast is the intracellular acidification or alkalinization that also promotes the increase or decrease of the cAMP concentration respectively (Trevillyan and Pall 1979; Casado, Gonzalez et al. 2011). Besides the regulation of PKA activity by cAMP, the phosphorylation of either Tpk by Pkh or Bcy1 by Yak1 (Garrett, Menold et al. 1991), that at the same time is negatively regulated by PKA, seems to affect the cellular localization and, therefore, the affinity of PKA for different substrates (Griffioen and Thevelein 2002). Through the phosphorylation of several targets which include metabolic enzymes, kinases and several transcription factors, the PKA activity regulates biological processes such cell growth, cell cycle progression, heat and osmotic shock tolerance sporulation and autophagy (Estruch 2000; Norbeck and Blomberg 2000; Budovskaya, Stephan et al. 2004). In addition, single catalytic subunits participate in specific biological processes such as invasive growth in response to glucose limitation (Tpk2) or mitochondrion organization (Tpk3) (Harashima and Heitman 2002; Chevtzoff, Yoboue et al. 2010). Among the transcription factors regulated by PKA, Mns2 and Mns4 bind DNA at the STRE (Stress Response Elements) of responsive genes, inducing gene expression and

were found as multicopy suppressors of a *snf1^{ts}* at the restrictive temperature (Estruch and Carlson 1993). The mutation of either *msn2* or *msn4* does not present a clear phenotype while the deletion of both genes increases the sensibility to heat shock, as well as osmotic and oxidative stress (Martinez-Pastor, Marchler et al. 1996). Interestingly, the lethality of *tpk1 tpk2 tpk3* triple mutant cells is rescued by the deletion of both *MNS2* and *MNS4* (Smith, Ward et al. 1998). In absence of stress or presence of glucose, Mns2 and Mns4 are phosphorylated and localized to the cytoplasm. In opposite conditions when the cell is under stress conditions or with low availability of glucose, the transcription factors are translocated to the nucleus. The nuclear localization of Mns2 is inhibited by its direct phosphorylation by PKA. Moreover, PKA inhibits Mns2 and Mns4 function by the negative regulation of Yak1 or Rim15. The deletion of either Yak1 or Rim15 suppresses the lethality of the lack of PKA activity (Garrett, Menold et al. 1991). Yak1 phosphorylates and activates Mns2 with a different mechanism that does not implicate the nuclear localization (Lee, Cho et al. 2008). Another transcription factor downstream of PKA is Hsf1. Hsf1 acts in coordination with Mns2 and Mns4 in a heat shock response, having each of them distinct contributions to the heat-induced gene expression. Contrary to Mns2 and Mns4, PKA negatively regulates the expression of Hsf1 since deletion of PKA causes an increase in Hsf1 phosphorylation (Ferguson, Anderson et al. 2005).

1.5.2.3 Ypk1/2

Ypk1 and Ypk2, the first Pkh substrates identified (Casamayor, Torrance et al. 1999). have a high homology with the mammalian counterparts SGK and PKB/Akt. The sequence of Ypk1 and Ypk2 share a sequence similarity of 90% with almost identical N-terminal and catalytic domain and a more distant very short C-terminal region. Their activity is essential for the cell survival since *ypk1 ypk2* double mutant is not viable. It was shown that the overexpression of mammalian SGK rescues the phenotype reinforcing the shared role between Ypk1/2 and SGK; furthermore, like SGK and PKB/Akt, Ypk1 and Ypk2 are targets of Tor2 (Kamada, Fujioka et al. 2005; Niles, Mogri et al. 2012) but, unlike SGK and PKB/Akt, they do not require PIP₃, consistent with the absence of PH domains. This lack of PH domain is remediated by a physical interaction with Slm1 and Slm2, two proteins with a PH domain that recognize PI(4,5)P₂. Slm1 interacts directly with Ypk1 to facilitate its localization at the PM and then assist the phosphorylation of the turn motif and HM by Tor2 (Niles,

Mogri et al. 2012). Ypk1 and Ypk2 have the same activation loop sequence (Casamayor, Torrance et al. 1999) and it is essential for the Ypk activity (Kamada, Fujioka et al. 2005). Pkh1 preferentially phosphorylates and activates Ypk1, whereas Pkh2 prefers Ypk2. Nevertheless, all double mutants (*pkh1 ypk1*, *pkh2 ypk1*, *pkh2 ypk1*, *pkh2 ypk2*) are viable, and the remaining Ypk in the double mutant cells is still phosphorylated in the activation loop site by the Pkh left. At the restrictive temperature, *ypk1^{ts}ypk2* cells lyse rapidly, but this defect is remediated with osmotic support such as 1M sorbitol. Moreover, an overexpression of either *PKC1* or the downstream Pkc1 target, *BCK1-20* allele can suppress the lysis phenotype indicating a role in the CWI pathway (Roelants, Torrance et al. 2002). In addition, Ypk1/2 is also implicated in the regulation of receptor-mediated endocytosis, actin polarization and sphingolipid metabolism.

To date, only two families of Ypk substrates have been characterized, the lipid translocases Fpk1 and Fpk2 responsible, in part, of the turnover to the inner leaflet of the PM of aminophospholipids such PE and PSer (Roelants, Baltz et al. 2010) and the Orm1 and Orm2 proteins that mediate the sphingolipid biosynthesis response to heat stress (Sun, Miao et al. 2012). Although a transcription factor directly phosphorylated by Ypk1/2 has not been described, an analog-sensitive allele for Ypk1/2 shows a direct implication in the inhibition of the transcription factor Crz1, involved in stress response and positively regulated by the calcium dependent phosphatase calcineurin (Niles, Mogri et al. 2012).

1.5.2.4 Pkc1

In mammals, there are nine different PKC isoforms subdivided in conventional, novel and atypical PKCs (see Item 1.2.2.3). In addition, there are three PKC-related protein kinases (PRKs) (Mellor and Parker 1998). By contrast, there is only one PKC isoform (Pkc1) in *S. cerevisiae* (Levin, Fields et al. 1990). Pkc1 is larger than any other mammalian PKC isoforms. Pkc1 possesses at the N-terminus two homologous regions (HR1) that interact with Rho1. This characteristic resembles the mammalian protein kinase C-related kinases PRKs, also termed PKNs that contain three N-terminal HR1 domains in the N-terminal regulatory region. In addition, it possesses an extended regulatory domain with all the subdomains found in all the different mammalian PKCs: two C1 domains, a C2 domain and a pseudosubstrate (Figure

1.5). The pseudosubstrate binds to the active site inhibiting its activity and is considered an essential component of the mechanism of regulation of PKCs. When the pseudosubstrate site is mutated, Pkc1 becomes constitutive active, being able to suppress lethality of *rho1* mutants (Nonaka, Tanaka et al. 1995). The C1 domains are present in all mammalian PKC isoforms. In conventional PKCs, the C1 domains bind to diacylglycerol and phorbol esters. However, similarly to atypical PKCs, the yeast C1 domains lack several aminoacids essential for the diacylglycerol/phorbol ester binding and do not respond to diacylglycerol. Pkc1 also possesses a C2 domain that in conventional PKCs is responsible for binding Ca^{2+} . However, the C2 domain from yeast Pkc1 also does not bind Ca^{2+} . From the C-terminal to the catalytic core, Pkc1 contains the typical extension present in AGC kinases, with a terminal HM. The HM can be phosphorylated.

Pkc1 is the core kinase in the CWI pathway and both external and internal cell wall stress signaling are driven through Pkc1. Pkc1 signaling turns in the activation of a set of genes responsible of the cell wall remodeling. Both catalytic and localization functions are tightly regulated, and its domains are required for a proper targeting, e.g. C1 domain localizes in the cell periphery, C2 domain in the mitotic spindle and HR1 to the bud tip (Denis and Cyert 2005). Pkc1 phosphorylation by either Pkh1 or Pkh2 is required to obtain active Pkc1 (Roelants, Torrance et al. 2004) and the activation is also needed for the localization in the bud neck. Pkc1 contains nuclear localization signals and it may play a role in the regulation of microtubule function (Denis and Cyert 2005). It was shown that the CWI through Pkc1 plays a role in the oxidative stress response by signaling ribosomal gene repression (Mitjana, Petkova et al. 2011), participates in membrane fluidity homeostasis (Lockshon, Olsen et al. 2012) and also acts as mitotic check point by controlling both the cell size and the morphogenesis, which explains at the same time how membrane growth is integrated within the cell cycle progression (Anastasia, Nguyen et al. 2012).

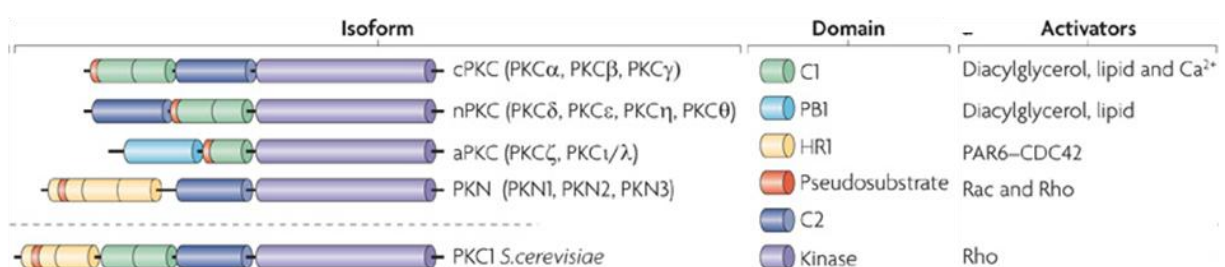


Figure 1.5 PKC family in mammalian cells in comparison to Pkc1 in *S. cerevisiae*. Adapted from (Rosse, Linch et al. 2010).

1.6 The plasma membrane

The PM in eukaryotic cells is a lipid bilayer that separates the intracellular space from the extracellular environment. It is composed fundamentally by proteins and amphipathic lipids in part glycosylated. Based on the head group, the lipids can be classified in sterols, glycerophospholipids and sphingolipids.

Sterols are formed by a polar head group, a non polar hydrocarbon tail and a planar steroid ring structure with a hydroxyl substituent that confers the molecule an amphipathic character. In yeast, the sterol product is ergosterol: It is only present in fungi and plants which makes ergosterol synthesis a potential drug target (see Item 1.3.2). Sterols are present in high abundance in the PM and contribute to fluidity and permeability. A change in sterol composition results in hypersensitivity to certain drugs such as brefedin A, cycloheximide and fluconazole (Table 1.2) (Zweytick, Hrastnik et al. 2000).

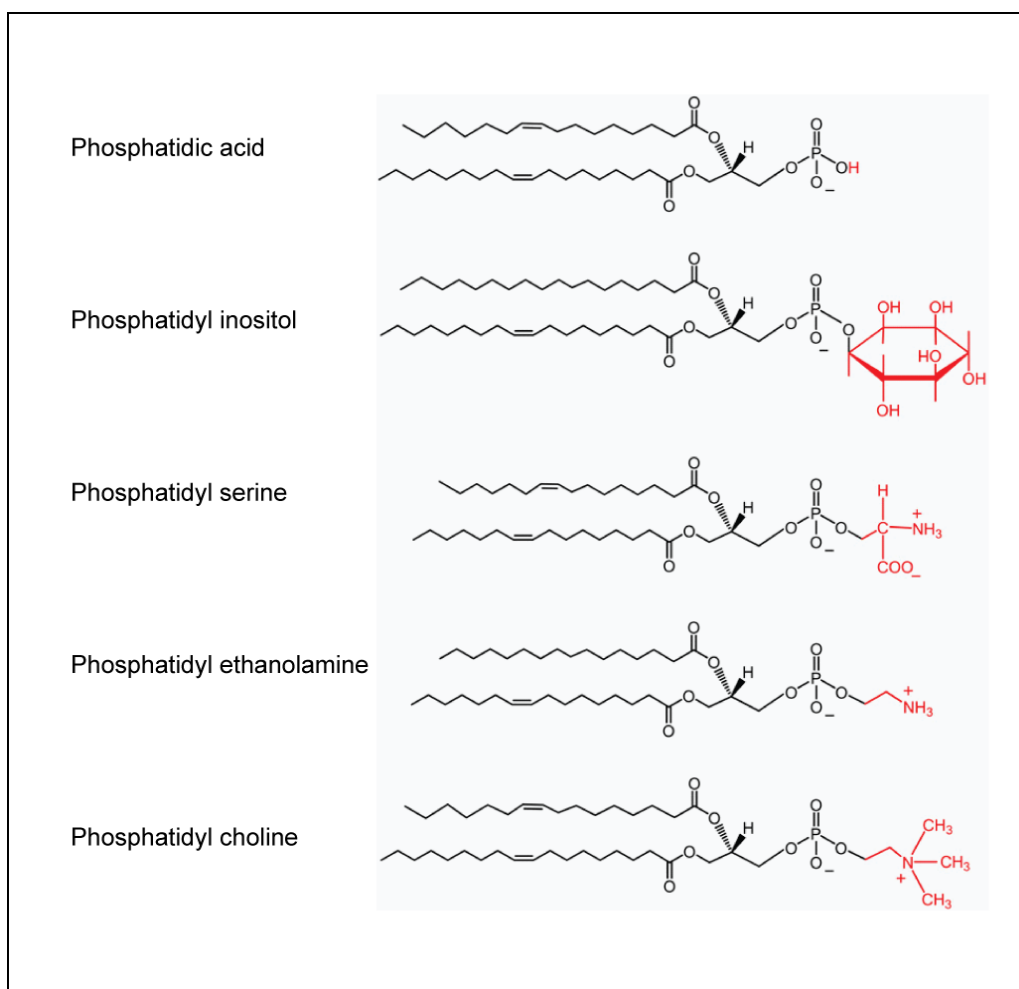
Glycerolphospholipids are formed by a glycerol molecule bound to a phosphate group and to a two long hydrocarbon chains. The most common phospholipids are phosphatidic acid (PA), phosphatidylcholine (PC), phosphatidylethanolamine (PE), phosphatidylserine (PSer) and phosphatidylinositol (PI).

PA is the precursor in *de novo* pathways of all membrane glycerolphospholipids. It is also implicated in the regulation of gene phospholipid synthesis. It is synthesized in the endoplasmatic reticulum (ER) and transported to the PM or to the mitochondria to serve as a precursor for intramitochondrial phospholipid synthesis (Connerth, Tatsuta et al. 2012). PE, PSer and PI are synthesized in the ER, although PSer can as well be decarboxylated to form PE in mitochondria (Henry, Kohlwein et al. 2012). PI serves also as a precursor for phosphatidylinositol-phosphates (PIPs), which are phosphorylated at several positions of the inositol ring. PIPs are in low abundance in comparison to PIs, but they are implicated in many signaling and regulatory activities. An example of their function is the recruitment of proteins to membranes such as actin proteins which have a PH domain that serve as an anchor between the cytoskeleton and the PM through PI(4,5)P₂ (Strahl and Thorner 2007).

Another phospholipid implicated in regulatory processes is PSer. It is found in low abundance in cell organelles and is enriched asymmetrically in the inner layer of the

PM through the regulation of Pkh-Ypk (Roelants, Baltz et al. 2010). Furthermore, PSer is present at high concentrations in the cell cycle during the bud emergence with localization near the septin ring and decreasing in the following cell cycle. This behavior contrasts with the levels of PC and PE with a lineal increased concentrations during the cell cycle progression (Fairn, Hermansson et al. 2011).

Table 1.3 Main Glycerolphospholipids in *S. cerevisiae*



PA, PI, PSer, PE and PC share the amphipathic part (black) of the molecule and only differ in the group bound to phosphate (red).

Sphingolipids or the long chain bases (LCBs) are the last lipid family members that form the PM. Their synthesis takes place in the ER and begins with the condensation of a fatty acid-CoA with serine that yields an intermediate product called 3-ketodihydrosphingosine with short life, which is reduced to form dihydrosphingosine (DHS) (Figure 1.6). This reaction is inhibited by myricin, stopping the sphingolipid synthesis at the beginning of the biosynthetic pathway. DHS can yield ceramide by N-acylation or phytosphingosine (PHS) by hydroxilation. Both, PHS and DHS form

phytoceramide, the precursor of complex sphingolipids bound to phosphatidylinositol groups. This reaction can be suppressed by the addition of aureobasidin with results in an accumulation of Phytoceramide, Ceramide, PHS and DHS (Dickson and Lester 1999).

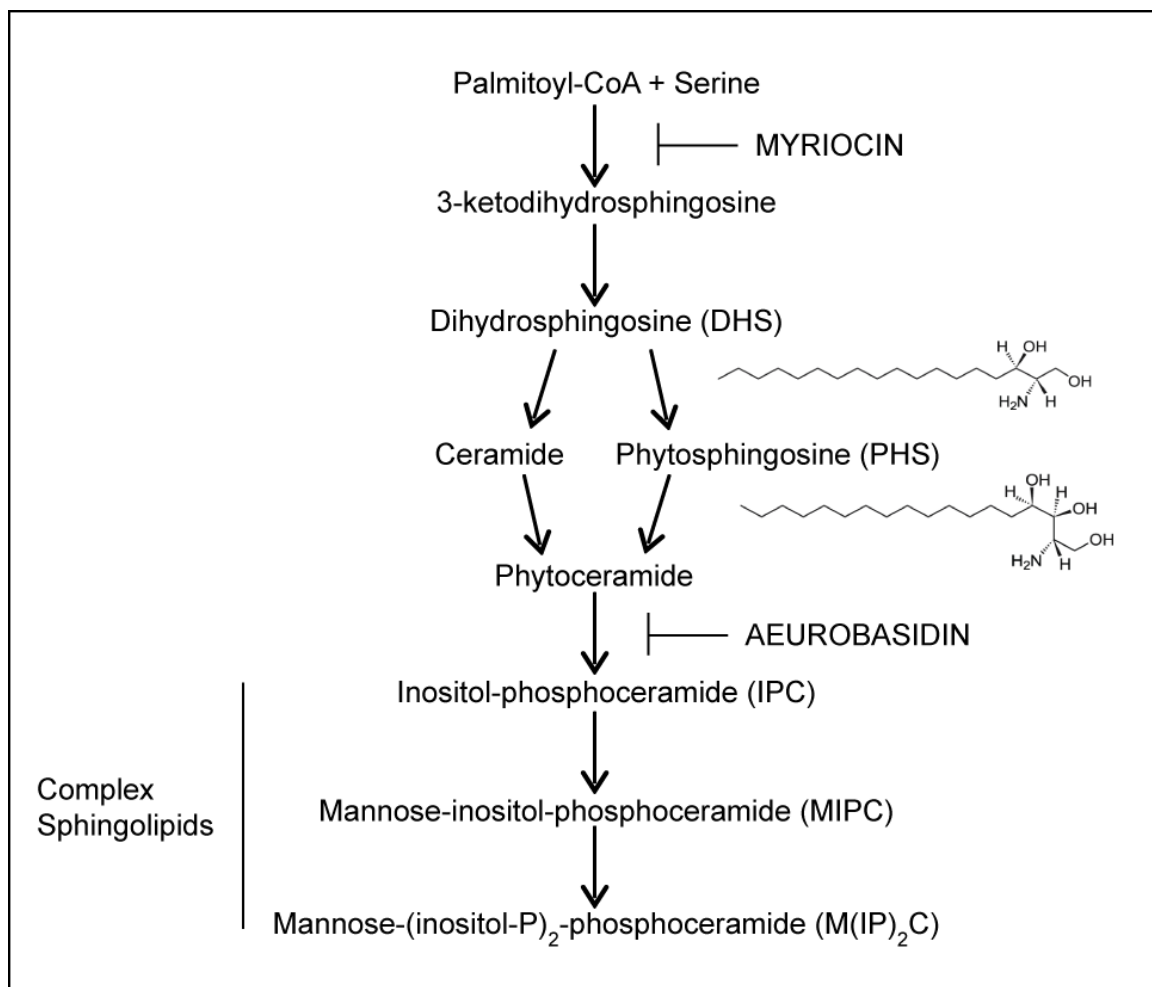


Figure 1.6 Sphingolipid biosynthetic pathway. Myriocin and aerobasidin are drugs used for the study of the regulation of the sphingolipid biosynthetic pathway. Adapted from (Tanigawa, Kihara et al. 2012).

Sphingolipids have been associated to certain essential functions. Some biological functions are signal transduction, nutrient transport, cellular growth, endocytosis, exocytosis and life span. Moreover, at high concentrations PHS has an inhibitory effect on growth and nutrient import and was shown to induce apoptosis in certain fission yeast such as *Aspergillus nidulans* and mammalian cells (Cheng, Park et al. 2003; Park, Kang et al. 2003).

1.6.1 Signal transduction function of sphingolipids

The heat stress is the major factor that affects sphingolipid concentrations. A shift in temperature from 25°C to 37°C generates a heat shock response that produces a

rapidly but transient increase in LCBs (Dickson, Nagiec et al. 1997);(Morano, Grant et al. 2012). Upon increased levels of LCBs, Pkh1/2 are autophosphorylated in the activation loop which trigger the phosphorylation of Pkhs kinase substrates Ypk1/2, Sch9 and Pkc1 by Pkh1/2 (Figure 1.7). In the sphingolipid signaling, two additional substrates of Pkh1/2, Pil1 and Lsp1, are also implicated. These are proteins that belong to the endocytosis pathway (Zhang, Lester et al. 2004; Luo, Gruhler et al. 2008)

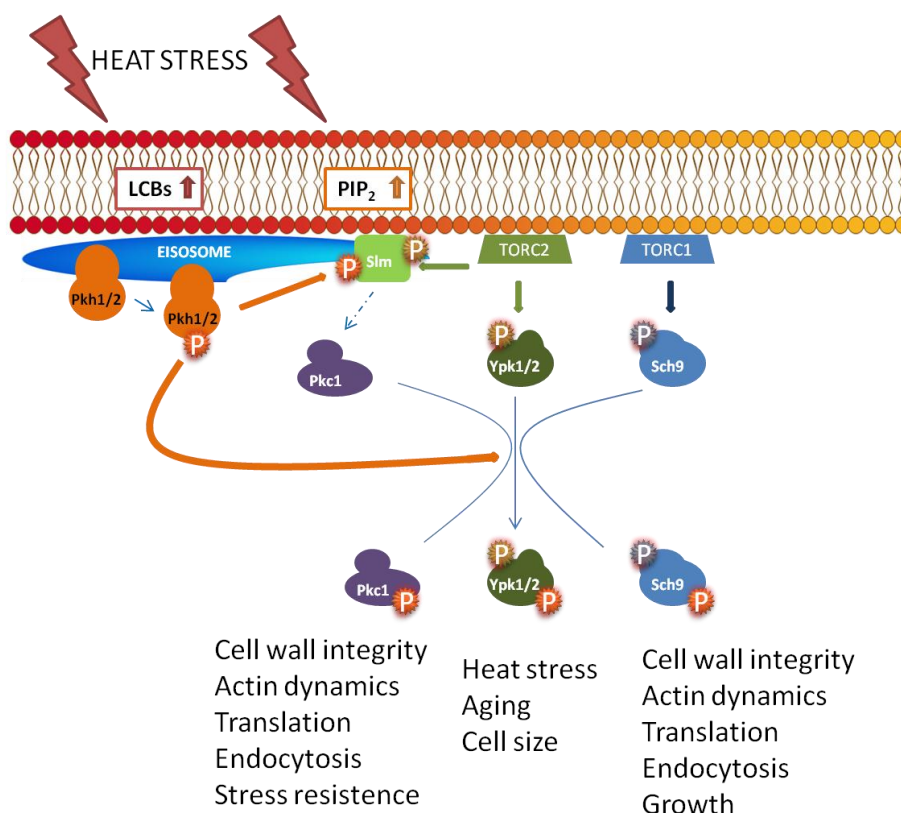


Figure 1.7 Signaling pathways regulated by LCBs. Summary of the signaling pathways regulated by LCBs in *S. cerevisiae*. Heat stress produce a transient increase in LCBs, which then activate Pkh1 and Pkh2. Pkh1/2 phosphorylate Ypk1, Ypk2, Sch9, and Pkc1 in their activation loop (PDK1 site), but the proteins need to be phosphorylated in the activation loop by TOR1/2 to become enzymatically active. Phosphorylation of these sites in Ypk2 is mediated by TORC2, and for Sch9 phosphorylation is mediated by TORC1. Ypk1/2 and Pkc1 are shown working in parallel pathways to control CWI. Adapted from (Dickson 2008).

1.6.2 Organization in the plasma membrane

The PM is the only organelle with high concentrations of sphingolipids; nevertheless, the distribution is not homogeneous. Sphingolipids form, in interaction with sterols lipid rafts, small domains of clusters where the length of the fatty acyl chains and the concentration of sphingolipids form a lipid bilayer system (Bagnat and Simons 2002). The function is still unclear, and there is no evidence that sphingolipid functions are dependent on their segregation into a particular type of lipid domains (Aresta-Branco,

Cordeiro et al. 2011). However, it is well established that the PM is formed by three different compartments: the membrane compartment of TOR2 (MCT), the membrane compartment of Can1 (MCC) and the membrane compartment of Pma1 (MCP) (Malinska, Malinsky et al. 2003; Berchtold and Walther 2009). From the three of them, MCC is the best characterized which is formed by the permease Can1 and 26 more proteins (Grossmann, Malinsky et al. 2008).

In addition, cellular structures termed eisosomes are found intimately associated with the cytoplasmic layer of the PM. It is calculated that a yeast cell possesses around 40 eisosomes and the most abundant protein cluster found are Pil1 and its homolog Lsp1. Pil1 and Lsp1 consist on a banana-shaped BAR domain positively charged in the concave surface that is required for normal localization and function (Ziolkowska, Karotki et al. 2011). On the other side, Pil1 and Lsp1 might not share the same biological function since in the absence of Pil1, Lsp1 is not attached to the membrane and only few larger clusters are formed in the PM. In addition the eisosomes are formed normally with Pil1 in *lsp1* mutants (Walther, Brickner et al. 2006). Thus, it might be related with the unknown function of both N- and C-terminal residues that differ in both proteins. Eisosomes are essential for marking static sites for endocytosis. Although the sequence is highly conserved in fungi, Pil1 does not seem to have the same biological role in other fungal species. For instance, unlike *S. cerevisiae* Pil1 is implicated in endocytosis, Pil1 is essential for cell growth in *C. albicans* (Reijnst, Walther et al. 2011).

The proteins Pkh1 and Pkh2 of *S. cerevisiae* physically interact with the eisosomes; moreover, Pil1 and Lsp1 were shown to be Pkh substrates in vitro and in vivo (Zhang, Lester et al. 2004; Walther, Aguilar et al. 2007). The crystal structure of Pil1 and the model suggested (Olivera-Couto, Grana et al. 2011; Reijnst, Walther et al. 2011) showed that many of the phosphorylated residues and positive charges of Pil1 lie on the concave face of the BAR domain. Both kinases, Pkh1 and Pkh2, are partially localized in eisosomes. Pkh1 needs Pil1 for its localization while Pkh2 is located independently from Pil1. The synthesis of LCBs affects the eisosome assembling and the phosphorylation of Pil1 by Pkh is part of this regulation. The eisosome disassemble upon low LCB concentrations and high Pkh activity that prompts Pil1 phosphorylated. On the other side, eisosomes are assembled upon high LCBs concentration or upon low Pkh activity (Walther, Aguilar et al. 2007) The

mechanism of how Pil1 phosphorylation is regulated by Pkh is still unclear since it was shown that LCBs triggers Pkh activity, and the activation of its AGC kinase substrates. In contrast (Friant, Lombardi et al. 2001), Pil1 was found and described as a negative regulator of Pkh proteins (Zhang, Lester et al. 2004).

Chapter II: Materials and Methods

2. Materials and Methods

2.1 Bacterial strains

Escherichia coli strains used are listed in Table 2.1. *E. coli* DH5 α was used as a host for DNA cloning and amplifying experiments. *E. coli* cells were grown at 37 °C in LB medium (10 g/l Bacto-tryptone, 5 g/l yeast extract and 10 g NaCl) containing, when needed, 50 μ g/ml ampicilin. *E. coli* DH10Bac Chemically Competent Cells were used for bacmid production containing 50 g/ml kanamycin, 7 g/ml gentamicin, 10 g/ml tetracycline, 100 g/ml Bluo-gal and 40 g/ml IPTG for the bacmid selection.

Table 2.1 Bacterial strains

Strain	Relevant genotype	Reference
DH5 α	fhuA2 Δ (argF-lacZ)U169 phoA glnV44 Φ 80 Δ (lacZ)M15 gyrA96 recA1 relA1 endA1 thi-1 hsdR17	Invitrogen
DH10Bac	F- <i>mcrA</i> Δ (<i>mrr-hsdRMS- mcrBC</i>) Φ 80/lacZ Δ M15 Δ lacX74 <i>recA1 endA1</i> <i>araD139</i> Δ (<i>ara leu</i>) 7697 <i>galU galK</i> λ - <i>rpsL nupG</i> / pMON14272/pMON7124	Invitrogen

2.2 General molecular biology methods

Polymerase chain reaction (PCR) were performed with Taq polymerase (Sigma-Aldrich) for cloning into TOPO vector using TOPO TA cloning kit (Invitrogen), and PfuUltra polymerase (Stratagene) for extremely accurate amplification of genomic DNA targets or mutagenesis. Mutagenesis was followed according to QuikChange (Stratagene) recommendations. Restriction digests were performed by incubation of DNA with the specific restriction enzymes and supplied buffers (NEB England biolabs) for 2h at the required temperature. Desphosphorilation and ligation were performed with the Shrimp Alkaline Phosphatase (SPA) kit (ROCHE) and the rapid ligation kit (Roche) respectively, following the manufacturer instructions. Agarose gel and electrophoresis method was used for PCR size analysis and band separation.

DNA Extraction from agarose gels were performed using Gel Extraction Kit (Qiagen) along with the provided protocol. For *E. coli* transformations DH5 α high efficiency competent cells were prepared as described in Inoue et al 1990 (Inoue, Nojima et al. 1990). For plasmid selection Qiagen mini-prep kit for small-scale plasmid purification (~20 μ g) and Qiagen mega-prep kit for large scale purification (~3mg) was used. DNA sequencing was performed by the dideoxy chain-termination method using BigDye Terminator v3.1 Cycle Sequencing Kit (Applied Biosystems) and detection was performed with an Applied Biosystems model 3100 Avant Genetic Analyzer according to the manufacturer's instructions. Oligos used are described in Table 2.2

Table 2.2. Oligonucleotides used

Name	Nucleotide sequence (from 5' to 3')
OACG304	<u>CGACACATTGTTGATGGAATAATTGGTCCCTAGTTAAACAGCTGAAGCTTCGTACGC</u>
OACG305	<u>ACGGCCTAGGGCTCATGGAATTATCCTTATCAAAATACAT</u> ATAGGCCACTAGTGGATCTG
OACG300	<u>CGCACGTGTACTTGCTTGAATACTGCTACTATATCATTAAGAGCTTGGTGAGCGC</u>
OACG301	<u>TATTATGCATTACACTTTCCCTTACCATGTCTTACATATGCATCCGTCGAGTTCAAGAG</u>
ODP18	CCTAGCCGTTGCAACTGCTG
ODP19	GGACGAGGGTATGGACGGTGG
MCA1-nat1_fw1	<u>TCTAAACTACCACCAAAGAAGACCGACTAGATTTACAATCCGTACGCTGCAGGTCGAC</u>
MCA1-nat1_rv1	<u>CAGTCTGAATACATCTACCAACGTACACATTCATATATTTCGATGAATTCGAGCTCG</u>
SMARTIII oligo	AAGCAGTGGTATCAACGCAGAGTGGCCATTATGGCCGGG
CDS III Primer	ATTCTAGAGGCCGAGGCGGCCGACATG-d(T) ₃₀ VN*
5'PCR primer 2-Hybrid	TTCCACCCAAGCAGTGGTATCAACGCAGAGTGG
3'PCR primer 2-Hybrid	GTATCGATGCCACCCTCTAGAGGCCGAGGCGGCCGACA
pUC/M13 Forward	CCCAGTCACGACGTTGTAAAACG
pUC/M13 Reverse	AGCGGATAACAATTCACACAGG
T7 Sequencing	TAATACGACTCACTATAGGG

*N=A,G,C or T V=A, G, or C.

2.3 Mammalian and insect cell lines

Mammalian cell lines used are listed in Table 2.3. HEK293 cells were used to express and purify proteins GST-fusion proteins. Breast cancer cell line (4T1) was

used for Cell Proliferation and Viability Assays (MTT). Cells were cultured in DMEM medium supplemented with 10% FBS and 1% antibiotic antimycotic at 37°C with 5% CO₂ and incubated for the required time. Sf9 insect cells were used for His-tagged protein production. Insect cells were grown in Grace's Insect Medium, supplemented with 10 µg/ml of gentamycin and for some conditions, 10% FBS and at 27°C with continuous shaking.

Table 2.3. Cell lines used

Cell line	Reference
HEK293	a
4T1	b
Sf9	c

HEK293 and 4T1 correspond to mammalian cell lines while Sf9 corresponds to insect cell line. a : (Graham, Smiley et al. 1977) b : (Aslakson and Miller 1992) c : (Vaughn, Goodwin et al. 1977)

2.4 MTT Assay

MTT Cell Proliferation and Viability Assay was used to test the cytotoxicity of small compounds. The cells were cultured in DMEM + 10% FBS until cells reached confluency. Then, the cells were diluted for a final concentration of 10⁴ cfu and seeded in 96 well tissue culture plates. The cells were treated in sixuplicate with compound dilutions in DMSO of 200 100 50 25 µM and DMSO and DMEM control for an incubation time of 24 hours. The tetrazolium compound MTT (3-[4, 5-dimethylthiazol-2-yl]-2, 5-diphenyltetrazolium bromide) is added to the wells and the cells were incubated for 2 h. The MTT is reduced by active cells to insoluble formazoan dye crystals. The crystals were resuspended in DMSO + 20% SDS detergent so that the absorbance can be measured at 570nm.

2.5 Transfection and expression in HEK293 cells by PEI method

HEK293 cells were transfected with pEBG2T with the cDNA insert coding for the protein in the study. The PEI stock powder was dissolved in Mili-Q water at a final concentration of 1 mg/ml. Dilutions of PEI (Polysciences) were tested for optimal transfection. The green fluorescent protein (GFP) was used to detect the efficiency of plasmid transfection. Only PEI concentration that reached >80% of GFP transfected were used for further pGEBG2T transfection.

Confluent cells were split in 8 x 14,5 petri dishes and incubated for 24 hours. A mix 1 ml PEI 1mg/ml and 100 µg of plasmid in 20 ml of DMEM medium without FBS was used to transfect the 8 petri dishes. The cells were incubated for 48 hours and lysed for protein purification.

2.6 Bacmid production, transfection and protein expression in Sf9 cells

For bacmid production, cDNA was cloned in pFastBac and the plasmids transformed using competent DH10Bac *E. coli* cells from MAX Efficiency DH10Bac *E. coli* kit (Invitrogen) for blue/white selection and followed the instructions of Bac-to-Bac Baculovirus Expression System manual supplied with Bac-to-Bac Baculovirus Expression kit (Invitrogen). The recombinant bacmid was purified from the DH10Bac white colonies, then correct size of bacmid and insert were analysed by PCR with primers pUC/M13 Forward and pUC/M13 Reverse. The bands can be analyzed by size: Bacmid alone ~300 bp. Bacmid transformed with pFastBac HT ~2430 bp + size of insert. The bacmid concentration was measured and used for virus production.

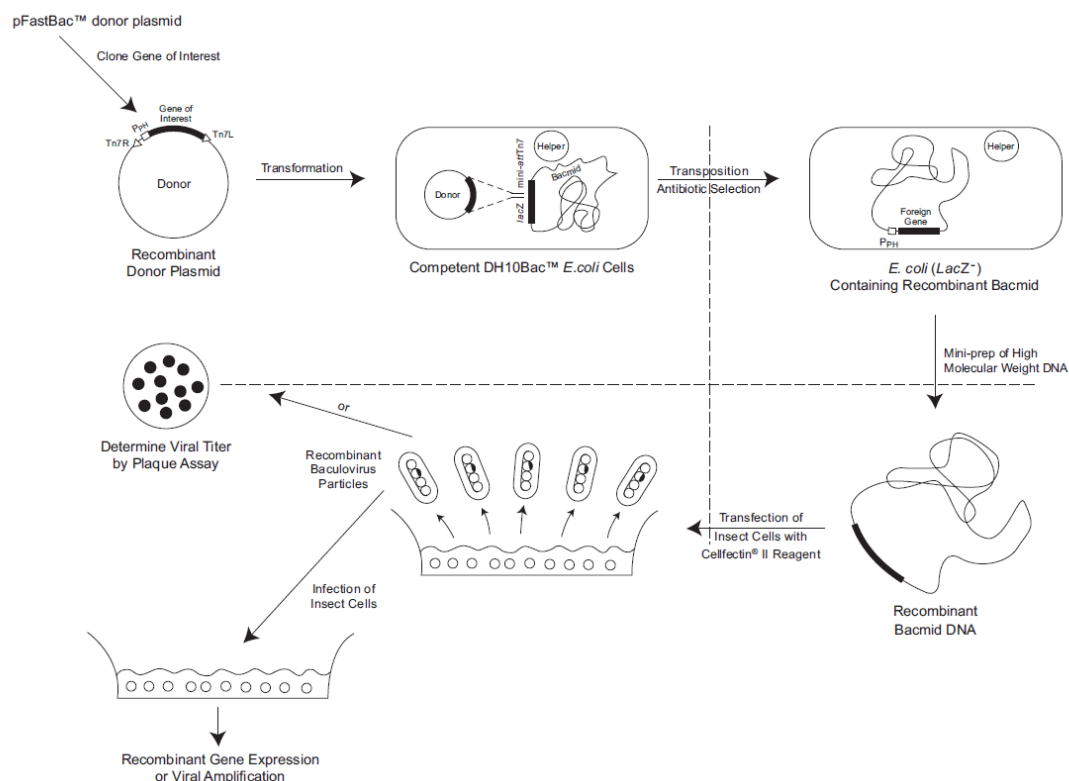


Figure 2.1 Schematic representation of virus production in insect cells. (Extracted from Bac-to-Bac® Baculovirus Expression System manual, Invitrogen).

2.6.1 Virus production

The transfection was carried out using materials from Invitrogen and following the protocol of Bac-to-Bac baculovirus expression system manual (Invitrogen) (Figure 2.1) as it follows:

- 1) The Sf9 cells were maintained between 1.0 million cells/ml to 3.0 million cells/ml.
- 2) Proper volume of plating medium was prepared by mixing 1.5% of supplemented Grace's Insect Medium (Invitrogen) containing 10% FBS (without antibiotics) and 85% of Grace's Insect Medium (Invitrogen).
- 3) 8×10^5 Sf9 cells were plated into each well of the 6-well-cell culture plate. The cells were allowed to attach to the bottom of the well for 15 min at 26°C. The medium was then aspirated; 2.5 ml of plating medium were added into the well.
- 4) Cellfectin II (Invitrogen) stock was re-suspended before use. Eight μ l of cellfectin II was diluted in 100 μ l of Grace's Insect Medium (Invitrogen). One μ l of bacmid was also diluted with 100 μ l of Grace's Insect Medium. The two were combined, gently mixed and incubated at roomtemperature for 15 min.
- 5) The resultant mixture of cellfectin and bacmid was added drop by drop into the well. The cells were incubated at 26°C for 3-5 h.
- 6) At the end of the incubation, the plating medium was aspirated and 2 ml of supplemented Grace's Insect Medium (Invitrogen) containing 10% FBS was added into the well and incubated at 26°C for 72 h.
- 7) At the end of the incubation, the medium was collected. It was labeled as P0 virus and was used to infect another 10 ml of Sf9 cells at 1.5 million/ml (healthy culture with antibiotics). The mixture was transferred into a 250 ml Erlenmeyer culturing bottle and incubated again at 26°C for 96 h.
- 8) At the end of the incubation, 12 ml of the culture was centrifuged at 2000 rpm, for 10 min in Centrifuge 5804 R and supernatant was collected. The supernatant was called P1 virus and continued to be passaged to P2 virus by infecting 50 ml of Sf9 cells at 1.5 million/ml (healthy culture with antibiotics) with 5 ml of the virus. The rest of the P1 virus was kept in -80°C supplied with 2% FBS.
- 9) 5 ml of the P2 virus was passaged to P3 by infecting 500 ml of the Sf9 cells. The rest of the virus was kept in -80°C supplied with 2% FBS.
- 10) The P3 virus was used on protein expression. P3 virus was not passaged further. For each 500 ml more P3 virus production, 5 ml of stored P2 was thawed and used. Infection was evaluated by microscopy observation of the cell morphology.

2.6.2 Start a new culture of the Sf9 cells

Twenty seven ml of Sf-900 SFM medium (Invitrogen) was warmed up in a water bath at 26°C and transferred into a 250 ml Erlenmeyer bottle. An aliquot of Sf9 cells (Invitrogen) were thawed quickly in 37°C water bath and transferred into the medium bottle. The cells were passaged in small scale until the cells recovered and multiplied at an optimal rate (1 million/ml to 3 million/ml in every two days) before they can be amplified for large scale protein expression.

2.6.3 Sf9 cell culture methods

Sf9 cells were kept at 100 ml volume in 250 ml of Erlenmeyer bottle and maintained at concentration below 3 million cells/ml, when they were not used for protein production. Every other day, the cell culture was diluted to 1 million cells/ml with Sf-900 SFM medium supplied with 1x of antibiotics and antimycotics solution 100x (Sigma-Aldrich). When cell cultures were amplified for protein production or virus production, the cell culture volume was transferred into 500 ml cell roller flasks with filter cap (Greiner) and doubled in volume with every other day while its concentration still remains under 3 million cells/ml until the cell culture reach the demanded amount (described below).

2.6.4 Infection and harvest of Sf9 cells for protein production

For each protein production, 2.5 L-3.5 L of cell culture at 1.8 million cells/ml was used. Five ml of P3 virus were added for every 500 ml of Sf9 cells. The culture was kept at 26°C shaking for 72 h and then centrifuged 8500 rpm for 20 min (with Ja-10 rotor in Beckman J2-HS centrifuge). Then the pellets were re-dissolved in 30 ml of insect cells lysis buffer. The lysate was then snap frozen and kept at -80°C until being used for protein purification.

2.6.5 Freezing and preserving a Sf9 cell culture

A healthy Sf9 cell culture was grown to reach the desired concentration in complete Sf9 cell medium, supplemented with antibiotics and antimycotics. The amount of required freezing medium was calculated and made in advance, which is composed of 50% fresh medium and 50% conditioned growth medium (day 2-4 cell conditioned media collected from Sf9 cultures during subculture procedure) and DMSO to a final concentration of 7.5%. The cells were pelleted and re-suspended in freezing medium

to reach a density of 1×10^7 cells/ml. The culture is moved gently and aliquoted into cryo vials of proper volume. The vials were snap frozen at a controlled rate of decreasing temperature ($-1 \text{ }^\circ\text{C}/\text{min}$) in a -20°C rack system.

2.6.6 Purification of recombinant protein from Sf9 cells

The protein purification from Sf9 cells was performed with affinity chromatography to isolate the over expressed protein:

- 1) The pellet of the cells in the 50 ml falcon tube was thawed and transferred to a Glass Dounce homogenizer, where the cells were lysed by physical force.
- 2) The homogenate was centrifuged at 8500 rpm for 20 min (Ja-10 rotor in Beckman J2-HS centrifuge) to pellet the cell debris. The supernatant was transferred into an empty clean 50 ml falcon tube. Thirty μl of the supernatant was kept for SDS-PAGE in step 11. Then, 2.5 ml of Ni-NTA (resin volume) and 0.5 M NaCl was added into the supernatant. The 50ml Falcon tube was rotated at 4°C for 1.5-3 h to bind the recombinant His-tagged protein onto the resin. The blue resin turns into light blue when the protein is bound.
- 3) After the incubation, the resin was pelleted by 2 min centrifugation at 5000 rpm (Eppendorf 5804 R). The resin was washed in batch with Buffer A (1 L, 50 mM Tris, 0.5 M NaCl, 10 mM Imidazol, PMSF, 200 μl of β -mercaptoethanol) 20 times to remove unspecific lipid and proteins bound to the resin.
- 4) The resin was placed in a column and then washed in the column by a gravity flow using 1L of buffer A overnight.
- 5) Forty ml of elution buffer (Buffer A with 200 mM Imidazol) was added to re-suspend the resin. The resin was allowed to re-settle and the elution buffer was collected by gravity flow. The resin returned to its original color when the bound protein was released.
- 6) The eluent was measured for its protein concentration using the Bradford assay. Thirty μl of the eluent was removed and kept for the SDS-PAGE. The fractions containing the protein of interest were pooled and measured for protein concentration.
- 7) The pooled sample was then injected into the sample loop of the ÄKTA purifier 900 (GE healthcare), which is equipped with Hiload 16/60 superdex 200 gel filtration column (GE healthcare). The FPLC was programmed for size exclusion

chromatography with the filtered running buffer (containing 200 mM NaCl, 20 mM Tris, 1 mM DTT).

8) The fractions containing the protein of interest were pooled and measured for protein concentration.

9) The sample was then concentrated in a viva spin 20 concentrators (Sartorius). The concentrator was centrifuged for 3-5 min at 4000 rpm to reduce the sample volume. The Centrifugation step was repeated until the sample volume was optimal for gel filtration (concentration not higher than 5 $\mu\text{g}/\mu\text{l}$). In the interval between each centrifugation, the sample was homogenized to assure that no precipitate was formed by over concentration of protein near the filter.

10) In the end, the sample was filtered in Ultrafree-MC (Milipore) tubes to remove any remaining precipitates or contaminants and was then aliquoted, snap frozen and stored at -80°C .

2.6.7 Purification analysis of recombinant protein from Sf9 cells

The concentration of His-CaPkh2 reached after step 9 of Item 2.6.6 was of 5,6 $\mu\text{g}/\mu\text{l}$. The spectrophotometry analysis of the AKTÄ purification showed 3 overlapped peaks of different sizes (Figure 2.2B). This phenomena usually indicates that the protein is forming multimers in the buffer solution. In this case it may be equilibrium of monomer, dimer and tetramer. To verify that it is a reversible equilibrium and discard the possible contamination of others size proteins I then loaded each peak onto a SDS gel PAGE to check whether the putative dimers and tetramers are formed by single CaPkh2 proteins that after a denaturation process with DTT and β -mercaptoethanol are forming single species. The result of SDS PAGE confirmed that the protein is pure and is not contaminated with any other substance (Figure 2.2A). For PDK1 it was suggested recently a dimeric state giving an additional role to its PH domain, which collaborates in the interaction (Ziemba, Pilling et al. 2013). Thus, the different behaviors of CaPkh2 open future studies to see whether the oligomerization of CaPkh2 existed also in vivo.

CaPkh2 has an isoelectric point of ~ 7.3 (Figure 2.2C) which corresponds with the theoretical estimation (Figure 2.2D) and from the SDS gel PAGE results, the molecular weight fit with the full length. It is also interesting to emphasize that neither the GST-Pkh2 nor His-Pkh2 showed important degradation products.

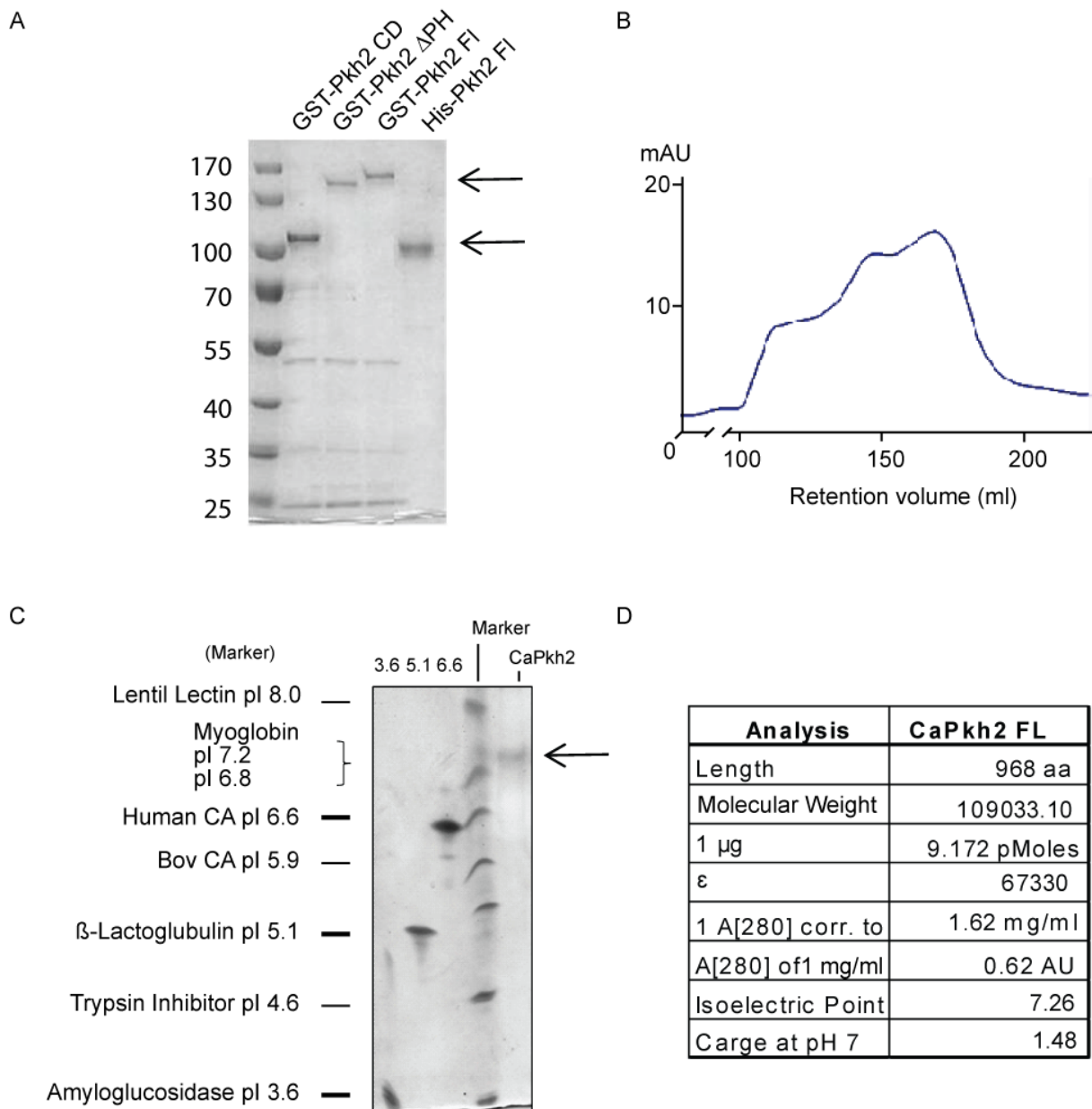


Figure 2.2 Analysis of CaPkh2 purification constructs. A) SDS PAGE gel with CaPkh2 constructs. On each well 1 μ g was loaded. PageRuler Prestained Protein Ladder was used as a molecular weight marker. B) Gel filtration chromatography of CaPkh2 FL over-expressed in Sf9 cells. Purification was performed on ÄKTA purifier. X-axis is the retention volume of the protein samples. Y-axis marks the absorbance measured in real-time by UV unit at 280nm. C) IEF gel. One μ g of His-Pkh2 FL protein was loaded. D) Biocomputational analysis of His-Pkh2 FL protein.

2.7 Isoelectric focussing

Isoelectric focussing (IEF) was used to check the homogeneity of protein samples. For IEF, precast Novex IEF Gel, 50X Novex IEF Anode Buffer, Novex IEF Cathode Buffer pH 3-10 (10X), pH marker and loading buffer (Invitrogen) were used. The upper chamber was filled with 200 ml of cathode buffer (1X) and lower chamber with 600 ml of anode buffer (1X). A 1:1 mixture of loading buffer and protein sample were loaded into the gel. The gels were run at 100 V constant for 1 h, 200 V constant for 1

h and then 300 V 30 min. After electrophoresis, samples on gel were fixed with 12% of TCA (Sigma-Aldrich) containing 3.5% sulfosalicylic (Sigma-Aldrich) acid for 30 min. Gels were stained with Commassie blue, dried and kept.

2.8 Western Blot

Forty μg of total protein was fractionated by 10% SDS-PAGE and transferred to nitrocellulose membranes (Protran BA83, Whatman). Membranes were incubated with the indicated antibodies for 12 h at 4°C. For immunodetection of actin, membranes were stripped with the Restore Western Blot Stripping Buffer (Thermo Scientific) for 30 min at 37 °C. Membranes were then incubated for one hour with a 1:2000 dilution of the AC-15 monoclonal anti- β -actin antibody (Sigma-Aldrich). A 1:5000 dilution of horseradish peroxidase-conjugated anti-rabbit (BioRad) or anti-mouse IgG (Sigma-Aldrich) were used as secondary antibodies. Immunodetection was carried out in all cases using the Luminata Forte Western HRP substrate detection system (Millipore) and chemiluminescence detected using the LAS-4000 imaging system (Fuji).

2.9 In vitro measurement of protein kinase activity

We have modified the traditional in vitro protein kinase activity assays using radio-labelled ATP (ATP γ) and performed in 96 well format followed by evaluation using phosphoimager technology (Fuji FLA9000). The kinase activity was performed principally for PDK1 and its homolog in *C. albicans*, CaPkh2. In addition, other kinase activity such as PKB/Akt and SGK were measured. As a substrate for PDK1 and CaPkh2, the PDK1 substrate T308tide (KTFCGTPEYLAPEVRR) was used, polypeptide sequence for the phosphorylation site on PKB/Akt. This peptide substrate allows the characterization of activators and inhibitors of PDK1. PIFtide was used to activate the kinase. It is a polypeptide that corresponds with the 24 C-terminal residues of PRK2. The components of the reactions varied in different experiments. The kinase and substrate were mixed with 50 mM Tris-HCl pH 7,5 and β -mercapthoethanol. To test different concentrations of compounds, a stock compound of 20-25 mM was dissolved in DMSO. The final v/v percentage of DMSO in the reaction was 1%. The compound was incubated with the kinase mix at RT and a second mix of [γ 32P] ATP (5–50 c.p.m./pmol) (GE Healthcare, stock solution at 3000 Ci/mmol), cold ATP (100 μM) and MgCl_2 (10 mM) in a final volume of 20 ml. To

stop the reaction 5 μ l 0,01% of phosphoric acid was added. The reaction was spotted on to P81 phosphocellulose paper (Whatman) by a pipetting station (ep motion 5070, Eppendorf). The P81 paper was washed three times with 0,01 % of phosphoric acid to remove [32P] ATP unbound. The dried P81 paper was then exposed on the phosphoimager cassettes (Fuji) overnight. Then the cassettes were read in LAS-9000 imaging system (Fuji).

2.10 His-CaPkh2 and His-PDK1 interaction with biotin-PIFtide and displacement of the Interaction using AlphaScreen technology

The AlphaScreen assay (Perkin-Elmer) was performed according to the manufacturer's protocol in 384-well microtiter plates. The His-CaPkh2 interaction with biotin-PIFtide was evaluated in a similar setup as previously performed with His-PDK133 but with variations in the order of addition of the beads and the incubation times and varying PIFtide and PDK1/CaPkh2 concentrations according to the cross-tritration set up experiment (Figure 2.3). Incubations were performed in white 384-well microtiter plates (Greiner) containing 20 μ L of a reaction mix and 5 μ L of beads. The reaction mix contained 50 mM Tris-HCl (pH 7.4), 100 mM NaCl, 1 mM dithiothreitol, 0.01% (v/v) Tween-20, 0.1% (w/v) BSA, 1 mM DMSO, 100 nM His-CaPkh2 or 100 nM His-PDK1, 50 nM Biotin-PIFtide, and the indicated concentrations of unlabeled PIFtide or small compounds. Subsequently, 5 μ L of beads solution containing nickel chelate-coated acceptor beads and streptavidin-coated donor beads (20 μ g/mL final concentrations) was added to the reaction mix. The reaction mix and the beads were incubated in the dark for 45 min at RT and the emission of light from the acceptor beads was measured in the EnVision reader (Perkin- Elmer) and analyzed using the GraphPad Prism software.

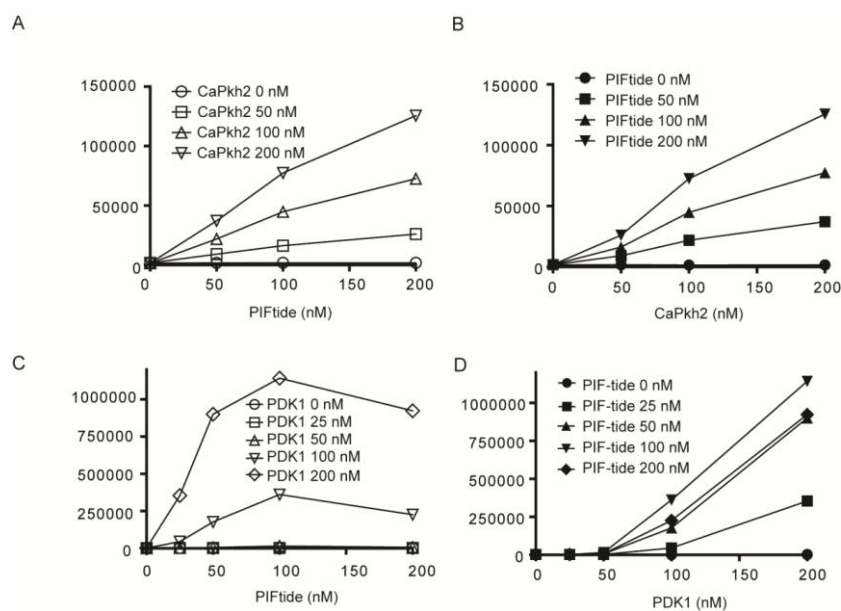


Figure 2.3 Conditions for measuring the interaction of PDK1 and CaPkh2 with PIFtide using AlphaScreen technology. Kinase and PIFtide cross-titrations are performed to identify the conditions to be used for the interaction-displacement assay with compounds. A-B) His-CaPkh2 and Biotin-PIFtide cross-titration. C-D) His-PDK1 and Biotin-PIFtide cross-titration.

2.11 Interaction of GST-Pkh2 with lipids

Protein domains that specifically bind phosphoinositides have emerged as major determinants in localizing proteins to their site of function for the regulation of kinase activity. These phosphoinositide-binding motifs, which include the C2 (PKC conserved region 2), PH (Pleckstrin homology), FYVE (Fab1p/YOTP/Vac1p/EEA1), ENTH (Epsin NH2-terminal homology) and PX (Phox homology) domains, are found in proteins implicated in a diverse array of cellular processes, such as actin cytoskeletal organization, cell growth regulation, control of gene expression, protein transport, exocytosis and endocytosis. With PIP Strips and Sphingostrips is possible to identify in a protein lipid overlay assay (Dowler, Kular et al. 2002).

Experimental procedure:

- 1) The membrane was blocked using TBS-T + 3% fatty acid-free BSA, and gently agitated for one hour at room temperature.
- 2) The membrane was Incubated using 0.5 $\mu\text{g}/\text{mL}$ of the desired protein (Table 3.1) in TBS-T + 3% fatty acid-free BSA at room temperature.
- 3) The membrane was washed with TBS-T + 3% fatty acid-free BSA three times using gentle agitation for 10 minutes each time. This wash step was repeated between all incubation steps and before detection.

4) For detection of GST fusion proteins, a highly purified rabbit polyclonal anti-GST antibody (A5800) in conjunction with horseradish peroxidase (Sigma-Aldrich) was used and chemiluminescence was detected using LAS-4000 imaging system (Fuji).

2.12 Yeast cell strains and culture conditions

Yeast strains used in this work derive from CML476 and BY4741. In the case of Two-hybrid screenings, AH109 strain was used. The strains are described in Table 2.4. *S. cerevisiae* cells were grown in YPD medium (10 g/l yeast extract, 20 g/l peptone and 20 g/l dextrose) at a constant temperature of 28° except when stated otherwise. The SD medium, Synthetic Completed Medium (6.70g/l yeast nitrogen base, 20 g/l glucose) supplemented with *drop-out* medium (a mix of aminoacids that lacks the adequate components for select auxotrophy) was used for the selection of mutations plasmids and check positive interactions in Two-hybrid experiments.

Table 2.4 Yeast strains used

Strain	Relevant genotype	Source/Ref.
CML476	<i>MATa ura3-52 leuΔ1 his3Δ200 GAL2 CMVp(tetR¹-SSN6)::LEU2 trp1::tTA</i>	a
MB002	<i>MATa CML476 KanMX4-(tetO₇):PKH2</i>	Present study
MB005	<i>MATa CML476 KanMX4-(tetO₇):PKH2 pkh1::HIS3</i>	Present study
SDP7	<i>MATa CML476 KanMX4-(tetO₇):PKH2 pkh3::nat1</i>	Present study
SDP8	<i>MATa CML476 KanMX4-(tetO₇):PKH2 pkh1::HIS3 pkh3::nat1</i>	Present study
SDP10	<i>MATa ura3-52 leuΔ1 his3Δ200 GAL2 CMVp(tetR¹-SSN6)::LEU2 erg6::TRP1</i>	Present study
YAB100	<i>MATa CML476 KanMX4-(tetO₇):PKH2 pkh1::HIS3 mca1::nat1</i>	Present study
BY4741	<i>MATa his3Δ1 leu2Δ met15Δ ura3Δ</i>	b
Y04300	<i>BY4741 pkh3::KanMX4</i>	b
Y06988	<i>BY4741 pil1::KanMX4</i>	b
Y07338	<i>BY4741 lsp1::KanMX4</i>	b
Y01328	<i>BY4741 bck1::KanMX4</i>	b
YPP64T	<i>MATa ade2 trp1-901 leu2-3,112 lys2-801am his3-200 lys2::(lexAop)4-HIS3 ura3-52::ura3 (lexAop)8-lacZ pdr5:: loxP, snq2:: loxP, yor1:: loxP, pdr1:: loxP, pdr3:: loxP</i>	c
YPP66	<i>MATa Gal4-452 Gal80-538 ade2-101 his3-200 leu2-3,112 trp1-901 ura3-52 lys2-801 URA3::UASGAL1-LacZ lys2::GAL1UAS-GAL1TATA-HIS3 cyhR pdr5:: loxP, snq2:: loxP, yor1:: loxP, pdr1:: loxP, pdr3:: loxP</i>	c
AH109	<i>MATa leu2-3, 112 ura3-52 trp1-901 his3-200 gal4Δ gal80Δ GAL2-ADE2 lys2::GAL1-HIS ura3::MEL1-lacZ</i>	d

a: (Yen, Gitsham et al. 2003), b: (Winzeler, Shoemaker et al. 1999), c: kindly provided by Hybrigenics Services, France. d: (James, Halladay et al. 1996),

2.13 Construction of mutated yeast strains

2.13.1 Insertion of *tetO₇* promoter

In order to drive the expression of *PKH2* from the regulatable *tetO₇* promoter, we replaced, by homologous recombination, the region comprised between nucleotide -487 and the initiating codon of the chromosomal *PKH2* coding region in the CML476 (WT) strain, with a KanMX4-*tetO₇* cassette, obtaining the MB002 strain (Table 2.4). This substitution is positioned in a 1.3 Kbp intergenic region containing divergent promoters. The KanMX4-*tetO₇* cassette, containing long flanking homology regions, was PCR-amplified, from the pCM325 plasmid, with the forward oligonucleotide OACG304, where the underlined sequence corresponds to nucleotides -487 to -446 respect the *PKH2* initiator codon, and the reverse oligonucleotide OACG305, where the underlined sequence begins at +37 and finishes at the ATG start codon of *PKH2* (in bold) (Table 2.2). Italicized nucleotides in the primers correspond to pCM325 sequences.

To generate the *pkh1Δ::HIS3* mutation, the *HIS3* gene was amplified using the forward oligonucleotide OACG300 and the reverse OACG301 as primers. The underlined sequences correspond to nucleotides -41 to -1 respect the *PKH1* initiator codon (OAC300) and to nucleotides 69 to 25 after the *PKH2* stop codon (OAC301). Italicized sequences correspond to the limits of the *HIS3* gene present in the pRS423 plasmid, used as a template.

The disruption the coding region *PKH3* with *nat1* in MB002 and MB005 strains gave rise to the SDP7 and SDP8, respectively. The KanMX4 cassette from the *pkh3Δ::KanMX4* strain in the BY4741 background, generated in the context of the *Saccharomyces* Genome Deletion Project, was replaced by homologous recombination with the 1.2 Kbp BamHI/EcoRI restriction fragment from the pAG25 plasmid containing the *natMX4* cassette. The insertion of the cassette in the proper genomic localization was verified by PCR and also by the ability of the strains to grow in the presence of nourseothricin but not G418. A genomic region from this new strain, including the full neoMX4 cassette inserted into the *PKH3* ORF, that comprise from the nucleotide -512 upstream the ATG of *PKH3* to the nucleotide +400 respect the *PKH3* stop codon was PCR-amplified with the oligonucleotides ODP18 and (Table 2.2) as a forward and reverse primers, respectively. This ~1.5 kbp PCR-

amplified fragment was used to disrupt the *PKH3* ORF in the MB002 and MB005 strains, giving rise to the SDP7 and SDP8 strains, respectively. The correct insertion of the cassette was verified by PCR.

The natMX4 cassette was amplified from pAG25 using the forward MCA1-nat1_fw1 primer 4, where the underlined sequence corresponds to nucleotides –40 to –1 from the *MCA1* initiator codon, and the reverse primer MCA1-nat1_rv1 4, where the underlined sequences correspond to nucleotides +41 to +1 respect the *MCA1* stop codon. The italicized nucleotides correspond to limits of the natMX4 cassette present in pAG25 plasmid. To generate the YAB100 strain, the *MCA1* coding region in the MB002 strain was disrupted with the PCR-obtained natMX4 cassette. Disruption was verified by PCR with appropriate primers.

2.13.2 Depletion of Pkh

To evaluate the effect of depletion of Pkh2, wild type CML476 as well as the conditional *tetO:PKH2* mutant (MB002) and the different derivative strains used in this study were grown overnight in YPD, diluted in the presence of 100 µg/ml doxycycline to A_{660} of 0.05, growth resumed at 28 °C for 8 h, re-diluted to A_{660} of 0.01 in the presence of doxycycline (100 µg/ml) and grown for 16 h. Samples were taken at the indicated time points, the A_{660} of the culture measured and the cells centrifuged for 5 min at 1200 g. Doxycycline treatment was renewed every 12 hours to account for possible degradation of the drug.

2.14 RNA isolation

For RNA preparation, cultures were grown for 8 h in the presence of doxycycline until they reached an optical density of 0.55-0.60, and samples were taken for RNA purification (8 h time-point). For the time-point of 24 h and heat shocked cells, the appropriate quantity of cells were collected by centrifugation, resuspended in 50 ml of YPD at an optical density of 0.01, treated with 100 µg/ml of fresh doxycycline and grown for additional 16h. At this point, cells for the 24 time-point were collected and cell for the heat shock experiment were incubated either at 40 °C or 28° C for 40 minutes. Collected samples were washed with cold water and the dried cells pellet kept at -80 °C until RNA purification.

Total RNA was extracted with a RiboPure™ Yeast (Ambion) kit and treated with DNase to eliminate traces of genomic DNA. RNA quality was assessed by electrophoresis in a denaturing 0.8% agarose gel and quantified by measuring A_{260} in a BioPhotometer (Eppendorf).

2.15 DNA microarray analysis

In total, 8 µg of total RNA was employed for cDNA synthesis and labeling, using the indirect labeling kit (CyScribe Post-Labeling kit, GE-Amersham Biosciences) in conjunction with Cy3-dUTP and Cy5-dUTP fluorescent nucleotides. The cDNA obtained was dried and resuspended in the hybridization buffer. DNA amount and labeling efficiency was evaluated with a Nanodrop spectrophotometer (Nanodrop Technologies). Fluorescently labeled cDNAs were combined and hybridized to yeast genomic microchips constructed in our laboratory (Autonomous University of Barcelona) by arraying 6014 different PCR-amplified open reading frames (ORFs) from *S. cerevisiae* (Alberola, Garcia-Martinez et al. 2004). Pre-hybridization, hybridization and washing conditions were essentially as described previously (Hegde, Qi et al. 2000). Slides were scanned with a ScanArray 4000 apparatus (Packard BioChips Technologies) and the output analyzed using GenePix Pro 6.0 software. Spots with either a diameter smaller than 120 µm, or fluorescence intensity of Cy3 (indocarbocyanine) and Cy5 (indodicarbocyanine) lower than 150 units, were not considered for further analysis.

Four different microarray experiments were performed, each in duplicate (dyes were swapped to avoid dye-specific bias). In a first set of experiments we compared the expression profile of WT CML476 cells with that of SDP8 cells, both exposed to doxycycline for a total time of 8 or 24 h in YPD media. In the second series of experiments we compared the transcriptomic profiles of WT CML476 and SDP8 cells treated with doxycycline for 24 h and heat-shocked for 40 minutes at 40 °C with those of the same cells in the absence of the stress. The data from duplicate experiments were combined, and the mean was calculated. A given gene was considered to be induced or repressed when the expression ratio was higher than 2.0 or lower than 0.50 respectively. The GEPAS3.0 software, now implemented in the Babelomics tool (<http://babelomics.bioinfo.cipf.es/>) was used to pre-process the data. The MIPS Functional Catalogue Database (available at http://mips.helmholtz-muenchen.de/proj/funcatDB/search_main_frame.html) was used for the functional

distribution of gene lists. To identify the potential role of Pkh in the regulation of transcription factors under a heat stress, we used the documented direct evidences for transcription factor binding sites available at the YEASTRACT database.

2.16 Preparation of yeast extracts and immunoblot analysis

For immunodetection of the Slr2 MAPK, cultures were stressed by an alkaline shock by the addition of KOH (or KCl in control experiment) to reach a final concentration of 35 mM, as described in Serrano et al. (Serrano, Martin et al. 2006). After 15 min, 50 ml of the cell culture was harvested by sedimentation (1500 x g) at 4 °C, washed with prechilled phosphate-buffered saline (PBS), snap-frozen, and kept at –80 °C.

2.17 Reactive Oxygen Species detection

Cultures in YPD medium at A_{660} 0.01 were incubated and grown as described in Item 2.13.2 for 24 h in the presence of doxycycline (100 µg/ml). Cells were then incubated for 1 h with 2.5 µg/ml of the fluorogenic indicator dihydrorhodamine 123 (DHR 123) (Sigma-Aldrich), harvested by centrifugation, resuspended in PBS solution and examined through a fluorescein filter using an Olympus FluoView™ FV1000 confocal. Images were processed with the ImageJ 1.44p software (<http://rsb.info.nih.gov/ij/>). For evaluation of oxidative stress by flow cytometry, cells from the same treated cultures were fixed with 3.7% (vol/vol) formaldehyde for 30 min and sonicated for 10 seconds with intervals of 1 second on ice before analysis. The fluorescence of 10000 cells included in the SSC-H, FSC-H upper right quadrant was then analyzed using a BD Biosciences FACScan Cytometer. Parameters were set at excitation and emission settings of 304 nm and 551 nm (filter FL-1), respectively.

2.18 Programmed cell death assays

Programmed cell death (PCD) assays were conducted by detecting the terminal deoxynucleotidyl transferase-mediated dUTP nick end labeling (TUNEL) with the In Situ Cell Death Detection Kit, Fluorescein (Roche) in cell cultures treated with doxycycline for 24 h as described in the previous section. Cells contained in 50 ml of culture were then washed, resuspended in PBS at $A_{660} \approx 1$ and fixed with 3.7% (vol/vol) formaldehyde for 30 min at room temperature. Fixed cells were washed three times with PBS and resuspended in 2 ml of PBS. Cell walls of WT, MB005 and SDP8 strains were digested with 20 mg/ml Zymolyase 20T (Seikagaku Biobusiness)

at 37 °C for 55 min, 45 or 20 min, respectively, in order to reach the same number of spheroplasts for each strain (about 80% of the cells). Spheroplasted cells were washed three times with PBS containing 1M sorbitol, incubated for 2 min on ice with permeabilization solution [0.1% Triton X-100 and 0.1% sodium citrate], washed twice with the PBS-sorbitol buffer, incubated for 60 min at 37 °C with 50 µl buffer and the incubated Spheroplasts were finally rinsed three times with PBS-sorbitol, resuspended in 2 ml of PBS and analyzed using Becton Dickinson FACSCalibur apparatus. For microscope visualization, 10 µl Vectashield antifading agent (Invitrogen) was added. Microscopy observation and processing of images were performed as described for ROS analysis (Item 2.14 RNA). The percentage of TUNEL-positive nuclei was calculated from the 10000 counts of FACS and was analyzed with the software Cyflogic v.1.2.1 (Cyflo Ltd.).

2.19 Generation of Pkh2 *Candida albicans* synthetic gene

For the expression of Pkh2 of *C. albicans* in insect and mammalian cells, a new synthetic gene coding for the aminoacids in the universal codon usage were used (See Appendix 4.1). The codon usage was optimized for a better expression in mammalian cells. Therefore, the codons were changed keeping the same coded aminoacids for the most useable codons in *Homo sapiens*.

To develop a synthetic gene, bioinformatic tools were used. NCBI data base was used to find gene sequences. The codon usage of the study organism was identified in the Codon Usage Database (<http://www.kazusa.or.jp/>). Mr.Gene software was used to optimize the code sequence and CUG nucleotide codon was translated in *C. albicans* for Serine and not for Leucine.

2.20 Two-hybrid screening

Yeast Two-hybrid system is a powerful assay to identify novel protein-protein interactions inside a eukaryotic cell environment. The assay is based on the fusion of a bait protein with part of the transcription factor Gal4, the GAL DNA-binding domain while another gene or cDNA is expressed with the other part of Gal4, GAL4 activation domain (Figure 2.4). When both bait protein and cDNA interact inside the nucleus, GAL DNA-binding domain and GAL4 activation domain are brought into proximity and activate the transcription of reporter genes under the control of the upstream activating sequences (UAS) (Fields and Song 1989).

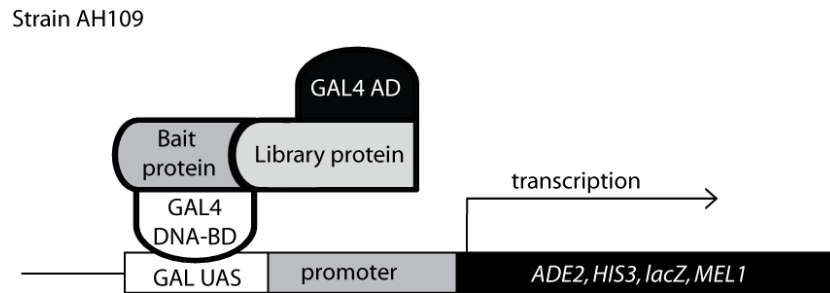


Figure 2.4 The interaction between proteins activates a set of reporter genes in AH109 strain. AH109 includes *ADE2* and *HIS3* nutritional markers and *lacZ* reporter gene. *MEL1* is a GAL4-endogenous-responsive gene. *HIS3*, *ADE2*, *lacZ* and *MEL1* genes are under the control of 3 heterologous GAL4-responsive UAS and promoter elements (GAL1, GAL2, MEL1, MEL1 respectively).

2.20.1 RNA isolation of the different morphogenetic states of *C. albicans*

To increase the positive hits in the Two-hybrid screening of the protein Pkh2, a cDNA library of the three different morphogenic forms of *C. albicans* was generated. For the yeast bud state, cells were grown in YPD and collected in log phase. For the preparation of the inocula for the two morphogenic states, pseudo hyphae and hyphae, the same procedure was done. Yeast were grown during 48 hours in YPD agar + Uridine (25 ug/ul) 28°C. Uridine was used as a complement for the mutation of *ura3Δ* in the CA14 Candida strain. A loopful of yeast was inoculated in YPD + Uridine (25μg/ml) and grown at 26°C overnight with continuous shaking. The cells were harvested by centrifugation and washed twice in sterile water. Then, 5×10^6 cells/ml were starved by growing them in 0,15 M NaCl, in phosphate buffer pH 6,8 for 24 h with continuous shaking at 26°C. Cells were then counted to check that the cfu should be $< 7 \times 10^6$. The nonuse aliquots were stored with 15% glycerol at -80°C . For the hyphae form, 199 Medium with glutamate and carbonate (Sigma-Aldrich) was used. Starved cells at $> 10^6$ cells/ml were inoculated in a ratio of 1/1000 in 199 Medium and grown with continuous shaking at 37°C for 6 hours. Then, culture was measured in a spectrophotometer and the cells checked in a confocal microscope to verify the hyphae state. For the pseudohyphae state, cells from starvation were inoculated with a ratio of 1/1000 in Soll medium (10g glucose, 10g Bacto-peptone, 1g $\text{MfSO}_4 \cdot 7\text{H}_2\text{O}$, 2,2g KH_2PO_4 , 1g K_2HPO_4 , 1g yeast extract, 20g Bacto-agar) + 25ug/ml uridine. The culture was grown with continuous shaking at 28°C for 48 h. Cells from the saturated culture were inoculated in new Soll medium and grown 3-5 h at 37°C and continuous shaking. The cells were stored harvested by centrifugation

and stored at -80°C . RNA was extracted as described in Item 2.14 (Odds 1985; Merson-Davies and Odds 1989; Sudbery, Gow et al. 2004).

2.20.2 LiAc yeast transformation for Two-hybrid assay

Simultaneous vs. sequential transformations

The efficiency of preparing competent yeast cells by the LiAc method is about 10^5 colonies per μg of DNA when using a single type of plasmid. In experiments where the presence of 2 plasmids inside the host cell is required, such as two-hybrid assay, the simultaneous cotransformation reduces the efficiency to a magnitude lower due to lower probability that a particular yeast cell will take both plasmids. The efficiency is even lower if one of the plasmids is lineal and is transformed with a ssDNA fragment that keeps homology in the 3' and 5' ends with the 3' and 5' ends of the linealized plasmid. In this case, the homology recombination reduces the probability of transformation and recircularization

Therefore, to increase the probability of cotransformation with the linealized plasmid, the sequential transformation was chosen. To provide controls for cotransformation efficiency, the colonies were spread in serial dilutions on 100-mm SD agar plates of 1:10, 1:100 and 1:1000. The plates were incubated up-side-down at 30°C until colonies appear (generally, 2–4 days).

2.20.3 cDNA library *C. albicans* and pGBKt7-Pkh1 generation

cDNA library was generated according to the Matchmaker™ Library Construction & Screening Kits (Clontech). The RNA used for the cDNA construction was a mixture of RNA of the three different *Candida* morphogenic forms of *C. albicans* (See Item 2.20.1). Duplicates of firsts-strand cDNA synthesis were extended with SMART III oligonucleotides (Table 2.2) by MMLV Reverse transcriptase. The ss cDNA was amplified by Long Distance PCR (LD-PCR) and a small alicuot of $7\mu\text{l}$ (7% v/v of the total) was analyzed on a 1,2% agarose /EtBr gel. Then, the product was purified with a CHROMA SPIN TE-400 column; the TE-400 columns are used to select for DNA molecules $>200\text{bp}$. The duplicate experimental samples were combined in a single tube and 1/10 vol of sodium acetate (3M; pH 4.8) and 2.5 vol. 95% ethanol (-20°C) for the cDNA precipitation was added.

2.20.4 Constructing and screening the Two-hybrid library

To increase the efficiency, the screening of the Matchmaker library was made by cotransformation in two steps. First, pGBKT7-Pkh2 was transformed in AH109 cells. Then, the cells containing the plasmid were cotransformed with the SMART-cDNA library and pGADT7-Rec open plasmid. The procedure followed was the subsequent.

The following SD plates were prepared: Five 100-mm plates of each Drop out medium SD/-Leu, SD/-Trp, SD/-Leu/-Trp. And 20 150-mm plates of each drop out medium SD/-His/-Leu/-Trp, SD/-Ade/-His/-Leu/-Trp/X- α -Gal. The plates were allowed to dry at RT for 2-3 days.

A control in small-scale was done before the cDNA library transformation (Table 2.5). A standard yeast transformation was followed with an additional step after the heat shock at 42°C that consists in the incubation of the cells in 1ml YPD Plus Liquid Medium at 30°C for 90 min. The sample was mixed every 15 min by gentle vortexing. After the incubation, 100 μ l cells of 1:10, 1:100 and 1:1000 were spread onto 100-SD agar plates SD/-Leu/-Trp to check cotransformation efficiency and SD/-Leu/-Trp/X- α -Gal to select for cotransformants expressing interaction proteins. The plates were incubated at 30°C for 2-4 until colonies appear.

Table 2.5. Small scale control

Component	Positive control (μ l)	Negative control (μ l)
SV40 Large T PCR Fragment	5,0	5,0
pGADt7-Rec (Small-linearized; 500ng/ μ l)	0,5	0,5
pGBKT7-53 (500ng/ μ l)	0,5	-
pGBKT7-Lam (500 ng/ μ l)	-	0,5
Herring Testes Carrier DNA (10mg/ml), denatured	5	5
AH109 Competent Yeast Cells	50	50
PEG/LiAc Solution	500	500

2.20.5 Set-up for control Two-hybrid cotransformation

To increase the efficiency, pGBKT7-CaPKH2 was transformed in AH109 competent cells (Table 2.3). AH109 cells containing pGBKT7-CaPKH2 were used as competent cells for the cotransformation of the SMART cDNA library and the linearized plasmid

pGADt7-Rec. For the transformation, the protocol from the manufacturer was followed (Matchmaker, Clontech). The transformation mixture was spread onto a triple drop out media (TDO) lacking His, Leu and Trp (SD/-His/-Leu/-Trp), 150µl on each, and incubated at 30°C until colonies appear. The colonies grown onto TDO were streaked onto quadruple drop out media (QDO), SD/-His/-Leu/-Trp/-Ade, to recheck positive colonies and incubated at 30°C until new colonies appear. An additional control was used streaking QDO colonies onto SD/-Leu/-Trp/X-α-Gal to select interactions. For the rescue of Library cDNA insert, blue colonies were catalogued and the pGAD-cDNA plasmid was extracted and transformed in *E. coli* competent cells. The cells were spread onto 50µg/ml ampicillin LB plates. *E. coli* colonies containing pGAD-cDNA plasmid were incubated at 37°C for further plasmid extraction by miniprep (Qiagen). The plasmid was sequenced with T7 Sequencing (Table 2.2). The sequences were verified with the presence of an open reading frame fused to the GAL4AD sequence and compared to those in GenBank database.

2.21 Novel protocols performed for testing compounds in vivo

2.21.1 Assay for testing compounds in yeast cells on agar

The classical problems found working with small compounds are:

- Few amount of compound available that limits the use of big YPD agar volume.
- Low compound solubility.
- The less YPD agar used for the plates preparation the faster solidification.

Solutions: Pre-heat medium with agar in small volume (1 ml or 5 ml). Use thermo-block of 15 ml falcon or Eppendorf. Temperature below of 65 °C is required due to the possibility of compound degradation if the temperature is higher. Add compound to the 1 ml or 5 ml medium and homogenize pipetting few times (0,2-0,5 % DMSO maximum). As a control, plates are prepared containing the equivalent concentration of DMSO.

2.21.2 Test compounds in suspension growth in 96 well plates

To determine the cell growth inhibition in presence of compounds, a suspension growth assay in parallel with the growth in agar plates was performed. Yeast colonies were picked from a fresh agar dish, grown overnight and diluted into a new YPD

media at OD_{630nm} 0.01. The compound diluted in DMSO was added for a final volume of 200 µl of YPD and a maximum DMSO concentration of 0,5%. The 96 well plate was incubated in a humid chamber at 30°C for 16 hours and the culture was measured every 2 hours in a 96well plate reader (Eppendorf) at the absorbance of 595_{nm}.

Compounds found targeting Aurora B in mammalian cells are toxic for *Candida* cells.

The validation of in vitro initial hits of our focused compound library of 800 small compounds and our 14000 compounds commercial library (Hit-finder, Malbridge) is usually tested in mammalian cells with the aim of finding selective compounds against certain cancer types. However, it was of our interest to set up a platform for testing the effect of drugs in yeast. One project followed in Research Group Phosphosites was the screening to find selective compounds for Aurora B in mammalian cells. Thus, some compounds found inhibiting Aurora B were potential inhibitors for the homolog in *S. cerevisiae* and *C. albicans*, Ipl1. In both organisms it is conserved only one isoform of Aurora that encompasses the function of the three mammalian isoforms Aurora A, B and C. To check if compounds targeting Aurora B in mammalian cells are also toxic in yeast cells I tested with the above described protocols in suspension and solid medium the growth effect under different concentrations of compound PSX137 in *Candida* strains kindly provided by Dr. Volkhard A. J. Kempf from the "Institute for Medical Microbiology and Infection Control, University Hospital of Frankfurt" and all experiments were done in the S2 laboratory facility of the Institute (Figure 2.5). Additional controls to verify the specificity of the compound in *C. albicans* Aurora (Ipl1) are listed in Appendix 4.2. The results revealed that PSX137 is toxic to different *Candida* strains.

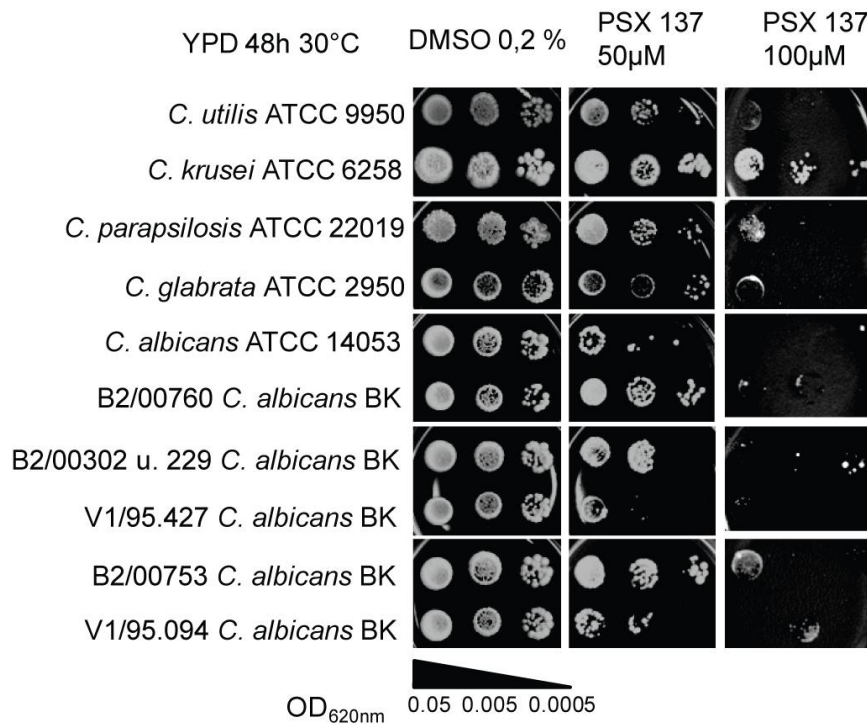


Figure 2.5 Toxicity of PSX137 in *Candida* strains in solid growth. Five *Candida* strains from a ATCC collection and five multiresistant *C. albicans* from blood samples were tested. Yeast cells were grown at 30°C until they reached the exponential phase. 10-Fold dilutions of the cultures were prepared, and spotted on YPD medium containing 0,2 DMSO as a control, and 50μM and 100μM of PSX137compound.

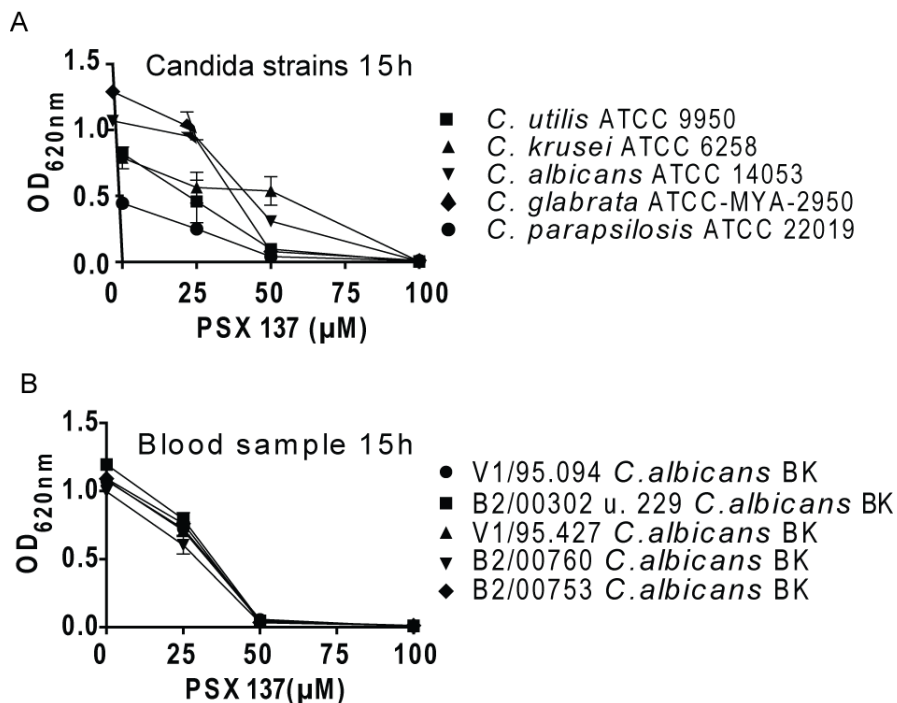


Figure 2.6 Toxicity of PSX137 in *C. albicans* strains in suspension growth. Five *Candida* strains from a ATCC collection and five multiresistant *C. albicans* from blood samples were tested. Yeast cells were grown at 30°C until they reached the exponential phase. 10-Fold dilutions of the cultures were prepared, and spotted on YPD medium containing 0,2 DMSO as a control, 50μM and 100μM of PSX 137.

2.21.3 Heat shock assay for Cell Wall Integrity pathway (CWI) kinases

This protocol was developed for testing compounds with low solubility and problems to pass through the yeast cell wall. It allows a maximum DMSO concentration of 10%. The compounds tested are targets of Pkc1 and Pkh, kinases that belong to the CWI pathway.

The SDP10 strain (*ergΔ*) is the CML476 with a deletion in *erg6* gene to permeabilize the cell wall (See Table 2.3). SDP10 colonies that contain either pRS316 or pRS316-*BCK1-20* plasmid were picked from a SD/-URA fresh dish. Those were grown in liquid medium shaking overnight at 30°C. The saturated cultures were diluted in 50 ml YPD in 125 ml Erlenmeyer at OD₆₃₀ 0,5 and grown until reaching log phase (250 rpm, 30°C). The pellet was washed with H₂O in MQ and gently resuspended in 500 µl TE/Li (1x Tris-EDTA buffer + 0.1M Lithium acetate final concentration) and 3 ml of PEG 50% TE/Li was added. The master-mix was incubated 30 min at 30°C. Gently turning the tube up and down every 10 minutes

Eppendorf tubes (1,5ml) were prepared with 20 mM of the compound diluted in DMSO for a final volume of 30µl in each tube.

To each tube, 300 µl of master-mix containing the cells (PEG 50% + Te/Li) was added, vortexed, and incubated in a water bath 15 min, 42°C. The samples were then left on ice for 2 min and spin at maximum g for 1 min. Then, the pellets were washed with cold PBS and resuspended in 1,5 ml PBS. The proper OD₆₃₀ to be added to agar plates and 96 well plate is around 1OD₆₆₀ to make the final volume a OD₆₃₀ of 0,1 – 0,2 in the well. Therefore, the OD₆₃₀ of each sample was measured and modified to a final OD₆₃₀ of 1 in the eppendorf tube adding cold PBS. Same amount of cells were spread onto SD/-URA agar dishes and were as well made triplicates of 15 µl of the culture into 200 µl SD/-URA medium in 96 well plate. In the 96 well plates the final OD₆₃₀ was measured at time point 0 h and incubated at 30°C 15h in a humid chamber. Then, measures were taken at OD₆₃₀ every 2 hours. As well, dots were made with 10-fold serial dilutions with an initial OD₆₃₀ of 1 and spotted in SD/-URA plates.

Validation of protocol: The compounds tested that affected the growth of yeasts were part of a library designed to bind to the PIF-pocket on AGC kinases. Two AGC

kinases, Pkhs and Pkc1, are described to be part of the CWI pathway upstream of Bck1.

Compounds from our focused library to the PIF-pocket of human α PKC inhibit the growth of yeast cells. Under the *erg6 Δ* genetic background, we then generated two strains containing either an empty plasmid (pRS316) or the plasmid coding for the Bck1 constitutively active mutant (pRS316-*BCK1-20*) and tested the effect of a set of our PIF-pocket allosteric inhibitor compounds of mammalian PKC isoforms, PSX933, PSX034, PSX134, PSX234 and PSX434 (all compounds variants from the same scaffold) in the presence of 200 μ M of each compound. In this assay, the compounds that specifically inhibit the AGC kinases Pkh1-3 or Pkc1 would affect the growth of the WT cells, but would be rescued by the overexpression of the constitutively active form of Bck1. Interestingly, we observed that PSX933 and PSX034 inhibited the growth of the WT yeast cells in solid and liquid media but had reduced effects on the yeast cells overexpressing *BCK1-20* (Figure. 2.7). The data indicate that PSX933 and PSX043 affect the growth of yeast cells. Moreover, since the effect is less pronounced in the cells expressing *BCK1-20*, the data supports the idea that the compounds are specifically acting upstream of Bck1 on the CWI pathway. Finally, we observed large differences in the effects by different compounds from this series; e.g. PSX043 had a strong effect on the growth of WT cells on solid media while PSX434, having the same scaffold but lacking a -Cl and a -CF₃ substituents, had greatly diminished effects. This result further provides support to the idea that the effects are specific and not due to general toxicity of the compound class.

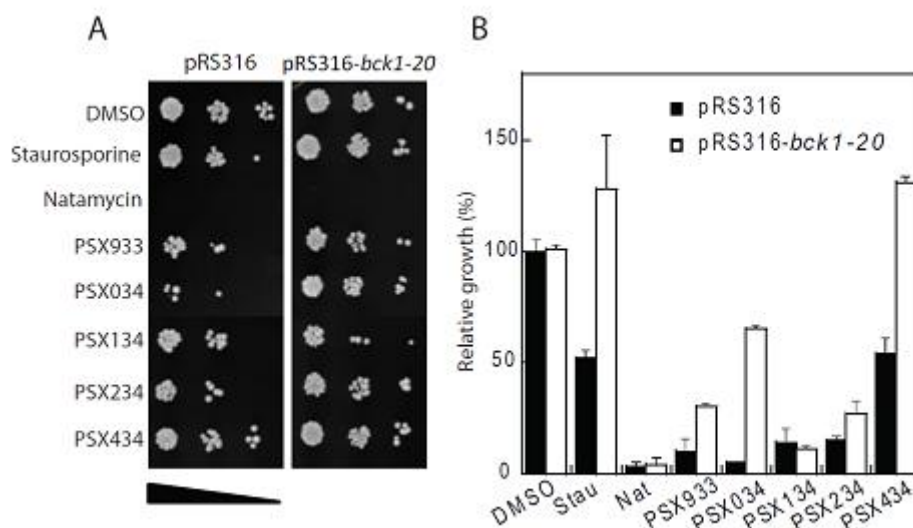


Figure 2.7. Compounds developed to target the PIF-pocket on AGC kinases inhibit growth of yeast cells and the effect is reverted by overexpression of *BCK1-20*. We tested the effect of DMSO (control), staurosporine, natamycin and PSX allosteric compounds on growth of yeast cells. A- Effect on growth on agar. Natamycin (control) inhibits vacuolar fission and therefore, growth and this effect is not reverted by overexpression of the CWI downstream target *BCK1-20*. In contrast, compounds from our focused library, e.g. PSX933 and PSX034 inhibit growth and the effect is reverted by the overexpression of *BCK1-20*. B- The effect on growth in suspension cultures quantified by absorbance at 600nm. PSX933 and PSX034 have a drastic effect on the growth of yeast cells in suspension that is reversed by the overexpression of *BCK1-20*.

2.22 Reproducibility of the results

All experiments described in this thesis were repeated at least twice. Most experiments were repeated multiple times with similar results with independent transformants and cultures.

Chapter III: Results

3. Results

3.1 Part I. Pkh *S. cerevisiae*. Genetic characterization

3.1.1 Characterization of depleted strains

To date, most of the information obtained about the functions of the Pkh proteins has been acquired using a Pkh1^{D398G} temperature-sensitive allele (see Item 1.5.1.2). Here I present a different genetic strategy to deplete the Pkh with no need to use high-temperature incubations, which may trigger the activation of the CWI pathway; using this strategy, I corroborate the importance of Pkh. I demonstrate that the depletion of Pkh induces: a) defect on the cell wall b) glycogen accumulation c) unfolded protein response d) an increase in the levels of cellular reactive oxygen species (ROS) and in DNA strand breaks that do not require the metacaspase Mca1, indicating that the absence of Pkh triggers metacaspase-independent programmed cell death (PCD). I also show that the expression in Pkh-deficient cells of a constitutively active form of Bck1 that activates Slk2 attenuates the signs of PCD and lethality, suggesting that at least some elements of the Pkh-Slk2 MAP kinase pathway play an important anti-PCD role. Finally, I determined that Pkh is important for the proper transcriptional response in basal conditions and to heat stress mainly driven by Hsf1 and Msn2/Msn4 transcription factors.

For study the effects of the lack of Pkh proteins in *S. cerevisiae*, avoiding incubations at 37°C that could activate the CWI-Slk2 MAP kinase pathway, I prepared a strain where the expression of *PKH2* is under the control of the doxycycline-repressible (tetO₇) promoter. This system was previously described by Yen and collaborators (Yen, Gitsham et al. 2003). Treatment of yeast cells with doxycycline was also previously described to have negligible effects at the transcriptomic level (Abdulrehman, Monteiro et al. 2011). In order to insert the *Kan* MX4-*tetO* cassette upstream of the *PKH2* coding region in the WT CML476 strain I replaced 487 bp located immediately upstream the *PKH2* start codon by the cassette containing the doxycycline-repressed promoter tetO₇, yielding the strain MB002. In addition, I disrupted the *PKH1* coding region in the MB002 strain, obtaining the MB005 strain (Table 2.4). According to quantitative RT-PCR measurements, the level of mRNA for *PKH2* in MB005 cells decreased nine-fold and two hundred fifty-fold after treatment with doxycycline for 20 h and 24 h respectively (Figure 3.1A). As shown in Figure

3.1B, the growth of MB005 cells in solid medium containing doxycycline is decreased compared with the wild type strain CML476. To study the phenotype of all disrupted Pkh combinations and to completely deplete the cell of Pkh I disrupted *PKH3* gene in MB002 and MB005 strains, obtaining the SDP7 and SDP8 strains, respectively. (Table 2.3). Since the growth of MB005 was severely affected on solid medium, deletion of *PKH3* did not apparently worsen the growth on agar (Figure 3.1B) but significantly aggravated the growth of the MB005 strain in liquid medium (Figure 3.1C). This growth defect was specifically caused by the lack of Pkh because expression of either yeast *PKH1* from the pRS316 centromeric plasmid from *ADH1*-driven promoter in the MB005 or SDP8 strain rescued the growth defect in doxycycline-containing media (Fig 3.1D). I then tested the viability of WT and Pkh depleted cells in YPD agar after treatment with doxycycline following the time course of the liquid growth. The results are consistent with the reduction of growth in the Pkh depleted cells. While the WT cells grew normally with a 100% of viability as reference, the cells depleted of Pkh decreased the viability up to 60% after 20 hours of growth (Figure 3.1F). The growth defect of several CWI-related mutants is often remediated by adding to the growth medium an osmotic stabilizer such as 1 M sorbitol. Addition of 1 M sorbitol, however, did not recover cell growth of MB005 or SDP8 cells in plates containing doxycycline (Figure 3.1E). These data indicate that the SDP8 strain, when treated with doxycycline, is depleted from functional Pkh and can be used as a model for the study of the phenotypes caused by lack of Pkh. The conclusion is that Pkh is required for normal yeast growth under standard growth conditions and that without thermal shift the growth defect of Pkh-deficient cells is not due to osmotically-induced cell lysis.

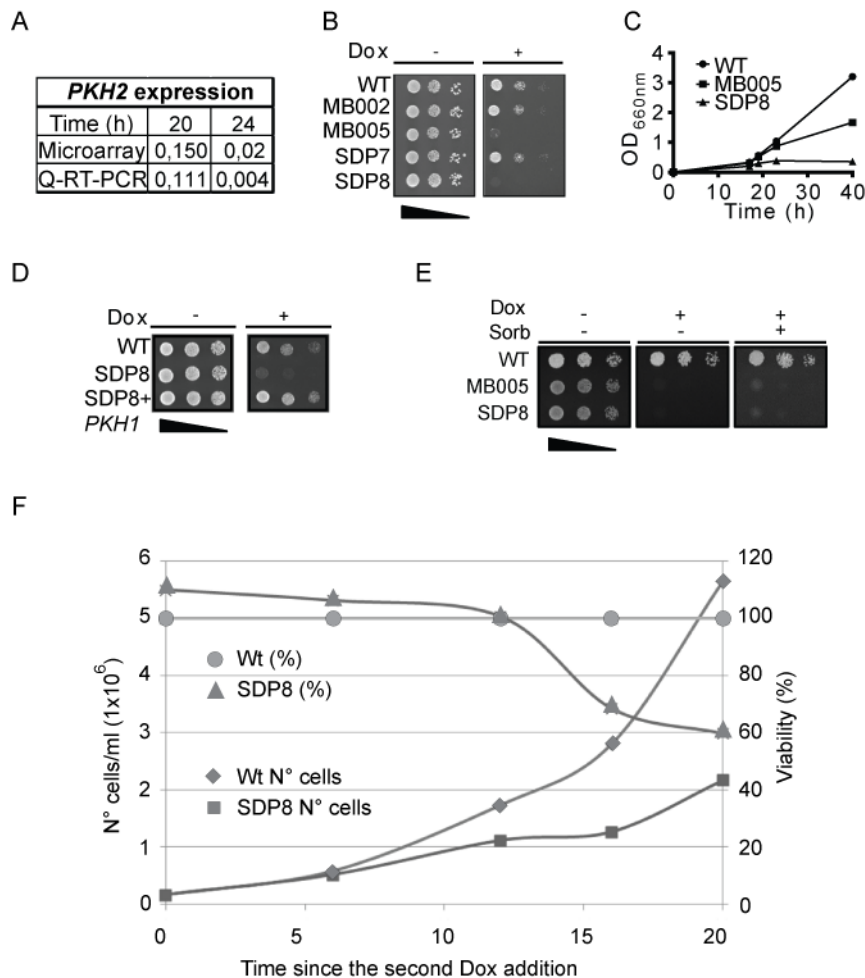


Figure 3.1 *S. cerevisiae* cells lacking *PKH1* and having reduced expression of *PKH2* are not viable. A) *PKH2* expression quantified by RT-PCR and microarray after 20 and 24 h of doxycycline (Dox) 100 µg/ml incubation. B) Serial 1:10 cell dilutions of the indicated strains spotted onto YPD agar plates in presence or absence of 100 µg/mL of doxycycline and incubated at 28 °C for 36 h. C) Suspension growth of the indicated yeast strains in the presence of 100 µg/mL doxycycline D) Expression of *PKH1* from the pRS316 centromeric plasmid under the control of its own promoter reconstitutes growth of SDP8 in the presence of 100 µg/mL doxycycline. E) Sorbitol does not recover growth of MB005 and SDP8 strains in the presence of doxycycline. Cultures of WT, MB005 and SDP8 yeast strains were diluted and spotted in YPD solid medium containing the indicated combinations of 100µg/ml doxycycline and 1M sorbitol (Sorb). F) Viability of the cells since the second doxycycline addition. Cells were incubated for 16 hours with doxycycline 100 µg/ml and inoculated in new fresh YPD + doxycycline medium. Cells were then counted and the viability analyzed by growth in agar plates and counted in each time point.

3.1.2 Pkh-depleted cells are defective in the activation of the CWI pathway

It is accepted that Pkh proteins are necessary for Pkc1 activation (Inagaki, Schmelzle et al. 1999; Friant, Zanolari et al. 2000) therefore, depletion of Pkh should inhibit the activation of Pkc1 and, consequently, compromise the CWI. In agreement with this hypothesis, MB005 cells were more sensitive than WT cells to the digestion with zymolyase, a cell-wall-degrading enzyme that promotes the activation of the Slk2 MAP kinase pathway (Serrano, Martin et al. 2006). Furthermore, additional deletion

of the *PKH3* gene (SDP8 strain) exacerbated cell lysis under the same treatment (Figure 3.2A). SDP8 cells, when treated with low concentrations of doxycycline, were also sensitive to incubation at 37 °C (Figure 3.2B). This could indicate that depletion of Pkh impedes or decreases the activation of the downstream Slt2 MAPK cascade. To test this hypothesis I produced a cell wall stress on SDP8 cells by alkalization of the media (Wishart, Osborn et al. 2006) and tested if the CWI pathway was affected by probing the phosphorylation state of Slt2 MAPK using a phospho-site-specific antibody (Figure 3.2C, upper panel). The alkaline stress induced by incubation with 35 mM KOH produced an important increase of Slt2 phosphorylation in doxycycline-treated WT cells when compared with the same cells incubated with 35 mM KCl as a negative control. Notably, the phosphorylation of Slt2 was drastically reduced when doxycycline-treated SDP8 cells were stressed in the same way, indicating that Slt2 phosphorylation was dependent on the presence of Pkh. A defect in Slt2 phosphorylation was also observed when doxycycline-treated SDP8 cells were subjected to heat stress by incubation for 40 min at 42 °C (Figure 3.2C, bottom panel), another well-known stress that induces Slt2 phosphorylation (de Nobel, Ruiz et al. 2000).

Yeast cells are sensitive to high concentrations of Calcofluor, a compound that is toxic and present antifungal activity at high concentrations. It works binding to chitin, the β -glucan chains that in turn cannot form microfibrils. Since chitin is one of the main structural polysaccharides in the cell wall, an abnormal deposition may cause weakness in the cell wall and lysis (Roncero, Valdivieso et al. 1988). Another cell wall disruptor is Congo red. It binds to β -D-glucan elementary fibrils and cells growth showing aberrant cell structures (Kopecka and Gabriel 1992). To study the implication of Pkh in the cell wall stress, we tested Pkh depleted strains under low doxycycline concentration (10 μ g/ml) (Fig. 3.2C) in order to avoid absence of phenotype consequence of depletion of Pkh and be able to analyze the sensitivity to the compounds (Figure 3.2D left). However, the growth was severely reduced when low quantities of Congo red or Calcofluor white were added (Figure 3.2D right), indicating that a decrease of the levels of Pkh increases the sensitivity to cell wall stressors. Together, the data indicate that Pkh is important for the proper response to cell wall stresses and is required for phosphorylation of the Slt2 MAP kinase.

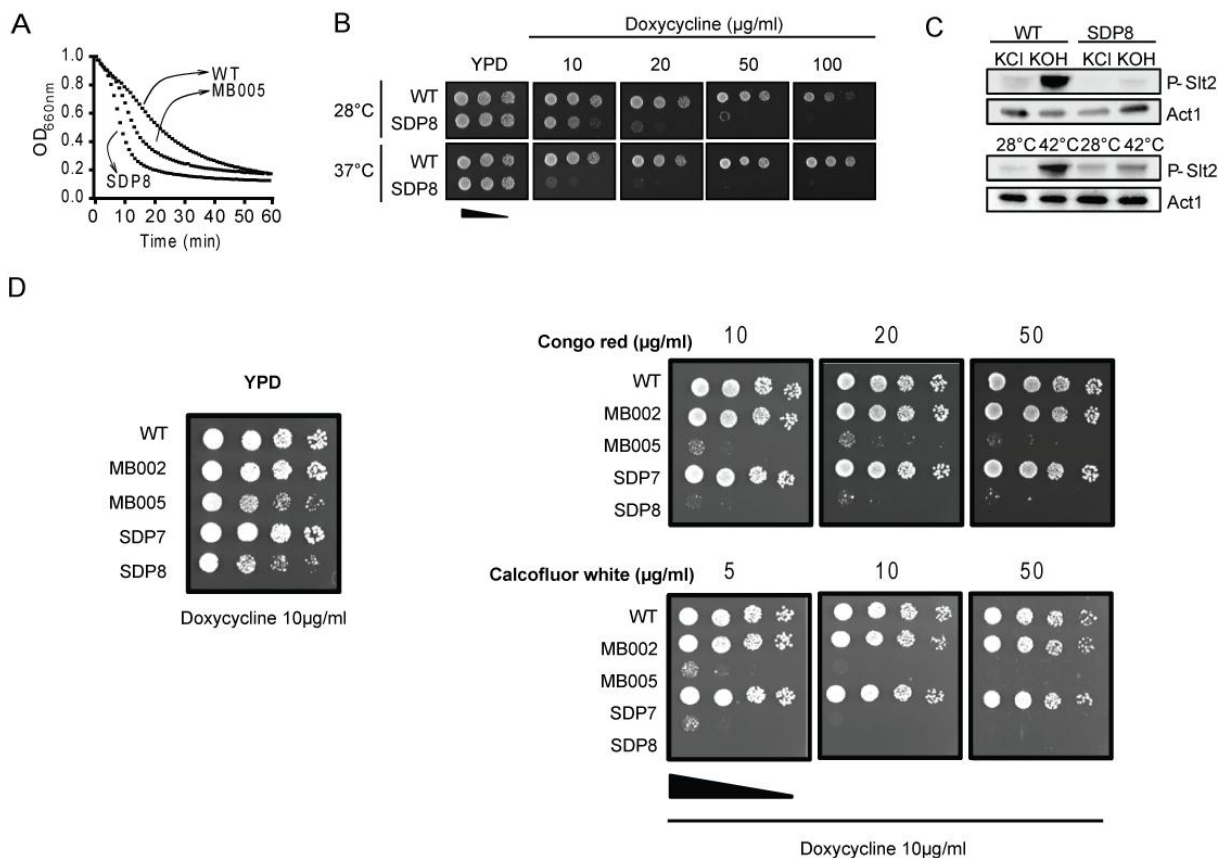


Figure 3.2 Depletion of Pkh decreases the ability of yeasts to activate the CWI pathway. A) Cultures of the indicated strains were incubated in the presence of zymolyase and the effect on the cell wall measured by absorbance at 660 nm. B) Heat shock decreases viability of SDP8 strain in the presence of doxycycline. WT and SDP8 cells were grown at 28°C until they reached the exponential phase. 10-Fold dilutions of the cultures were prepared, and spotted on YPD medium containing the specified concentrations of doxycycline. C) The activation of the CWI pathway was tested by stimulation of the pathway by KOH and a heat shock and following the phosphorylation of the downstream target, Slt2, by Western-blot; Actin (Act1) was used as a loading control. D) MB005 and SDP8 cannot grow under low concentrations of cell wall stress agents. B,D) Plates were then incubated at 28 °C or 37 °C for 2 days, except those containing 50 and 100 μg/ml of doxycycline (3 days).

3.1.3 Global transcriptional changes resulting from the depletion of Pkh

3.1.3.1 Cells depleted of Pkh accumulate mRNAs involved in stress responses

To gain further insight into the cellular roles of the Pkh kinases, I analyzed the global transcriptional changes resulting from the depletion of Pkh, using DNA microarrays. In contrast to the previously published data (Wishart, Hayes et al. 2005), we detected a number of transcriptional changes caused by doxycycline treatment (unpublished results). Therefore, I decided to compare the expression pattern of doxycycline-treated SDP8 cells and WT cells.

Treatment with doxycycline for 8 and 24 h changed more than 2 fold the expression of 113 and 368 genes, respectively. The levels of 156 mRNAs were decreased in

SDP8 cells after either 8 or 24 h of incubation with the antibiotic (included in clusters 1 and 2 in Figure 3.3). Among them, a set of 15 genes involved in ion transport (p-value $2.46e-06$, according to MIPS FunCat) was found to be repressed, most of them (14 genes, including *ARN1*, *ARN2*, *COT1*, *FET3*, *FET4*, *FIT1*, *FIT2*, *FIT3*, *FRE1*, *FTR1*, *PHO84*, *PMA1* and *SIT1*) specifically down-regulated only after 24 h of treatment with doxycycline. Also specifically down-regulated at 24 h of treatment with doxycycline was a group of 31 ribosomal proteins (p-value $9.98e-15$) (Figure 3.3, cluster 2 and Appendix Table A.1). We found 257 mRNAs with increased levels after either 8 or 24 h of incubation with doxycycline (Appendix Table A.1). The more relevant categories within the up-regulated genes were related to the metabolism of carbohydrates (p-value $2.53e-13$) and energy (p-value $1.17e-13$). For example, the expression of several genes involved in the synthesis of glycogen (such as *GSY1*, *GSY2*, *GAC1*, *GLG1* and *GLC3*) and fermentation (such as *ALD2*, *ALD3*, *ALD4*, *ALD6*, *AAD3*, *AAD6*, *AAD14*, *AAD15*, *AAD16*) were found to be increased at both 8 and 24 h of treatment with doxycycline (cluster 3 in Figure 3.3). Thus, the short-term transcriptional response to depletion of Pkh potentiates fermentation and increases the levels of glycogen. In addition, we observed a strong increase in the expression of genes involved in the response to stress (p-value $3.81e-13$; cluster 4 in Figure 3.3), specifically after 24 h of incubation with doxycycline. Among these up-regulated genes, we found a set of chaperones involved in the response to heat shock that belong to the functional category of unfolded protein response (such as *HSP12*, *HSP26*, *HSP30*, *HSP31*, *HSP33*, *HSP42*, *HSP78*, *HSP82*, *HSP104*, and *SSA4*). Similarly, we also found an excess of genes typically induced in response to oxidative stress (such as *PRX1*, *TSA2*, *SOD2*, *CTA1*, and *GRE1*). Thus, long-term depletion of Pkh proteins resulted in a transcriptional response related to that induced by heat shock, oxidative stress and energy reserves.

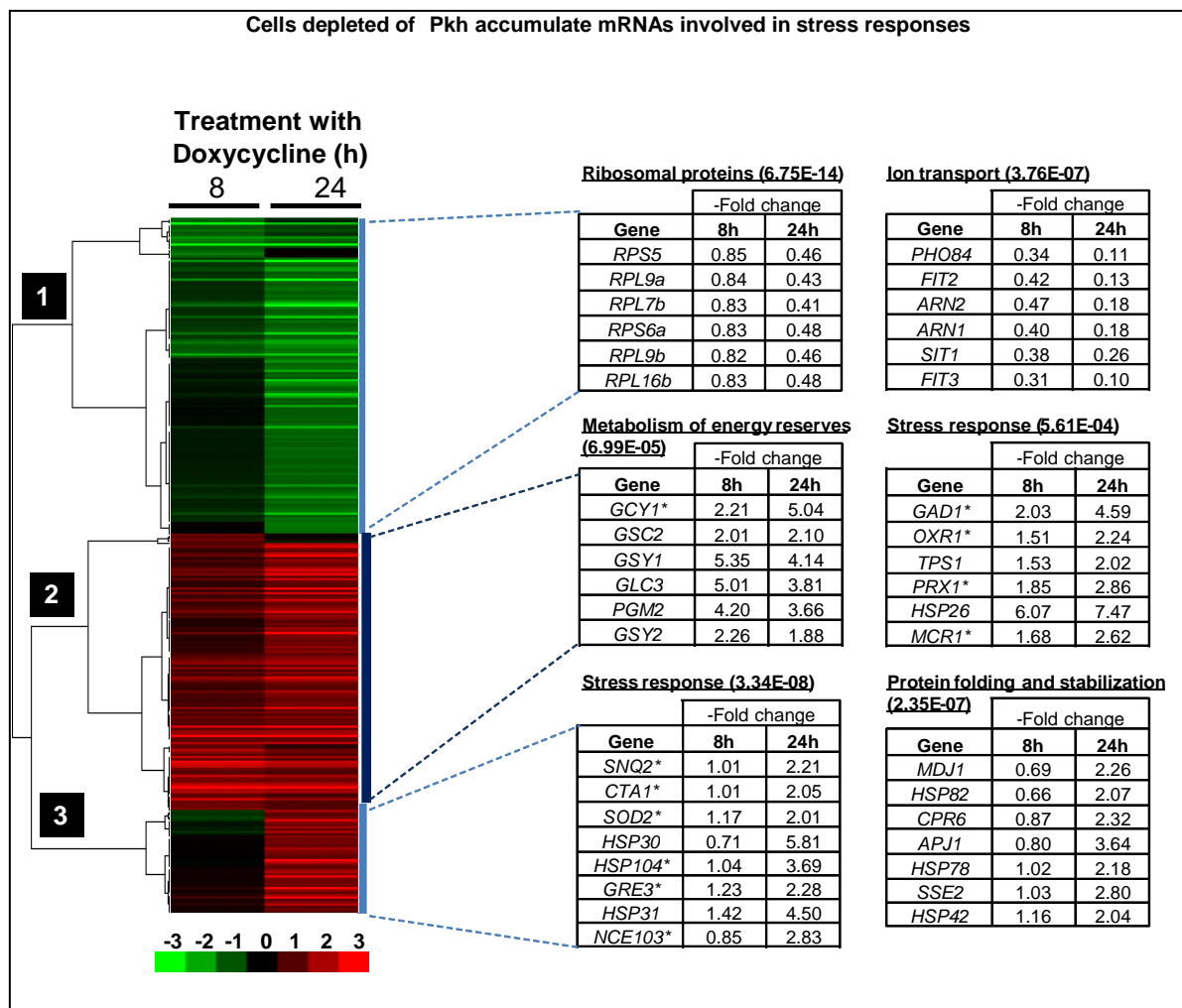


Figure 3.3 Clustering of the genes differentially expressed when Pkh is depleted. The expression patterns of SDP8 cells treated with doxycycline for 8 or 24 h were compared with those of equally treated WT cells. A set of 297 genes with data in both conditions that are differentially expressed in at least in one condition were hierarchically clustered (complete linkage clustering, uncentered correlation) using the Cluster software (v. 2.11) and visualized with Java TreeView (v. 1.1.5r2). The more relevant functional categories for each of the four clusters, according to MIPS FunCat, is detailed in the table.

3.1.3.1.1 Short term depletion of Pkh alters glycogen

In order to verify the effect of depletion of Pkh on glycogen synthesis we decided to examine the glycogen accumulation in SDP8 cells treated with low doses of doxycycline (10 $\mu\text{g/ml}$), to avoid cell dead. We found with Iodine staining of glycogen (Figure 3.4) that a non-lethal partial depletion of Pkh (MB005 and SDP8) activated the accumulation of glycogen, when compared with WT and Pkh-expressing cells (MB002 and SDP7). Thus, low levels of Pkh triggered accumulation of glycogen, mimicking a low glucose-induced response. In fact, and according to the Publication Enrichment tool available at the YeastMine website (Balakrishnan et al, 2012), there was a significant overlap between the 81 genes up-regulated by short-term depletion

of Pkh and the 80 genes found up-regulated under an early quinine stress (11 genes, p-value: $2.80e-7$), whose transcriptional profile mimics the yeast response to glucose limitation (dos Santos et al, 2009). Thus, depletion of Pkh triggered the expression of 6 out of the 10 genes involved in glycogen biosynthesis (Figure 3.4).

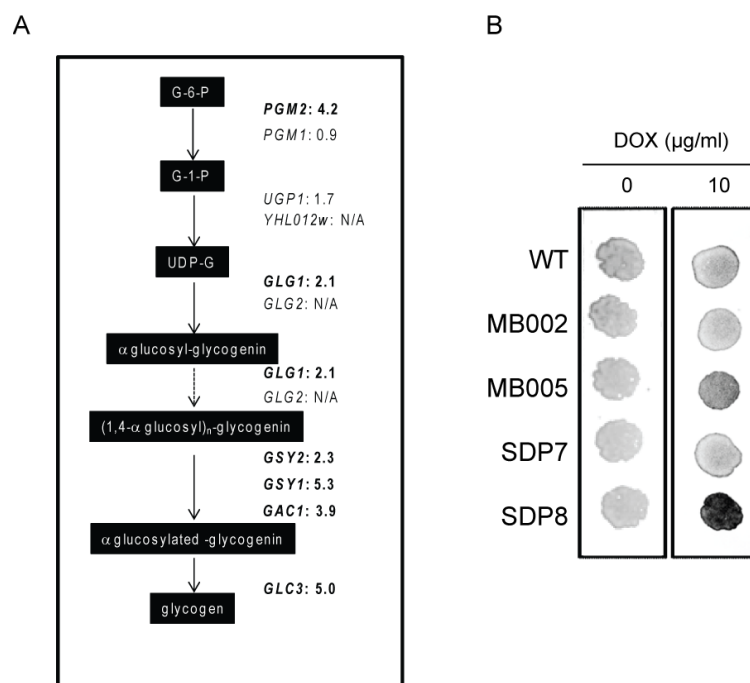


Figure 3.4 Depletion of Pkh affects the glycogen metabolism. A) Glycogen biosynthesis pathway, based on Yeast Biochemical Pathway Database (YeastCyc) at the SGD (Cherry et al, 2012). Numbers indicate the $-$ fold induction of the indicated genes in SDP9 versus WT cells after incubation for 8 h in the presence of doxycycline. Genes considered up-regulated are denoted in bold. N/A: no good quality data were obtained. B) Iodine staining of WT cells and its indicated derivatives growing in YPD plates without or with a low quantity of doxycycline.

3.1.3.1.2 Unfolded Protein Response genes induced after 24 hours treatment

The typical Unfolded Protein Response (UPR) is triggered by the transcription factor Hac1 which binds to the UPR elements at the target gene promoters. In order to identify if the canonical UPR was activated in cells depleted for Pkh1 we transformed SDP8 cells with UPRE fused to the β -galactosidase reporter. Our results indicated that incubation of SDP8 cells with doxycycline did not affect the activation of the UPR (data not shown). However, long-term depletion of Pkh caused sensitivity to the reducer agent β -mercaptoethanol, able to promote the UPR (Figure 3.5). The results suggested that Pkh is required for the proper UPR.

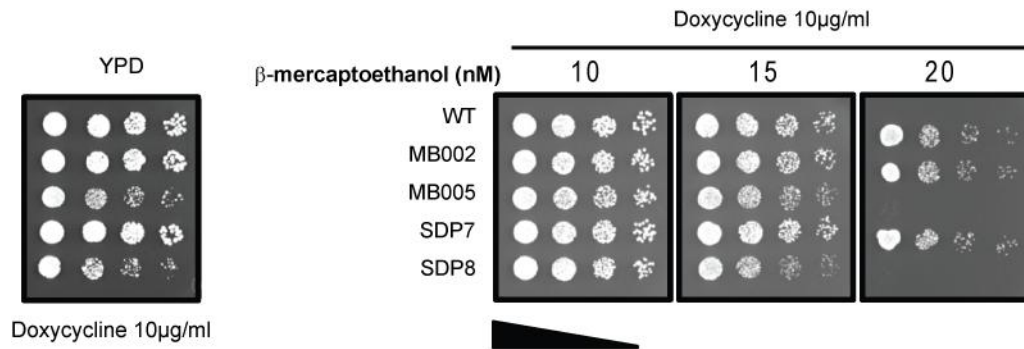


Figure 3.5 Cells with low Pkh expression are affected under reducer agent. β -mercaptoethanol affected the growth of MB005 and SDP8 at low concentrations. Fold dilutions of the cultures were prepared, and spotted on YPD medium containing 10 μ g/ml of doxycycline.

3.1.3.2 The absence of Pkh affects the transcriptional response to heat shock

To study the effect of depleted cells for Pkh under heat shock, I performed a microarray to identify the transcriptional changes induced in 24-h doxycycline-treated WT and SDP8 cells by an incubation at 40 °C for 40 min. The number of genes considered differentially expressed in at least one of the strains under heat shock was 803 (Figure 3.6). Of the 433 up-regulated genes in WT cells, a set of 193 (44.6%) was found to be Pkh-dependent to some extent. Among these genes, several functional categories are especially relevant. For example, we found 39 genes involved in the response to stress (p -value 6.61e-10) that were up-regulated in a Pkh-dependent manner, but only 15 were induced independently of Pkh (p -value 5.76e-01). Similarly, genes involved in protein folding and stabilization were over-represented in the set of Pkh-dependent up-regulated genes (18 genes, p -value 1.59e-10, Figure 3.6) when compared to the 6 genes up-regulated in a Pkh-independent fashion (p -value 9.69e-02). The regulation of genes encoding ribosomal proteins was independent of Pkh, as 74 out the 89 genes coding for ribosomal proteins down-regulated by heat shock were also repressed in the absence of Pkh (Figure 3.6). It is worth noting the presence of genes with altered expression levels under heat shock in SDP8 but not in WT cells. For example, an excess of the seripauperin multigene family (*PAU* genes) encoded mainly by subtelomeric regions were found up-regulated in response to the heat shock in Pkh-depleted cells (Figure 3.6) Similarly, the mRNA levels of a set of genes involved in the maturation of rRNA were down-regulated after heat shock in SDP8 but not in WT cells (Figure 3.6). Together, the above data indicate that Pkh is an essential mediator of the transcriptional response elicited by heat stress.

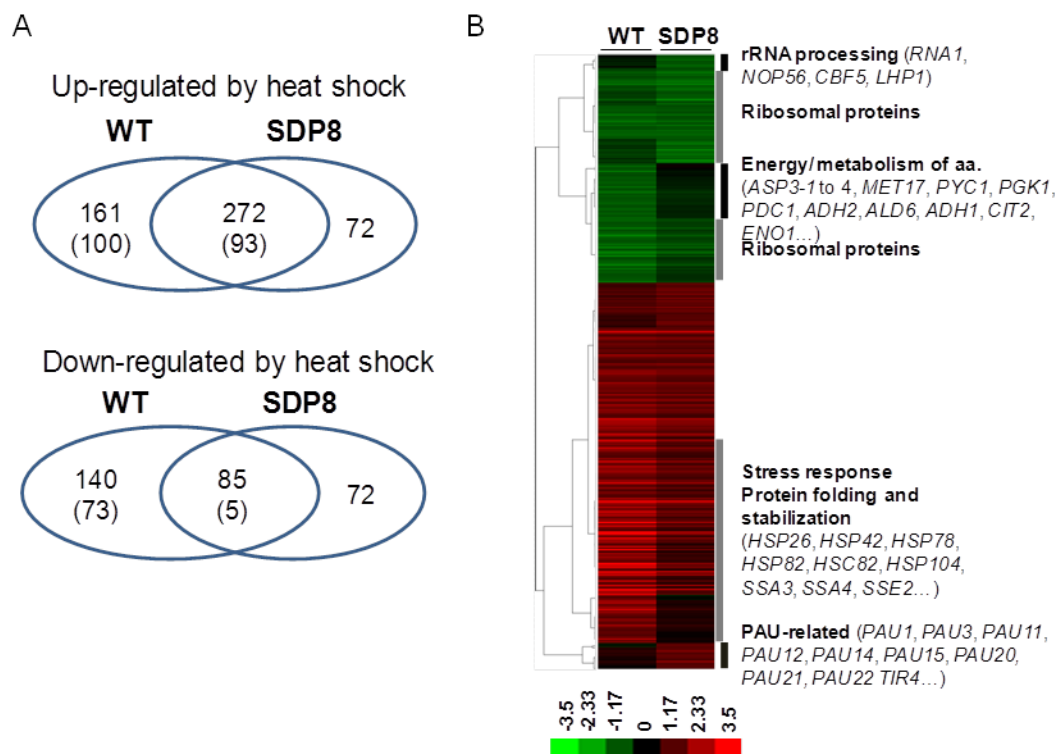


Figure 3.6 The transcriptional response to heat shock requires Pkh. Left: Venn diagrams of the number of genes with considered up-regulated (upper panel) and down-regulated (lower panel) mRNA expression under heat shock stress in the WT and SDP8 strains. Right: The expression patterns of the WT and SDP8 cells treated with doxycycline for 16 h and incubated at 42 °C for 40 min were compared with those of the same cells in the absence of the heat stress. A set of 803 genes with data in both strains that are differentially expressed at least in one of the strains were hierarchically clustered (complete linkage clustering, uncentered correlation) using the Cluster software (v. 2.11) and visualized with Java TreeView (v. 1.1.5r2). The relevant functional categories of genes in some clusters are denoted.

3.1.3.3 Pkh is important for regulating the Hsf1 and Msn2/Msn4 transcription factors after heat stress

Yeast cells respond to heat shock by modifying gene expression. Among the dozens of transcription factors implicated in the regulation of the heat shock response (Wu and Li 2008), the conserved heat shock factor (Hsf1) and the general stress response Msn2/Msn4 are responsible for almost the entirety of the heat shock response (Morano, Grant et al. 2012). To investigate whether the Pkh proteins are important for the normal transcriptional response to heat stress, I studied the most abundant transcription factors that regulate the Pkh-dependent up-regulated genes but not the Pkh-independent up-regulated genes. From the 96 genes up-regulated in a Pkh-dependent manner, 42 (43.8%) are targets for Hsf1, 26 (27.1%) for Msn2 and 18 (18.8%) for Msn4. There are 34 genes (35.4%) targeted by the combination of Msn2 and Msn4, and 23 genes, which correspond mostly to the categories of stress

response, that are simultaneously targeted by all three transcription factors (*APJ1*, *GAC1*, *HSP12*, *HSP26*, *HSP30*, *HSP42*, *HSP82*, *HSP78*, *HSP104*, *MDJ1*, *MGA1*, *SIS1*, *SSA4*, *TSL1* and *XBP1*; p-value: 7.76e-10). By contrast, from the 240 genes found up-regulated in a Pkh-independent fashion, 21 (8.8%) are targets for Hsf1, 16 (6.7%) for Msn2 and 7 (2.9%) for Msn4. Only 30 of those genes (12.5%) are targets for the combination of Msn2 and Msn4 (Figure 3.7).

The above data suggest that Pkh is important for the induction of genes involved in protein folding and the response to stress that are regulated by the Hsf1 and the Msn2/Msn4 transcription factors (See introduction for Hog1 pathway, Sch9 and PKA *S. cerevisiae*).

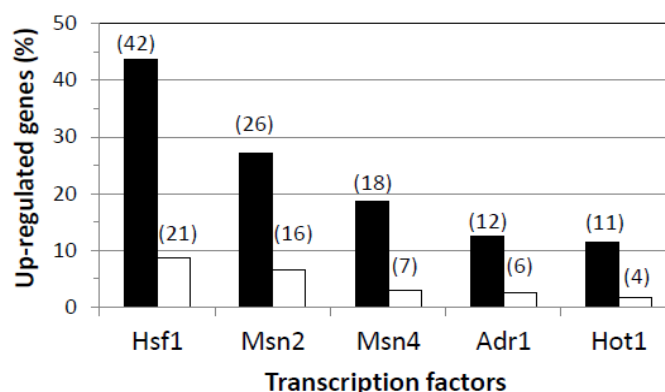


Figure 3.7 Transcription factors that are affected by the lack of Pkh under heat shock. The set of genes considered induced by incubation at 42 °C for 45 min in WT cells were scanned for documented transcription factor regulators (direct evidence) in the YEASTRACT database. The graphic represents the percentage of the genes regulated by each transcription factor (in parentheses) respect the total number of genes induced in a Pkh-dependent (96 genes, filled bars) or Pkh-independent manner (240 genes, empty bars) for those transcription factors with 10 or more target genes in at least one circumstance. Only those with a percentages of Pkh-dependent vs Pkh-independent ratio of 4 or higher are shown.

3.1.4 Cells depleted for Pkh accumulate ROS

The up-regulation of genes involved in the response to oxidative stress response (Figure 3.3) prompted us test the effects of low levels of Pkh on the sensibility to oxidative agents. As shown in the Figure 3.8, incubation of SDP8 cells with low quantity of doxycycline caused hypersensitivity to oxidizing agents such as the thiol oxidant diamide (Jamieson 1998).

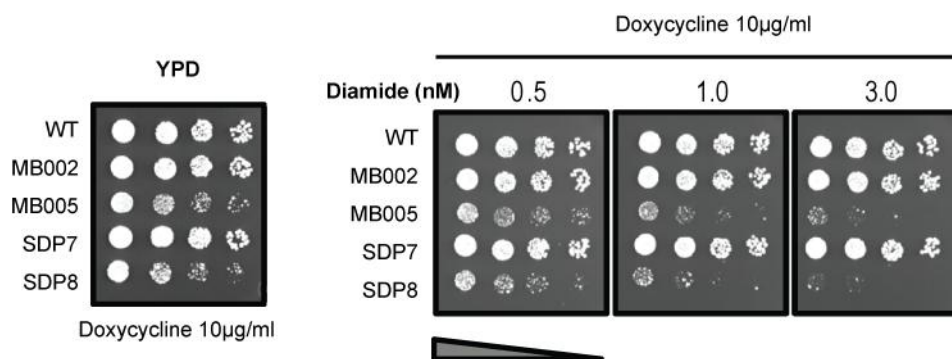


Figure 3.8 Low expression of Pkh exacerbates the cell lethality of oxidizing agents. Cultures of the indicated strains were incubated in the presence of diamide at the specified concentrations. Yeast cells were grown at 28°C until they reached the exponential phase. 10-Fold dilutions of the cultures were prepared, and spotted on YPD medium containing 10 µg/ml of doxycycline.

The data obtained from the DNA microarray experiments in Pkh-depleted cells were also consistent with the hypothesis that depletion of Pkh may trigger oxidative stress and the effect is exacerbated when an oxidizing agent is included.

To further test the possibility of endogenous reactive oxygen species (ROS) when low Pkh is expressed, WT, MB005 and SDP8 cells were treated with doxycycline for 24 h and then incubated with DHR 123 to monitor the generation of ROS and examined by fluorescence microscopy (Figure 3.9). The fluorescence signal was also quantified by flow cytometry. MB005 and SDP8 cells displayed more intense fluorescent staining than WT cells (Figure 3.9A). Analysis by flow cytometry revealed that the quantity of ROS in MB005 cells was higher than in the WT cells and that the additional deletion of *PKH3* further increased the appearance of ROS because SDP8 cells produced stronger signals than MB005 cells (Figure 3.9B). These results were also supported by quantifying the staining of at least 200 individual cells of each strain with the Wasabi image analyzer (Hamamatsu v. 1.5, data not shown). Therefore, we conclude that the lack of Pkh induces the accumulation of ROS.

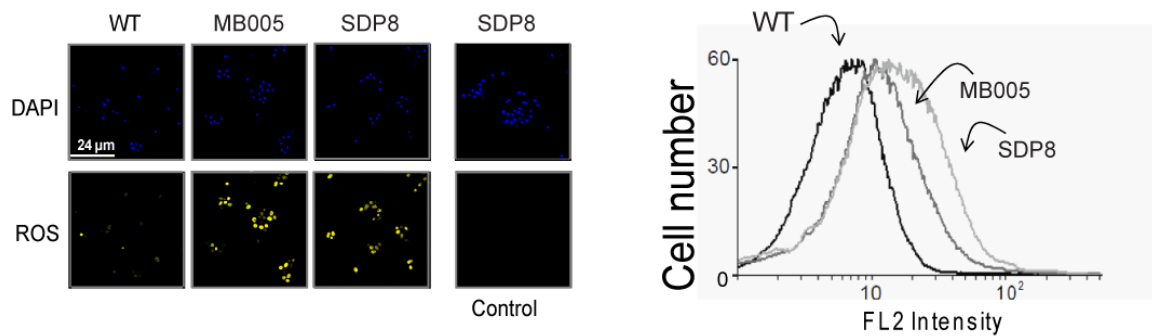


Figure 3.9 Depletion of Pkh activity induces oxidative stress in *S. cerevisiae*. A) The depletion of Pkh under doxycycline produces the accumulation of ROS. B) Quantification of ROS by FAC sorting. A-B) WT and its derivative strains, MB005 and SDP8, were treated with doxycycline for 24 h and loaded with dihydrorhodamine 123.

3.1.5 Activation of the Slit2 MAP kinase pathway reduces the oxidative stress of cells depleted of Pkh

Pkh proteins phosphorylate and activate the yeast members of the AGC protein kinase family Sch9, Ypk1/2, and Pkc1. It has been shown that Pkc1 is required for survival and for the adaptation to oxidative stress provoked by different oxidizing agents (Vilella, Herrero et al. 2005). Pkc1 directly phosphorylates and activates Bck1, the MAPKKK of the Slit2-MAPK pathway, thereby activating the CWI pathway. I wondered whether the state of oxidative stress caused by the lack of Pkh activity could be a consequence of a defect in the activation of the Pkc1-Slit2 pathway or, contrarily, whether it was independent of this pathway. To answer this question, I expressed the constitutively active *BCK1-20* allele of Bck1, which renders an active Slit2 (Lee and Levin 1992), in both WT and SDP8 cells. As shown in Figure 3.10A and B, activation of the Slit2 pathway did not affect the growth rate of the WT cells in the presence of doxycycline. However, the severe growth defect of SDP8 cells in the presence of doxycycline was partially suppressed by the activation of the Slit2 MAPK pathway in both liquid and solid medium, indicating that the lethality of Pkh-depleted cells was rescued, at least in part, by activation of the CWI pathway. I next asked if the oxidative stress detected in Pkh-depleted cells was also due to Pkc1 downstream effects. Staining and quantification of ROS showed that both the MB005 and SDP8 strains carrying the *BCK1-20* allele notably decreased the quantity of ROS when compared with the same strains harboring the empty plasmid (Figure 3.10C and D). Taken together, these results suggest that activation of the Pkc1-Bck1- MAP kinase pathway partially suppresses both the growth defect and the accumulation of ROS caused by the lack of Pkh.

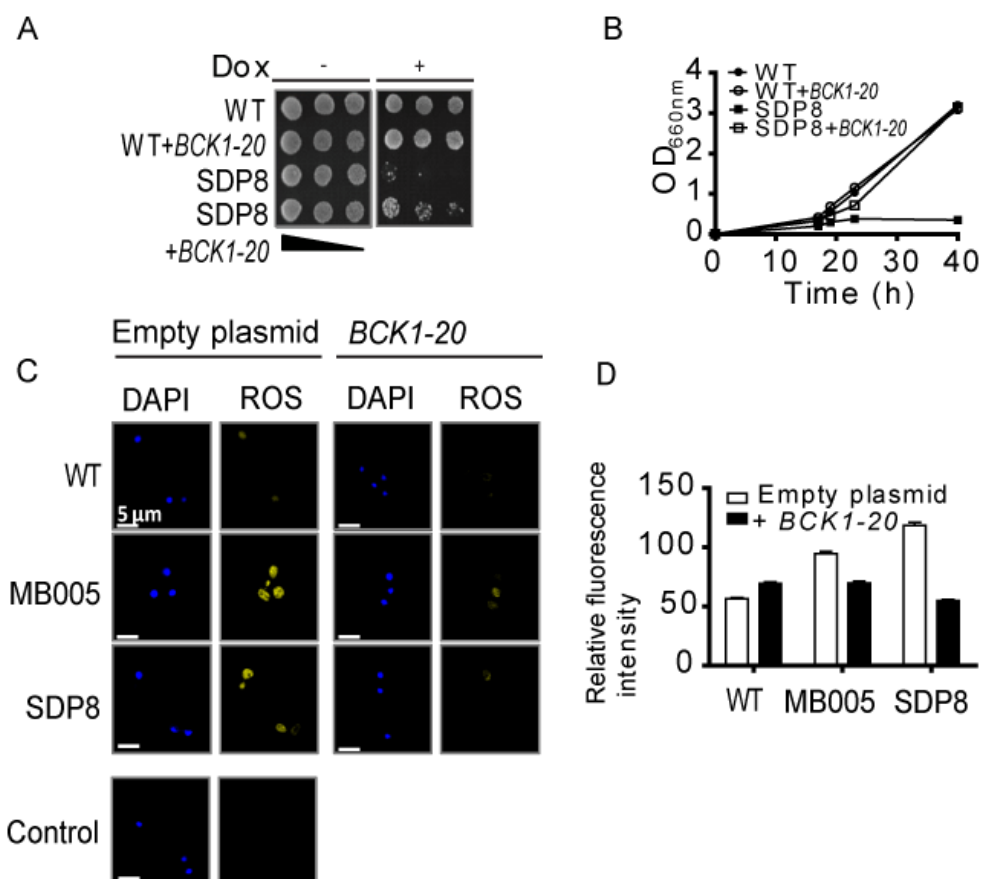


Figure 3.10 *BCK1-20* expression reverts the accumulation of ROS in the absence of Pkh. A–B) Expression of *BCK1-20* reconstitutes growth of the SDP8 strain in YPD agar (A) and in liquid media (B). C–D) Quantification of ROS by microscope and FAC sorting. WT and its derivative strains, MB005 and SDP8, were treated with doxycycline for 24 h and loaded with DHR 123. The fluorescence of a sample of SDP8 cells not treated with DHR123 is also shown as a control (–DHR 123). C) Nuclei were visualized by DAPI staining. Representative fields of the indicated strains are shown. Error bars denote the standard deviations.

3.1.6 Depletion of Pkh induces PCD in a Mca1-independent manner

The presence of ROS could be a signal of apoptotic-like cell death in yeast (Madeo, Frohlich et al. 1999). Then, ROS detected in cells lacking Pkh proteins could be triggering a PCD process. Several types of PCD have been described in metazoan organisms, such as apoptosis, autophagy, mitotic catastrophe, and anoikis. (Kroemer, El-Deiry et al. 2005). Although a number of physiological forms of apoptosis have been identified, it can also be exogenously induced. The accumulation of ROS is an evolutionary conserved key regulator of both exogenous and endogenous forms of apoptosis (Rockenfeller and Madeo 2008). One key feature of apoptosis in mammalian and yeast cells is the appearance of DNA fragmentation. Therefore, I examined the occurrence of double-strand DNA breaks in WT and Pkh-depleted yeast strains using the TUNEL assay. As shown in Figure

Figure 3.11A, MB005 cells displayed stronger staining for TUNEL than WT cells. This signal of DNA fragmentation was even more pronounced in SDP8 cells. In both strains, the activation of the Slr2-MAP kinase pathway by the expression of the *BCK1-20* allele decreased the number of double-strand breaks (Figure 3.11A and B). It is worth noting that the signal displayed by SDP8 cells carrying the empty pRS316 plasmid, is not due to autofluorescence nor to RNA fragmentation in the cytoplasm since all strains were treated with RNase. Also the cells not treated with fluorescein displayed almost no signal according to the FACS quantification (Figure 3.11B). The above result is in agreement with the hypothesis that the lack of Pkh induces DNA fragmentation and that this effect is also mediated by the lack of Pkh-dependent activation of the Pkc1 downstream signaling cascade.

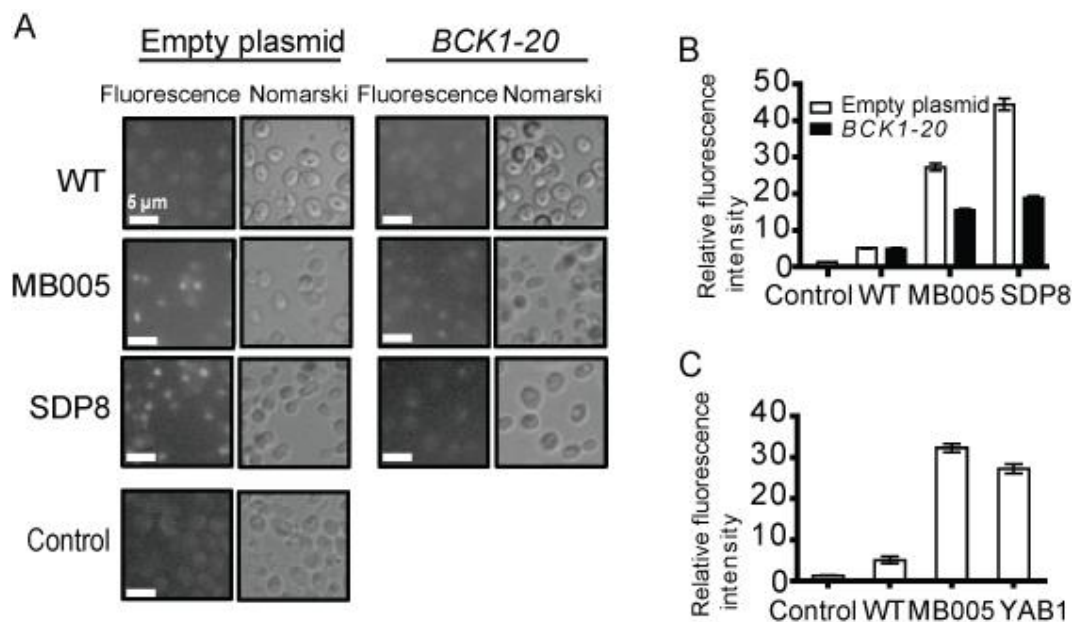


Figure 3.11 Depletion of Pkh causes DNA fragmentation. A) Double strand DNA breaks visualized by TUNEL staining. B- C) Quantification of double-strand DNA breaks by FACS sorting. B) *BCK1-20* expression reverts DNA fragmentation induced by depletion of Pkh. C) DNA fragmentation induced by Pkh depletion is not reverted by deletion of the metacaspase gene *MCA1*. The control corresponds to the autofluorescence of MB005 cells containing the empty pRS316 plasmid. Error bars denote the standard deviations.

Some of the apoptotic stimuli in yeast, including treatment with H_2O_2 (Madeo, Herker et al. 2002), require the yeast metacaspase Mca1 to trigger the apoptotic process, but other stimuli induce Mca1-independent apoptosis (Wilkinson and Ramsdale 2011). To investigate if the programmed cell death process elicited by the depletion of Pkh is dependent on Mca1, I deleted the *MCA1* gene in the MB005 strain, generating the YAB100 strain, and measured the DNA double-strand breaks after

incubation with doxycycline. As shown in Figure 3.11C, MB005 cells displayed at least 6-fold more fluorescence than WT cells. Additional disruption of *MCA1* (YAB100 strain) still showed approximately 6-fold the signal of WT cells. These results indicate that the apoptotic process triggered by the lack of Pkh is partially dependent on the activation of the Slit2 MAP kinase cascade and is not dependent on the Mca1 yeast metacaspase.

3.2 Part II Characterization of CaPkh2

The first part of this project revealed that the depletion of Pkh in *S. cerevisiae* eventually induces oxidative stress and DNA double-strand breaks, leading to programmed cell death. This finding supports that Pkh is a potential antifungal target since pharmacological inhibition of Pkh would lead to the death of yeast cells, the ultimate goal of antifungals. It was therefore of interest to further investigate the possibility of developing Pkh inhibitors with selectivity for the pathogen fungal *Candida* Pkh that would not inhibit the human ortholog. Here, I characterize *C. albicans* Pkh2 biochemically, structurally and by using chemical approaches in comparison to human PDK1. I found that a regulatory site on the *C. albicans* Pkh2 catalytic domain, the PIF-pocket, diverges from human PDK1. I will describe the identification and characterization of PS77, a small new allosteric inhibitor directed to the PIF-pocket, which has increased selectivity for *C. albicans* Pkh2. Together, these results describe novel features of the biology of yeast Pkh and chemical biology approaches that support the validation of Pkh as a drug target for selective antifungals.

3.2.1 Biochemical similarities and differences between CaPkh2 and PDK1

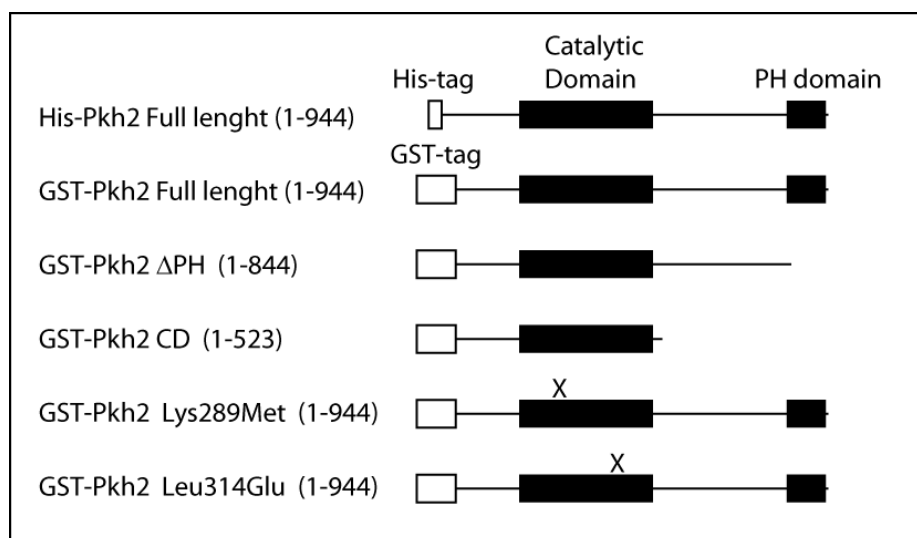
C. albicans is an obligatory diploid organism, which contains two genes encoding putative orthologs of Pkh proteins (*CaPKH2* and *CaPKH3*). Heterozygous deletion of *CaPKH2* in the CAI4 *C. albicans* strain rendered viable cells. However, the heterozygous cells had an effect in glycogen accumulation, suggesting that the Pkh phosphorylation of Tpk1 and Tpk2, the catalytic subunits of PKA, mediating basic cellular processes including glycogen accumulation (Giacometti, Kronberg et al. 2009), was sensitive to the haploinsufficiency of CaPkh2 (Pastor-Flores, Schulze et al. 2013). Moreover, our collaborator, R. Gionametti in S. Passeron's laboratory, was not able to obtain homozygous null *C. albicans* cells. Based on these observations it

is likely to assume that CaPkh is also essential for *C. albicans*. It was then in our interest to express CaPkh2 protein in order to characterize and test it as a possible target protein for antifungal drugs.

3.2.2 Design of *PKH2 C. albicans* synthetic gene for protein expression in mammalian and insect cells

Candida spp. are Ascomycota fungi that belong to the family of Saccharomycetaceae. The genome of *C. albicans* suffered 100 million years ago a reassignment event where CTG codon encoded a serine rather than a leucine as in the other organisms (Fitzpatrick, Logue et al. 2006). Consequently, the handling of *Candida* genome using current molecular biology is affected since the standard expression organisms translate CTG as a leucine. It was therefore necessary for the recombinant expression of CaPkh2 to design a complete new gene by changing the codon usage to maximize its expression in mammalian cells (See Appendix 4.2). I then cloned, expressed and purified different constructs of CaPKH2 in pFastBac and pGEB2T plasmids for the expression of His-CaPkh2 in insect cells and GST-CaPkh2 in mammalian cells. Table 3.1 (See material and methods for purification analysis Item 2.6).

Table 3.1. *Candida* Pkh2 constructs



Candida Pkh2 constructs expressed with affinity tags (white squares) and purified in Mammalian or Insect cells. The predicted domains are highlighted in black.

3.2.3 Two-hybrid system

As a part of the characterization of CaPkh2, I used Two-hybrid technology to find CaPkh2 interaction partners which may help to identify novel regulation process or signaling pathways.

CaPKH2 synthetic gene was fused to pGBKT7 (*TRP1*, Kanr) a vector with a high protein expression (*ADH* promoter). It contains the DNA-Binding domain GAL4. The *C. albicans* library was fused into pGADT7 (LEU2, Ampr) with a pool of cDNA that contains cells in log growth and stationary phase, hyphae and pseudohyphae morphogenetic state. The cDNA library is fused to GAL4 AD. With this approach, the possibilities to find CaPkh2 interaction partners may be higher that with a single growth condition. After the transformation of pGBKT7-CaPkh2 plasmid with pGADT7-cDNA library into AH109 cells, the first selection was carried onto a triple drop out media (TDO) lacking His, Leu and Trp (SD/-His/-Leu/-Trp). One hundred and twenty 9 colonies where obtained within 2 and 6 days. From each colony it was done a replicate onto a plate with a quadruple drop out media (QDO), SD/-His/-Leu/-Trp/-Ade. Eighty five colonies from TDO were positive in QDO.

A second control was done restreaking the positive colonies onto a plate containing SD/-Trp/-Leu and X-Gal, pH 7. This control allowed us to discard white colonies (negative) from blue colonies (positive) which have reacted with x-Gal.

The plasmid containing the cDNA library of each colony was isolated from the genomic DNA and the inserts where sequenced. Those genes or partial gene sequences that were not in frame with Gal4 activation domain where not consider for analysis. After sequentiating, a third check was done using the transformation of positives pGADT7-cDNA from X-Gal plate with the empty plasmid pGBKT7. In this case, the cDNA hits that interact with β -galactosidase will turn into blue colonies and therefore will be false positives. From 15 positives in X-Gal plate, only 5 colonies did not turn blue. In the following table (Table 3.2) are listed the positive interactions from the QDO that were restriking onto X-Gal. For the gene identification, the database from National Center for Biotechnology Information (NCBI) was used.

Table 3.2 Proteins interacting with CaPkh2 by Two-hybrid system

Gene name	Identities	Gene length	Description
RPB3	356/357	957	Putative RNA polymerase II subunit B44; heterozygous null mutant exhibits resistance to parnafungin in the <i>C. albicans</i> fitness test; Spider biofilm repressed
HSP60	308/420	1701	Tetradecameric mitochondrial chaperonin required for ATP-dependent folding of precursor polypeptides and complex assembly; prevents aggregation and mediates protein refolding after heat shock; role in mtDNA transmission; phosphorylated. Heat shock protein; soluble in hyphae; regulated by Nrg1 and by iron; induced in high iron; heavy metal (cadmium) stress-induced; sumoylation target; protein present in exponential and stationary phase cells; Hap43-repressed
TPI1	746/747	747	Triose-phosphate isomerase; antigenic in mouse/human; mutation affects filamentation; macrophage-repressed; protein in exponential and stationary growth phase yeast; possibly essential; flow model biofilm induced; Spider biofilm repressed
orf19.3874	192/206	1851	Predicted cation transmembrane transporter; Spider biofilm induced
RPS20	244/244	359	Putative ribosomal protein; repressed upon phagocytosis by murine macrophage; transcript positively regulated by Tbf1; Spider biofilm repressed

Five proteins out of 129 colonies were found as true positive interacting partners of CaPkh2. Triose Phosphate Isomerase was the only protein fully cloned into pGADT7. Description of each gene is subtracted from the Candida Genome Database (www.candidagenome.org).

From the 5 isolates, none of them belong to kinase family, typically substrates of PDK1. However, ScPkh was found to phosphorylate Pil1 and Lsp1, primary component of eisosomes and member of the BAR domain family (Zhang, Lester et al. 2004). This fact was found in yeast and was, at least for now, not found in mammalian cells. For that reason, it would not be unusual to find other protein families phosphorylated by CaPkh2.

Although the cDNA library was generated following the protocol to amplify whole genes and not random cDNA parts, in 4 clones the identified region corresponded to the C-terminal region of the protein. This may be related with the low affinity that the full packed proteins have in the Pkh-protein interaction. From the 5 positive isolates,

a full length protein was found in only one, the Triose-phosphate isomerase. The other four have a length average of 80-100 aa of the c-terminal part. This finding does not imply that the generated library does not have full length proteins, but only that strong interactions may be promoted by short aminoacidic sequences. Therefore, the unfolded proteins, and especially, extended polypeptides could interact with some folded protein regions with better affinity that could be identified by this technique (Biondi 2004).

From the 5 interaction proteins, Hsp60, Tpi1 and Rps20 are phosphorylated in a specific Ser in *S. cerevisiae* (Gruhler, Olsen et al. 2005; Reinders, Wagner et al. 2007; Albuquerque, Smolka et al. 2008; Holt, Tuch et al. 2009) and only Rpb3 and the predicted transmembrane transporter, have not been characterized yet. Those phosphorylation sites may be potential phosphorylation sites of CaPkh2, however, to present stronger conclusions, further analysis and characterizations such as in vitro protein-protein interaction assays should be done.

3.2.4 CaPkh2 as antifungal target

3.2.4.1 CaPkh2 crystal structure and the PIF-pocket as a target for the modulation of PDK1 activity

Protein kinase inhibitors to be employed as anti-infectives in humans should have high selectivity and have preference for the pathogen over the human ortholog kinase to avoid side effects. To investigate the potential selectivity of the ATP-binding site and the allosteric regulatory PIF-pocket, I used the purified GST-CaPkh2 expressed in mammalian cells and N-terminally His-tagged CaPkh2 expressed in insect cells (Table 3.1) to test their activity. Similarly to PDK1, CaPkh2 phosphorylated T308tide and was activated ~3-4 fold by PIFtide (Figure 3.12), the prototype 24-residue-polypeptide that binds to the PIF-pocket and activates PDK1 (Biondi, Cheung et al. 2000; Silber, Antal et al. 2004).

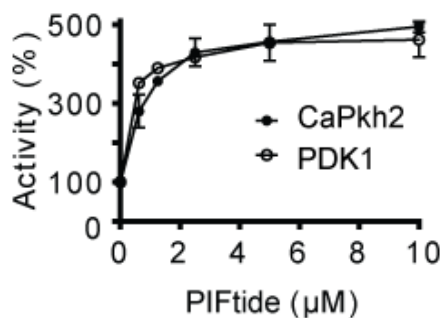


Figure 3.12 Activity assay of CaPkh2 and PDK1 activated by PIFtide

Furthermore, to investigate possible differences between PDK1 and CaPkh2 that could be targeted for the development of selective inhibitors, we attempted to crystallize full-length His-CaPkh2. The protein crystallized and we solved the crystal structure of CaPkh2 by molecular replacement using the PDK1 structure (PDB ID: 3HRC), and refined the CaPkh2 structure to 3.16 Å resolution (PDB ID: 4C0T). The structure comprises the CD (aa 237-510) of CaPkh2. In the solved structure, the main chain and most side chains can be accurately traced, allowing the comparison of the CD of PDK1 and CaPkh2. The CD shows the typical bilobal protein kinase structure, with the ATP-binding site in the cleft between both lobes (Figure 3.13A). The structure is in an overall active conformation, similar to the structures of PDK1 in crystal packing I (Biondi, Komander et al. 2002) and crystal packing II (Hindie, Stroba et al. 2009). However, similar to PDK1 structures in the absence of allosteric compounds, the active site is not in the fully closed-active conformation but in an intermediate conformation (Figure 3.13A), comparable to the structure of PKA in complex with staurosporine (PDB ID: 1STC).

The ATP-binding site is almost identical between CaPkh2 and PDK1 (Figure 3.13A and Figure 3.15). In spite of the general similarities between PDK1 and CaPkh2, significant differences were observed at the allosteric PIF-pocket regulatory site. The PIF-pocket is located between the β -strands β 4 & β 5 and helices α B & α C. Interestingly, CaPkh2 contains an additional Gly residue in the loop following the regulatory helix α C (Figure 3.13B). In addition, some key residues in the helix α C, corresponding to Thr128 and Arg131 in PDK1, are replaced by Asn and Lys, respectively. Since these residues are constituents of the allosteric PIF-pocket binding site where small compounds bind (Hindie, Stroba et al. 2009; Busschots, Lopez-Garcia et al. 2012), may participate in selective interactions. Mutation of the residue at the center of the hydrophobic PIF-pocket in PDK1, Leu155, to Ser, Asp or

Glu renders proteins that have 3-fold higher specific activity (Biondi, Cheung et al. 2000). In sharp contrast, the CaPkh2 mutant equivalent to Leu155Glu (CaPkh2 [Leu314Glu]) had vastly reduced specific activity (13 % of the activity of wild type CaPkh2). Similarly, mutation of Arg131 to Met renders a mutant PDK1 protein that has 2-fold higher specific activity (Frodin, Antal et al. 2002) while the equivalent CaPkh2 mutant (Lys289Met) had a slightly lower specific activity (63 % of the activity of wild type CaPkh2) (Figure 3.19). Together, the structural differences between the PIF-pockets of PDK1 and CaPkh2 and the additional differences in the activities of PDK1 and CaPkh2 proteins mutated at the PIF-pockets, provided a first indication that the PIF-pocket was structurally and functionally different between the human PDK1 and the *C. albicans* orthologs and it may provide selectivity for the development of CaPkh2-selective allosteric small compounds.

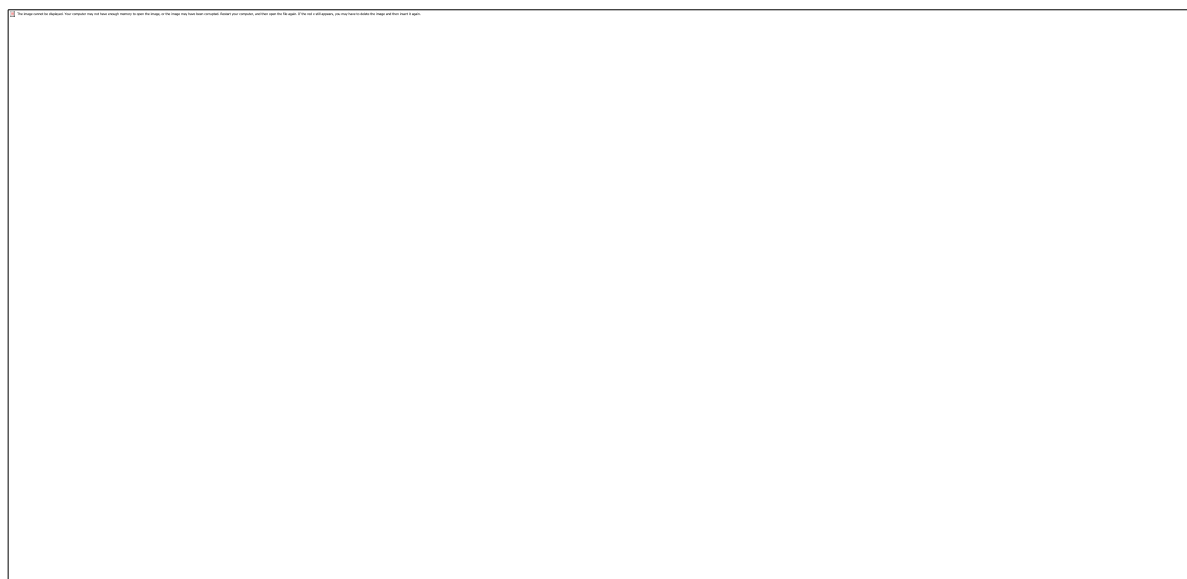


Figure 3.13 Structural characterization of CaPkh2. A) Crystal structure of the catalytic domain of CaPkh2 (blue) superimposed on the structure of human PDK1 (yellow) (PDB code 1H1W). The structures are shown in cartoon representation; ATP and the phosphorylations at the activation loops are depicted as sticks. B) Close-up view of the PIF-pocket with side chains constituting the pocket shown as sticks. The perspective in comparison to part B is rotated by $\sim 180^\circ$ along a vertical axis. Although the PIF-pocket of CaPkh2 is structurally similar to the PIF-pocket of PDK1, essential residues differ (indicated with red labels), and one additional residue is inserted in the loop C-terminal to helix αC (red circle).

3.2.4.2 Effect of compounds that target ATP binding site in Pkh2 activity

It was recently identified that the protein kinase inhibitor KP-372 inhibited the CWI pathway and had antifungal activity (Baxter, DiDone et al. 2011). KP-372 was originally identified as a non-selective ATP-binding site inhibitor of the protein kinase PKB/Akt (Mandal, Kim et al. 2005) and later found to inhibit PDK1 activity (Zeng, Samudio et al. 2006). However the direct inhibition of Pkh by KP-372 had not been verified *in vitro*.

We therefore tested the relative ability of KP-372 to inhibit PDK1 and CaPkh2 in kinase assays using 100 μM ATP, a relatively low concentration that favors binding of inhibitors to the ATP-binding site. Surprisingly, we observed that KP-372 failed to inhibit PDK1 and CaPkh2 *in vitro*, with 75% remaining activity at 50 μM , whereas, KP-372 inhibited PKB/Akt. Since the previous determination of PDK1 inhibition was determined using an indirect assay by measuring the activation of the substrate SGK (Zeng, Samudio et al. 2006), it was possible that KP-372 actually inhibited SGK (Figure 3.14). We indeed confirmed that KP-372 inhibited both PKB/Akt and SGK, but not PDK1 or CaPkh2. PKB/Akt and SGK are most similar to the yeast protein Ypk. Therefore, KP-372 may inhibit different yeast kinases including Ypk, although the identity of the kinase or kinases inhibited by KP-372 in yeast cells remains to be determined.

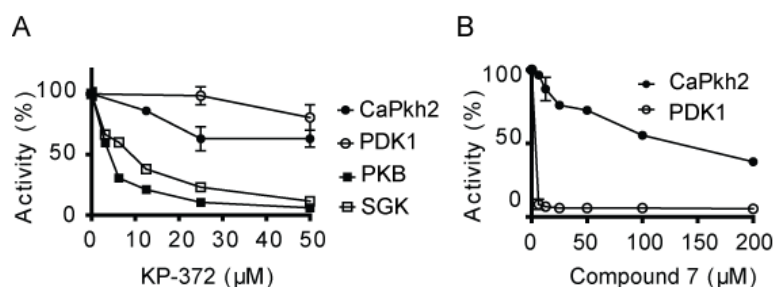


Figure 3.14 Effect of ATP-competitive inhibitors KP-372 and Compound 7. A) Effect of KP-372 on PDK1, CaPkh2, PKB/Akt and SGK1. KP-372 was identified as an inhibitor of PKB/Akt and later described to inhibit PDK1. KP-372 inhibited PKB/Akt but not PDK1 or CaPkh2. B) Effect of Compound 7 in PDK1 and CaPkh2. The selective type II inhibitor, compound 7 inhibited PDK1 activity but fail to inhibit CaPkh2.

More recently a very selective ATP-competitive inhibitor (selective type II inhibitor) called “compound 7” was described. The compound binds to the DFG-out conformation and has one ring overlapping with the site where ATP binds. Thus, even if it is termed “allosteric” inhibitor, it still overlaps with the ATP binding site (Nagashima, Shumway et al. 2011). One part of compound 7 is binding to the hinge region of human PDK1 by a classical hydrogen bonding pattern that mimics adenosine binding of ATP. It interacts with the main chain O-atom and N-atom of Ser160 and Ala162, respectively. An important property of this compound is that it is binding to the inactive “DFG-out” conformation. Moreover, compound 7 induces a cavity between the active site and the PIF-pocket. As a result, the PIF-pocket is distorted and pushed upward. The published crystal structure shows a distinct conformation of the PIF-pocket. However, it should be noted that this conformation is stabilized by a crystal contact and

that the PIF-pocket of this complex may be quite flexible in solution. The displacement of the PIF-pocket also disrupts a crucial salt bridge between Glu130 and Lys111, which holds Lys111 in position for ATP-binding. Instead, the Lys111 side chain is now bound by the amide group of compound 7. The kinase activity data of PDK1 and CaPkh2 in presence of compound 7 indicated indeed a high selectivity for human PDK1 but a very poor or unspecific inhibition for CaPkh2 (Figure 3.14).

Protein kinase inhibitor ATP-competitive drugs, e.g. staurosporine or UCN-01 have been tested as antifungals as well (Baxter, DiDone et al. 2011). However, the use of unspecific inhibitors is expected to inhibit multiple other human kinases leading to extensive side effects.

It was previously reported that the active site of PDK1 and Pkh share only 50 % sequence identity (Baxter, DiDone et al. 2011). In contrast to those estimations, the structure of CaPkh2 shows that the side chains that would be in close proximity to ATP or an ATP-competitive inhibitor, like staurosporine or UCN-01, are almost identical to those present in PDK1 (Figure 3.15). Although CaPkh2 was crystallized in the presence of ADP, we did not observe electron density for the nucleotide. By contrast, all published crystal structures of PDK1 have been obtained in the presence of ATP or an ATP-competitive inhibitor. And even though the CaPkh2 structure features an unoccupied active site, all residues directly participating in the binding of ATP are positioned almost identically. We evaluated whether the differences in the active site may permit a selective inhibition of CaPkh2: There are two conservative substitutions in the outer limits of the ATP-binding site (CaPkh2 Leu292 and Tyr251 that are Met and Phe in PDK1), which are too distant to interfere with the binding of inhibitors such as staurosporine (PDB ID: 1OKY) or UCN-01 (PDB ID: 1OKZ). Interestingly, one of these residues, Tyr251, is positioned similarly as the equivalent residue in the crystal structure of the PDK1-staurosporine complex. One additional difference is the replacement of PDK1 Val143 by Ile302 in CaPkh2. The CaPkh2 structure shows that the bulkier isoleucine protrudes into the ATP-binding site, where it could sterically clash with the inhibitor UCN-01. Based on comparisons with the PDK1/UCN-01 structure (Figure 3.15B) UCN-01 is a more selective kinase inhibitor than staurosporine and differs only by the presence of the 7-hydroxyl group (Figure 3.15A and B). In this manner, UCN-01 can potentially clash to some extent with Ile302 in CaPkh2, whereas staurosporine, smaller, may not. In agreement with these

structural observations, staurosporine inhibits CaPkh2 and PDK1 with equal potency, while UCN-01 has a 4-fold increased IC_{50} towards CaPkh2 (Figure 3.15C and D). The data indicate that there is indeed a difference in the ATP-binding pocket. However, since the substitution renders a smaller pocket in CaPkh2 than in human PDK1, this difference cannot be exploited for the development of selective CaPkh2 inhibitors. Together, our results stress the challenge of identifying selective CaPkh2 inhibitors by targeting the ATP-binding pocket.

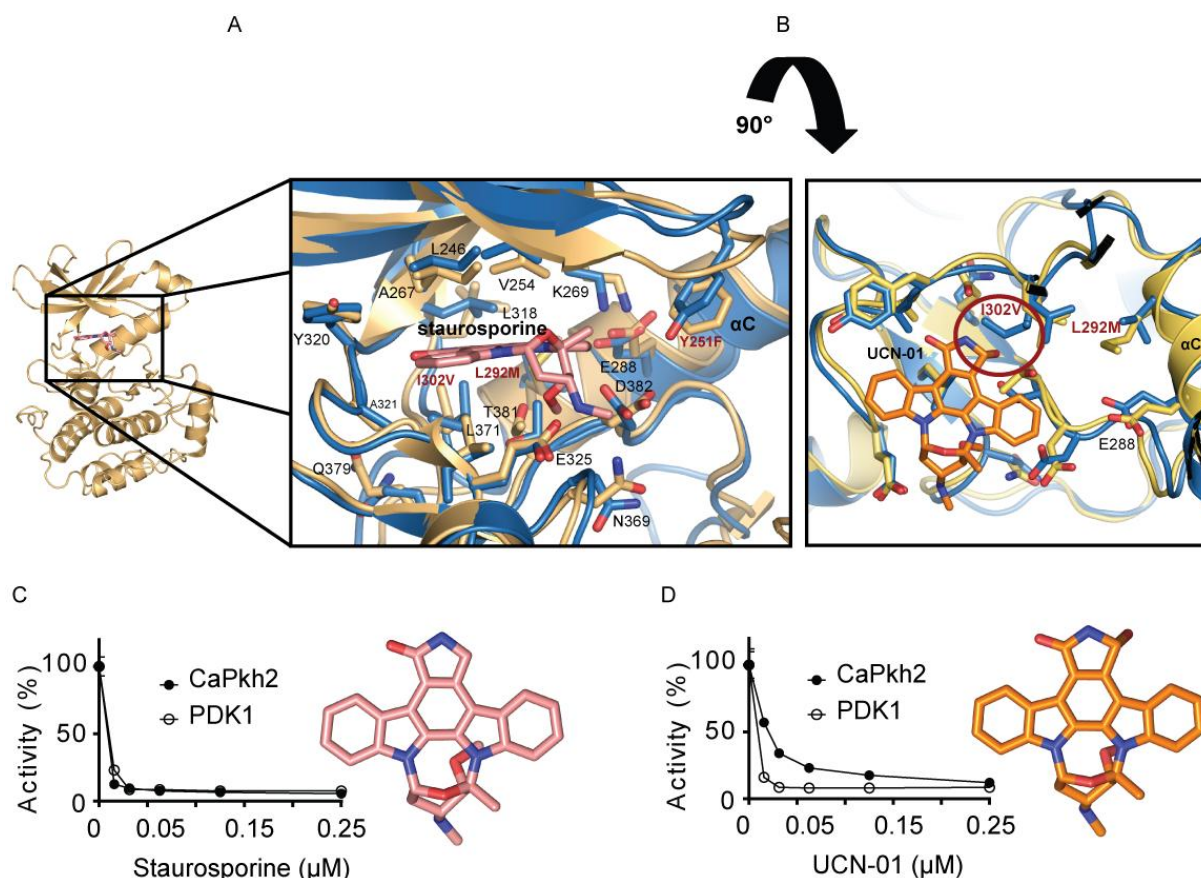
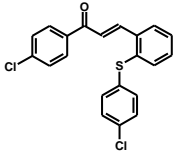
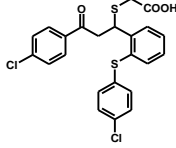
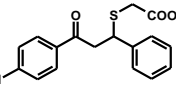
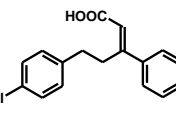
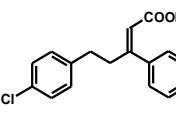
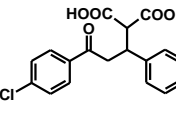
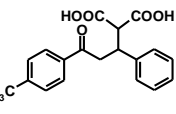
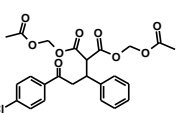


Figure 3.15 Comparison of the ATP-binding sites of CaPkh2 and human PDK1. A) The ATP-binding site is highly conserved between CaPkh2 (blue) and human PDK1 (light orange, PDB code 1OKY). Only side chains that may be in direct contact with an ATP-competitive inhibitor are shown as sticks. Non-conserved residues are marked with red labels. Staurosporine is depicted with pink carbon atoms. B) Structural alignment of the CaPkh2 structure with that of UCN-01-bound PDK1 (yellow, PDB code 1OKZ). In comparison to A), the perspective is rotated by $\sim 90^\circ$ around a horizontal axis. The red circle highlights a predicted sterical clash of the 7-hydroxyl group of UCN-01 with Ile302. C) Effect of staurosporine on PDK1 and CaPkh2. D) Effect of UCN-01 on PDK1 and CaPkh2. Staurosporine and UCN-01 are shown as stick models. The results indicate that none of the ATP-competitive inhibitors of PDK1 have preference for CaPkh2 and highlight the challenge of developing inhibitors that preferentially inhibit CaPkh2 over PDK1. Although, staurosporine is an effective antifungal compound, it is very unspecific and inhibits multiple human protein kinases.

3.2.4.3 Biochemical differences at the PIF-pocket between PDK1 and CaPkh2

We then tested small molecules from our PIF-pocket-directed focused library for their ability to affect the activity of CaPkh2. PS48, PS210 and PS182 (Table 3.3) are *in vitro* activators of PDK1 that have been co-crystallized with PDK1 (Hindie, Stroba et al. 2009; Busschots, Lopez-Garcia et al. 2012), confirming their binding to the PIF-pocket. Interestingly, PS48, PS210 and PS182 are not able to activate CaPkh2 (Figure 3.16A and C). In order to further characterize the interaction of small compounds with the PIF-pocket, I established AlphaScreen interaction-displacement assays using His-CaPkh2 or His-PDK1 and the biotinylated polypeptide PIFtide. Whereas inactive compounds (e.g. PS47 and PS220) did not displace the PDK1-PIFtide interaction, low-molecular-weight activators readily displaced the PDK1-PIFtide interaction. In comparison, PS48, PS210 and PS182 had decreased abilities to selectively displace the CaPkh2-PIFtide interaction (Figure 3.16B and D). Together, the data suggest that PS48, PS210 and PS182 had decreased abilities to bind to the PIF-pocket and decreased abilities to fully activate CaPkh2, providing further evidence that the PIF-pocket of CaPkh2 differed from that of PDK1.

Table 3.3 Effect of Compounds on PDK1 and CaPkh2 ordered by families

Compound name	Formula	CaPkh2					PDK1				
		Kinase activity			AlphaScreen		Kinase activity			AlphaScreen	
		Activity (%) 50 μ M	AC ₅₀ (μ M)	IC ₅₀ (μ M)	PIFtide bound (%) 100 μ M	EC ₅₀ (μ M)	Activity (%) 50 μ M	AC ₅₀ (μ M)	IC ₅₀ (μ M)	PIFtide bound (%) 100 μ M	EC ₅₀ (μ M)
PS76		96	-	n.e.	89	n.d.	45	-	n.d.	100	n.d.
PS77		3	-	17	5	44	37	-	38	91	n.d.
PS46		209	65	-	44	85	237	38 ^a	-	27	n.d.
PS47		123	n.e.	-	25	n.d.	80	n.e. ^b	-	2	n.d.
PS48		194	48	-	37	n.d.	281	8 ^b	-	39	97
PS182		331	n.d.	-	95	66	706	2 ^c	-	65	26
PS210		389	42	-	98	60	950	4 ^c	-	65	39
PS220		126	n.e.	-	100	n.e.	116	n.e.	-	100	n.e.

n.d. = not determined; n.e. = no effect. ^bRef (Engel, Hindie et al. 2006). ^cRefs (Hindie, Stroba et al. 2009) and (Stroba, Schaeffer et al. 2009). ^dRefs (Busschots, Lopez-Garcia et al. 2012) and (Wilhelm, Lopez-Garcia et al. 2012).

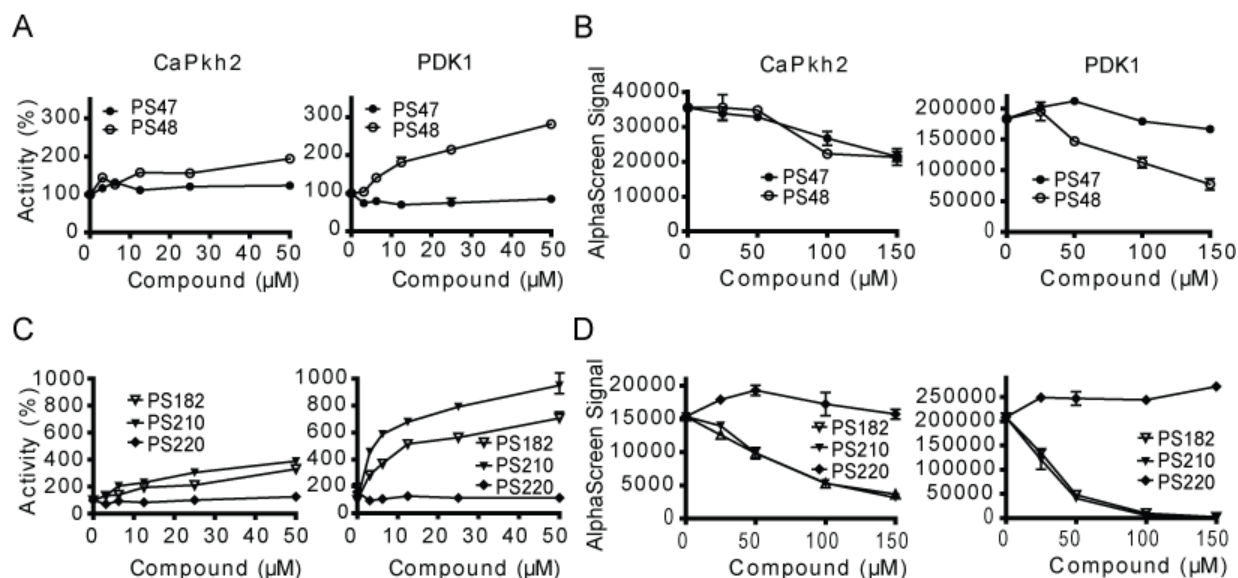


Figure 3.16 Comparison of the PIF-pocket of CaPkh2 and human PDK1 using small compounds allosteric activators that bind to the PIF-pocket of PDK1. A) Effect of related compounds PS47 and PS48 on the activity of CaPkh2 and PDK1. B) Displacement of PIFtide by PS47 and PS48. C) Effect of related compounds PS182, PS210, and PS220 on the activity of CaPkh2 and PDK1. D) Displacement of PIFtide PS182, PS210, and PS220. The ability of compounds to displace the CaPkh2-PIFtide or PDK1-PIFtide interaction was evaluated using an AlphaScreen interaction-displacement assay. Error bars denote the standard deviations.

3.2.4.4 Small molecule PS77 is a CaPkh2 PIF-pocket allosteric inhibitor with selectivity over PDK1

Within this in-home screen of own focused library, I also identified that 2-(3-(4-chlorophenyl)-1-(2-(4-chlorophenylthio)phenyl)-3-oxopropylthio) acetic acid (PS77; Table 3.3) inhibited CaPkh2 (Fig. 3.17A). PS77 is a variant of PS46, which is a low-molecular-weight PDK1 activator (Table 3.3; compound 1 in (Engel, Hindie et al. 2006)). Biochemical and mutagenesis experiments showed that PS46 binds to the PIF-pocket (Engel, Hindie et al. 2006), a feature that was confirmed by the crystal structure of the PDK1-ATP-PS46 complex (Valerie Hindie, Pedro M. Alzari and RMB, unpublished). Most interestingly, PS77 specifically inhibited CaPkh2 but had marginal inhibitory effect on PDK1 (Figure 3.17A). As a control for the specificity, the related compound 1-(4-chlorophenyl)-3-(2-(4-chlorophenylthio)phenyl)prop-2-en-1-one (PS76) did not inhibit CaPkh2. In complete agreement with the inhibition of CaPkh2, PS77 also displaced the interaction between His-CaPkh2 and biotin-PIFtide (Figure 3.17B) whereas PS76 had no effect on the displacement. In contrast, PS77 had vastly decreased ability to displace PIFtide from PDK1 (Figure 3.17B). Together, the results provided evidence that PS77 is a selective CaPkh2 allosteric inhibitor that competes with PIFtide for the binding to CaPkh2.

Since we have obtained the crystal structure of diverse allosteric activators and allosteric inhibitors bound to the PIF-pocket of PDK1 (Figure 3.17C), it was of interest to model the binding of PS77 to the PIF-pocket of CaPkh2. PS77 does not fit into the PIF-pocket in an equivalent manner to compound 1, PS48 or PS210 in the overall active structure of CaPkh2 or PDK1 since there is no apparent space for the diphenyl sulfide system. Since the helix α C of AGC kinases in solution has a large degree of mobility, we envisage that the 2-phenylthio moiety of PS77 may occupy a novel pocket behind helix α C (Figure 3.17E).

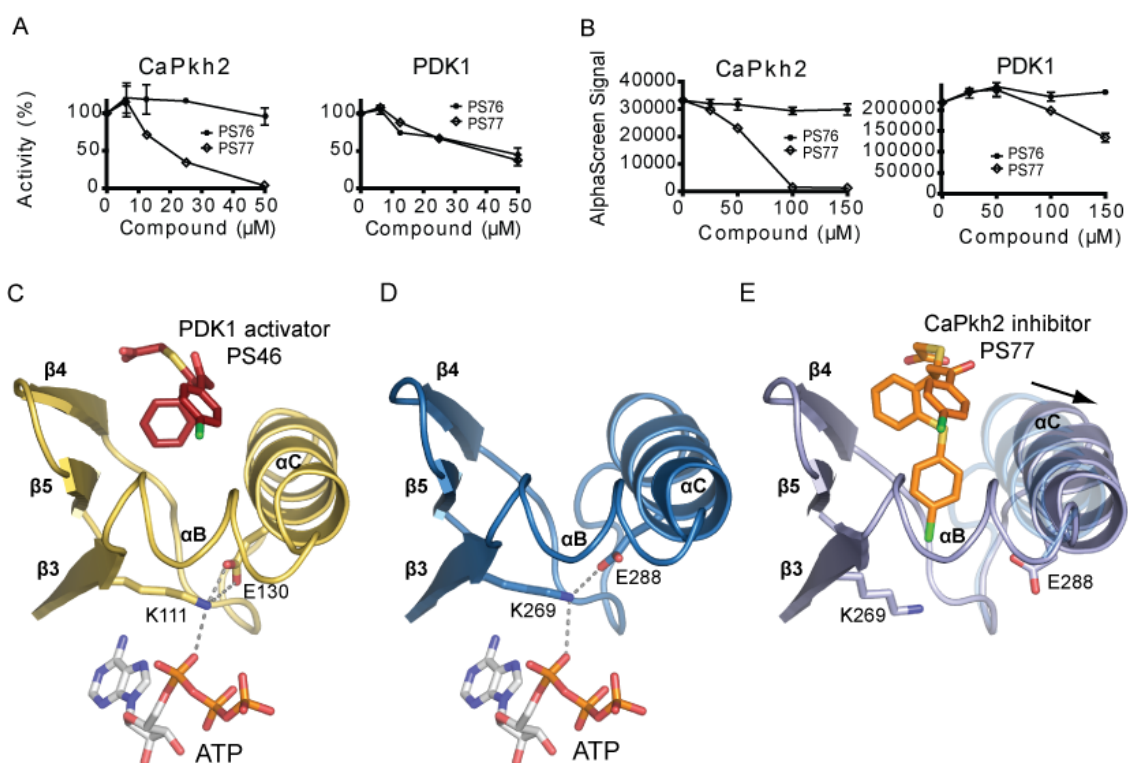


Figure 3.17 Novel compound PS77 is a selective allosteric inhibitor of CaPkh2. A) PS77 selectively inhibits the kinase activity CaPkh2. B) PS77 selectively displaces the interaction between CaPkh2 and PIFtide. Error bars denote the standard deviations. (C–E) Binding mode of PS46 and schematic representation of the possible binding mode of PS77 to the PIF-pocket of CaPkh2. C) Binding of activator PS46 (shown as sticks with red carbon atoms) to human PDK1 (yellow cartoon representation). This compound stabilizes the active conformation where the salt-bridge network among Glu130, Lys 111, and the α -phosphate of ATP is stabilized and primed for catalysis. D) The crystal structure of CaPkh2 (blue cartoon representation) also revealed an active conformation and the highly conserved salt bridges. E) Proposed binding mode of inhibitor PS77 to CaPkh2. Compound PS77 was docked manually into the PIF-pocket of CaPkh2 by (1) positioning the 3-(4-chlorophenyl) and 1-phenyl ring systems, similarly to the position of the two ring systems found in PS48, PS182, and PS210 crystal structures in complex with PDK1, and (2) allowing an opening movement of the helix α -C (translated outward) and positioning the third ring system ((4-chlorophenyl)sulfonyl) in a newly formed deep tunnel, behind helix α -C. For comparison, the original location of helix α -C is shown in transparent blue. Consequently, the model shows that Glu288 is moved out of salt-bridging distance with Lys269 and is not held in position any longer to interact with ATP, suggesting a possible mechanism for the inhibition of CaPkh2 kinase activity.

3.2.4 .5 Small molecule PS77 inhibited the growth of *S. cerevisiae* strains with ABC transporter deletions

In follow-up experiments I found that compound PS77 was not toxic to wild type *S. cerevisiae* cells or a yeast strain with deletion in *ERG6*, a mutation that often facilitates the permeability of small compounds into yeast cells. However, PS77 was toxic to yeast strains YPP66 and YPP64T (EC_{50} approximately 5 μ M), that had deleted Pdr5, Snq2 and Yor1 ABC transporters and transcription factors Pdr1 and Pdr3 that regulate the expression of ABC transporters (Figure 3.18). This indicated that PS77 permeated yeast cells, but that it needs to be improved to avoid interaction with yeast ABC transporters. In addition, I found that PS77, at higher concentrations (25 μ M), was also toxic to mammalian cells in culture (Appendix Figure A.5) suggesting that more selective and potent compounds to CaPkh2 may be required to provide a therapeutic window. At any rate, PS77 represents a proof-of-principle that can be considered a starting point for drug development.

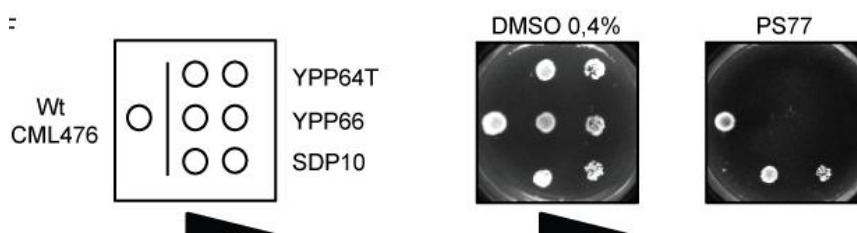


Figure 3.18 PS77 is toxic to YPP66 and YPP64T. Wild type, SDP10, YPP66, and YPP64T yeast strains were spotted onto YPD agar plates in presence or absence of 50 μ M PS77 and incubated at 28 °C for 36 h. SDP10, YPP66, and YPP64T were spotted also at 1:10 dilution.

Together, the present work sheds light on the potential of CaPkh as an antifungal drug target, the potential to use Pkh inhibitors in combination with drugs producing cell wall stress to synergize effects in fungal infectious organisms, and further provides evidence that the PIF-pocket regulatory site on CaPkh provides the desired selectivity to distinguish CaPkh from PDK1 for selective anti-fungal drugs. Similar strategies may be envisaged for other AGC kinases and other organisms producing fungal and parasitic infections.

3.2.5 Characterization of a putative CaPkh2 PH domain

PDK1 is a fundamental regulator of many essential cellular processes being one of the few ancient highly conserved kinases that have been maintained since the

divergence of the eukaryotic groups. The number of PDK1 homologues and the conserved domains within organisms vary from one species to another (Dittrich and Devarenne 2012). Furthermore, these domains could differ between PDK1 proteins found in the same organism, suggesting that some isoforms described as redundant homologues may have specific signal pathways not essential for the cell survival but that can complement cellular processes. In contrast to mammalian PDK1, Pkh proteins in *S. cerevisiae* do not possess a PH domain and analysis of the amino acid sequence did not show any relevant conserved region apart from the catalytic core. However, it is possible that the tools used to identify PH domains were not powerful enough to identify putative described and conserved domains.

In the present work, I identified that CaPkh2 proteins have at least two high affinity lipid binding domains that interact with the structural lipids phosphatidylserine (PSer) and phosphatidic acid (PA) and with signaling lipid PIP2, which inhibit CaPkh2 activity. On the other hand, I showed that sphingolipid dihydrosphingosine (DHS) is activator of CaPkh2 in vitro and released the inhibition produced by PSer. The data suggest that the specific activity of CaPkh2, in contrast to PDK1, may be actively regulated by the interaction with the PM structural lipids.

3.2.5.1 In vitro activity and binding to lipids of Pkh constructs

To investigate a possible regulation of Pkh by lipids, I first expressed and purified three different constructs of CaPkh fused to GST (GST-CaPKH2 1-944; GST-CaPKH2 1-844; GST-CaPKH2 1-521; Table 3.1). In parallel, I also expressed and purified GST-PDK1. Similarly to PDK1, CaPkh2 1-944 and CaPkh2 1-844 phosphorylated the polypeptide T308tide and were activated by PIFtide. In contrast, GST-Pkh2 1-521 (Catalytic domain, CD) was inactive (Figure 3.19). This is different to the effect of deleting the C-terminal region in PDK1, where the equivalent catalytic domain construct of PDK1 has similar specific activity as the full length construct. I previously also observed differences between PDK1 and CaPkh2 in relation to the PIF-pocket, where mutations that activated PDK1 produced inhibition when performed on CaPkh2 (See Item 3.2.5). These data suggested that the C-terminal region of CaPkh2 was required for the activity of the kinase domain, but the mechanism by which the residues between 521-844 are required for activity is not well understood.

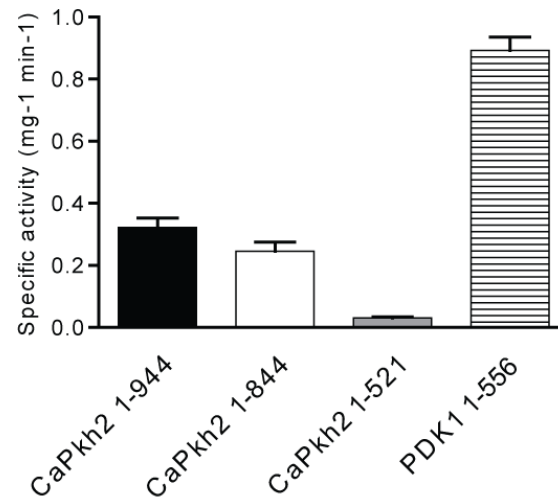


Figure 3.19 Specific activity of PDK1 and CaPkh2 constructs in basal conditions. PDK1 and CaPkh2 FL had different specific activity. The deletion of C-terminal domain in CaPkh2 resulted in loss of activity. In contrast the deletion of the last 100 aminoacids did not affect the activity.

Pkh proteins regulated by the long-chain bases (LCBs) are implicated in the regulation of different important processes such as cell wall integrity, actin dynamics and endocytosis (Walther, Aguilar et al. 2007; Dickson 2008). It was then of interest to identify the ability of Pkh to bind different lipids. For that reason, I employed GST-constructs (Table 3.1) of Pkh and PDK1 in an assay that consists on incubating the GST-fusion proteins with lipids spotted onto membranes and quantifying the lipid-protein binding of Pkh and PDK1 using anti-GST antibodies in a Lipid overlay assay. As previously described, PDK1 interacts with high affinity with PIP₂ and PIP₃ (Figure 3.20B). Interestingly, I observed that CaPkh2 1-944 full length also interacted with PIP₂ and PIP₃. (Figure 3.20C). In addition, CaPkh2 also interacted with P_{Ser}, PA (Figure 3.20C) and sulfatide (Figure 3.20D). Of these, sulfatide and PI(3,4,5)P₃ are not present in yeasts and therefore, are not considered biologically significant. Of interest, neither lysophosphatidic acid (LPA), sphingosine, sphingosine-1P, phytosphingosine nor ceramide bound with high affinity to CaPkh2. This was surprising because sphingosine signaling is considered to activate Pkh downstream pathways. However, we should note that in the assay we identify the remaining GST-Pkh2 protein only after extensive 1 h washing and therefore we are only identifying those lipids to which CaPkh2 binds with high affinity and low OFF-rates.

I then investigated which domains of Pkh participated in the binding to lipids. CaPkh21-844 lacking the last 100 amino acids still interacted with most lipids, but lost its binding affinity for sulfatide, PI(3,5)P₂, PI(3,4)P₂ and PI(4,5)P₂ (Figure 3.20C and

D). On the other hand, the catalytic domain of CaPkh2 did not bind any lipid in the lipid overlay assay (Figure 3.20C and D). Together, the data indicated that the last 100 residues provided the ability of CaPkh2 to bind to the physiologically relevant PIP2 second messenger, while the 521-844 linker region was required to bind with high affinity PS, PA, PI-mono-phosphates and PIP3.

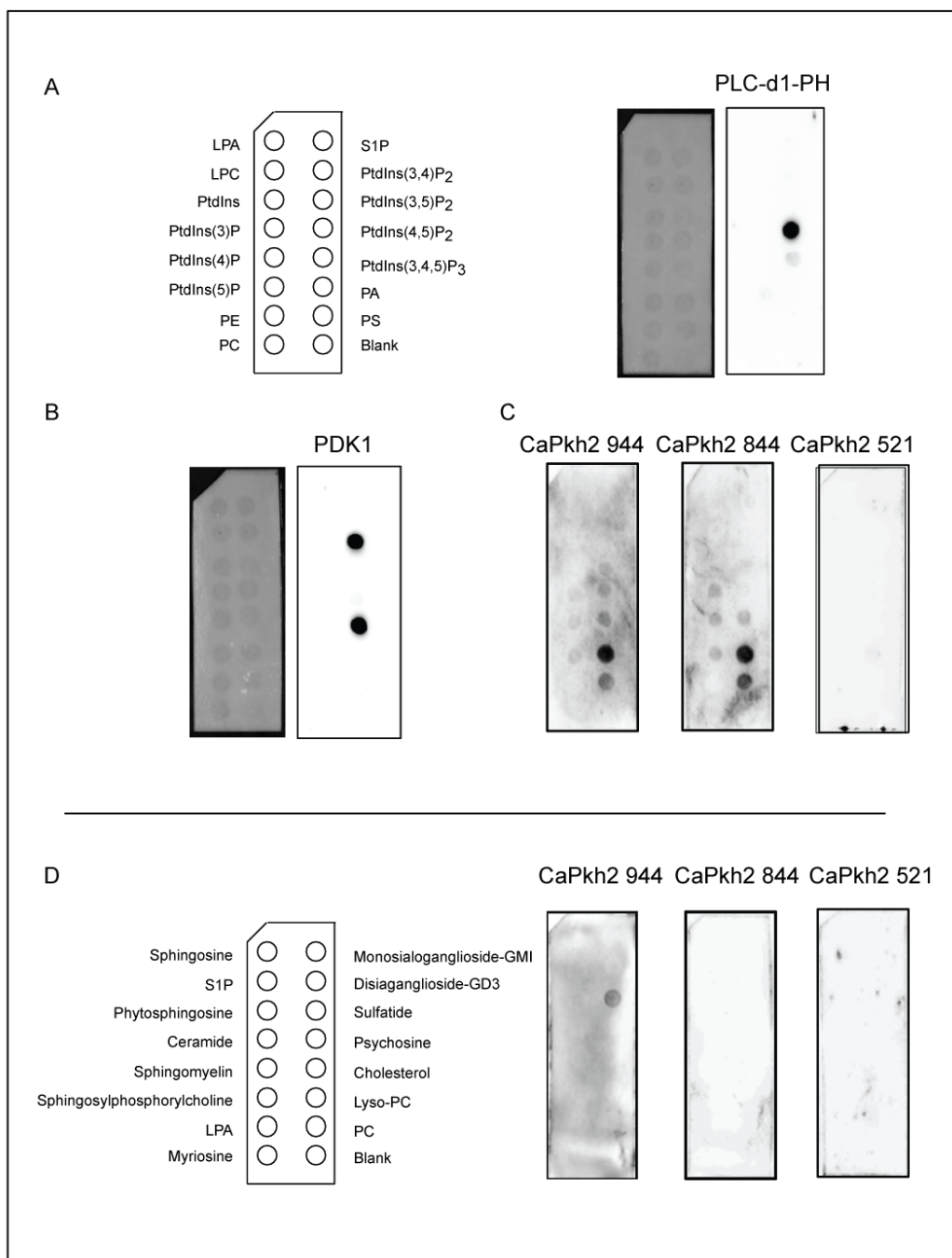


Figure 3.20 Lipid strips interact with PDK1 and CaPkh2 constructs. The proteins were incubated with the membranes containing the lipids in parallel and were developed using the same time conditions for all of them. A) (left) Glycerolphospholipids (PIPstrip). (right) PLC δ 1 that binds PtdIns(4,5)P₂ was used as a positive control. B) PIPstrip. FL and PH delta have affinity for PA, Pser and for the Pins family while CD was is not bound to any lipid. D) Sphingostrips. CaPkh2 FL but not CaPkh 844 or CaPkh2 521 binds to Sulfatide.

Previous studies had not identified any domain at the C-terminal region of Pkhs. However, the ability of the C-terminal region to provide binding affinity to lipids prompted us to carefully revise the possible existence of lipid binding domains. By using structural modeling software and attempting the structural modeling of fragments of the C-terminal region, we indeed identified that the last 100 amino acids of CaPkh2 could be accurately folded into a PH domain (Appendix Table A.3 and Table A.4); similarly, we could also identify a PH domain in the equivalent position in ScPkh2 (Figure 3.21), but not in ScPkh1 nor in Ca or ScPkh3 (data not shown). On the other hand, the same approach could not identify accurately the existence of any domain in the linker region. Together, the data indicated the existence of a putative C-terminal PH domain in CaPkh2, that, like in PDK1, has binding specificity to membrane lipids.

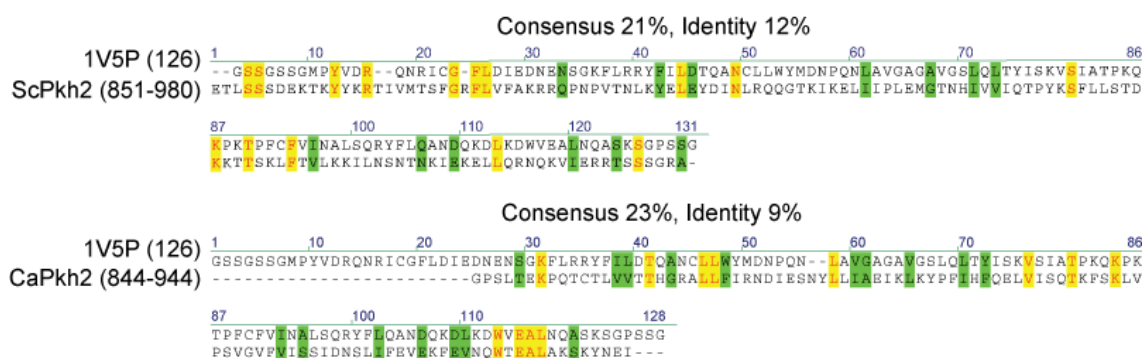


Figure 3.21 Alignment of the N-terminal Pleckstrin Homology Domain of TAPP2 from mouse (1V5P) with ScPkh2 and CaPkh2.

Then, it was of interest to know if the interaction with any of the lipids would affect the specific activity of CaPkh2. As previously described, the *in vitro* specific activity of PDK1 was not significantly affected by lipids. On the contrary, the structural phospholipids PA and PSer significantly inhibited the activity of CaPkh2 (Figure 3.22A). In sharp contrast, PE and PC did not inhibit CaPkh2 but slightly increased its specific activity. The results indicated a high degree of selectivity since PSer bound to CaPkh2 with high affinity and inhibited the kinase while PE, that differs from PSer only in the absence of a carboxylate group, did not bind with high affinity and slightly activated CaPKH2. Next, I investigated whether the PIPs signaling intermediates that bound with high affinity to CaPkh2 had any effect on the activity of CaPkh2. PI(3,4)P₂ and PI(4,5)P₂ inhibited CaPkh2 with high affinity with IC₅₀ below 1 μM (Figure 3.22B). Since PIP₂ is physiologically immersed in phospholipid membranes, we prepared PC vesicles and verified that CaPkh2 was also inhibited by PIP₂ included in PC vesicles

(100 μM) (Figure 3.22B). Finally, it appeared that sulfatide, whose binding was lost upon deletion of the PH domain, did not affect the activity of CaPkh2 (Figure 3.22C). Interestingly, the full length CaPkh2 and the construct lacking the C-terminal PH domain (CaPkh2 1-521) responded almost identically to all lipids tested, including the lack of effect by sulfatide. The results suggest that the PH domain of CaPkh2 may play a similar role to that of the PH domain of PDK1, which does not affect the intrinsic activity of the kinase *in vitro* and only provides localization to the kinase in cells. The fact that sulfatide selectively binds to the C-terminal PH domain indicates that it is functional and very selective for lipid binding. On the other hand, the fact that yeast cells do not possess sulfatide suggests that the physiological target lipid may not be within those tested or may be a yet-to be identified signaling lipid. To end, as it was described, the addition of LCBs such as DHS slightly activated CaPkh2. However the major effect was produced when DHS is added in presence of Pser which inhibits the enzyme activity. DHS stimulated the specific activity of CaPkh2 in a concentration dependent manner. At concentrations of DHS of 50 μM the Pkh activity was restored up to 50% but and at 200 μM it reached almost to 100% (Figure 3.22 C).

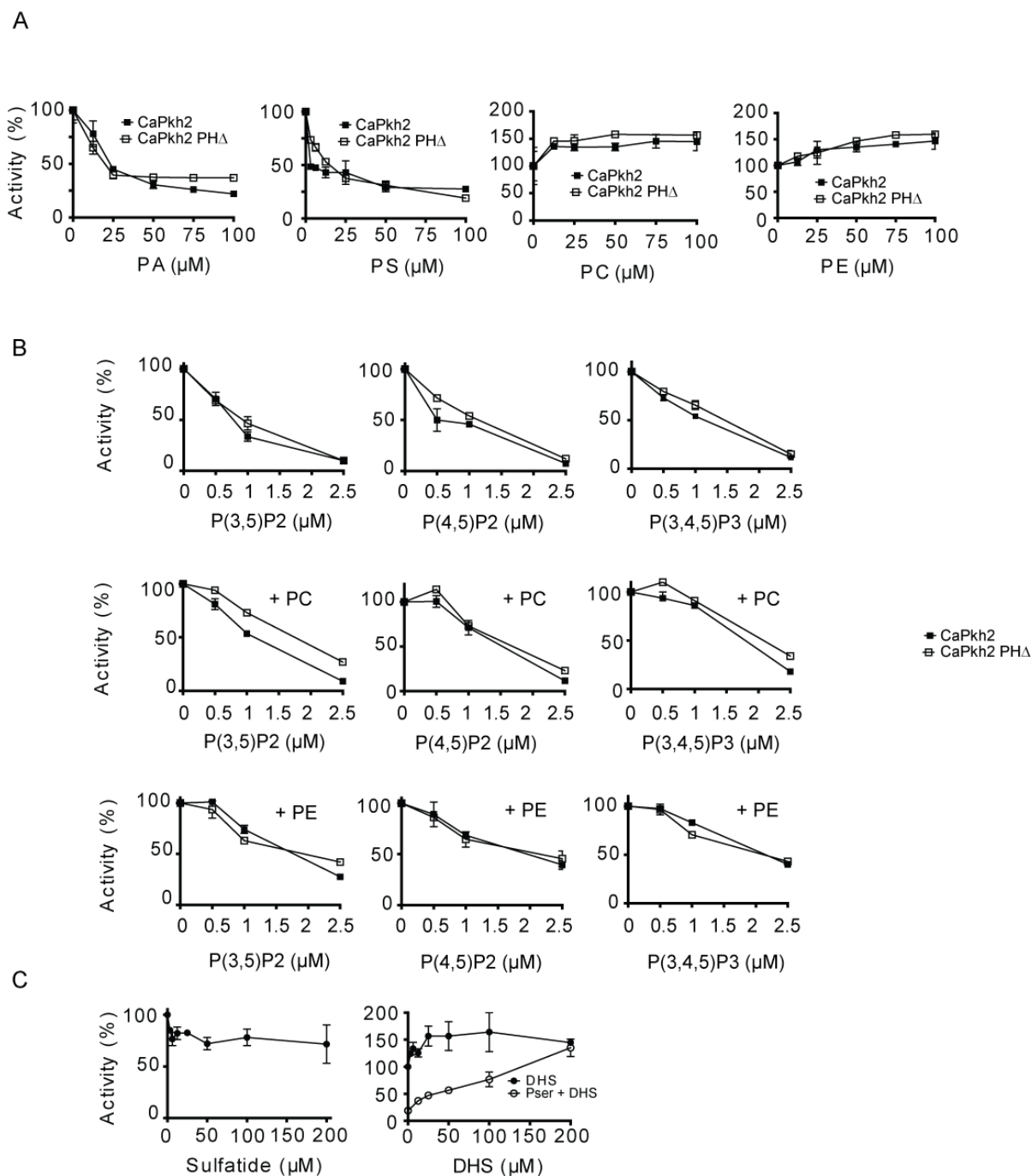


Figure 3.22 Pkh constructs activity with structural lipids and regulatory lipids. A) Pkh activity is inhibited by the addition of PA and Pser while PC and PE partially increased the activity. B) PIP2 and PIP3 inhibited Pkh activity at low concentrations with and without a carrier (PC or PE). C) Sulfatide did not affect Pkh activity. DHS released the inhibition caused by Pser.

In contrast to PDK1's apparently simple mechanism of co-localization with its substrate PKB/Akt by lipids, our overall data indicates that CaPkh2 has a much more elaborated mechanism of regulation by structural and signaling lipids.

Chapter IV: Discussion

Discussion

Previous studies opened the door to explore the possibility of Pkh as a drug target for antifungal therapy (Casamayor, Torrance et al. 1999). Because cells carrying simultaneous deletions of *PKH1* and *PKH2* are not viable, previous works evaluated the role of Pkh in *S. cerevisiae* using temperature-sensitive Pkh proteins (Inagaki, Schmelzle et al. 1999). The use of high temperatures triggers the activation of the CWI pathway and may activate the heat shock response. Results obtained by this strategy could not be a direct consequence of the absence of Pkh activity but be, at least in part, affected by the responses to high stressful temperatures. To evaluate the role of the Pkh proteins in the absence of a temperature shift and corroborate the possible role of Pkh as antifungal target, I developed a strategy based on the doxycycline-repressible tetO promoter to control the expression of *PKH2* (Arino, Casamayor et al. 2007) and I studied the effect of Pkh2 depletion in cells lacking the *PKH1* and *PKH3* genes.

Pkh is an essential protein implicated in a Programmed Cell Death

The use of this strategy allowed us to observe that cells depleted of Pkh had increased ROS and DNA fragmentation, both signatures of apoptosis-like PCD. The activation of the Slr2-MAPK pathway by the expression of the BCK1-20 allele partially rescued the lethality of Pkh-depleted cells. Activation of the CWI pathway also circumvented the presence of intracellular ROS when Pkh-depleted cells grew under standard conditions and also prevented programmed cell death in these cells. Thus, our data provide evidence that the lack of growth due to the apoptotic process in Pkh-deficient cells was caused, at least in part, by a deficient activation of the CWI pathway. Interestingly, previous studies showed that Slr2-deficient cells are hypersensitive to ROS, and this phenotype correlated with high levels of PCD (Krasley, Cooper et al. 2006). A cell death process also occurs in response to mating hormones in the absence of a mating partner in cells deficient for the CWI pathway (Zhang, Dudgeon et al. 2006). In addition, it has been described that the activation of the CWI pathway recues cells from a ROS-dependent farnesol-induced cell death event that was not affected when cells were grown in the presence of sorbitol (Fairn, MacDonald et al. 2007). Thus, our work is in agreement with previous findings and provides evidences that the whole Pkh-Pkc1-Slr2-MAP kinase protein kinase

cascade plays an important role in the response to ROS and that might be important for regulation of PCD.

Notably, the deletion of Pkh triggered an important increase in intracellular ROS. Because the accumulation of ROS is an evolutionary conserved key regulator of diverse forms of apoptosis (Perrone, Tan *et al.* 2008), I investigated whether the loss of cell viability observed in Pkh-depleted cells could be due to an apoptotic process and determined that these cells had higher levels of DNA double-strand breaks than WT cells and that the apoptotic process induced by the lack of Pkh is independent of the yeast metacaspase Mca1. There are other Mca1-independent forms of yeast apoptosis, which are induced by the addition of copper or C2-ceramide to the medium. Physiological scenarios, such as replicative aging and colony differentiation, also induce an Mca1-independent apoptosis (Madeo, Carmona-Gutierrez *et al.* 2009; Carmona-Gutierrez, Reisenbichler *et al.* 2011a). Because sphingolipids have been implicated in the regulation of apoptosis in yeast (Almeida, Marques *et al.* 2008; Aerts, Zabrocki *et al.* 2008; Carmona-Gutierrez, Reisenbichler *et al.* 2011b), Pkh proteins could be important in mediating this process. Interestingly, the Pkh ortholog PDK1 is upstream of a PKB/Akt signaling pathway in mammals that is important for blocking the apoptotic process (reviewed in Duronio 2008). Interestingly, we observed in Pkh depleted cells, an up-regulation of an AIF-like mitochondrial-associate inducer of cell death gene called Ndi1 (Li, Sun *et al.* 2006) which is associated with caspase-independent apoptosis in humans (Wu, Xu *et al.* 2002). The pro-apoptotic gene Ybh3, a BH3 homolog identified during the realization of this thesis (Buttner, Ruli *et al.* 2011), was also found up-regulated in the absence of Pkh. Thus, it may contribute to the apoptotic PCD where the mitochondria would be implicated. At any rate, this work provides an evidence of the fundamental role of Pkh in the cell survival. The major problem of antifungal drugs is the absence of effective compounds that are cytotoxic rather than cytostatic. According to our results we can conclude that Pkh proteins, essential for cell survival, are potential drug targets for antifungal therapy.

Structural differences in the PIF-pocket but not in the ATP-binding site of *C. albicans* can be used to develop specific compounds.

The development of drugs targeting the ATP-binding site of protein kinases has been one of the biggest concerns in the last decade, being approximately one third of all protein targets under investigation in the pharmaceutical industry (Fabbro, Cowan-Jacob et al. 2012). Unfortunately, the ATP-binding site is very conserved not only among most of the human protein kinases but even among kinases of evolutionary distant organisms. This high conservation between the ATP-binding sites of human kinases made it almost impossible to gain selectivity for targeting specific kinases. Recently, protein kinase inhibitors that inhibited the CWI pathway and had antifungal activity against *C. albicans* were identified (Baxter, DiDone et al. 2011). The compounds (e.g. KP-372, staurosporine and UCN-01) are known to inhibit several human protein kinases including PDK1 and may also target other kinases in yeasts. Because of the low specificity of most of the developed drugs targeting the ATP-binding site of protein kinases, compounds targeting fungal Pkh are expected to inhibit the human PDK1 and also multiple additional human kinases, producing unwanted side effects. Indeed, based on our crystal structure of CaPkh2 and activity assays, the kinase inhibitors suggested to target fungal kinases, inhibited human PDK1 at a nanomolar range with equal (staurosporine) or even better potency (UCN-01) than CaPkh2. Therefore, this difference cannot be exploited for the development of selective CaPkh2 inhibitors.. In addition, we confirmed that the compound KP-372 did not inhibit CaPkh2 activity, nor human PDK1 activity. Therefore, this difference cannot be exploited for the development of selective CaPkh2 inhibitors.

It has been speculated that higher selectivity could be achieved by targeting sites different than the ATP-binding site on fungal Pkh1. Recently, our group developed novel small compounds that, targeting the regulatory PIF-pocket site, allosterically activate or inhibit the activity of AGC kinases (Hindie, Stroba et al. 2009; Lopez-Garcia, Schulze et al. 2011). This technology can be employed for any eukaryotic organism since AGC kinases have a high conservation between species (Arencibia, Pastor-Flores et al. 2013). In contrast to the high similarity in the ATP-binding site, I found biochemical and structural differences between the PIF-pockets of PDK1 and CaPkh2 and additional differences in the activities of PDK1 and CaPkh2 proteins mutated at the PIF-pockets. Our data showed differences in the residues constituting

the CaPkh2 PIF-pocket of is formed amino acids, suggesting that these differences could give more selectivity versus small compounds. In addition, a bigger loop following the

regulatory α C helix of CaPkh2 could allow an opening movement of the α C helix forming a deep tunnel between α C helix and the β -sheet. Previous observations by deuterium exchange in our laboratory showed that the α C helix is a very flexible region in atypical PKCs and that this flexibility may allow the formation of a deep tunnel, creating space for compounds to enter deeper into the structure. I corroborated these structural differences with the small compound PS77, which specifically inhibited CaPkh2 but had marginal inhibitory effect on PDK1. These data are a first indication that the PIF-pocket is structurally and functionally different between the human PDK1 and the *C. albicans* orthologs and that it may provide selectivity for the development of CaPkh2-selective antifungal drugs. In addition, our work may also impinge on the drug development strategies against other eukaryotic infective organisms.

Depleting genes by an alternative strategy to avoid high temperatures

The doxycycline repressible promoter technology used in *S. cerevisiae* shed light to an alternative approach to avoid the side effects generated by incubation of cells harboring temperature-sensitive alleles to higher-than-optimal temperatures, and that could be considered by the cells as stressful conditions. During the realization of this thesis, similar approaches to study the effects of the depletion of either, the Sch9 kinase or the essential Lcb1/2 proteins in the sphingolipid production (Huang, Liu et al. 2012). The observed phenotypes in this project, after long-term incubations times with doxycycline are a sum of direct and indirect effects produced by the decreased levels, and eventually the depletion, of Pkh. My studies showed that decreased levels of Pkh and depletion of Pkh affects the transcription of a remarkably large number of genes including the up-regulation of many genes involved in the response to heat shock and oxidative stresses. Interestingly, a relevant fraction of the Pkh-dependent up-regulated genes are known to be transcribed by the Msn2/Msn4 or Hsf1 transcription factors, providing evidence for the endpoint effectors of Pkh signaling after a heat shock. The phosphorylation in the activation loop of Sch9 and PKA by Pkh proteins suggested a direct evidence of the implication of Pkh in Hsf1,

Msn2/Msn4 regulation. A non-phosphorylated activation loop conformation of Tpk1 decreases its association with Bcy1 and phosphorylation of the activation loop of Tpk1 is capable to interact with a Bcy1 dimer to form the holoenzyme molecule forming an inactive form (Haesendonckx, Tudisca et al. 2012). Taking into account that PKA negatively regulates the expression of Hsf1, Mns2 and Mns4 it may be an explanation for the activation of heat shock factors since in a *pkh1^{ts} pkh2 pkh3* strain, the phosphorylation in the activation loop of both Tpk2 and Tpk3 is completely abolished at the restrictive temperature of 37°C (Levin and Zoller 1990; Haesendonckx, Tudisca et al. 2012) and mutations in the Tpk1 Phe-Xaa-Xaa-Phe motif drastically reduces Pkh1-Tpk1 interaction (Voordeckers, Kimpe et al. 2011). On the other side Pkh acts upstream activating Sch9 by the phosphorylation of its activation loop. Since the transcription factor Hsf1 has been linked to Sch9, it also may explain the increment in the heat shock factors activity (Morano and Thiele 1999). Some of the transcriptional changes induced by the depletion of Pkh were already evident in SDP8 after 8 h of doxycycline treatment. At this time point, I found an up-regulation of seven genes out of the eleven involved in the synthesis of glycogen. Reduction of Pkh2 expression in a *pkh1pkh3* background increased glycogen accumulation. This response was a previously observed response to some stresses that are mediated by the Msn2/Msn4 transcription factors (Smith, Ward et al. 1998).

The depletion of Pkh also showed the importance of Pkh proteins in the CWI pathway demonstrating for the first time that Pkh is necessary for the phosphorylation of the Slit2 MAP kinase in the presence of cell wall stress. Accordingly, I revealed that Pkh-deficient cells were hypersensitive to cell wall stressors. I also presented evidence that the death of Pkh-depleted cells growing in standard conditions was not only due to a cell lysis defect as a consequence of a defect in the cell wall because, in contrast to what occurs with cells lacking Pkc1, the addition of an osmotic stabilizer to the medium did not restore cell survival. My results are in agreement with those obtained by Voordeckers and co-workers, where sorbitol rescued the growth defect of the *pkh1^{ts} pkh2* strain but could not completely rescue the growth of the *pkh1^{ts} pkh2 pkh3* strain when cells were grown at 35 °C (Voordeckers, Kimpe et al. 2011). Thus, Pkh proteins might also be involved in additional CWI-independent essential functions. This hypothesis is also supported by the very different transcriptional profiles

obtained under standard growth conditions by the depletion of Pkh (this work) and the deletion of *Slr2* (van Wageningen, Kemmeren *et al.* 2010).

Pkh is tightly regulated by structural and signaling lipids

I showed that CaPkh2 proteins have at least two high-affinity lipid-binding domains that interact with the structural lipids Pser and PA and with signaling lipids Pins(3,5)P2 and Pins(4,5)P2, which inhibit CaPkh2 activity while PE and PC did not affect CaPkh2 activity. Pser is found in *S. cerevisiae* in low abundance in cell organelles and is enriched asymmetrically in the inner layer of the plasma membrane through the regulation of the lipid translocase (flippase) by Pkh-Ypk (Roelants, Baltz *et al.* 2010). In addition, Pser is present at high concentrations in the cell cycle during the bud emergence with localization near the septin ring and decreasing in the following cell cycle. This behavior contrasts with the levels of PC and PE which increase linearly during the cell cycle (Fairn, Hermansson *et al.* 2011). The specific binding of CaPkh2 to Pser and not to PE and the inhibitory effect that Pser has on CaPkh2 specific activity may be linked with these events. Our biochemical data is consistent with the model presented in Figure 4.1. The finding that the CaPkh 1-844 construct is active but that the CaPkh 1-521 is inactive, suggests that the linker region including 521-844 may bind to the catalytic core, complementing the kinase domain and stabilizing the active conformation of the kinase. In addition, the linker region also binds with high affinity to inhibitory structural lipids Pser and PA. Therefore, the proposal is that the binding to Pser and PA prevents the linker region from its activating function, effectively inhibiting the intrinsic activity of CaPkh2. Previous work showed that Pkh1 and Pkh2 are localized in the plasma membrane by eisosome assembly and that Pkh1 but not Pkh2 requires the major eisosome component, Pil1, for this association. One possibility is that the binding to Pser and PA enhances the binding of Pkh2 to the plasma membrane only when the PH domain binding lipid is accumulated. Thus, the C-terminal PH domain may play a role to trigger Pkh interaction with the membrane –and hence inhibition- only upon the accumulation of a sulfatide-like signaling lipid. In mammals, the lipid co-localization strategy appears to be employed only for phosphorylation of PKB/Akt while the regulated docking-site between a HM and the PIF-pocket of PDK1 appears to be the more widely used mechanism for regulated interaction and phosphorylation of substrates. The finding that CaPkh2 has conserved its ability to bind an HM

polypeptide (PIFtide) and regulate its activity suggests that the mechanism of docking interaction with substrates is conserved. In this line, all kinase substrates of Pkh, i.e. Pkc1, Ypks, Tpk1 and Sch9, possess a conserved HM with the potential to dock to the PIF-pocket of Pkh to enhance the activity of Pkh when the substrates dock.

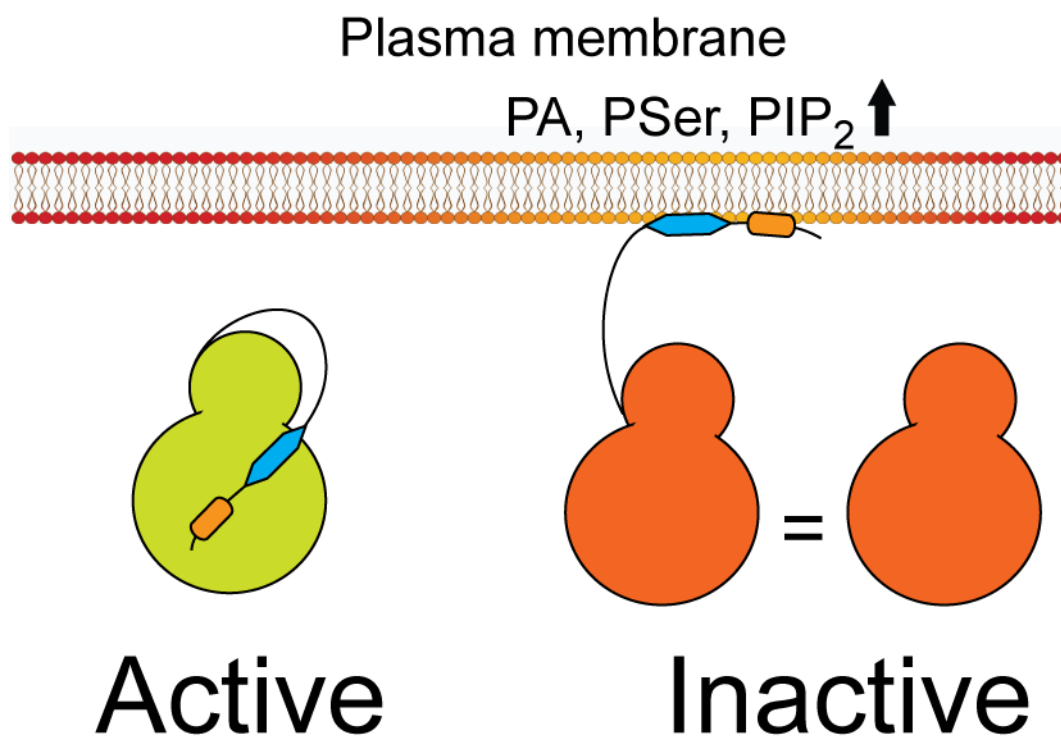


Figure 4.1 Model mechanism of CaPkh2 regulation by phospholipids.

4.1 Perspectives

Together, the results of my work indicate the existence of structural features that are different between mammalian PDK1 and CaPkh2. Notably, my work shows that CaPkh2 has evolved a different mechanism of regulation by structural and signaling lipids. At this point, it would be ideal to identify the exact domains that are binding to the regulatory and structural lipids and to structurally and biochemically characterize its molecular mechanism of allosteric regulation. In addition to the understanding of the evolution of the mechanisms of regulation of AGC kinases, such studies may uncover additional sites for CaPkh-selective drug developments.

In this study I validated Pkh as a target for antifungal agents. In addition, I demonstrated that it is possible to gain selectivity between kinases conserved in both organisms. This finding clears the way for a novel drug development approach

against fungal organisms. Selective Pkh inhibitors would indirectly act as antifungal agents by abolishing Pkh activity, leading infective fungal organisms to a PCD. In addition, the Pkh signaling pathway is activated by different stresses and its function is required for survival mechanisms in response to current antifungal drugs that target the cell wall or plasma membrane. In this regard, it is possible to speculate that selective Pkh inhibitors may be employed in combination with current drugs, synergizing their antifungal effects. Thus, as a final perspective, I suggest that it is important to investigate the relationship between Pkh inhibition in combination with standard antifungal drugs, in view of its potential future use in the effective treatment and cure of systemic mycoses that are currently deadly.

Bibliography

Bibliography

- Abdulrehman, D., P. T. Monteiro, et al. (2011). "YEASTRACT: providing a programmatic access to curated transcriptional regulatory associations in *Saccharomyces cerevisiae* through a web services interface." *Nucleic Acids Res* **39**(Database issue): D136-140.
- Alberola, T. M., J. Garcia-Martinez, et al. (2004). "A new set of DNA macrochips for the yeast *Saccharomyces cerevisiae*: features and uses." *Int Microbiol* **7**(3): 199-206.
- Albuquerque, C. P., M. B. Smolka, et al. (2008). "A multidimensional chromatography technology for in-depth phosphoproteome analysis." *Mol Cell Proteomics* **7**(7): 1389-1396.
- Alonso-Monge, R., F. Navarro-Garcia, et al. (1999). "Role of the mitogen-activated protein kinase Hog1p in morphogenesis and virulence of *Candida albicans*." *J Bacteriol* **181**(10): 3058-3068.
- Anastasia, S. D., D. L. Nguyen, et al. (2012). "A link between mitotic entry and membrane growth suggests a novel model for cell size control." *J Cell Biol* **197**(1): 89-104.
- Arana, D. M., C. Nombela, et al. (2005). "The Pbs2 MAP kinase kinase is essential for the oxidative-stress response in the fungal pathogen *Candida albicans*." *Microbiology* **151**(Pt 4): 1033-1049.
- Arenas, R., G. Moreno-Coutino, et al. (2012). "Classification of subcutaneous and systemic mycoses." *Clin Dermatol* **30**(4): 369-371.
- Arencibia, J. M., D. Pastor-Flores, et al. (2013). "AGC protein kinases: from structural mechanism of regulation to allosteric drug development for the treatment of human diseases." *Biochim Biophys Acta* **1834**(7): 1302-1321.
- Aresta-Branco, F., A. M. Cordeiro, et al. (2011). "Gel domains in the plasma membrane of *Saccharomyces cerevisiae*: highly ordered, ergosterol-free, and sphingolipid-enriched lipid rafts." *J Biol Chem* **286**(7): 5043-5054.
- Aslakson, C. J. and F. R. Miller (1992). "Selective events in the metastatic process defined by analysis of the sequential dissemination of subpopulations of a mouse mammary tumor." *Cancer Res* **52**(6): 1399-1405.
- Bagnat, M. and K. Simons (2002). "Lipid rafts in protein sorting and cell polarity in budding yeast *Saccharomyces cerevisiae*." *Biol Chem* **383**(10): 1475-1480.
- Balendran, A., A. Casamayor, et al. (1999). "PDK1 acquires PDK2 activity in the presence of a synthetic peptide derived from the carboxyl terminus of PRK2." *Curr Biol* **9**(8): 393-404.
- Balendran, A., G. R. Hare, et al. (2000). "Further evidence that 3-phosphoinositide-dependent protein kinase-1 (PDK1) is required for the stability and phosphorylation of protein kinase C (PKC) isoforms." *FEBS Lett* **484**(3): 217-223.
- Bauer, A. F., S. Sonzogni, et al. (2012). "Regulation of protein kinase C-related protein kinase 2 (PRK2) by an intermolecular PRK2-PRK2 interaction mediated by its N-terminal domain." *J Biol Chem* **287**(24): 20590-20602.
- Baxter, B. K., L. DiDone, et al. (2011). "Identification, in vitro activity and mode of action of phosphoinositide-dependent-1 kinase inhibitors as antifungal molecules." *ACS Chem Biol* **6**(5): 502-510.
- Berchtold, D. and T. C. Walther (2009). "TORC2 plasma membrane localization is essential for cell viability and restricted to a distinct domain." *Mol Biol Cell* **20**(5): 1565-1575.
- Biondi, R. M. (2004). "Phosphoinositide-dependent protein kinase 1, a sensor of protein conformation." *Trends Biochem Sci* **29**(3): 136-142.
- Biondi, R. M., P. C. Cheung, et al. (2000). "Identification of a pocket in the PDK1 kinase domain that interacts with PIF and the C-terminal residues of PKA." *EMBO J* **19**(5): 979-988.
- Biondi, R. M., A. Kieloch, et al. (2001). "The PIF-binding pocket in PDK1 is essential for activation of S6K and SGK, but not PKB." *EMBO J* **20**(16): 4380-4390.
- Biondi, R. M., D. Komander, et al. (2002). "High resolution crystal structure of the human PDK1 catalytic domain defines the regulatory phosphopeptide docking site." *EMBO J* **21**(16): 4219-4228.

- Blankenship, J. R., S. Fanning, et al. (2010). "An extensive circuitry for cell wall regulation in *Candida albicans*." *PLoS Pathog* **6**(2): e1000752.
- Bockmuhl, D. P., S. Krishnamurthy, et al. (2001). "Distinct and redundant roles of the two protein kinase A isoforms Tpk1p and Tpk2p in morphogenesis and growth of *Candida albicans*." *Mol Microbiol* **42**(5): 1243-1257.
- Budovskaya, Y. V., J. S. Stephan, et al. (2004). "The Ras/cAMP-dependent protein kinase signaling pathway regulates an early step of the autophagy process in *Saccharomyces cerevisiae*." *J Biol Chem* **279**(20): 20663-20671.
- Busschots, K., L. A. Lopez-Garcia, et al. (2012). "Substrate-selective inhibition of protein kinase PDK1 by small compounds that bind to the PIF-pocket allosteric docking site." *Chem Biol* **19**(9): 1152-1163.
- Buttner, S., D. Ruli, et al. (2011). "A yeast BH3-only protein mediates the mitochondrial pathway of apoptosis." *EMBO J* **30**(14): 2779-2792.
- Calabrese, D., J. Bille, et al. (2000). "A novel multidrug efflux transporter gene of the major facilitator superfamily from *Candida albicans* (FLU1) conferring resistance to fluconazole." *Microbiology* **146 (Pt 11)**: 2743-2754.
- Cannon, R. D., E. Lamping, et al. (2009). "Efflux-mediated antifungal drug resistance." *Clin Microbiol Rev* **22**(2): 291-321, Table of Contents.
- Cao, F., S. Lane, et al. (2006). "The Flo8 transcription factor is essential for hyphal development and virulence in *Candida albicans*." *Mol Biol Cell* **17**(1): 295-307.
- Carmody, S. R., E. J. Tran, et al. (2010). "The mitogen-activated protein kinase Slt2 regulates nuclear retention of non-heat shock mRNAs during heat shock-induced stress." *Mol Cell Biol* **30**(21): 5168-5179.
- Casado, C., A. Gonzalez, et al. (2011). "The role of the protein kinase A pathway in the response to alkaline pH stress in yeast." *Biochem J* **438**(3): 523-533.
- Casamayor, A., P. D. Torrance, et al. (1999). "Functional counterparts of mammalian protein kinases PDK1 and SGK in budding yeast." *Curr Biol* **9**(4): 186-197.
- Chauhan, N., J. P. Latge, et al. (2006). "Signalling and oxidant adaptation in *Candida albicans* and *Aspergillus fumigatus*." *Nat Rev Microbiol* **4**(6): 435-444.
- Cheetham, J., D. A. Smith, et al. (2007). "A single MAPKKK regulates the Hog1 MAPK pathway in the pathogenic fungus *Candida albicans*." *Mol Biol Cell* **18**(11): 4603-4614.
- Cheng, J., T. S. Park, et al. (2003). "Induction of apoptosis by sphingoid long-chain bases in *Aspergillus nidulans*." *Mol Cell Biol* **23**(1): 163-177.
- Chevtzoff, C., E. D. Yoboue, et al. (2010). "Reactive oxygen species-mediated regulation of mitochondrial biogenesis in the yeast *Saccharomyces cerevisiae*." *J Biol Chem* **285**(3): 1733-1742.
- Colombo, S., P. Ma, et al. (1998). "Involvement of distinct G-proteins, Gpa2 and Ras, in glucose- and intracellular acidification-induced cAMP signalling in the yeast *Saccharomyces cerevisiae*." *EMBO J* **17**(12): 3326-3341.
- Connerth, M., T. Tatsuta, et al. (2012). "Intramitochondrial transport of phosphatidic acid in yeast by a lipid transfer protein." *Science* **338**(6108): 815-818.
- Csank, C., K. Schroppel, et al. (1998). "Roles of the *Candida albicans* mitogen-activated protein kinase homolog, Cek1p, in hyphal development and systemic candidiasis." *Infect Immun* **66**(6): 2713-2721.
- Daquinag, A., M. Fadri, et al. (2007). "The yeast PH domain proteins Slm1 and Slm2 are targets of sphingolipid signaling during the response to heat stress." *Mol Cell Biol* **27**(2): 633-650.
- Davis-Hanna, A., A. E. Piispanen, et al. (2008). "Farnesol and dodecanol effects on the *Candida albicans* Ras1-cAMP signalling pathway and the regulation of morphogenesis." *Mol Microbiol* **67**(1): 47-62.
- de Nobel, H., C. Ruiz, et al. (2000). "Cell wall perturbation in yeast results in dual phosphorylation of the Slt2/Mpk1 MAP kinase and in an Slt2-mediated increase in FKS2-lacZ expression, glucanase resistance and thermotolerance." *Microbiology* **146 (Pt 9)**: 2121-2132.

- Deak, M., A. Casamayor, et al. (1999). "Characterisation of a plant 3-phosphoinositide-dependent protein kinase-1 homologue which contains a pleckstrin homology domain." *FEBS Lett* **451**(3): 220-226.
- Denis, V. and M. S. Cyert (2005). "Molecular analysis reveals localization of *Saccharomyces cerevisiae* protein kinase C to sites of polarized growth and Pkc1p targeting to the nucleus and mitotic spindle." *Eukaryot Cell* **4**(1): 36-45.
- Dettori, R., S. Sonzogni, et al. (2009). "Regulation of the interaction between protein kinase C-related protein kinase 2 (PRK2) and its upstream kinase, 3-phosphoinositide-dependent protein kinase 1 (PDK1)." *J Biol Chem* **284**(44): 30318-30327.
- Dickson, R. C. (2008). "Thematic review series: sphingolipids. New insights into sphingolipid metabolism and function in budding yeast." *J Lipid Res* **49**(5): 909-921.
- Dickson, R. C. and R. L. Lester (1999). "Yeast sphingolipids." *Biochim Biophys Acta* **1426**(2): 347-357.
- Dickson, R. C., E. E. Nagiec, et al. (1997). "Sphingolipids are potential heat stress signals in *Saccharomyces*." *J Biol Chem* **272**(48): 30196-30200.
- Diez-Orejas, R., G. Molero, et al. (1997). "Reduced virulence of *Candida albicans* MKC1 mutants: a role for mitogen-activated protein kinase in pathogenesis." *Infect Immun* **65**(2): 833-837.
- Dittrich, A. C. and T. P. Devarenne (2012). "Perspectives in PDK1 evolution: insights from photosynthetic and non-photosynthetic organisms." *Plant Signal Behav* **7**(6): 642-649.
- Dowler, S., G. Kular, et al. (2002). "Protein lipid overlay assay." *Sci STKE* **2002**(129): pl6.
- Engel, M., V. Hindie, et al. (2006). "Allosteric activation of the protein kinase PDK1 with low molecular weight compounds." *EMBO J* **25**(23): 5469-5480.
- Estruch, F. (2000). "Stress-controlled transcription factors, stress-induced genes and stress tolerance in budding yeast." *FEMS Microbiol Rev* **24**(4): 469-486.
- Estruch, F. and M. Carlson (1993). "Two homologous zinc finger genes identified by multicopy suppression in a SNF1 protein kinase mutant of *Saccharomyces cerevisiae*." *Mol Cell Biol* **13**(7): 3872-3881.
- Fabbro, D., S. W. Cowan-Jacob, et al. (2012). "Targeting cancer with small-molecular-weight kinase inhibitors." *Methods Mol Biol* **795**: 1-34.
- Fabrizio, P., F. Pozza, et al. (2001). "Regulation of longevity and stress resistance by Sch9 in yeast." *Science* **292**(5515): 288-290.
- Fairn, G. D., M. Hermansson, et al. (2011). "Phosphatidylserine is polarized and required for proper Cdc42 localization and for development of cell polarity." *Nat Cell Biol* **13**(12): 1424-1430.
- Feng, Q., E. Summers, et al. (1999). "Ras signaling is required for serum-induced hyphal differentiation in *Candida albicans*." *J Bacteriol* **181**(20): 6339-6346.
- Ferguson, S. B., E. S. Anderson, et al. (2005). "Protein kinase A regulates constitutive expression of small heat-shock genes in an Msn2/4p-independent and Hsf1p-dependent manner in *Saccharomyces cerevisiae*." *Genetics* **169**(3): 1203-1214.
- Fields, S. and O. Song (1989). "A novel genetic system to detect protein-protein interactions." *Nature* **340**(6230): 245-246.
- Fitzpatrick, D. A., M. E. Logue, et al. (2006). "A fungal phylogeny based on 42 complete genomes derived from supertree and combined gene analysis." *BMC Evol Biol* **6**: 99.
- Fox, G. C., M. Shafiq, et al. (2007). "Redox-mediated substrate recognition by Sdp1 defines a new group of tyrosine phosphatases." *Nature* **447**(7143): 487-492.
- Friant, S., R. Lombardi, et al. (2001). "Sphingoid base signaling via Pkh kinases is required for endocytosis in yeast." *EMBO J* **20**(23): 6783-6792.
- Friant, S., B. Zanolari, et al. (2000). "Increased protein kinase or decreased PP2A activity bypasses sphingoid base requirement in endocytosis." *EMBO J* **19**(12): 2834-2844.
- Frodin, M., T. L. Antal, et al. (2002). "A phosphoserine/threonine-binding pocket in AGC kinases and PDK1 mediates activation by hydrophobic motif phosphorylation." *EMBO J* **21**(20): 5396-5407.
- Garrett, S., M. M. Menold, et al. (1991). "The *Saccharomyces cerevisiae* YAK1 gene encodes a protein kinase that is induced by arrest early in the cell cycle." *Mol Cell Biol* **11**(8): 4045-4052.

- Gbelska, Y., J. J. Krijger, et al. (2006). "Evolution of gene families: the multidrug resistance transporter genes in five related yeast species." *FEMS Yeast Res* **6**(3): 345-355.
- Giacometti, R., F. Kronberg, et al. (2012). "Cross regulation between *Candida albicans* catalytic and regulatory subunits of protein kinase A." *Fungal Genet Biol* **49**(1): 74-85.
- Giacometti, R., F. Kronberg, et al. (2009). "Catalytic isoforms Tpk1 and Tpk2 of *Candida albicans* PKA have non-redundant roles in stress response and glycogen storage." *Yeast* **26**(5): 273-285.
- Giacometti, R., F. Kronberg, et al. (2011). "*Candida albicans* Tpk1p and Tpk2p isoforms differentially regulate pseudohyphal development, biofilm structure, cell aggregation and adhesin expression." *Yeast* **28**(4): 293-308.
- Gow, N. A., A. J. Brown, et al. (2002). "Fungal morphogenesis and host invasion." *Curr Opin Microbiol* **5**(4): 366-371.
- Graham, F. L., J. Smiley, et al. (1977). "Characteristics of a human cell line transformed by DNA from human adenovirus type 5." *J Gen Virol* **36**(1): 59-74.
- Griffioen, G. and J. M. Thevelein (2002). "Molecular mechanisms controlling the localisation of protein kinase A." *Curr Genet* **41**(4): 199-207.
- Grosshans, B. L., A. Andreeva, et al. (2006). "The yeast Igl family member Sro7p is an effector of the secretory Rab GTPase Sec4p." *J Cell Biol* **172**(1): 55-66.
- Grossmann, G., J. Malinsky, et al. (2008). "Plasma membrane microdomains regulate turnover of transport proteins in yeast." *J Cell Biol* **183**(6): 1075-1088.
- Grubb, S. E., C. Murdoch, et al. (2008). "*Candida albicans*-endothelial cell interactions: a key step in the pathogenesis of systemic candidiasis." *Infect Immun* **76**(10): 4370-4377.
- Gruhler, A., J. V. Olsen, et al. (2005). "Quantitative phosphoproteomics applied to the yeast pheromone signaling pathway." *Mol Cell Proteomics* **4**(3): 310-327.
- Guo, S., X. Shen, et al. (2009). "A MAP kinase dependent feedback mechanism controls Rho1 GTPase and actin distribution in yeast." *PLoS One* **4**(6): e6089.
- Haesendonckx, S., V. Tudisca, et al. (2012). "Activation loop of PKA catalytic isoforms is differentially phosphorylated by Pkh protein kinases in *Saccharomyces cerevisiae*." *Biochem J*.
- Harashima, T. and J. Heitman (2002). "The Galpha protein Gpa2 controls yeast differentiation by interacting with kelch repeat proteins that mimic Gbeta subunits." *Mol Cell* **10**(1): 163-173.
- Hauge, C., T. L. Antal, et al. (2007). "Mechanism for activation of the growth factor-activated AGC kinases by turn motif phosphorylation." *EMBO J* **26**(9): 2251-2261.
- Hegde, P., R. Qi, et al. (2000). "A concise guide to cDNA microarray analysis." *Biotechniques* **29**(3): 548-550, 552-544, 556 passim.
- Henry, S. A., S. D. Kohlwein, et al. (2012). "Metabolism and regulation of glycerolipids in the yeast *Saccharomyces cerevisiae*." *Genetics* **190**(2): 317-349.
- Herrero, A. B., M. C. Lopez, et al. (1999). "*Candida albicans* and *Yarrowia lipolytica* as alternative models for analysing budding patterns and germ tube formation in dimorphic fungi." *Microbiology* **145 (Pt 10)**: 2727-2737.
- Hindie, V., A. Stroba, et al. (2009). "Structure and allosteric effects of low-molecular-weight activators on the protein kinase PDK1." *Nat Chem Biol* **5**(10): 758-764.
- Hindie, V., A. Stroba, et al. (2009). "Structure and allosteric effects of low molecular weight activators on the protein kinase PDK1." *Nat. Chem. Biol.* **5**(10): 758-764.
- Hohmann, S. (2002). "Osmotic stress signaling and osmoadaptation in yeasts." *Microbiol Mol Biol Rev* **66**(2): 300-372.
- Holt, L. J., B. B. Tuch, et al. (2009). "Global analysis of Cdk1 substrate phosphorylation sites provides insights into evolution." *Science* **325**(5948): 1682-1686.
- Hong, F., M. D. Larrea, et al. (2008). "mTOR-raptor binds and activates SGK1 to regulate p27 phosphorylation." *Mol Cell* **30**(6): 701-711.
- Huber, A., B. Bodenmiller, et al. (2009). "Characterization of the rapamycin-sensitive phosphoproteome reveals that Sch9 is a central coordinator of protein synthesis." *Genes Dev* **23**(16): 1929-1943.

- Ikenoue, T., K. Inoki, et al. (2008). "Essential function of TORC2 in PKC and Akt turn motif phosphorylation, maturation and signalling." *EMBO J* **27**(14): 1919-1931.
- Inagaki, M., T. Schmelzle, et al. (1999). "PDK1 homologs activate the Pkc1-mitogen-activated protein kinase pathway in yeast." *Mol Cell Biol* **19**(12): 8344-8352.
- Inoue, H., H. Nojima, et al. (1990). "High efficiency transformation of Escherichia coli with plasmids." *Gene* **96**(1): 23-28.
- Irie, K., M. Takase, et al. (1993). "MKK1 and MKK2, which encode Saccharomyces cerevisiae mitogen-activated protein kinase-kinase homologs, function in the pathway mediated by protein kinase C." *Mol Cell Biol* **13**(5): 3076-3083.
- James, P., J. Halladay, et al. (1996). "Genomic libraries and a host strain designed for highly efficient two-hybrid selection in yeast." *Genetics* **144**(4): 1425-1436.
- Jamieson, D. J. (1998). "Oxidative stress responses of the yeast Saccharomyces cerevisiae." *Yeast* **14**(16): 1511-1527.
- Jones, T., N. A. Federspiel, et al. (2004). "The diploid genome sequence of Candida albicans." *Proc Natl Acad Sci U S A* **101**(19): 7329-7334.
- Jorgensen, P., J. L. Nishikawa, et al. (2002). "Systematic identification of pathways that couple cell growth and division in yeast." *Science* **297**(5580): 395-400.
- Jorgensen, P., I. Rupes, et al. (2004). "A dynamic transcriptional network communicates growth potential to ribosome synthesis and critical cell size." *Genes Dev* **18**(20): 2491-2505.
- Kamada, Y., Y. Fujioka, et al. (2005). "Tor2 directly phosphorylates the AGC kinase Ypk2 to regulate actin polarization." *Mol Cell Biol* **25**(16): 7239-7248.
- Karathia, H., E. Vilaprinyo, et al. (2011). "Saccharomyces cerevisiae as a model organism: a comparative study." *PLoS One* **6**(2): e16015.
- Klengel, T., W. J. Liang, et al. (2005). "Fungal adenylyl cyclase integrates CO₂ sensing with cAMP signaling and virulence." *Curr Biol* **15**(22): 2021-2026.
- Knighton, D. R., N. H. Xuong, et al. (1991). "Crystallization studies of cAMP-dependent protein kinase. Cocrystals of the catalytic subunit with a 20 amino acid residue peptide inhibitor and MgATP diffract to 3.0 Å resolution." *J Mol Biol* **220**(2): 217-220.
- Knighton, D. R., J. H. Zheng, et al. (1991). "Crystal structure of the catalytic subunit of cyclic adenosine monophosphate-dependent protein kinase." *Science* **253**(5018): 407-414.
- Kopecka, M. and M. Gabriel (1992). "The influence of congo red on the cell wall and (1----3)-beta-D-glucan microfibril biogenesis in Saccharomyces cerevisiae." *Arch Microbiol* **158**(2): 115-126.
- Kornev, A. P., N. M. Haste, et al. (2006). "Surface comparison of active and inactive protein kinases identifies a conserved activation mechanism." *Proc Natl Acad Sci U S A* **103**(47): 17783-17788.
- Krause, S. A., M. J. Cundell, et al. (2012). "Functional specialisation of yeast Rho1 GTP exchange factors." *J Cell Sci* **125**(Pt 11): 2721-2731.
- Kroemer, G., W. S. El-Deiry, et al. (2005). "Classification of cell death: recommendations of the Nomenclature Committee on Cell Death." *Cell Death Differ* **12 Suppl 2**: 1463-1467.
- Kumamoto, C. A. (2005). "A contact-activated kinase signals Candida albicans invasive growth and biofilm development." *Proc Natl Acad Sci U S A* **102**(15): 5576-5581.
- Kumamoto, C. A. and M. D. Vences (2005). "Alternative Candida albicans lifestyles: growth on surfaces." *Annu Rev Microbiol* **59**: 113-133.
- LaFayette, S. L., C. Collins, et al. (2010). "PKC signaling regulates drug resistance of the fungal pathogen Candida albicans via circuitry comprised of Mkc1, calcineurin, and Hsp90." *PLoS Pathog* **6**(8): e1001069.
- Lalla, R. V., M. C. Latortue, et al. (2010). "A systematic review of oral fungal infections in patients receiving cancer therapy." *Support Care Cancer* **18**(8): 985-992.
- Lee, K. S. and D. E. Levin (1992). "Dominant mutations in a gene encoding a putative protein kinase (BCK1) bypass the requirement for a Saccharomyces cerevisiae protein kinase C homolog." *Mol Cell Biol* **12**(1): 172-182.

- Lee, P., B. R. Cho, et al. (2008). "Yeast Yak1 kinase, a bridge between PKA and stress-responsive transcription factors, Hsf1 and Msn2/Msn4." *Mol Microbiol* **70**(4): 882-895.
- Lengeler, K. B., R. C. Davidson, et al. (2000). "Signal transduction cascades regulating fungal development and virulence." *Microbiol Mol Biol Rev* **64**(4): 746-785.
- Levin, D. E. (2005). "Cell wall integrity signaling in *Saccharomyces cerevisiae*." *Microbiol Mol Biol Rev* **69**(2): 262-291.
- Levin, D. E., F. O. Fields, et al. (1990). "A candidate protein kinase C gene, PKC1, is required for the *S. cerevisiae* cell cycle." *Cell* **62**(2): 213-224.
- Levin, L. R. and M. J. Zoller (1990). "Association of catalytic and regulatory subunits of cyclic AMP-dependent protein kinase requires a negatively charged side group at a conserved threonine." *Mol Cell Biol* **10**(3): 1066-1075.
- Li, W., L. Sun, et al. (2006). "Yeast AMID homologue Ndi1p displays respiration-restricted apoptotic activity and is involved in chronological aging." *Mol Biol Cell* **17**(4): 1802-1811.
- Lockshon, D., C. P. Olsen, et al. (2012). "Rho signaling participates in membrane fluidity homeostasis." *PLoS One* **7**(10): e45049.
- Lopez-Garcia, L. A., J. O. Schulze, et al. (2011). "Allosteric regulation of protein kinase PKCzeta by the N-terminal C1 domain and small compounds to the PIF-pocket." *Chem Biol* **18**(11): 1463-1473.
- Luo, G., A. Gruhler, et al. (2008). "The sphingolipid long-chain base-Pkh1/2-Ypk1/2 signaling pathway regulates eisosome assembly and turnover." *J Biol Chem* **283**(16): 10433-10444.
- Ma, P., S. Wera, et al. (1999). "The PDE1-encoded low-affinity phosphodiesterase in the yeast *Saccharomyces cerevisiae* has a specific function in controlling agonist-induced cAMP signaling." *Mol Biol Cell* **10**(1): 91-104.
- Madden, K., Y. J. Sheu, et al. (1997). "SBF cell cycle regulator as a target of the yeast PKC-MAP kinase pathway." *Science* **275**(5307): 1781-1784.
- Madeo, F., E. Frohlich, et al. (1999). "Oxygen stress: a regulator of apoptosis in yeast." *J Cell Biol* **145**(4): 757-767.
- Madeo, F., E. Herker, et al. (2002). "A caspase-related protease regulates apoptosis in yeast." *Mol Cell* **9**(4): 911-917.
- Malinska, K., J. Malinsky, et al. (2003). "Visualization of protein compartmentation within the plasma membrane of living yeast cells." *Mol Biol Cell* **14**(11): 4427-4436.
- Mandal, M., S. Kim, et al. (2005). "The Akt inhibitor KP372-1 suppresses Akt activity and cell proliferation and induces apoptosis in thyroid cancer cells." *Br J Cancer* **92**(10): 1899-1905.
- Martinez-Pastor, M. T., G. Marchler, et al. (1996). "The *Saccharomyces cerevisiae* zinc finger proteins Msn2p and Msn4p are required for transcriptional induction through the stress response element (STRE)." *EMBO J* **15**(9): 2227-2235.
- Mashhoon, N., G. Carmel, et al. (2001). "Structure of the unliganded cAMP-dependent protein kinase catalytic subunit from *Saccharomyces cerevisiae*." *Arch Biochem Biophys* **387**(1): 11-19.
- Mellor, H. and P. J. Parker (1998). "The extended protein kinase C superfamily." *Biochem J* **332** (Pt 2): 281-292.
- Merson-Davies, L. A. and F. C. Odds (1989). "A morphology index for characterization of cell shape in *Candida albicans*." *J Gen Microbiol* **135**(11): 3143-3152.
- Mitjana, F. V., M. I. Petkova, et al. (2011). "Pkc1 and actin polymerisation activities play a role in ribosomal gene repression associated with secretion impairment caused by oxidative stress." *FEMS Yeast Res* **11**(8): 656-659.
- Monge, R. A., E. Roman, et al. (2006). "The MAP kinase signal transduction network in *Candida albicans*." *Microbiology* **152**(Pt 4): 905-912.
- Morano, K. A., C. M. Grant, et al. (2012). "The response to heat shock and oxidative stress in *Saccharomyces cerevisiae*." *Genetics* **190**(4): 1157-1195.
- Morano, K. A. and D. J. Thiele (1999). "The Sch9 protein kinase regulates Hsp90 chaperone complex signal transduction activity in vivo." *EMBO J* **18**(21): 5953-5962.

- Moseley, J. B. and B. L. Goode (2006). "The yeast actin cytoskeleton: from cellular function to biochemical mechanism." *Microbiol Mol Biol Rev* **70**(3): 605-645.
- Nagahashi, S., T. Mio, et al. (1998). "Isolation of CaSLN1 and CaNIK1, the genes for osmosensing histidine kinase homologues, from the pathogenic fungus *Candida albicans*." *Microbiology* **144** (Pt 2): 425-432.
- Navarro-Garcia, F., M. Sanchez, et al. (1995). "Functional characterization of the MKC1 gene of *Candida albicans*, which encodes a mitogen-activated protein kinase homolog related to cell integrity." *Mol Cell Biol* **15**(4): 2197-2206.
- Niimi, M., K. Niimi, et al. (2004). "Regulated overexpression of CDR1 in *Candida albicans* confers multidrug resistance." *J Antimicrob Chemother* **54**(6): 999-1006.
- Niles, B. J., H. Mogri, et al. (2012). "Plasma membrane recruitment and activation of the AGC kinase Ypk1 is mediated by target of rapamycin complex 2 (TORC2) and its effector proteins Slm1 and Slm2." *Proc Natl Acad Sci U S A* **109**(5): 1536-1541.
- Nonaka, H., K. Tanaka, et al. (1995). "A downstream target of RHO1 small GTP-binding protein is PKC1, a homolog of protein kinase C, which leads to activation of the MAP kinase cascade in *Saccharomyces cerevisiae*." *EMBO J* **14**(23): 5931-5938.
- Norbeck, J. and A. Blomberg (2000). "The level of cAMP-dependent protein kinase A activity strongly affects osmotolerance and osmo-instigated gene expression changes in *Saccharomyces cerevisiae*." *Yeast* **16**(2): 121-137.
- Odds, F. C. (1985). "Morphogenesis in *Candida albicans*." *Crit Rev Microbiol* **12**(1): 45-93.
- Olivera-Couto, A., M. Grana, et al. (2011). "The eisosome core is composed of BAR domain proteins." *Mol Biol Cell* **22**(13): 2360-2372.
- Park, H., C. L. Myers, et al. (2005). "Role of the fungal Ras-protein kinase A pathway in governing epithelial cell interactions during oropharyngeal candidiasis." *Cell Microbiol* **7**(4): 499-510.
- Park, M. T., J. A. Kang, et al. (2003). "Phytosphingosine induces apoptotic cell death via caspase 8 activation and Bax translocation in human cancer cells." *Clin Cancer Res* **9**(2): 878-885.
- Pastor-Flores, D., J. O. Schulze, et al. (2013). "The PIF-pocket as a target for *C. albicans* Pkh selective inhibitors." *ACS Chem Biol*.
- Pfaller, M. A., D. J. Diekema, et al. (2010). "Results from the ARTEMIS DISK Global Antifungal Surveillance Study, 1997 to 2007: a 10.5-year analysis of susceptibilities of *Candida* species to fluconazole and voriconazole as determined by CLSI standardized disk diffusion." *J Clin Microbiol* **48**(4): 1366-1377.
- Piekarska, K., E. Mol, et al. (2006). "Peroxisomal fatty acid beta-oxidation is not essential for virulence of *Candida albicans*." *Eukaryot Cell* **5**(11): 1847-1856.
- Raz-Pasteur, A., Y. Ullmann, et al. (2011). "The pathogenesis of *Candida* infections in a human skin model: scanning electron microscope observations." *ISRN Dermatol* **2011**: 150642.
- Reijntj, P., A. Walther, et al. (2011). "Dual-colour fluorescence microscopy using yEmCherry-/GFP-tagging of eisosome components Pil1 and Lsp1 in *Candida albicans*." *Yeast* **28**(4): 331-338.
- Reinders, J., K. Wagner, et al. (2007). "Profiling phosphoproteins of yeast mitochondria reveals a role of phosphorylation in assembly of the ATP synthase." *Mol Cell Proteomics* **6**(11): 1896-1906.
- Rinaldi, J., J. Wu, et al. (2010). "Structure of yeast regulatory subunit: a glimpse into the evolution of PKA signaling." *Structure* **18**(11): 1471-1482.
- Rockenfeller, P. and F. Madeo (2008). "Apoptotic death of ageing yeast." *Exp Gerontol* **43**(10): 876-881.
- Roelants, F. M., A. G. Baltz, et al. (2010). "A protein kinase network regulates the function of aminophospholipid flippases." *Proc Natl Acad Sci U S A* **107**(1): 34-39.
- Roelants, F. M., P. D. Torrance, et al. (2002). "Pkh1 and Pkh2 differentially phosphorylate and activate Ypk1 and Ykr2 and define protein kinase modules required for maintenance of cell wall integrity." *Mol Biol Cell* **13**(9): 3005-3028.
- Roelants, F. M., P. D. Torrance, et al. (2004). "Differential roles of PDK1- and PDK2-phosphorylation sites in the yeast AGC kinases Ypk1, Pkc1 and Sch9." *Microbiology* **150**(Pt 10): 3289-3304.

- Rolland, F., J. H. De Winde, et al. (2000). "Glucose-induced cAMP signalling in yeast requires both a G-protein coupled receptor system for extracellular glucose detection and a separable hexose kinase-dependent sensing process." *Mol Microbiol* **38**(2): 348-358.
- Roncero, C., M. H. Valdivieso, et al. (1988). "Effect of calcofluor white on chitin synthases from *Saccharomyces cerevisiae*." *J Bacteriol* **170**(4): 1945-1949.
- Roosen, J., K. Engelen, et al. (2005). "PKA and Sch9 control a molecular switch important for the proper adaptation to nutrient availability." *Mol Microbiol* **55**(3): 862-880.
- Roosen, J., E. Frans, et al. (2000). "Comparison of premortem clinical diagnoses in critically ill patients and subsequent autopsy findings." *Mayo Clin Proc* **75**(6): 562-567.
- Rosse, C., M. Linch, et al. (2010). "PKC and the control of localized signal dynamics." *Nat Rev Mol Cell Biol* **11**(2): 103-112.
- Ryan, O., R. S. Shapiro, et al. (2012). "Global gene deletion analysis exploring yeast filamentous growth." *Science* **337**(6100): 1353-1356.
- Sanglard, D., F. Ischer, et al. (2003). "Calcineurin A of *Candida albicans*: involvement in antifungal tolerance, cell morphogenesis and virulence." *Mol Microbiol* **48**(4): 959-976.
- Sanglard, D., F. Ischer, et al. (1997). "Cloning of *Candida albicans* genes conferring resistance to azole antifungal agents: characterization of CDR2, a new multidrug ABC transporter gene." *Microbiology* **143 (Pt 2)**: 405-416.
- Sarbassov, D. D., D. A. Guertin, et al. (2005). "Phosphorylation and regulation of Akt/PKB by the rictor-mTOR complex." *Science* **307**(5712): 1098-1101.
- Serrano, R., H. Martin, et al. (2006). "Signaling alkaline pH stress in the yeast *Saccharomyces cerevisiae* through the Wsc1 cell surface sensor and the Slr2 MAPK pathway." *J Biol Chem* **281**(52): 39785-39795.
- Sharp, P. M. and W. H. Li (1987). "The codon Adaptation Index--a measure of directional synonymous codon usage bias, and its potential applications." *Nucleic Acids Res* **15**(3): 1281-1295.
- Silber, J., T. L. Antal, et al. (2004). "Phosphoinositide-dependent kinase-1 orthologues from five eukaryotes are activated by the hydrophobic motif in AGC kinases." *Biochem Biophys Res Commun* **321**(4): 823-827.
- Smith, A., M. P. Ward, et al. (1998). "Yeast PKA represses Msn2p/Msn4p-dependent gene expression to regulate growth, stress response and glycogen accumulation." *EMBO J* **17**(13): 3556-3564.
- Soll, D. R. (2004). "Mating-type locus homozygosity, phenotypic switching and mating: a unique sequence of dependencies in *Candida albicans*." *Bioessays* **26**(1): 10-20.
- Strahl, T. and J. Thorner (2007). "Synthesis and function of membrane phosphoinositides in budding yeast, *Saccharomyces cerevisiae*." *Biochim Biophys Acta* **1771**(3): 353-404.
- Stroba, A., F. Schaeffer, et al. (2009). "3,5-Diphenylpent-2-enoic acids as allosteric activators of the protein kinase PDK1: structure-activity relationships and thermodynamic characterization of binding as paradigms for PIF-binding pocket-targeting compounds." *J Med Chem* **52**(15): 4683-4693.
- Sudbery, P., N. Gow, et al. (2004). "The distinct morphogenic states of *Candida albicans*." *Trends Microbiol* **12**(7): 317-324.
- Sun, Y., Y. Miao, et al. (2012). "Orm protein phosphoregulation mediates transient sphingolipid biosynthesis response to heat stress via the Pkh-Ypk and Cdc55-PP2A pathways." *Mol Biol Cell* **23**(12): 2388-2398.
- Tan, J., Z. Li, et al. (2013). "PDK1 Signaling Towards PLK1-Myc Activation Confers Oncogenic Transformation and Tumor Initiating Cell Activation and Resistance to mTOR-targeted Therapy." *Cancer Discov*.
- Tanigawa, M., A. Kihara, et al. (2012). "Sphingolipids regulate the yeast high-osmolarity glycerol response pathway." *Mol Cell Biol* **32**(14): 2861-2870.
- Tebarth, B., T. Doedt, et al. (2003). "Adaptation of the Efg1p morphogenetic pathway in *Candida albicans* by negative autoregulation and PKA-dependent repression of the EFG1 gene." *J Mol Biol* **329**(5): 949-962.

- Toda, T., S. Cameron, et al. (1987). "Three different genes in *S. cerevisiae* encode the catalytic subunits of the cAMP-dependent protein kinase." *Cell* **50**(2): 277-287.
- Trevillyan, J. M. and M. L. Pall (1979). "Control of cyclic adenosine 3',5'-monophosphate levels by depolarizing agents in fungi." *J Bacteriol* **138**(2): 397-403.
- Urban, J., A. Soulard, et al. (2007). "Sch9 is a major target of TORC1 in *Saccharomyces cerevisiae*." *Mol Cell* **26**(5): 663-674.
- Vaughn, J. L., R. H. Goodwin, et al. (1977). "The establishment of two cell lines from the insect *Spodoptera frugiperda* (Lepidoptera; Noctuidae)." *In Vitro* **13**(4): 213-217.
- Vilella, F., E. Herrero, et al. (2005). "Pkc1 and the upstream elements of the cell integrity pathway in *Saccharomyces cerevisiae*, Rom2 and Mtl1, are required for cellular responses to oxidative stress." *J Biol Chem* **280**(10): 9149-9159.
- Voordeckers, K., M. Kimpe, et al. (2011). "Yeast 3-phosphoinositide-dependent protein kinase-1 (PDK1) orthologs Pkh1-3 differentially regulate phosphorylation of protein kinase A (PKA) and the protein kinase B (PKB)/S6K ortholog Sch9." *J Biol Chem* **286**(25): 22017-22027.
- Wachtler, B., D. Wilson, et al. (2011). "From attachment to damage: defined genes of *Candida albicans* mediate adhesion, invasion and damage during interaction with oral epithelial cells." *PLoS One* **6**(2): e17046.
- Walther, T. C., P. S. Aguilar, et al. (2007). "Pkh-kinases control eisosome assembly and organization." *EMBO J* **26**(24): 4946-4955.
- Walther, T. C., J. H. Brickner, et al. (2006). "Eisosomes mark static sites of endocytosis." *Nature* **439**(7079): 998-1003.
- Whiteway, M. and C. Bachewich (2007). "Morphogenesis in *Candida albicans*." *Annu Rev Microbiol* **61**: 529-553.
- Wilhelm, A., L. A. Lopez-Garcia, et al. (2012). "2-(3-Oxo-1,3-diphenylpropyl)malonic acids as potent allosteric ligands of the PIF pocket of phosphoinositide-dependent kinase-1: development and prodrug concept." *J Med Chem* **55**(22): 9817-9830.
- Wilkinson, D. and M. Ramsdale (2011). "Proteases and caspase-like activity in the yeast *Saccharomyces cerevisiae*." *Biochem Soc Trans* **39**(5): 1502-1508.
- Winzeler, E. A., D. D. Shoemaker, et al. (1999). "Functional characterization of the *S. cerevisiae* genome by gene deletion and parallel analysis." *Science* **285**(5429): 901-906.
- Wishart, J. A., A. Hayes, et al. (2005). "Doxycycline, the drug used to control the tet-regulatable promoter system, has no effect on global gene expression in *Saccharomyces cerevisiae*." *Yeast* **22**(7): 565-569.
- Wishart, J. A., M. Osborn, et al. (2006). "The relative merits of the tetO2 and tetO7 promoter systems for the functional analysis of heterologous genes in yeast and a compilation of essential yeast genes with tetO2 promoter substitutions." *Yeast* **23**(4): 325-331.
- Wu, M., L. G. Xu, et al. (2002). "AMID, an apoptosis-inducing factor-homologous mitochondrion-associated protein, induces caspase-independent apoptosis." *J Biol Chem* **277**(28): 25617-25623.
- Wu, W. I., W. C. Voegtli, et al. (2010). "Crystal structure of human AKT1 with an allosteric inhibitor reveals a new mode of kinase inhibition." *PLoS One* **5**(9): e12913.
- Wu, W. S. and W. H. Li (2008). "Systematic identification of yeast cell cycle transcription factors using multiple data sources." *BMC Bioinformatics* **9**: 522.
- Yen, K., P. Gitsham, et al. (2003). "An improved tetO promoter replacement system for regulating the expression of yeast genes." *Yeast* **20**(15): 1255-1262.
- Yeo, S. F. and B. Wong (2002). "Current status of nonculture methods for diagnosis of invasive fungal infections." *Clin Microbiol Rev* **15**(3): 465-484.
- Zeng, Z., I. J. Samudio, et al. (2006). "Simultaneous inhibition of PDK1/AKT and Fms-like tyrosine kinase 3 signaling by a small-molecule KP372-1 induces mitochondrial dysfunction and apoptosis in acute myelogenous leukemia." *Cancer Res* **66**(7): 3737-3746.

- Zhang, X., R. L. Lester, et al. (2004). "Pil1p and Lsp1p negatively regulate the 3-phosphoinositide-dependent protein kinase-like kinase Pkh1p and downstream signaling pathways Pkc1p and Ypk1p." J Biol Chem **279**(21): 22030-22038.
- Zhao, B., R. Lehr, et al. (2007). "Crystal structure of the kinase domain of serum and glucocorticoid-regulated kinase 1 in complex with AMP PNP." Protein Sci **16**(12): 2761-2769.
- Ziemba, B. P., C. Pilling, et al. (2013). "The PH Domain of Phosphoinositide-Dependent Kinase-1 Exhibits a Novel, Phospho-Regulated Monomer-Dimer Equilibrium with Important Implications for Kinase Domain Activation: Single-Molecule and Ensemble Studies." Biochemistry.
- Ziolkowska, N. E., L. Karotki, et al. (2011). "Eisosome-driven plasma membrane organization is mediated by BAR domains." Nat Struct Mol Biol **18**(7): 854-856.
- Zweytick, D., C. Hrastnik, et al. (2000). "Biochemical characterization and subcellular localization of the sterol C-24(28) reductase, erg4p, from the yeast *saccharomyces cerevisiae*." FEBS Lett **470**(1): 83-87.

Appendix

Appendix

Table A.1 Genes up-regulated by depletion of Pkh at the indicated times of incubation with doxycycline

INDUCED GENES				INDUCED GENES			
ORF	GENE	-fold increase		ORF	GENE	-fold increase	
		at 8h	at 24h			at 8h	at 24h
YAL054C	ACS1		12.32	YDL113C	ATG20	1.71	2.06
YAL061W	BDH2	2.66	4.19	YDL124W		1.63	2.32
YAR028W		1.05	2.56	YDL149W	ATG9		2.07
YAR035W	YAT1		2.92	YDL169C	UGX2		3.47
YBL015W	ACH1	1.40	2.60	YDL174C	DLD1	1.97	4.20
YBL042C	FUI1		3.42	YDL204W	RTN2	1.33	2.43
YBL064C	PRX1	1.85	2.86	YDL222C	FMP45		12.70
YBL075C	SSA3		8.28	YDL223C	HBT1		5.00
YBL078C	ATG8		4.98	YDL233W		1.67	2.25
YBR005W	RCR1	2.05	1.87	YDL234C	GYP7	2.75	3.68
YBR006W	UGA2		2.07	YDR011W	SNQ2	1.01	2.21
YBR008C	FLR1	0.94	2.58	YDR043C	NRG1	1.58	3.14
YBR050C	REG2		4.78	YDR055W	PST1	1.06	3.01
YBR056W		1.72	2.30	YDR059C	UBC5	1.26	2.02
YBR072W	HSP26	6.07	7.47	YDR070C	FMP16		5.90
YBR083W	TEC1	2.95		YDR085C	AFR1	2.05	1.88
YBR101C	FES1	0.58	2.66	YDR096W	GIS1	2.12	1.82
YBR112C	CYC8	1.18	2.57	YDR123C	INO2		2.35
YBR117C	TKL2		9.88	YDR171W	HSP42	1.16	2.04
YBR126C	TPS1	1.53	2.02	YDR178W	SDH4	1.69	2.27
YBR132C	AGP2	2.43	1.22	YDR216W	ADR1		4.68
YBR169C	SSE2	1.03	2.80	YDR223W	CRF1		3.05
YBR203W	COS111		2.44	YDR256C	CTA1	1.01	2.05
YBR214W	SDS24	1.65	2.89	YDR258C	HSP78	1.02	2.18
YBR230C	OM14	2.37	2.73	YDR342C	HXT7	4.39	2.30
YBR284W			3.02	YDR380W	ARO10		13.25
YBR287W		1.64	2.34	YDR453C	TSA2		2.24
YBR298C	MAL31	3.13		YDR533C	HSP31	1.42	4.50
YCL040W	GLK1	1.84	2.02	YEL011W	GLC3	5.01	3.81
YCR021C	HSP30	0.71	5.81	YEL039C	CYC7	2.72	
YCR051W		2.01	2.20	YEL045C		1.10	2.10
YCR091W	KIN82	2.10		YEL049W	PAU2		2.90
YCR102C			5.51	YEL060C	PRB1	2.08	3.55
YCR107W	AAD3	0.69	4.11	YER020W	GPA2	2.04	2.17
YCRX21C			3.68	YER053C	PIC2	1.03	2.64
YDL014W	NOP1		2.77	YER054C	GIP2		3.43
YDL085W	NDE2		4.34	YER067W		5.72	3.61

INDUCED GENES				INDUCED GENES			
ORF	GENE	-fold increase		ORF	GENE	-fold increase	
		at 8h	at 24h			at 8h	at 24h
YER103W	SSA4		18.71	YHR139C	SPS100	0.96	4.50
YER143W	DDI1	1.05	2.34	YHR209W	CRG1	1.72	2.35
YER150W	SPI1	1.74	9.21	YIL017C	VID28	1.55	2.04
YFL014W	HSP12		52.73	YIL136W	OM45	2.07	
YFL016C	MDJ1	0.69	2.26	YIL144W	TID3	1.18	4.11
YFL054C		2.37	1.91	YIL169C		2.02	0.78
YFL056C	AAD6		10.71	YIR016W		2.09	1.70
YFL057C	AAD16		10.58	YJL016W			3.51
YFR015C	GSY1	5.35	4.14	YJL048C	UBX6		4.09
YFR053C	HXK1	4.84	3.86	YJL066C	MPM1	1.41	2.10
YGL006W	PMC1	1.53	2.96	YJL116C	NCA3	0.80	2.22
YGL053W	PRM8	1.46	2.11	YJL141C	YAK1	1.96	2.71
YGL055W	OLE1	1.24	2.66	YJL153C	INO1		95.70
YGL121C	GPG1		2.34	YJL165C	HAL5	1.89	3.45
YGL156W	AMS1		2.45	YJL166W	QCR8	2.21	
YGL231C	EMC4	2.10		YJL219W	HXT9		2.74
YGR008C	STF2	2.32	2.27	YJL221C	FSP2		2.19
YGR032W	GSC2	2.01	2.10	YJR073C	OPI3	1.94	3.30
YGR043C	NQM1		8.04	YJR096W			2.88
YGR110W	CLD1		3.72	YJR115W		4.14	
YGR142W	BTN2		22.19	YKL001C	MET14	1.87	2.68
YGR197C	SNG1	1.19	2.88	YKL062W	MSN4	2.23	1.41
YGR201C			3.37	YKL071W		0.95	7.36
YGR213C	RTA1		4.71	YKL087C	CYT2	1.16	2.32
YGR243W	FMP43	2.97	4.02	YKL109W	HAP4	2.08	2.14
YGR248W	SOL4	2.66	5.90	YKL150W	MCR1	1.68	2.62
YGR249W	MGA1	2.11		YKL163W	PIR3		2.67
YGR256W	GND2		4.00	YKL216W	URA1	3.93	4.27
YHL021C	AIM17	3.14	3.50	YKL218C	SRY1	1.41	2.19
YHL027W	RIM101	1.44	2.13	YKR024C	DBP7	1.14	2.78
YHR008C	SOD2	1.17	2.01	YKR058W	GLG1	2.15	
YHR033W			2.24	YKR061W	KTR2	1.22	2.08
YHR087W	RTC3	2.65	6.42	YKR075C		6.89	4.80
YHR092C	HXT4	6.37		YKR076W	ECM4	2.47	2.86
YHR096C	HXT5		7.88	YKR091W	SRL3	2.40	1.89
YHR104W	GRE3	1.23	2.28	YKR097W	PCK1		8.44
YHR138C		2.17	2.86	YKR098C	UBP11	1.45	2.81

INDUCED GENES				INDUCED GENES			
ORF	GENE	-fold increase		ORF	GENE	-fold increase	
		at 8h	at 24h			at 8h	at 24h
YLR054C	OSW2		8.44	YMR105C	PGM2	4.20	3.66
YLR120C	YPS1	2.17	2.99	YMR110C	HFD1	1.83	2.33
YLR142W	PUT1	5.31	4.68	YMR114C		1.82	2.66
YLR149C		1.81	3.14	YMR135C	GID8	1.51	2.00
YLR174W	IDP2		3.77	YMR136W	GAT2	2.31	10.53
YLR177W		2.19	1.47	YMR140W	SIP5		2.07
YLR178C	TFS1	2.73	5.41	YMR169C	ALD3		15.20
YLR194C		2.53	5.92	YMR170C	ALD2	1.46	7.73
YLR216C	CPR6	0.87	2.32	YMR180C	CTL1	0.85	2.02
YLR257W		1.85	2.74	YMR250W	GAD1	2.03	4.59
YLR258W	GSY2	2.26	1.88	YMR280C	CAT8		5.48
YLR267W	BOP2		2.46	YMR284W	YKU70		2.11
YLR272C	YCS4	2.33	6.68	YMR291W		2.27	1.11
YLR277C	YSH1	1.15	2.81	YMR304C-A		1.44	2.39
YLR282C		3.39	3.25	YMR316C-A		2.62	5.04
YLR294C		2.27		YNL013C			4.87
YLR312C			3.90	YNL014W	HEF3		2.09
YLR327C	TMA10	2.77	2.67	YNL015W	PBI2	1.20	2.41
YLR331C	JIP3	2.89	2.05	YNL036W	NCE103	0.85	2.83
YLR350W	ORM2	1.61	2.10	YNL077W	APJ1	0.80	3.64
YLR392C	ART10		2.50	YNL093W	YPT53		6.67
YLR414C		3.25	6.25	YNL134C		1.60	3.56
YLR460C		1.18	6.32	YNL144C		2.51	2.16
YLL026W	HSP104	1.04	3.69	YNL192W	CHS1	1.81	2.71
YLL039C	UBI4	1.71	2.14	YNL195C		1.46	2.51
YLL056C			4.80	YNL208W		1.60	2.14
YML118W	NGL3		3.25	YNL305C		1.65	2.02
YML128C	MSC1	2.91	8.54	YNL331C	AAD14		2.61
YMR008C	PLB1	1.50	2.16	YNR002C	ATO2		6.64
YMR011W	HXT2	9.13	7.44	YNR059W	MNT4		2.28
YMR020W	FMS1	1.43	2.42	YNR064C			3.46
YMR030W	RSF1		2.35	YOL016C	CMK2	2.81	4.38
YMR081C	ISF1	4.75	3.49	YOL032W	OPI10	1.07	2.47
YMR084W			8.43	YOL052C-A	DDR2		5.39
YMR085W			4.79	YOL084W	PHM7		18.34
YMR090W			4.18	YOL126C	MDH2	3.49	3.66
YMR096W	SNZ1	0.63	3.72	YOL143C	RIB4	2.11	1.83

INUCED GENES			
ORF	GENE	-fold increase	
		at 8h	at 24h
YOL165C	AAD15	1.33	2.21
YOR019W		2.18	
YOR028C	CIN5		5.17
YOR036W	PEP12	2.08	2.39
YOR065W	CYT1	1.41	2.59
YOR120W	GCY1	2.21	5.03
YOR121C			5.74
YOR134W	BAG7		5.73
YOR137C	SIA1	2.35	
YOR162C	YRR1	1.35	2.65
YOR178C	GAC1	3.88	3.52
YOR202W	HIS3	9.34	10.29
YOR208W	PTP2		2.74
YOR220W	RCN2	2.36	3.94
YOR273C	TPO4	3.23	5.80
YOR289W		2.40	1.95
YOR347C	PYK2	2.06	1.03
YOR374W	ALD4	2.06	2.68
YOR385W		2.08	4.08
YOR391C	HSP33		2.18
YPL057C	SUR1	2.95	2.42
YPL061W	ALD6	1.38	3.44
YPL070W	MUK1	1.11	2.60
YPL149W	ATG5	1.48	2.20
YPL186C	UIP4	1.61	2.53
YPL195W	APL5	1.96	2.22
YPL196W	OXR1	1.51	2.24
YPL223C	GRE1		6.23
YPL240C	HSP82	0.66	2.07
YPR001W	CIT3		4.59
YPR005C	HAL1		2.32
YPR030W	CSR2	2.37	6.03
YPR093C	ASR1	1.29	2.18
YPR150W			10.86
YPR154W	PIN3	1.18	2.43

Table A.2 Genes down-regulated by depletion of Pkh at the indicated times of incubation with doxycycline

REPPRESSED GENES				REPPRESSED GENES			
ORF	GENE	-fold decrease		ORF	GENE	-fold decrease	
		at 8h	at 24h			at 8h	at 24h
YAL023C	PMT2	0.84	0.47	YER145C	FTR1	0.55	0.28
YAR071W	PHO11	0.30	0.31	YFL004W	VTC2	0.78	0.42
YBR031W	RPL4A	0.77	0.47	YFR031C-A	RPL2A	0.81	0.49
YBR048W	RPS11B	0.92	0.49	YGL008C	PMA1	0.68	0.22
YBR067C	TIP1	0.98	0.41	YGL012W	ERG4	0.81	0.33
YBR069C	TAT1	0.71	0.49	YGL039W		0.71	0.48
YBR092C	PHO3	0.49	0.34	YGL103W	RPL28	0.88	0.49
YBR093C	PHO5	0.37	0.45	YGL123W	RPS2	0.79	0.46
YBR158W	AMN1	0.94	0.49	YGL147C	RPL9A	0.84	0.43
YBR231C	SWC5	0.44	1.12	YGL245W	GUS1	0.83	0.44
YBR238C		0.65	0.36	YGR035C		0.80	0.43
YBR249C	ARO4	0.67	0.44	YGR061C	ADE6	0.67	0.44
YCL030C	HIS4	0.51	0.35	YGR079W			0.33
YCR013C		0.82	0.49	YGR108W	CLB1	0.67	0.41
YDL003W	MCD1	0.41		YGR168C		0.82	0.27
YDL061C	RPS29B	0.86	0.45	YGR211W	ZPR1	0.45	1.06
YDL083C	RPS16B	0.78	0.48	YGR234W	YHB1	0.79	0.30
YDL157C		0.86	0.48	YGR264C	MES1	0.72	0.47
YDL191W	RPL35A	0.82	0.49	YHL035C	VMR1		0.50
YDR023W	SES1	0.71	0.44	YHL040C	ARN1	0.40	0.18
YDR025W	RPS11A	0.81	0.48	YHL047C	ARN2	0.47	0.18
YDR033W	MRH1	0.75	0.27	YHR019C	DED81	0.76	0.48
YDR240C	SNU56		0.49	YHR020W		0.60	0.38
YDR300C	PRO1	0.71	0.44	YHR068W	DYS1	0.69	0.40
YDR324C	UTP4	0.49	0.66	YHR143W	DSE2	1.10	0.38
YDR490C	PKH1	0.05	0.09	YHR182C-A		0.94	0.48
YDR508C	GNP1	0.76	0.47	YHR203C	RPS4B		0.49
YDR534C	FIT1	0.75	0.18	YHR215W	PHO12	0.25	0.19
YEL021W	URA3	0.10	0.21	YIL018W	RPL2B	0.87	0.45
YEL022W	GEA2	0.68	0.50	YIL052C	RPL34B	0.88	0.48
YEL065W	SIT1	0.38	0.26	YJL006C	CTK2	1.02	0.44
YEL071W	DLD3	0.41	0.53	YJL012C	VTC4	0.64	0.29
YER011W	TIR1	0.82	0.34	YJL078C	PRY3	0.62	0.44
YER056C	FCY2	0.80	0.46	YJL079C	PRY1	0.85	0.38
YER070W	RNR1	0.74	0.18	YJL080C	SCP160	0.79	0.49
YER082C	UTP7	0.29		YJL138C	TIF2	0.90	0.49
YER131W	RPS26B	0.98	0.42	YJL178C	ATG27		0.47

REPPRESSED GENES				REPPRESSED GENES			
ORF	GENE	-fold decrease		ORF	GENE	-fold decrease	
		at 8h	at 24h			at 8h	at 24h
YJL190C	RPS22A	0.68	0.41	YMR058W	FET3	0.54	0.20
YJR029W		0.72	0.48	YMR116C	ASC1	0.78	0.49
YJR123W	RPS5	0.85	0.46	YMR120C	ADE17	0.84	0.47
YJR148W	BAT2	0.94	0.48	YMR189W	GCV2	0.70	0.39
YKL008C	LAC1	0.90	0.42	YMR205C	PFK2	0.73	0.48
YKL081W	TEF4	0.71	0.47	YMR272C	SCS7	0.91	0.48
YKL180W	RPL17A		0.35	YMR303C	ADH2	0.81	0.45
YKR103W	NFT1		0.32	YMR317W			0.25
YKR104W			0.49	YMR319C	FET4	1.07	0.40
YLR027C	AAT2	0.67	0.46	YNL066W	SUN4	0.95	0.49
YLR029C	RPL15A	0.94	0.48	YNL067W	RPL9B	0.83	0.46
YLR048W	RPS0B	0.75	0.50	YNL069C	RPL16B	0.83	0.48
YLR056W	ERG3	0.66	0.47	YNL145W	MFA2		0.33
YLR058C	SHM2	0.72	0.43	YNL164C	IBD2	0.49	1.02
YLR073C	RFU1	0.46	0.77	YNL209W	SSB2	0.65	0.49
YLR134W	PDC5	0.65	0.44	YNL231C	PDR16	0.52	0.45
YLR167W	RPS31	0.90	0.48	YNL289W	PCL1	0.36	1.06
YLR188W	MDL1	0.63	0.44	YNR056C	BIO5		0.34
YLR214W	FRE1	0.50	0.61	YNR067C	DSE4	0.65	0.42
YLR300W	EXG1	0.65	0.38	YOL058W	ARG1	0.47	0.39
YLR304C	ACO1	0.47	0.28	YOL086C	ADH1	0.82	0.48
YLR332W	MID2	0.50	0.55	YOR009W	TIR4		0.29
YLR339C		0.83	0.40	YOR010C	TIR2		0.50
YLR340W	RPP0	0.78	0.46	YOR011W	AUS1		0.38
YLR348C	DIC1	0.73	0.42	YOR063W	RPL3	0.80	0.47
YLR349W		0.80	0.43	YOR096W	RPS7A	0.80	0.48
YLR355C	ILV5	0.41	0.50	YOR135C	IRC14	0.65	0.29
YLR406C	RPL31B	0.78	0.48	YOR136W	IDH2	0.58	0.31
YLR413W		0.69	0.36	YOR153W	PDR5	0.75	0.41
YLR441C	RPS1A		0.48	YOR306C	MCH5		0.34
YLL044W		0.72	0.42	YOR316C	COT1	0.80	0.44
YML027W	YOX1	0.34		YOR345C		0.67	0.40
YML052W	SUR7	0.83	0.46	YOR359W	VTS1	0.45	0.71
YML063W	RPS1B	0.91	0.46	YOR382W	FIT2	0.42	0.13
YML080W	DUS1	0.46	0.66	YOR383C	FIT3	0.31	0.10
YML123C	PHO84	0.34	0.11	YPL019C	VTC3	0.51	0.21
YMR006C	PLB2	0.81	0.43	YPL030W	TRM44	0.49	0.61

REPRESSED GENES			
ORF	GENE	-fold decrease	
		at 8h	at 24h
YPL068C		0.34	
YPL090C	RPS6A	0.83	0.48
YPL131W	RPL5	0.73	0.47
YPL178W	CBC2	0.88	0.26
YPL198W	RPL7B	0.83	0.41
YPR074C	TKL1	0.71	0.42
YPR136C			0.47
YPR145W	ASN1	0.50	0.42

A.1 codon usage frequency vs. relative adaptiveness

For the gene design, and based in the similarity codon usage between mammalian and insect cells, I used human codon usage for a better gene expression in both organisms. The codon quality of coding sequences can be depicted in two different ways. The simplest way of depiction is to plot the codon usage frequency that can be found in common codon usage tables. A more elaborate way to depict the codon quality is to convert the codon usage frequency into relative adaptiveness values. In contrast to the codon usage frequency the relative adaptiveness takes into account the number of codons which code for the respective amino acid. The basic principle for deriving relative adaptiveness values out of codon usage frequency values is the following: For each amino acid the codon with the highest frequency value is set to 100% relative adaptiveness. All other codons for the same amino acid are scaled accordingly. The codon usage table for *Escherichia coli* at Kazusa lists the following values for Glycine and Glutamate codons (Sharp and Li 1987):

Aa	Codon	Number	/1000	Fraction
Gly	GGG	17628.00	10.99	0.15
Gly	GGA	12696.00	7.92	0.11
Gly	GGT	39862.00	24.85	0.34
Gly	GGC	47212.00	29.44	0.40
Glu	GAG	28529.00	17.79	0.31
Glu	GAA	63484.00	39.58	0.69

The frequency of each codon is listed in the 5th column named "Fraction". Comparing the fraction values for the best Glutamate codon GAA (0.69) with the best

Glycine codon GGC (0.40) shows clearly that codon frequency values for one aminoacid cannot be compared to those of other aminoacids even within the same codon usage table. The relative adaptiveness values can be deduced from the 5th column:

Aa	Codon	Number	/1000	Fraction	Rel.Adapt.
Gly	GGG	17628.00	10.99	0.15	38
Gly	GGA	12696.00	7.92	0.11	28
Gly	GGT	39862.00	24.85	0.34	85
Gly	GGC	47212.00	29.44	0.40	100
Glu	GAG	28529.00	17.79	0.31	45
Glu	GAA	63484.00	39.58	0.69	100

The best codon (e.g. GAA for Glu) is set to 100. All others values (e.g. GAG for Glu) are calculated using the rule of proportion ($0.31 * (100/0.69)$)

The codon quality of the following sequence of *CaPKH2* is analyzed by plotting codon usage frequencies and relative adaptiveness values (Figure A.1 and Figure A.3). Then, an analysis of aminoacids coded by wild type *CaPKH2* gene expressed in mammalian cells versus aminoacids coded of *CaPKH2* synthetic gene was done (Figure A.4).

Codontable 1 (red):

<http://www.kazusa.or.jp/codon/cgi-bin/showcodon.cgi?species=5476&aa=12&style=N>

Codontable 2 (black): Homo_sapiens

Mean difference: 19.78 % Ordinate (y-axis): frequency

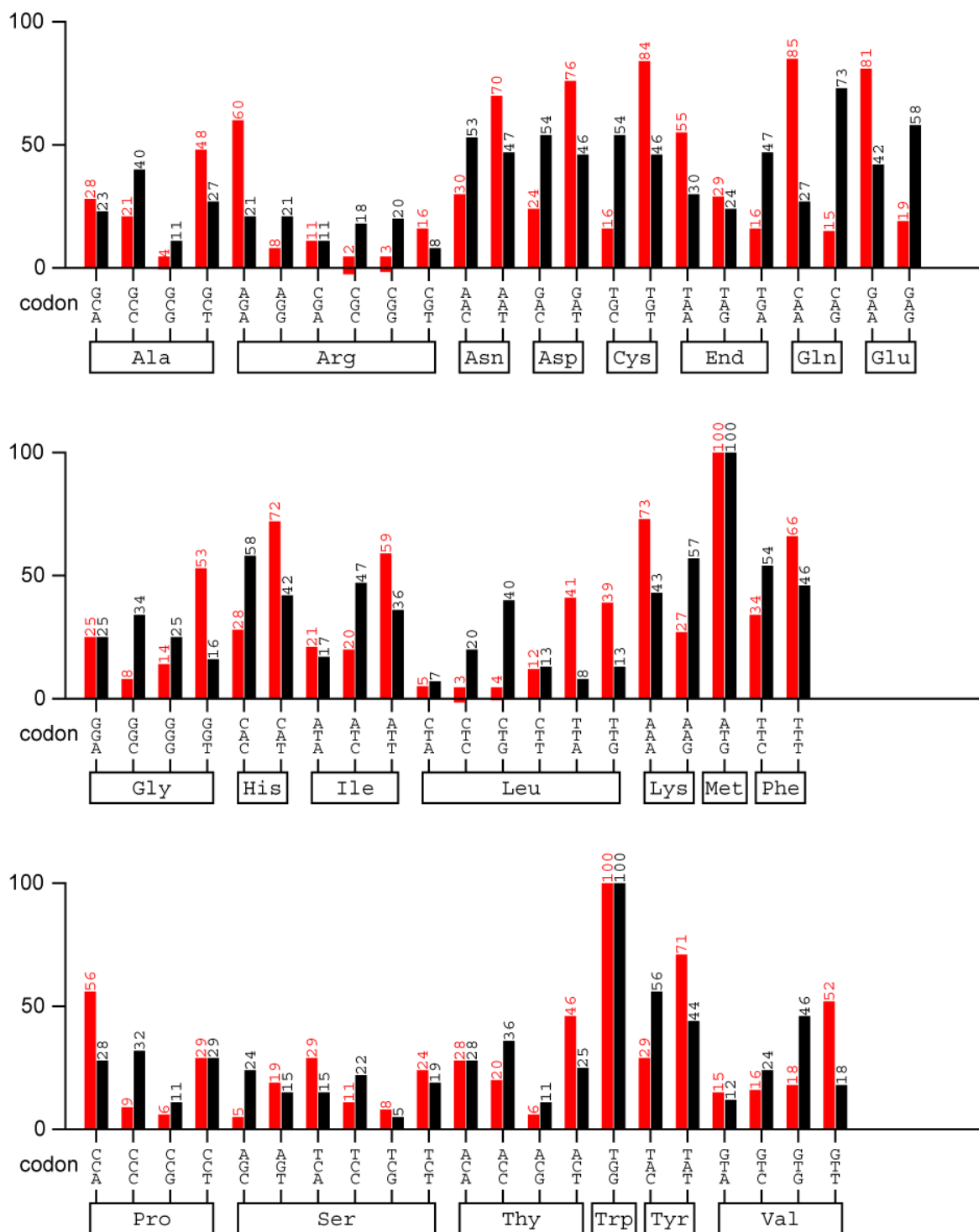


Figure A.1 Codon usage of alternative yeast *C. albicans* (red) versus Standard code of *Homo sapiens* (black) measured by frequency.

Codontable 1 (red):

<http://www.kazusa.or.jp/codon/cgi-bin/showcodon.cgi?species=5476&aa=12&style=N>

Codontable 2 (black): Homo sapiens

Mean difference: 39.72 % Ordinate (y-axis): relative adaptiveness

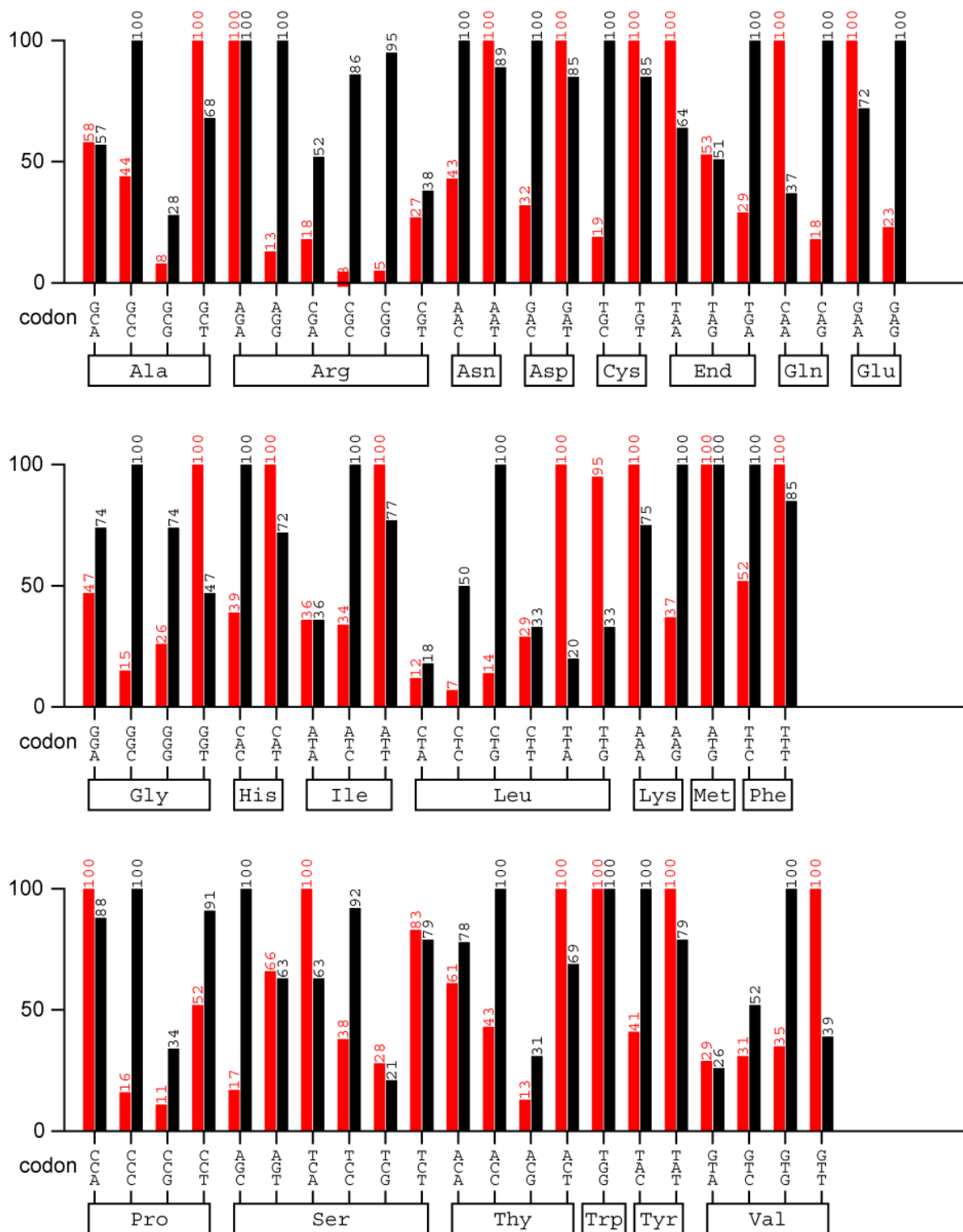


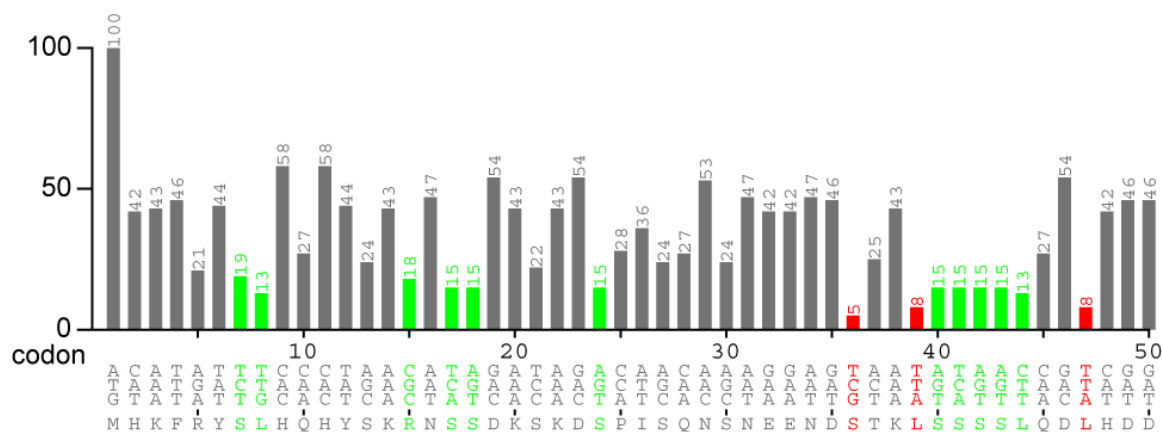
Figure A.2 Codon usage of alternative yeast *C. albicans* (red) versus Standard code of Homo sapiens (black) measured by relative adaptiveness.

A

CaPKH2 gene (1-50 aa)Codontable: sequence derived from *Candida albicans*

Ordinate (y-axis): frequency

<20% <10%



B

CaPKH2 optimised gene (1-50 aa)Codontable: sequence derived from *Candida albicans*

Ordinate (y-axis): frequency

<20% <10%

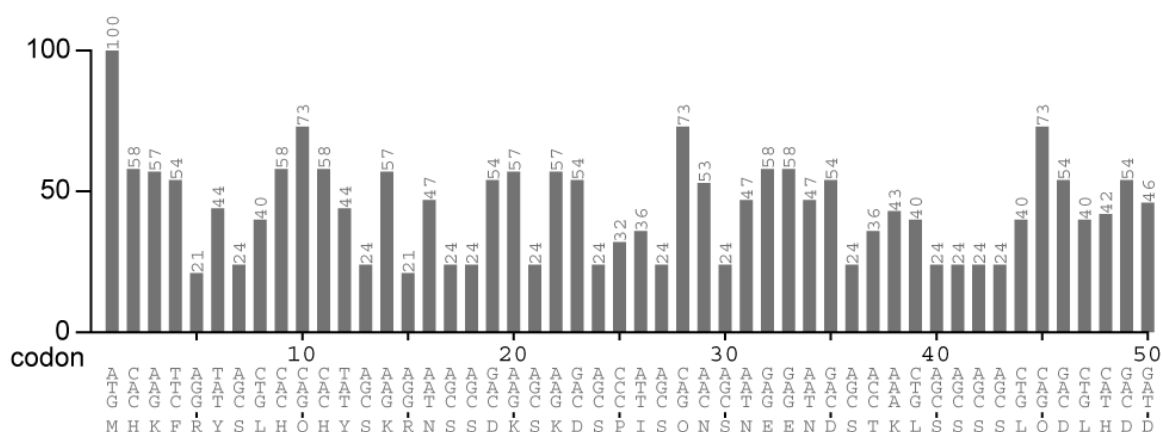


Figure A.3 Codon table of 50 first aminoacids coded by wild type *CaPKH2* gene (A) expressed in mammalian cells versus 50 first aminoacids coded of *CaPKH2* synthetic gene (B).

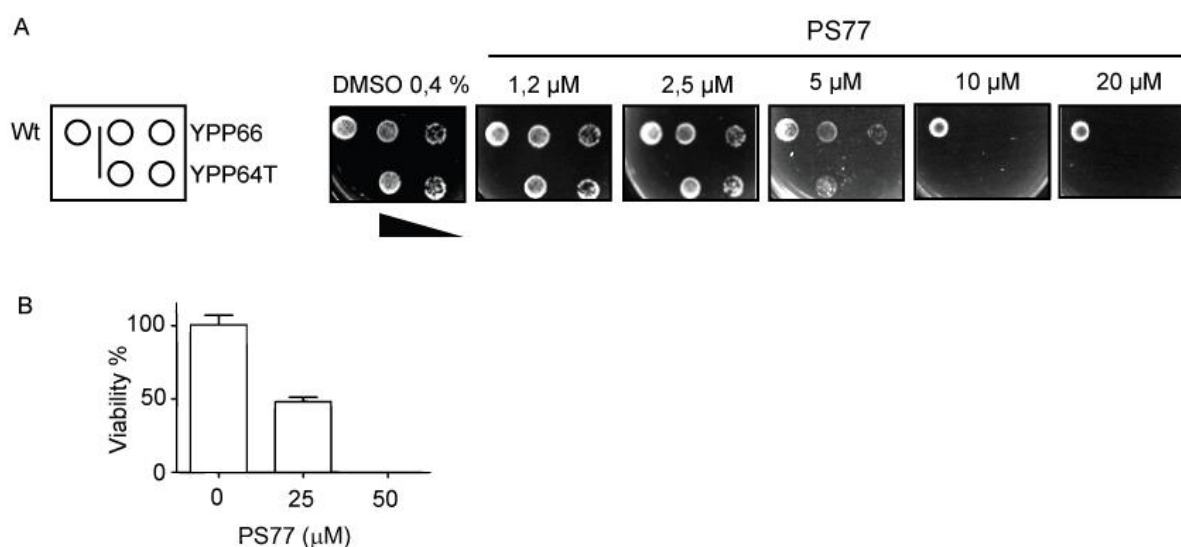


Figure A.4 Effect of PS77 on yeast strains and a mammalian cell line. A) Wild type, YPP66 and YPP64T yeast strains were spotted onto YPD agar plates in presence or absence of the indicated concentrations of PS77 and incubated at 28°C for 36 h. SDP10, YPP66 and YPP64T were spotted also at 1:10 dilution. The results show that PS77 was toxic to yeast strains YPP66 and YPP64T with EC₅₀ approximately 5 μM. B) The effect of PS77 was tested on HepG2 hepatocellular carcinoma cells. HepG2 cells were incubated with PS77 at the indicated concentrations and the viability estimated using the MTT method. About 50% viable cells remained after treatment with 25 μM PS77.

Table A.3 Results of FFAS03 search in PDB0113

#	Score	Template	%id
1	-13.800	1v5p_A mol:protein length:126 pleckstrin homology domain-containing, family	14
2	-13.100	2rsg_A mol:protein length:94 Collagen type IV alpha-3-binding protein	21
3	-12.900	2dhj_A mol:protein length:125 Rho GTPase activating protein 21	10
4	-12.600	2j59_M mol:protein length:168 RHO-GTPASE ACTIVATING PROTEIN 10	10
5	-12.600	1w1d_A mol:protein length:151 3-PHOSPHOINOSITIDE DEPENDENT PROTEIN KINASE-1	7
6	-12.500	2d9v_A mol:protein length:130 Pleckstrin homology domain-containing protein	10
7	-12.400	1v5u_A mol:protein length:117 SET binding factor 1	9
8	-12.200	2rlo_A mol:protein length:128 Centaurin-gamma 1	12
9	-12.100	2d9w_A mol:protein length:127 Docking protein 2	10
10	-11.900	2coc_A mol:protein length:112 FYVE, RhoGEF and PH domain containing protein	14
11	-11.800	3aj4_A mol:protein length:112 Pleckstrin homology domain-containing family	9
12	-11.800	2dhi_A mol:protein length:120 Pleckstrin homology domain-containing family	7
13	-11.800	2dhk_A mol:protein length:119 TBC1 domain family member 2	13
14	-11.500	2d9x_A mol:protein length:120 Oxysterol binding protein-related protein 11	15
15	-11.500	1wi1_A mol:protein length:126 calcium-dependent activator protein for secre	8
16	-11.200	1x05_A mol:protein length:129 Pleckstrin	9
17	-11.200	3rcp_A mol:protein length:103 Pleckstrin homology domain-containing family	15
18	-11.200	1h10_A mol:protein length:125 RAC-ALPHA SERINE/THREONINE KINASE	11
19	-11.100	1zc4_B mol:protein length:120 exocyst complex protein Exo84	15
20	-11.100	1xx0_A mol:protein length:127 Pleckstrin	9

Table A.4 Results of FFAS03 search in PfamA26U

	Score	Template	%id
1	-12.900	PF15413; E9C7L7.1/130-226; Pleckstrin homology domain	13
2	-12.400	PF14593; E9CBD6.1/483-586; PH domain	14
3	-11.300	PF12814.2; Q6CF84_YARLI/3022-3141; Meiotic cell cortex C-terminal pleckstrin homology	11
4	-11.300	PF15409; E3RG70.1/221-309; Pleckstrin homology domain	17
5	-10.100	PF15410; E3WPL5.1/343-456; Pleckstrin homology domain	9
6	-9.670	PF00169.24; MYO10_BOVIN/1207-1304; PH domain	13
7	-8.480	PF15406; B2A9W4.1/92-199; Pleckstrin homology domain	14
8	-7.800	PF05131.9; Q9C2Y9_EMENI/279-434; Pep3/Vps18/deep orange family	15
9	-7.540	PF12305.3; Q8EJX5_SHEON/5-99; Protein of unknown function (DUF3630 topsan)	8
10	-7.190	PF03574.10; A0YWJ2_LYNBP/54-202; Peptidase family S48	6

A.2 Initial hits found targeting Aurora B in mammalian cells inhibited Ipl1 in *C. albicans*

To test if small compounds found inhibiting Aurora B of mammalian cells were also active compounds for the homolog in yeast Ipl1, I grew *S. cerevisiae* cells BY4742 until they reached the logarithmic phase. Then I split the culture in 3 equal parts and I added DMSO and PSX237 as a control, and the active compound PSX137. PSX237 belongs to the same family as PSX137 but with slightly modifications in the radical groups. I then incubated for 2.5 h and collected the cells. The protein extract measured by western blot revealed a decrease in P-Histone H3, a phosphorylation site of Ipl1 (Figure A.5).

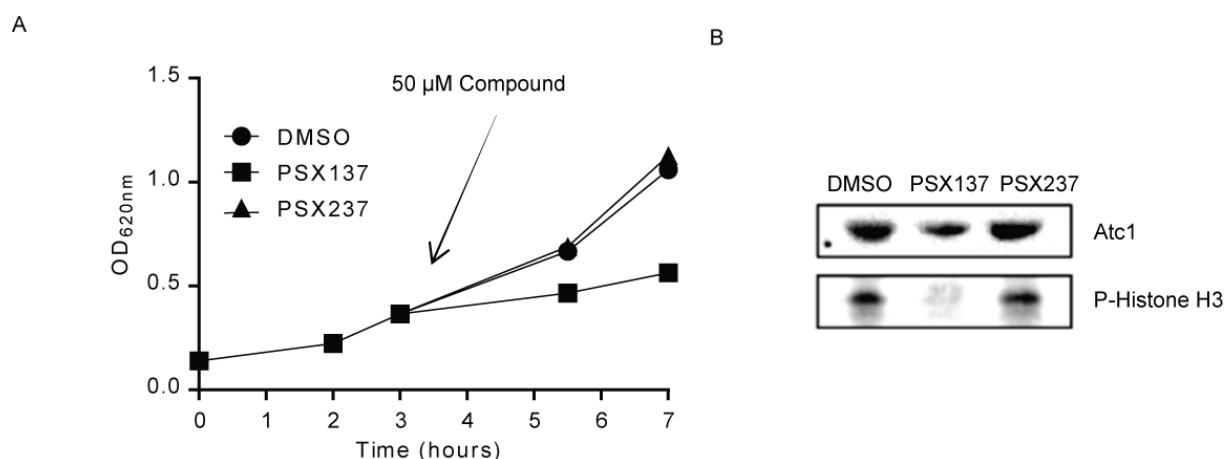


Figure A.5 PSX137 inhibit growth in *S. cerevisiae* targeting Ipl1. A) Suspension growth of *S. cerevisiae*. 50 μ M of DMSO, PSX137 and PSX237 were added to log phase *S. cerevisiae* cultures. After 1.5 hours of incubation part of the cells were collected and frozen. Additionally, 4 hours of incubation were done. B) Western blot of cells collected of suspension growth with DMSO and PSX237 as a control and PSX137. P-Histone H3 was detected by anti-phospho-histone antibody. Atc1 was measured as a control.

Acknowledgement

I would like to dedicate the next paragraphs to all the (very special people) that have helped, supported, advised and stand me throughout the elaboration of this project.

I would like to begin by giving my sincerely gratitude to my supervisor in Frankfurt, Dr. Ricardo Biondi, who has given me the opportunity of undertaking an interdisciplinary project between Barcelona and Frankfurt. His advises, strong knowledge, consistent guidance and enthusiasm were indispensable to me and the project. I also greatly appreciate his support out of the laboratory during all these years.

I would also particularly like to thank my supervisor from the Autonomous University of Barcelona, Prof. Dr. Antonio Casamayor. Thanks to him I was able to set up a Yeast Laboratory in the University Hospital of Frankfurt. His advises, tutelage, discussions, hundreds of mails and deep knowledge in yeast were indispensable for the elaboration of the thesis. I also specially appreciated his sense of humor!

A warm thank as well to Prof. Dr. Amparo Acker-Palmer for being my Ph.D. advisor and for her kind support.

Thank you to PD Dr. Dr. Albrech Piiper for reviewing my thesis, for his support but also for our talks about science, our politic discussions and in general for his company.

I also thank and appreciated the support of Prof. Dr. Stefan Zeuzem for letting me using his facilities for setting up a Yeast Laboratory.

I will extend my thanks to Dr. Thomas Pleli who has been a good friend. In addition to be a good advisor, he helped me with new methods and suggested new ideas to advance in the project. I also would like to thank Christian Schmithals for giving me his support in implementing new collaborations.

I would also like to sincerely thank my colleagues in the Research Group Phosphosites. Dr. Jose Arencibia and Magda Krupa for their friendship, support and very important advises regarding methods, molecular biology and writing. To Dr. Jörg Schulze for making all the crystallographic work for CaPkh2, for his discussions

about model mechanisms, for actively contributing to the project as well. To Evelyn Süess for her support with biochemical experiments. Thank you also to Dr. Hua Zhang and Dr. Laura Lopez-Garcia for being an important part of the group and in my life.

Last but not least, I would like to greatly and fully thank the support from outside of the lab and specially my family, my parents and brother for being so supportive and very close to me all the time. My biggest thank to Leslie, my life partner, who has been there during all the situations.

Publications

- 1- **Pastor-Flores D**, Schulze JO, Bahí A, Giacometti R, Ferrer-Dalmau J, Passeron S, Engel M, Suess E, Casamayor A, Biondi RM.
“The PIF-pocket as a target for *C. albicans* Pkh selective inhibitors”.
ACS Chem. Biol. 2013, Aug (10), pp 2283–2292.
- 2- Arencibia JM, **Pastor-Flores D**, Bauer AF, Schulze JO, Biondi RM
“AGC protein kinases: from structural mechanism of regulation to allosteric drug development for the treatment of human diseases”.
Biochim Biophys Acta. 2013 Jul;1834(7):1302-21.
- 3- **Pastor-Flores D**, Schulze JO, Casamayor A, Biondi RM.
“Lipid effectors of CaPkh2, the protein kinase ortholog of PDK1”.
Manuscript in preparation.
- 4- **Pastor-Flores D**, Ferrer J, Bahi A, Boleda M, Biondi RM, Casamayor A.
“Depletion of yeast Pkh induces/triggers a stress-like transcriptional response”.
Manuscript in preparation.

PERSONAL DATA

Name: Daniel Pastor-Flores
Date and place of birth: 25/11/1981, Zaragoza, Spain
Nationality: Spanish
Address: Homburgerstr 5, 60486 Frankfurt, Germany
E-mail: pastor@med.uni-frankfurt.de
Telephone number: 0049/176 567 972 97

HIGHER EDUCATION

November 2008 to date	Ph.D. candidate at Internal Medicine I (Prof. Dr. Zeuzem), University Hospital Johann Wolfgang Goethe, Frankfurt am Main, in the group of Dr. Ricardo Biondi "Research Group PhosphoSites".
September 2006 to July 2008	M.Sc. Thesis in the group of Prof. M. Luisa Peleato and Prof. M. Fillat at the Department of Molecular and Cellular Biology in the University of Zaragoza, Spain. "Characterization of protein FurB in <i>Anabaena</i> and Identification of furb in <i>Microcystis aeruginosa</i> ".
February 2006 to September 2006	Diploma project in the group of Prof. Uwe Strotmann at the Department of Microbiology and Biotechnology in the University of Recklinghausen, Germany. "Development and evaluation of test bacteria luminescence with ISO 11348-1".
2003 to 2006	Degree in Biochemistry from the University of Zaragoza, Spain.
2000 to 2003	General Chemistry at the University of Zaragoza, Spain.

RESEARCH EXPERIENCE

During my PhD I have been trained in the Autonomous University of Barcelona, Spain and in the Research Group PhosphoSites, Frankfurt. I have been working within a multidisciplinary environment aiming at discovering - by genetic, chemical and biological approaches - the molecular mechanism and regulation of protein kinases of pathogen fungi such as *Candida*. My research can set the bases for the development of selective antifungal compounds with novel mode of action.

As part of the projects, I acquired experience on a large set of molecular biology, cellular and yeast genetic engineering techniques, including:

- Protein expression and purification:

GST-fusion proteins expressed in HEK293 cells and purification using glutathione sepharose. Protein expression in Sf-9 insect cells and high quality purification using FPLC for crystallogenesis.

- Biochemistry:

Protein kinase activity assays, thermal stability assays, protein-protein interaction assays, lipid-protein binding assays, Alpha screen technology (homogeneous assay used to measure the interaction of a protein-peptide and the displacement by small compounds).

- Molecular biology:

DNA cloning, DNA mutagenesis in vitro, DNA sequencing, design of synthetic gene, generation of recombinant baculovirus using the Bac-to-Bac system.

- Mammalian cell culture work:

Culture of 4T1, FLC and HEpG2 cells for Proliferation and Viability Assays (MTT assay). HEK293 and Sf-9 for protein expression and purification.

- Yeast culture and genetics work:

DNA suppression and complementation, microarrays, two-hybrid system, toxicity assays, FACsorting and confocal microscope. Set up novel protocol to test focused compounds with low solubility in yeast cells and test the selectivity for the cell wall integrity pathway kinases.

PERSONAL COMPETENCES

Languages: Spanish: mother tongue
English: fluent
German: basic (level B2)
French: beginner (level A2)

Organization competences: Set up a Yeast Genetic Laboratory when I moved to Frankfurt in 2010.
Active participation with my supervisor Dr. Biondi in the design of two successful proposals based in Yeast Genetics and granted by DFG (BI 1044/2-3) and Frankfurt Hospital Johann Wolfgang Goethe (Antrag auf Förderung von Innovation, 2011).

Computer competences: Good command of Microsoft Office (Word, Excel and Powerpoint), Adobe Creative Suite (Photoshop, Illustrator), data analysis software (Graphpad, Kaleidagraph) biocomputational (Vector NTI), FACS (Cyflogic, FlowJo) microscope (Wasabi, ImageJ 1.44p), and microarray software (GenePix Pro 6.0, GEPAS3.0).

PATENT

Pkh AS AN ANTIFUNGAL TARGET

Inventors: **Pastor-Flores D**, Schulze JO, Biondi RM.

EU patent application with filing N°EP13178104.9 and filed July 25, 2013.

REFERENCES

- Dr. Ricardo M. Biondi (Ph.D. Supervisor in Frankfurt)

Research Group PhosphoSites

Medizinische Klinik I, Universitätsklinikum Frankfurt

Theodor-Stern-Kai 7, 60590 Frankfurt, Germany

E-mail: biondi@med.uni-frankfurt.de

Tel: +49 (0)69 6301 4591

- Prof. Dr. Antonio Casamayor (Ph.D. Supervisor in Barcelona)

Institut de Biotecnologia i Biomedicina (Edifici IBB),

Autonomous University of Barcelona, 08193 Cerdanyola del Vallès, Spain.

E-mail: antonio.casamayor@uab.es

Tel.: +34 935 811 278

- Prof. Dr. Maria F. Fillat (M.Sc. Supervisor)

Department of Biochemistry and Molecular and Cellular Biology

University of Zaragoza, Spain.

E-mail: mfillat@unizar.es

Tel.: +34 976 761 282